AD-A123 776 TESTING OF A SHROUDED SHORT MIXING STACK GAS EDUCTOR MODEL USING HIGH TEMPERATURE PRIMARY FLOW(U) NAVAL POSTGRADUATE SCHOOL MONTEREY CA I J EICK OCT 82 1/3

UNCLASSIFIED F/G 21/2 NL

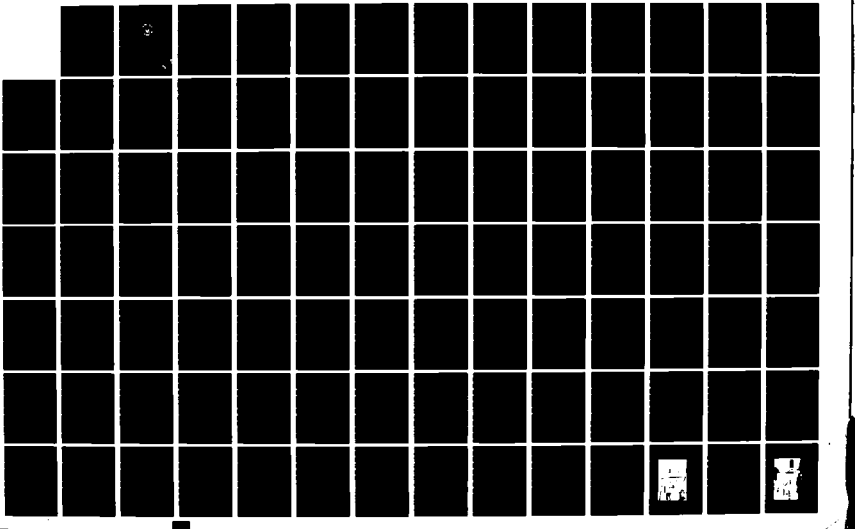

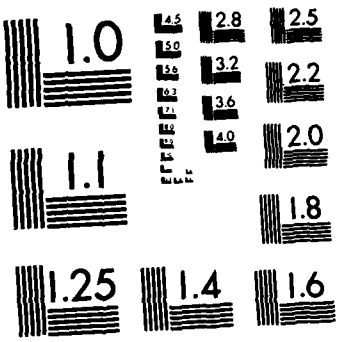

MICROCOPY RESOLUTION TEST CHART
NATIONAL BUREAU OF STANDARDS-1963-A

NAVAL POSTGRADUATE SCHOOL
Monterey, California

THESIS

TESTING OF A SHROUDED, SHORT MIXING STACK GAS EDUCTOR MODEL USING HIGH TEMPERATURE PRIMARY FLOW

by

Ira James Eick

October 1982

Thesis Advisor: P. F. Pucci

Approved for public release; distribution unlimited

Unclassified

SECURITY CLASSIFICATION OF THIS PAGE (When Data Entered)

REPORT DOCUMENTATION PAGE		READ INSTRUCTIONS BEFORE COMPLETING FORM
1. REPORT NUMBER	2. GOVT ACCESSION NO. AD A123776	3. RECIPIENT'S CATALOG NUMBER
4. TITLE (and Subtitle) Testing of a Shrouded, Short Mixing Stack Gas Eductor Model Using High Temperature Primary Flow		5. TYPE OF REPORT & PERIOD COVERED Master's Thesis October 1982
		6. PERFORMING ORG. REPORT NUMBER
7. AUTHOR(s) Ira James Eick		8. CONTRACT OR GRANT NUMBER(s)
9. PERFORMING ORGANIZATION NAME AND ADDRESS Naval Postgraduate School Monterey, California 93940		10. PROGRAM ELEMENT, PROJECT, TASK AREA & WORK UNIT NUMBERS
11. CONTROLLING OFFICE NAME AND ADDRESS Naval Postgraduate School Monterey, California 93940		12. REPORT DATE October 1982
		13. NUMBER OF PAGES 238
14. MONITORING AGENCY NAME & ADDRESS(if different from Controlling Office)		15. SECURITY CLASS. (of this report) Unclassified
		15a. DECLASSIFICATION/DOWNGRADING SCHEDULE

16. DISTRIBUTION STATEMENT (of this Report)

Approved for public release; distribution unlimited.

17. DISTRIBUTION STATEMENT (of the abstract entered in Block 20, if different from Report)

18. SUPPLEMENTARY NOTES

19. KEY WORDS (Continue on reverse side if necessary and identify by block number)

Gas Eductor	Hot Flow
Multiple Nozzle	Hot Primary Flow
Mixing Stack	Exhaust
Shroud	Cooling
Diffuser Rings	Thermal Imagery

20. ABSTRACT (Continue on reverse side if necessary and identify by block number)

An existing apparatus for testing models of gas eductor systems using high temperature primary flow was redesigned and modified to provide improved control and performance over a wide range of gas temperatures and flow rates. Pumping coefficient, temperature, and pressure data were recorded for two gas eductor system models. The first, previously tested under hot flow conditions, consisted of a

DD FORM 1 JAN 73 1473 EDITION OF 1 NOV 65 IS OBSOLETE S/N 0102-014-6601

Unclassified

SECURITY CLASSIFICATION OF THIS PAGE (When Data Entered)

(#20 - Abstract - continued)

primary plate with four straight nozzles and a slotted, shrouded mixing stack with two ring diffuser (L/D=2.5). The second was geometrically similar to a model previously tested in cold flow. This model employed a primary plate with four tilted-angled nozzles and a slotted, shrouded mixing stack with two ring diffuser (L/D=1.5). Thermal imagery was used to generalize the data obtained by direct temperature measurement. The validity of cold flow model testing is confirmed. The short stack with tilted-angled primary nozzles is shown to have superior mixing and pumping performance, but to exhibit significantly higher shroud and diffuser surface temperatures.

Approved for public release, distribution unlimited.

Testing of a Shrouded, Short Mixing Stack Gas Eductor Model Using High Temperature Primary Flow

by

Ira James Eick
Lieutenant Commander, United States Navy
B.A., University of Idaho, 1970

Submitted in partial fulfillment of the requirements for the degree of

MASTER OF SCIENCE IN MECHANICAL ENGINEERING

from the

NAVAL POSTGRADUATE SCHOOL
October 1982

Author Ira James Eick

Approved by: Paul F. Pucci

Thesis Advisor

Second Reader

Matthew Kelleher

Chairman, Department of Mechanical Engineering

William M. Tolles

Dean of Science and Engineering

ABSTRACT

An existing apparatus for testing models of gas eductor systems using high temperature primary flow was redesigned and modified to provide improved control and performance over a wide range of gas temperatures and flow rates. Pumping coefficient, temperature, and pressure data were recorded for two gas eductor system models. The first, previously tested under hot flow conditions, consisted of a primary plate with four straight nozzles and a slotted, shrouded mixing stack with two ring diffuser (L/D=2.5). The second was geometrically similiar to a model previously tested in cold flow. This model employed a primary plate with four tilted-angled nozzles and a slotted, shrouded mixing stack with two ring diffuser (L/D=1.5). Thermal imagery was used to generalize the data obtained by direct temperature measurement. The validity of cold flow model testing is confirmed. The short stack with tilted-angled primary nozzles is shown to have superior mixing and pumping performance, but to exhibit significantly higher shroud and diffuser surface temperatures.

TABLE OF CONTENTS

LIST OF FIGURES

LIST OF TABLES

TABLE OF SYMBOLS

ENGLISH LETTER SYMBOLS

A - Area, in^2, ft^2

B - Atmospheric pressure, in Hg

c - Sonic velocity, ft/sec

C - Coefficient of discharge

D - Diameter, in (as a reference quantity, refers to the inside diameter of the mixing stack)

DELPN - Pressure drop across the entrance reducing section, in H_2O

DELPU - Pressure drop across the burner U-tube, in H_2O

f - Friction factor

F_{fr} - Wall skin-friction force, lbf

g - Proportionality factor in Newton's Second Law
g = 32.174 lbm-ft/lbf-sec^2

h - Enthalpy, Btu/lbm

l - Arbitrary length, in

L - Length of the mixing stack assembly, in

P - Pressure, in H_2O

PMS - Static pressure in the mixing stack, referenced to atmoshperic, in H_2O

PNH - Inlet air pressure upstream of the reducing section, in Hg

PPLN - Pressure differential across the measurement plenum seconiary flow nozzles, in H_2O

PUPT - Pressure in the uptake, in H_2O

r - Radial distance from the axis of the mixing stack, in

R - Gas Constant, for air = 53.34 ft-lbf/lbm-°R

ROTA - Fuel mass flow rotameter reading

Rms - Interior radius of the mixing stack, in

s - Entropy, Btu/lbm-R

S - Standoff, distance between the discharge plane of the primary nozzles and the entrance plane of the mixing stack, in

T - Temperature, °F, °R

TAMB - Ambient temperature, °F

TAMBR - Ambient temperature, °R

TBURN - Burner temperature, °F

TEP - Exit plane temperature, °F

TMS - Mixing stack wall temperature, °F

TNH - Inlet air temperature, °F

TNHR - Inlet air temperature, °R

TSURF - Surface temperature of shroud and diffusers, °F

TUPT - Uptake temperature, °F

TUPTR - Uptake temperature, °R

u - Internal Energy (Btu/lbm)

U - Velocity, ft/sec

UM - Average velocity in the mixing stack, ft/sec

UP - Primary flow velocity at nozzle exit, ft/sec

UU - Primary flow velocity in uptake, ft/sec

v - Specific volume (ft^3/lbm)

W - Mass flow rate, lbm/sec

WF - Mass flow rate of fuel, lbm/sec

WP - Primary mass flow rate, lbm/sec

WS - Secondary mass flow rate, lbm/sec

WPA - Mass flow rate of primary air, lbm/sec

X - Axial distance from mixing stack entrance, in

DIMENSIONLESS GROUPINGS

A* - Secondary flow area to primary flow area ratio

A * - Tertiary flow area to primary flow area ratio

K_e - Kinetic energy correction factor

K_m - Momentum correction factor at mixing stack exit

K_p - Momentum correction factor at primary nozzle exit

M,UMACH - Mach number

p* - Pressure Coefficient for secondary flow

P * - Pressure coefficient for tertiary flow

PMS* - Pressure coefficient for mixing stack pressures

Re - Reynolds number

T* - Secondary flow absolute temperature to primary flow absolute temperature ratio

T_t* - Tertiary flow absolute temperature to primary flow absolute temperature ratio

W* - Secondary mass flow rate to primary mass flow rate ratio

W_t* - Tertiary mass flow rate to primary mass flow rate ratio

ρ_s^* - Secondary flow density to primary flow density ratio

ρ_t^* - Tertiary flow density to primary flow density ratio

GREEK LETTER SYMBOLS

β - $K + (f/2)*(A/A)$

β - Ratio of ASME long radius metering nozzle throat diameter to inlet diameter

γ - Ratio of specific heats for air

μ - Absolute viscosity, lbf-sec/ft^2

ρ - density, lbm/ft^3

ϕ - "Function of"

SUBSCRIPTS

0 - Section within the measurement plenum

1 - Section at primary nozzle exit

2 - Section at mixing stack exit

a - Atmospheric

b - Burner

m - Mixed flow

ms - Mixing stack

or - orifice

p - Primary

s - Secondary

t - Tertiary

u - Uptake

w - Mixing stack wall

ACKNOWLEDGEMENTS

The completion of this research is owed in a large part to the advice, assistance and support of a number of other people. In particular, I would like to express my thanks and appreciation to the following:

Professor Paul Pucci, of the Mechanical Engineering Department, my thesis advisor, whose counsel, support, and careful guidance has made this such a meaningful experience.

Mr. John Moulton, modelmaker and craftsman, his skill, innovation, and long hours of work are the foundation upon which this research rests.

Mr. John King, of the Naval Civil Engineering Laboratory, for his assistance in obtaining, and instruction in the use of, the thermal imaging equipment used.

Lieutenant Commander Michael Gehl, USN, a friend and shipmate, who, in spite of his own duties, was always ready to lend a hand when two weren't enough.

And, most importantly, my wife, Jan, whose patience, forebearance, and incredible flexibility have carried us through the years from one crazy project to another.

I. INTRODUCTION

Energy and momentum diffusion in a low Mach number gas eductor system is an interesting problem which has been under study at the Naval Postgraduate School for some time. This research has been motivated by the U. S. Navy's introduction of marine gas turbine propulsion systems in significant numbers of modern combatant ships. The marine gas turbine engine differs significantly from conventional steam boiler systems in air breathing characteristics. For an equivalent power output, the gas turbine engine processes four to five times the volume of combustion air and has a final exhaust temperature some 300 to 400 degrees Fahrenheit hotter than the steam system. Such characteristics create problems in the shipboard employment of these engines.

The high temperature gas heats uptake and stack surfaces, increasing the vessel's susceptibility to detection and targeting by thermal imaging (infra-red) equipment. The exhaust plume itself is also a detection problem but of less significance than the heated surfaces of shipboard structure. Various types of electronic equipments and sensors carried by a combatant vessel must be mounted as far above the water surface as possible to obtain the greatest area of coverage and to maximize effectiveness. The

materials used in construction of these equipments and their associated cabling are subject to accelerated deterioration in the presence of the heated exhaust plume. It is, therefore, desirable to reduce as far as possible the plume temperatures in the vicinity of such equipment. Finally, increasing numbers of small combatants are operating and carrying a variety of aircraft. Since landing areas are normally on the ship's fantail, it is necessary for these aircraft to approach from astern and to descend through the ship's exhaust plume during landing. This increases the hazard of operation within the ship's already turbulent wake and is a highly undesirable effect.

Due to the inherent design of a gas turbine engine, reduction of the volume of the exhaust plume is not feasible, consequently, reduction of the gas temperatures within the plume becomes highly desirable. The most attractive way to accomplish this goal would be to employ some sort of energy recovery system within the uptakes, thereby simultaneously reducing the plume temperatures and increasing overall plant efficiency. Such energy recovery systems are, of course, entirely feasible for certain engine applications. This is demonstrated by the waste heat boilers used to provide steam for auxiliary purposes in the DD 963 and CG 47 ship classes. These boilers, however, are installed in conjuction with the gas turbine generator sets used to provide shipboard electrical power and not with the

main proplusion engines. The wide and rapid range of power fluctuations associated with propulsion engine operation tend to make the installation of a waste heat boiler which serves a relatively constant load impractical.

An energy recovery design for use with propulsion engines which is currently receiving serious consideration is RACER (Rankine Cycle Energy Recovery). In this concept, steam from a waste heat boiler drives a steam turbine which is paired with the gas turbine power turbine through a combining gearbox. While preliminary designs for this system show great promise, it has not yet been demonstrated in full scale operation. In any event, it would not be suitable for retrofit into existing hulls, and installation is planned for only one or two cruise engines in a three or four engine ship. Thus, it is fairly certain that, although desirable, energy recovery is not a practicable solution to many aspects of the plume temperature problem.

A second means of reducing plume temperature is water suppression. In these systems, which are currently installed in some ships, salt water is sprayed into the exhaust near the stack exit. Such a method has many drawbacks. It requires a water supply which involves a system of pumps, piping and valves. This, of course, involves considerable installation weight and expense and levies additional maintenance requirements on the ship's force. Use of the suppression spray could also intensify problems

with mast mounted electronics equipment due to deposition of salts. In general, this system produces increased corrosion and maintenance problems for all exposed weather deck areas. At best, water suppression is an intermittent system, intended to be activated only when the ship is under threat of imminent attack. As an "in extemis" defense, some form of water suppression system will probably be a necessity in any design. It will not serve, however, to meet the requirement for a system which can operate continuously to reduce exhast plume temperatures and to cool stack surfaces.

A third method of cooling the exhaust plume, also in current use, is to dilute the exhaust gas flow with ambient air. The result is a larger volume of flow, but at significantly reduced temperatures and velocities. This dilution is achieved by employing the exhaust discharge as the primary jet in a gas eductor system. The eductor action causes ambient air to become entrained in the flow and to be drawn into the mixing section of the eductor where it mixes with the primary flow.

The mixing process under the highly turbulent conditions encountered in the gas eductor is complex and not well understood. The process has been studied by a number of researchers for a variety of purposes. Operation of gas eductors can be separated roughly into three regimes. At the upper end where Mach numbers based on the jet velocity approach and exceed one, there has been considerable

interest because of applications in thrust augmentation for aircraft and rocket engines. In the mid-region, particularly in the Mach number range of 0.4 to 0.6, research has been stimulated by the desire to obtain thrust enhancement in Vertical Takeoff and Landing (VTOL) aircraft. Relatively little work has been reported regarding gas eductor operation at jet Mach numbers of less than 0.2. This is the regime which has direct application for dilution cooling of engine exhaust flows and which has been the focus of continuing research at the Naval Postgraduate School. Moss [Ref. 1] provides a rather complete survey of the literature dealing with gas eductor systems.

II. BACKGROUND

Current U. S. Navy ship designs already include a simple gas eductor system installed on the propulsion gas turbine engine exhausts. These designs involve a solid wall mixing stack and rely on the length of the mixing stack to provide complete mixing. Work began at the Naval Postgraduate School in 1976 to investigate the effects of various parameters on the pumping and mixing performance of gas eductors. The object of this research is to effect reductions in the size and weight of the eductor structure while maintaining eductor performance measured in terms of plume temperatures and the temperatures of stack surfaces.

A. THE TEST FACILITIES

To carry out this research, two test facilities have previously been constructed. One, for cold flow testing, permits reasonably rapid analysis of a wide variety of eductor configurations. Since high temperatures are not involved, eductor models are constructed from easily fabricated materials and the basic investigation can go forward at minimal cost. A second facility, designed to test models at operating temperatures, has also been constructed. Using this facility, the actual operating performance of specific

models can be tested at realistic temperatures, confirming the results of cold flow testing.

B. INITIAL INVESTIGATIONS AT NPS

The initial investigation of gas eductor performance at the Naval Postgraduate school was undertaken by Ellin [Ref. 2]. This work was based on a simple one dimensional gas eductor model developed by Pucci [Ref. 3]. Ellin tested three basic eductor geometries to determine the effects of varying the area of the primary jet with respect to the area of the mixing stack, the effect of changing the number of primary nozzles, and the effect of standoff distance. Standoff distance is the axial distance between the exit plane of the primary nozzles and the entrance section of the mixing stack. Ellin verified a correlation between dimensionless parameters representing the pressure in a measurement plenum and the eductor's induced, or secondary, air mass flow which is derived from dimensional analysis of the one dimensional model. Ellin's work was was followed by Moss [Ref. 1], and Harrell [Ref. 4].

Working independently along parallel lines, Moss and Harrell verified that the dimensionless pumping coefficient was largely independent of the uptake Mach number. Moss further investigated the effects of mixing stack length, standoff distance, and mixing stack entrance geometry for models having four primary jets. Harrell tested similar

variables on a model of different scale using a single primary jet and on an additional model having four primary nozzles. Harrell's results verified that scaling was not a parameter in the non-dimensional correlation.

The preceeding work of Ellin, Moss, and Harrell all having been conducted in the cold flow facility, it was considered necessary to conduct verification testing at actual operating temperatures. Accordingly, Ross [Ref. 5] undertook construction and verification of the hot flow test facility used by this and other researchers. Using the facility constructed by Ross and acting on the recommendations of Moss and Harrell, Welch [Ref. 6] tested a four nozzle, solid walled mixing stack eductor system at five uptake temperatures between 160° F and 850° F. His investigation was conducted at a standoff ratio of 0.5 (the ratio of standoff distance to mixing stack inside diameter) and considered the effects of varying the mixing stack length (characterized by the ratio of mixing stack length to mixing stack diameter: L/D) and changing the ratio of mixing stack area to total primary nozzle area.

C. IMPROVEMENTS IN MIXING STACK CONFIGURATION

The initial work was conducted with straight, solid walled mixing stacks. Reports of significant pressure depression throughout the length of the mixing stack by Moss, Harrell, and Welch suggested that additional, or

tertiary flow could be induced into the mixing stack along its length and that this flow could be used to reduce externally detectable temperatures by means of film cooling flows. Staehli and Lemke [Ref. 7] used the cold flow facility to investigate the effects of both solid and ring diffusers, cooling ports in the mixing stack, and shrouding. Differing L/D's varying from 1.75 to 3.0 were tested. Two mixing stack area to primary jet area ratios (2.5 and 3.0) were included in the variables considered.

Hill [Ref. 8] followed Welch in hot flow testing by considering the performance of a solid wall mixing stack with L/D=2.5 and a slotted mixing stack of L/D=1.75 surrounded by shroud and diffusers with one and two rings. The shroud and diffuser combination increased the overall length of the mixing stack assembly to L/D=2.5. Hill's two ring diffuser assembly was tested again by this researcher and is used as one basis for comparison in this work.

In associated, but indirectly related work in 1980-1981, Shaw [Ref. 9] and Ryan [Ref. 10] developed a "plug stack" geometry intended to eliminate the infra-red signature presented to high angle seekers by diverting the flow around a central shielding structure which employs certain film cooling features. This work, though somewhat promising, remains to be pursued.

D. ENHANCED MIXING NOZZLE GEOMETRIES

In order to enhance the mixing process within the mixing stack it was considered desirable to facilitate mixing between the primary and secondary gas flows on a macroscopic scale. This was to be accomplished by using tilted and angled nozzles to create a swirling action within the primary jet. Davis [Ref. 11], in cold flow testing, considered the performance of four nozzle primary jets created by straight nozzles and a number of tilted-angled nozzles. His work was performed with three different solid walled mixing stacks with L/D's of 1.75, 1.5, and 1.25.

Acting on the results of this work, Drucker [Ref. 12] conducted some additional cold flow verification runs on the eductor geometeries tested by Davis and then extended this work to a shorter, slotted stack with cooling shroud and two ring diffuser. As with Davis, Drucker's primary jet was formed in four nozzles. Based on Davis' recommendations the nozzle discharge was tilted 15 degrees from the axial direction and angled in toward the center of the nozzle plate 20 degrees from the circumferential direction. Drucker's mixing stack contained four rows of cooling slots similar in layout to that of Hill and was surrounded by a film cooling shroud which terminated in a two ring diffuser. Two diffuser half-angles were tested, 7.3 and 10.8 degrees. Similiar pumping coefficient performance was obtained for both geometries, but areas of suspected low flow were found

in the vicinity of the second diffuser ring for the 10.8 degree model.

E. CURRENT OBJECTIVES

The specific goal of this investigation was to verify the high temperature performance of the particular eductor configuration which was developed by Davis and Drucker. After initial attempts to operate the high temperature test facility were unsatisfactory and after reviewing the work and recommendations of Welch [Ref. 6] and Hill [Ref. 8], a supplementary goal of improving the operating range and characteristics of the combustion gas generator was established.

III. THEORY AND MODELING

An eductor is a device in which a primary jet of fluid is directed into a co-axial mixing chamber in such a way that a volume of secondary fluid is entrained in the flow and a pumping action occurs. The primary and secondary fluids may be either liquids or gases in any combination. Even solids can be pumped in a slurry form. This research considers an eductor system in which both fluids are gases in incompressible flow.

An eductor is comprised of a primary nozzle plate which forms primary jet and a mixing chamber in which the primary fluid mixes with the pumped, or secondary fluid. The nozzle plate may contain one or several nozzles which may or may not impart a swirling motion to the jet. The jet is discharged into a co-axial mixing duct which has interior dimensions larger than the jet diameter. Surrounding the mixing chamber entrance is the secondary fluid which is to be pumped. This fluid is entrained in the primary flow by viscous shear interaction and drawn into the mixing chamber by a pressure depression created there. The pressure depression in the mixing chamber is found to persist for some distance along the chamber and is found capable of creating additional, or tertiary flows, into the chamber

through ports along its length. Figure (1) is a representation of a simple one dimensional eductor model.

Of interest in this work is the ability of a hot primary jet to entrain and mix with a cooler ambient fluid of the same species producing a uniform flow of fluid at an intermediate temperature. As this work is the continuation of research at the Naval Postgraduate School previously discussed, it was intended that similarity be maintained between this and previous work to permit correlation of data and to preserve the original error analysis conducted by Ellin [Ref. 2]. Similarity between the basic geometries tested has been maintained by all investigators and, in this instance, the model of interest is geometrically similar to a cold flow model previously tested by Drucker. Mach number similarity has been used to establish dynamic similarity between the primary gas flow rates of the models and the prototype. Dimensionless parameters controlling the flow as derived from a one-dimensional analysis of a simple eductor system are used throughout.

The basic analysis is presented for an eductor with only primary and secondary flows. Tertiary flows may be similarly non-dimensionalized using the same base parameters as the secondary flow. Tertiary flows, though present, were not measured in this work.

A. MODELING TECHNIQUE

The primary gas flow in the prototype mixing stack is turbulent ($Re > 10^5$) when based on the average flow properties within the mixing stack and the hydraulic diameter of the mixing stack. As a consequence of this, momentum exchange is predominent over shear interaction, and the kinetic and internal energy terms are more influential on the flow than are viscous forces. Since it can be shown that the Mach number represents the ratio of kinetic energy of a flow to its internal enerery, the Mach number is a more significant parameter than the Reynolds number in describing this turbulent flow. Because the effectiveness of the eductor changes the volume of the induced flows and consequently the average velocities and flow properties within the mixing stack, modeling similarity based on conditions within the mixing stack is not feasible. It is, however, possible to accurately model primary flow through the prototype uptake using Mach number similarity. It is this similarity which has been maintained.

B. ONE-DIMENSIONAL ANALYSIS OF A SIMPLE EDUCTOR

The following analysis is presented by Drucker [Ref. 12].

The theoretical analysis of an eductor may be approached in two ways. One method attempts to analyze the details of the mixing process of the primary and secondary air streams

as it takes place inside the mixing stack. This requires an interpretation of the mixing phenomenon which, when applied to a multiple nozzle system, becomes extremely complex. The other method, which was chosen here, analyzes the overall performance of the eductor system and is not concerned with the actual mixing process. To avoid repetition of previous reports only the main parameters and assumptions will be presented here. A complete derivation of the analysis used can be found in References [2] and [3]. The one-dimensional flow analysis of the simple eductor system (Figure 1) described depends on the simultaneous solution of the continuity, momentum, and energy equations coupled with the equation of state, all compatible with specific boundary conditions.

The idealizations made for simplifying the analysis are as follows:

1) The flow is steady state and incompressible.

2) Adiabatic flow exists throughout the eductor with isentropic flow of the secondary stream from the plenum (at section 0) to the throat or entrance of the mixing stack (at section 1) and irreversible adiabatic mixing of the primary and secondary streams occurs in the mixing stack (between sections 1 and 2).

3) The static pressure across the flow at the entrance and exit planes of the mixing-tube (at sections 1 and 2) is uniform.

4) At the mixing stack entrance (section 1) the primary flow velocity U_p and temperature T_p are uniform across the primary stream, and the secondary flow velocity U_s and temperature T_s are uniform across the secondary stream, but U_p does not equal U_s, and T_p does not equal T_s.

5) Incomplete mixing of the primary and secondary streams in the mixing stack is accounted for by the use of a non-dimensional momentum correction factor K_m which relates the actual momentum rate to the pseudo-rate based on the bulk-average velocity and density and by the use of a non-dimensional kinetic energy correction factor K_e which relates the actual kinetic energy rate to the pseudo-rate based on the bulk-average velocity and density.

6) Both gas flows behave as perfect gases.

7) Flow potential energy position changes are negligible.

8) Pressure changes P_{so} to P_{sl} and P_l to P_a are small relative to the static pressure, so that the gas density is essentially dependent upon temperature (and atmospheric pressure).

9) Wall friction in the mixing stack is accounted for with the conventional pipe friction factor term based on the bulk-average flow velocity U_m and the mixing stack wall area A_w.

The following parameters, defined here for clarity, will be used in the following development.

$\frac{A_p}{A_m}$	ratio of primary flow area to mixing stack cross section area
$\frac{A_w}{A_m}$	ratio of wall friction area to mixing stack cross sectional area
K_p	momentum correction factor for primary mixing
K_m	momentum correction factor for mixed flow
f	wall friction factor

Based on the continuity equation, the conservation of mass principle for steady flow yields

$$W_m = W_p + W_s + W_t$$

(eqn 3.1)

where:

$$W_p = \rho_p U_p A_p$$
$$W_s = \rho_s U_s A_s$$
$$W_t = \rho_t U_t A_t$$
$$W_m = \rho_m U_m A_m$$

(eqn 3.2)

All of the above velocity and density terms, with the exception of ρ_m and U_m, are defined without ambiguity by virtue of idealizations (3) and (4) above. Combining equations (3.1) and (3.2) above, the bulk average velocity at the exit plane of the mixing stack becomes

$$U_m = \frac{W_s + W_t + W_p}{\rho_m A_m}$$

(eqn 3.3)

where A_m is fixed by the geometric configuration and

$$\rho_m = \frac{P_a}{RT_m}$$

(eqn 3.4)

where T_m is calculated as the bulk average temperature from the energy equation (3.11) below. The momentum equation stems from Newton's second and third laws of motion and is the conventional force and momentum-rate balance in fluid mechanics.

$$K_p\left(\frac{W_p U_p}{g_c}\right) + \left(\frac{W_s U_s}{g_c}\right) + \left(\frac{W_t U_t}{g_c}\right) + P_1 A_1 = K_m\left(\frac{W_m U_m}{g_c}\right) + P_2 A_2 + F_{fr}$$

(eqn 3.5)

Note the introduction of idealizations (3) and (5). To account for a possible non-uniform velocity profile across the primary nozzle exit, the momentum correction factor K_p is introduced here. It is defined in a manner similar to that of K_m and by idealization (4), supported by work conducted by Moss, it is set equal to unity. K_p is carried through this analysis only to illustrate its effect on the final result. The momentum correction factor for the mixing stack exit is defined by the relation

$$K_m = \frac{1}{W_m U_m} \int_0^{A_m} U_m^2 \rho_2 dA$$

(eqn 3.6)

where U_m is evaluated as the bulk-average velocity from equation (3.3). The wall skin friction force F_{fr} can be related to the flow steam velocity by

$$F_{fr} = f A_w \left(\frac{U_m^2 \rho_m}{2 g_c}\right)$$

(eqn 3.7)

using idealization (9). As a reasonably good approximation for turbulent flow, the friction factor may be calculated from the Reynolds number

$$f = 0.046 \ (Re_m)^{-0.2}$$

(eqn 3.8)

Applying the conservation of energy principle to the steady flow system in the mixing stack between the entrance and exit planes,

$$W_p\left(h_p + \frac{U_p^2}{2g_c}\right) + W_s\left(h_s + \frac{U_s^2}{2g_c}\right) + W_t\left(h_t + \frac{U_t^2}{2g_c}\right)$$

$$= W_m\left(h_m + K_e \frac{U_m^2}{2g_c}\right)$$

(eqn 3.9)

neglecting potential energy of position changes (idealization 7). Note the introduction of the kinetic energy correction factor K_e, which is defined by the relation

$$K_e = \frac{1}{W_m U_m^2} \int_0^{A_m} U_2^3 \rho_2 dA$$

(eqn 3.10)

It may be demonstrated that for the purpose of evaluating the mixed mean flow temperature T_m, the kinetic energy terms may be neglected to yield

$$h_m = \frac{W_p}{W_m} h_p + \frac{W_s}{W_m} h_s + \frac{W_t}{W_m} h_t$$

(eqn 3.11)

where $T_m = \phi(h_m)$ only, with the idealization (6).

The energy equation for the isentropic flow of the secondary air from the plenum to the entrance of the mixing stack may be shown to reduce to

$$\frac{P_o - P_s}{P_s} = \frac{U_s^2}{2g_c}$$

(eqn 3.12)

similarly, the energy equation for the tertiary air flow reduces to

$$\frac{P_o - P_t}{\rho_s} = \frac{U_t^2}{2g_c}$$

(eqn 3.13)

The previous equations may be combined to yield the vacuum produced by the eductor action in either the secondary or tertiary air plenums. For the secondary air plenum, the vacuum produced is

$$P_c - P_{os} = \frac{1}{g_c A_m}\left(K_p \frac{W_p^2}{A_p \rho_p} + \frac{W_s^2}{A_s \rho_s}\left(1 - \frac{1}{2}\frac{A_m}{A_s}\right) - \frac{W_m^2}{A_m \rho_m}\left(K_m + \frac{f}{2}\frac{A_w}{A_m}\right)\right)$$

(eqn 3.14)

where it is understood that A_p and ρ_p apply to the primary flow at the entrance to the mixing stack, A_s and ρ_s apply to the secondary flow at this same section, and A_m and ρ_m apply to mixed flow at the exit of the mixing stack system. P_a is atmospheric pressure, and is equal to the pressure at the exit of the mixing stack. A_w is the area of the inside wall of the mixing stack.

For the tertiary air plenem, the vacuum produced is

$$P_a - P_{ot} = \frac{1}{g_c A_m}\left(K_p \frac{(W_p + W_s)^2}{(A_p \rho_p + A_s \rho_s)} + \frac{W_t^2}{A_t \rho_t}\left(1 - \frac{1}{2}\frac{A_m}{A_t}\right)\right.$$

$$\left. - \frac{W_m^2}{A_m \rho_m}\left(K_m + \frac{f}{2}\frac{A_w}{A_m}\right)\right)$$

(eqn 3.15)

where the primary flow now consists of both the primary and secondary air flows.

C. NON-DIMENSIONAL FORM OF THE SIMPLE EDUCTOR EQUATION

In order to satisfy the criteria of geometrically similiar flows, the non-dimensional parameters which govern the flow must be determined. The means chosen for determining these parameters was to normalize equations (3.14) and (3.15) with the following dimensionless groupings.

$$P^* = \frac{P_a - P_{os}}{\frac{\rho_s}{\frac{U_p^2}{2g_c}}}$$

a pressure coefficient which compares the pumped head ($P_a - P_{os}$) for the secondary flow to the driving head ($U_p^2/2g_c$) of the primary flow

$$P_t^* = \frac{P_a - P_{ot}}{\frac{\rho_t}{\frac{U_p^2}{2g_c}}}$$

a pressure coefficient which compares the pumped head ($P_a - P_{ot}$) for the tertiary flow to the driving head ($U_p^2/2g_c$) of the primary flow

$$W^* = \frac{W_s}{W_p}$$

a flow rate ratio, secondary to primary mass flow rate

$$W_t^* = \frac{W_t}{W_p}$$

a flow rate ratio, tertiary to primary mass flow rate

$$T^* = \frac{T_s}{T_p}$$

an absolute temperature ratio, secondary to primary

$$T_t^* = \frac{T_t}{T_p}$$

an absolute temperature ratio, tertiary to primary

$$\rho_s^* = \frac{\rho_s}{\rho_p}$$

a flow density ratio of the secondary to primary flow. Note that since the fluids are considered perfect gases,

$$\rho_s^* = \frac{T_p}{T_s} = \frac{1}{T^*}$$

$$\rho_t^* = \frac{\rho_t}{\rho_p}$$

a flow density ratio of the tertiary, or film cooling, flow to primary flow. Note that since the fluids are considered perfect gases,

$$\rho_t^* = \frac{T_p}{T_t} = \frac{1}{T_t^*}$$

$$A_s^* = \frac{A_s}{A_p}$$

a ratio of secondary flow area to primary flow area

$$A_t^* = \frac{A_t}{A_p}$$ a ratio of tertiary flow area to primary flow area

With these non-dimensional groupings, equations (3.14) and (3.15) can be rewritten in dimensionless form. Since both equations follow the same format, only the results for the secondary air plenum are presented here.

$$\frac{P^*}{T^*} = 2\,\frac{A_p}{A_m}\left(\left(K_p - \frac{A_p}{A_m}\beta\right) - W^*\left(K_p + T^*\right)\frac{A_p}{A_m}\beta\right.$$

$$\left. + W^{*2}T^*\left(\frac{1}{A^*}\left(K_p - \frac{A_m}{2A^*A_p}\right) - \frac{A_p}{A_m}\beta\right)\right)$$

(eqn 3.16)

where

$$\beta = K_m + \frac{f}{2}\,\frac{A_w}{A_m}$$

(eqn 3.17)

This may be rewritten as

$$\frac{P^*}{T^*} = C_1 + C_2 W^*(T+1) + C_3 W^{*2} T^*$$

(eqn 3.18)

where

$$C_1 = 2\frac{A_p}{A_m}(K_p - \frac{A_p}{A_m}\beta),$$

(eqn 3.19)

$$C_2 = -(\frac{A_p}{A_m})^2 \beta$$

(eqn 3.20)

$$C_3 = 2\frac{A_p}{A_m}(\frac{1}{A^*} - \frac{A_m}{2A^*A_p}\beta - \frac{A_p}{A_m}\beta).$$

(eqn 3.21)

As can be seen from equation (3.18)

$$P^* = \phi(W^*, T^*).$$

(eqn 3.22)

The additional dimensionless quantities listed below have been used in past research to correlate the static pressure distribution down the length of the mixing stack.

$$PMS^* = \frac{\frac{PMS}{\rho_s}}{\frac{U_p^2}{2g_c}}$$

a pressure coefficient which compares the pumping head (PMS/ρ_s) for the secondary flow to the driving head ($U_p^2/2g_c$) of the primary flow, where PMS = static pressure along the mixing stack length

$$\frac{X}{D}$$

ratio of the axial distance from the mixing stack entrance to the diameter of the mixing stack

D. EXPERIMENTAL CORRELATION

For the geometries and flow rates investigated, it was confirmed by Ellin [Ref. 2] and Moss [Ref. 1] that a satisfactory correlation of the variable P*, T* and W* takes the form

$$\frac{P^*}{T^*} = \phi(W^* T^{*n}) \qquad \text{(eqn 3.23)}$$

where the exponent "n" was determined to be equal to 0.44. The details of the determination of n = 0.44 as the correlating exponent for the geometric parameters of the gas eductor model being tested is given by Ellin. To obtain a

gas eductor model's pumping characteristic curve, the experimental data is correlated and analyzed by using equation (3.23), that is, P^*/T^* is plotted as a function of $W^*T^{*0.44}$. This correlation is used to predict the open-to-the-environment operating point for the gas eductor model. Variations in the model's geometry will change the pumping ability, which can be evaluated from the plot of equation (3.23). The value of parameter $W^*T^{*0.44}$ when $P^*/T^* = 0$ is referred to as the pumping coefficient.

IV. EXPERIMENTAL APPARATUS

The experimental facility used was originally constructed by Ross [Ref. 5] and later used by Welch [Ref. 6] and Hill [Ref. 8]. The gas generator was constructed from the combustor section and turbine nozzle box of a Boeing Model 502 gas turbine engine. Components of the engine's fuel system were modified by Ross and installed to support a simplified combustor layout. Only one of the original two combustor assemblies is used. Combustion air is provided by a three stage Carrier centrifugal air compressor located in building 230 adjacent to the test facility. The test facility is located in building 249 at the Naval Postgraduate School Annex. Appendix A gives complete instructions for the operation of the gas generator.

A. COMBUSTION AIR PATH

Combustion and cooling air pass from the compressor discharge via an underground pipe to building 249. Air enters the test facility through a vertical standpipe which contains an eight inch butterfly valve in parallel with a bypass globe valve (Figure 6). The butterfly valve is normally closed, flow through the bypass valve only being

sufficient to operate the gas generator. Figure (5) is the layout of the gas generator. At the top of the standpipe is a "T" connection. In one direction flow passes through an eight inch butterfly valve and enters a short section of piping which is used by other departments to supply various experiments. The second arm of the "T" supplies the combustion gas generator through an eight inch to four inch reducing section. The flow characteristics of this reducing section were determined by Welch and the pressure drop across this section is used to determine the air mass flow rate throught the gas generator assembly. A linear curve was fit to Welch's data for use in data reduction programs. The correlation is presented in Figure (49). Air flow next passes through a manual isolation valve and enters a splitter section which is shown in Figure (7).

In the splitter section, a portion of the air flow is directed through the motor operated burner air control valve and the U-tube to the combustor section. The flow characteristics of this section as determined by Ross are presented in Figure (50). The remaining air passes through the motor operated cooling air bypass valve and enters the mixing section. The mixing section was fabricated by Ross from the nozzle box of the Boeing engine. The turbine wheel was removed to permit the cooling air to enter parallel to the axis of the removed shaft. A device was installed in the nozzle box to introduce a swirl into the cooling air

which is counter to that produced by the nozzles. Hot gases from the combustion section enter the mixing section through the nozzles and the effect of the counter-rotating flows is to produce rapid and thorough mixing. Downstream of the mixing section is a flow straightener. This is followed by an uptake section which delivers the gas flow to the primary nozzles.

B. FUEL SYSTEM

1. System Arrangement

Service fuel is stored in a 55 gallon drum mounted on an elevated stand adjacent to the building. This arrangement is shown in Figure (22). Fuel flows from the storage tank through a tank isolation valve to a bulkhead isolation valve located just inside the building. A tank stripping and drain connection is located in the supply line just outside the building. Adjacent to the interior bulkhead valve is a thermocouple connection for measuring fuel temperature. Fuel then passes through the flow measuring rotameter to a fuel filter. Taking suction on the filter is a 24 vdc motor driven fuel supply pump. This positive displacement pump contains an internal bypass and pressure regulating feature. Normal pump discharge pressure is 14-16 PSIG.

The supply pump provides positive suction head for the high pressure pump. This pump, which was originally

shaft driven by the Boeing engine, was modified by Ross for use with a 115 vac electric motor. The attached Woodward governor was also removed by Ross and a blank housing installed. This pump has no internal bypass and must be provided with an external recirculation loop when in operation. Valves placed in the recirculation loop are used to control the pump discharge pressure and, thus, the flow of fuel to the burner nozzle. Downstream of the recirculation connection is a system drain valve and a manually operated discharge valve (Figure 25). From the discharge valve, fuel is piped to an electrically operated solenoid valve located at the entrance to the combustor.

2. Fuel System Modification and Verification

Early in the process of activating the hot flow test facility, the previously used Cox Vortex fuel mass flow meter failed. Since a replacement could not be obtained, a Fischer Porter Model 10A3565A rotameter was installed and calibrated. Calibration was performed in place, using the fuel supply pump to discharge fuel into a container for a fixed period of time. The quantity of fuel discharged was weighed on a gram scale and the mass determined. Flow rate was controlled using a needle valve at the pump outlet. Rotameter calibration data is given in Table (I). Figure (46) plots fuel mass flow against rotameter reading. A linear curve fit to the data results in the expression

$$WF = -3.076 + 0.4048 * ROTA$$

(eqn 4.1)

Hill [Ref. 8] had recommended that the system's fuel control valve be replaced with a needle valve to improve sensitivity and control. The existing arrangement used a ball valve mounted on the pump table as a fuel control valve. A long mechanical linkage extended across the building to the control station. Not only did this linkage seriously impede access around the gas generator, but as could easily be seen, this arrangement made difficult accurate adjustment of the fuel flow. Accordingly, 3/8 inch stainless steel tubing was used to extend the high pressure pump recirculation line to the control station. The ball valve was retained as the control valve and mounted on the bench at the control station. This valve permits the operator to rapidly select any desired operating pressure in a single motion.

To increase the sensitivity of the fuel control valve, a needle valve was installed in parallel with it close to the high pressure pump (Figure 25). This valve, which is always partially open, permits flow through the recirculation line even when the fuel control valve is fully closed. Thus, flow through the pump is assured even when

both the fuel control and the pump discharge valves are closed.

This needle valve, called the "trimmer", is used to establish the range of control for the fuel control valve. When properly adjusted this system provides smooth operation over a range of high pressure pump discharge pressures from 80 to 350 PSIG. Since the pump's maximum output pressure is specified to be 375 PSIG, control is obtained over most of the pump's useful range. Fuel pressure is easily adjusted to within 5 PSIG of a desired setpoint and with some care can accurately be varied in increments as small as 2 PSIG.

The first attempts to light off the gas generator were unsuccessful. It was noted that, when following the operating instructions provided by Hill, large quantities of liquid fuel were carried downstream and expelled at the primary nozzles almost immediately after the emergency fuel cutoff valve was opened. Lightoffs were attempted with a variety of high pressure pump discharge pressures and a number of different air flow settings, all to no avail. Refering to Hill's work [Ref. 8] it was found that he had noted that "Although desired Mach number can be achieved over a wide range of temperatures and pressures, the gas generator runs smoothly over a much narrower band." Further, he reports that during low temperature runs it was necessary to almost close a needle valve on the discharge of the high pressure pump. This valve is shown in system

drawings provided by both Welch and Hill, but no other reference to its setting or purpose is made by either writer. Since this valve was installed downstream of the high pressure pump gauge, it was reasoned initially that it should be fully open during operation in order that the pressure displayed accurately represent the pressures being experienced at the nozzle. However, from the evidence that the fuel mixture was far too rich, it was concluded that this valve must have been partially closed in previous operation. This supposition was confirmed in a personal conversation with Hill who recalled that the pump discharge valve was in fact nearly closed under all operating conditions. Thus, it is clear that the high pressure pump pressures reported in previous work do not accurately reflect the actual nozzle pressures obtained.

Further consideration led to the fact that fuel flows recorded by Welch and Hill ranged from approximately 4.0 to 6.0 gallons per hour (GPH). The burner nozzle supplied with the Boeing engine is rated at 9.5 GPH at 100 PSIG with an operating range of 30 to 375 PSIG. Fuel flows of four to six GPH raised further suspicion that the burner pressures previouly used were too low for proper atomization. This would account for the surging reported by Hill, the smoking reported by Hill and laboratory technicians familiar with the gas generator, and the difficulty experienced in obtaining combustion.

Accordingly, a number of burner nozzles of differing capacities were obtained. Three of the nozzles were tested using the system pumps and a spare combustor assembly rigged to discharge into a five gallon can. Tables (II), (III), and (IV) display the data obtained. The fuel mass flows were obtained by use of the rotameter readings and equation (4.1). Figure (47) compares the results for the original 9.5 GPH nozzle and for a 4.0 GPH and a 5.0 GPH nozzle. Considering the actual fuel mass flows reported by Hill of 0.008 to 0.011 lbm/sec it was concluded from the data presented in Figure (47) that the actual nozzle pressures obtained must have been below 50 PSIG in all cases and may have been as low as 6 PSIG during the 550° F data runs. It was determined visually that atomization did not occur in the 9.5 GPH nozzle at nozzle pressures of less than 37 PSIG and atomization was poor for nozzle pressures of less than 50 PSIG. On the basis of this information, the 5.0 GPH nozzle was installed in the test rig. Figure (48) displays the performance characteristics of this nozzle in greater detail.

Final modifications to the fuel system included moving the solenoid operated emergency fuel cutoff valve to a position immediately adjacent to the combustor and replacing the flexible hose which connected the high pressure pump to the combustor with 3/8 inch stainless steel tubing. Moving the cutoff valve eliminated a sizable volume

of pressurized fuel from being drained into the combustor after the unit was shut down. Replacing the hose with tubing reduced the pressure drop between the pump and the nozzle from 10 PSIG to 5 PSIG at maximum flow rates. A gauge was installed between the emergency fuel cutoff valve and the burner nozzle to provide an accurate indication of burner nozzle pressure.

The modified system has been found to be flexible and reliable. Combustion is easily and cleanly established within 6 to 12 seconds after the emergency fuel cutoff valve is opened. No raw fuel is expelled from the primary nozzles or the nozzle box drain under normal circumstances. The gas generator now runs smoke free over a wide range of uptake temperatures and Mach numbers.

Stable operation with uptake temperatures ranging from 400° F to more than 1200° F has been demonstrated, although routine operation at uptake temperatures exceeding 1000° F is not recommended. At an uptake temperature of 550° F, uptake Mach numbers of less than 0.060 to 0.261 have been demonstrated. At 950° F, Mach numbers ranging from 0.036 to 0.078 have been achieved. Higher Mach numbers are easily obtainable at intermediate and higher temperatures, but cannot currently be observed due to instrumentation limitations. Thus, the facility now has full capability to model the prototype eductor under all operating conditions and the flexibility to be used for investigations over a significantly wider range of uptake Mach numbers.

C. THE MEASUREMENT PLENUM

The gas generator uptake and the eductor model are enclosed in a plenum (Figure 2) which is used in the measurement of secondary flow. Appendix B presents the formulae used to determine the flow rates. Ten ASME long radius nozzles are installed in the sides and roof of the plenum allowing the flow entrance area to be varied accurately. Measurement of the pressure differential between the plenum interior and ambient and knowledge of ambient temperature permit calculation of the flow rate.

1. The Rear Seal

As designed by Ross, the plenum featured split aluminum seal plates at both the forward and rear ends. At the rear end, the seal plates bolted to the rear wall of the plenum and clamped around the stainless steel uptake pipe. Since the uptake experienced significant thermal expansion during operation, this seal was a potential source of leakage. In the past, various sealing compounds were applied, but due to the high temperatures involved, none was considered completely effective.

In order to improve the sealing of the plenum, and to minimize heat loss in the uptake, the fiberglass insulation and metal sheathing installed by Ross was removed and high-temperature pre-formed calcium silicate insulation was installed over the entire length of the uptake pipe. The uptake supports were first modified to carry the weight of

the pipe independent of the plenum rear seal and the joint to the turbine nozzle box. Figures (26) and (27) depict these supports. Next a layer of one inch thick fiberglass insulation was cemented to the pipe. In the area where the pipe passes through the plenum wall, the fiberglass insulation was replaced by calcium silicate tiles formed from the insulation and hand fitted and cemented to the pipe. This provided a firm base for the clamp attaching the diaphragm seal which was later installed. The split sections of preformed insulation were then fitted together over this base, sealed with refractory cement, and wrapped with a double layer of duct tape. The result was an airtight sheath around the uptake that develops maximum surface temperatures of less than 185° F when uptake temperature is 950° F. The highest surface temperature has been observed in a limited area around a coupling flange where the insulation thickness is reduced. Over the remainder of its length the uptake now has surface temperatures of less than 140° F.

With a cooler surface, it was possible to install a flexible seal at the rear wall. This diaphragm seal is formed from a rubberized fabric. The fabric was bedded in a layer of silicone sealant and clamped to the uptake with a band clamp. A similiar layer of sealant was applied to the plenum rear wall and the seal attached with a split clamping ring. Figure (28) is a view of the plenum interior showing the finished uptake and the diaphragm seal. A byproduct of this modification was increased uniformity in the uptake

gas temperature, with temperatures between the uptake mid-section and the primary nozzle now varying less than 2° F.

2. The Forward Seal

The original forward seal bolted to the front wall of the plenum and clamped around the exit end of the mixing stack. When only solid wall mixing stacks were being tested, as by Welch, this arrangement was probably satisfactory. However, when models involving shrouds and diffusers were introduced, the seal plate was enlarged to clamp to the outer diffuser ring. An effective seal to the diffuser could be produced, but there was no isolation between secondary and tertiary flows. During pumping coefficient measurement, the low pressures in the plenum caused backflow into the plenum through the film cooling clearances between the shroud and diffusers. This was observed and reported by Hill who then plugged the film cooling passages during measurements of pumping coefficients.

The cold flow test facility employs two seals at the forward end, one at the entrance plane of the mixing stack and the second at the mixing stack's exit. This arrangement permits independent determination of both secondary and tertiary flow rates. It was decided to more closely approximate cold flow test conditions by modifying the hot flow plenum to provide a seal at the entrance to the mixing stack. Thus, secondary flow rates are now measured in a

manner exactly analogous to the cold flow models. Measurement of tertiary flows in hot flow testing was not considered essential because correspondence of other measured parameters implies similarity in tertiary flows.

The forward sealing bulkhead was moved back within the plenum and new seal plates provided to clamp to the entrance section of the mixing stack. From mixing stack temperature data reported by Welch and Hill it was determined the the stack entrance section was relatively cool and that it would be possible to employ an o-ring seal at this point. Figures (29) and (38) show the mixing stack seal.

3. Model Installation and Alignment

An adjustable support stand was designed and constructed to support the mixing stack assembly independently of the seal plates. This stand facilitates model installation and alignment. Alignment is accomplished by mounting the model on the stand, installing centering plates in each end of the mixing stack and in the open uptake pipe, and adjusting the stand until the alignment bar passes freely through holes in the centering plates. The alignment apparatus can be seen in Figures (29) and (30). Standoff distance is then set by installing the straight primary nozzles on the uptake and measuring the required distance from the nozzle exit plane to the mixing stack entrance plane (the termination of the entrance radius) using a combination square.

During preliminary operation of the gas generator significant longitudinal expansion of the uptake was observed. The calculated expansion due to a temperature increase from 60° F to 950° F was 0.387 inches and the observed expansion was 0.3125 inches. This amount was considered appreciable when compared to the nominal 3.561 inch standoff distance. Accordingly, the installed standoff distance was increased by 0.1265 inches to 3.6875 inches to compensate for this effect.

D. INSTRUMENTATION

1. Temperature Measurement

Two types of thermocouple displays are installed, each has the capability to accept 18 input channels. A type K display provides data on combustion temperatures, uptake temperatures and mixing stack wall temperatures. Table (V) gives the current channel assignments. The Type T display is used to measure inlet air, ambient air, fuel, and shroud and diffuser surface temperatures. Table (VI) gives the current channel assignments. The display installation is shown in Figure (8).

2. Pressure Measurement

Five manometers, shown in Figure (10), are installed for gas generator operation and data collection. They include a 20 inch water manometer for measurement of differential pressure across the inlet reducing section (DELPN),

an oil manometer (range 0-17 inches H_2O) for measuring uptake pressure (PUPT), a 20 inch mercury manometer for measuring inlet air pressure (PNH), a 2 inch inclined water manometer currently used to measure the differential pressure across the burner U-tube (DELPU), and a 6 inch inclined water manometer connected to a distribution manifold. Five individual manfolds located in the main control panel (Figure 9) are interconnected to permit measurement of plenum and mixing stack pressures with respect to atmospheric pressure. Mixing stack pressures both above and below atmospheric can be displayed. Also installed is a laboratory mercury barometer.

E. THE MODELS

Two eductor models were tested. Each model consists of a primary nozzle plate mounted on the end of the uptake and a mixing stack assembly. The mixing stack assemblies include the mixing stack, a film cooling shroud and an exit diffuser. Characteristic eductor dimensions are given in Figure (3). In both models tested the mixing stack interior diameter, "D", was 7.122 inches. This dimension was the same as used in previous hot flow testing and is 0.6078 scale of the cold flow models. Both models tested employed a standoff ratio, "S/D", of 0.5. Table (VII) provides a comparison of key model characteristics.

1. Model A

Model A, which was previously tested by Hill, is shown in the current installation in Figure (31). This configuration includes a primary nozzle plate with four straight nozzles. The ratio of mixing stack area to primary area is 2.5. The mixing stack L/D is 1.75 and the stack contains six rows of film cooling slots as shown in Figure (32). When tested by Hill this mixing stack had a field of 12 thermocouples installed for wall temperature measurement. These thermocouples were removed prior to the present tests. This mixing stack has not been instrumented for pressure measurement.

The mixing stack is enclosed in an aluminum shroud extending from X/D = 0.25 to X/D = 2.0. Two aluminum diffuser rings 0.375 diameters wide are installed to bring the overall length of the assembly to 2.5 diameters. Film cooling clearance between the stack and the shroud and the shroud and diffuser rings is 0.1875 inches. The dimensions of this model are shown in Figure (33). Two rows of thermocouples were installed along the length of the shroud and diffuser by Hill. Not all of these thermocouples remain operational, however, enough were available to provide adequate comparison in the data taken.

2. Model B

The second model tested, shown in Figure (34), was geometrically similar to a cold flow model tested by

Drucker. This model's primary nozzle plate as contained four nozzles which were tilted and angled in the 15/20 configuration recommended by Davis and used by Drucker. The Model B nozzle plate is seen in Figure (43) Figures (39) and (43) compare the straight and tilted-angled nozzle plates. The mixing stack area to primary nozzle area ratio of 2.5 was retained in the second model. Both sets of nozzles are mounted in identical plates with dimensions shown in Figure (41).

The mixing stack for Model B is 1.0 diameters long and contains four rows of film cooling ports. For convenience in manufacture, the dimensions of the film cooling ports were changed slightly from that required by the scale factor. Due to the necessity to increase the port width, the length was decreased proportionately so that the ratio of total port area to mixing stack cross-sectional area has been maintained constant at 0.141. This mixing stack is seen in Figure (37). Eight pressure taps in locations identical to those used by Drucker are installed in the wall of the mixing stack. Twelve type K thermocouples are located in an array 180° from the pressure taps. Thermocouple locations were chosen to provide data comparable with Hill's for the 2.5 L/D stack and also to determine the cooling effect of the the stack ports. Unfortunately, a failed thermocouple at one of the two port locations chosen seriously reduced the information which could be obtained regarding port effects.

The shroud and diffuser rings for this model were made from 25 gauge cold rolled sheet steel. The arrangement in shown in Figure (36). The film cooling clearance is this model was reduced to 0.075 inches to be consistent with the geometry used by Drucker. Only a single row of type T thermocouples was installed along the length of the shroud and diffuser. Thermal imagery was used to verify that the thermocouples installed were providing data representative of the entire shroud/diffuser surface.

V. THERMAL IMAGERY

One of the difficulties involved in characterizing the effects of the highly turbulent flows in the eductor system is the lack of certainty that the locations selected for measurement are indeed representative of the general flow or surface conditions. Some advantage can be obtained from flow symmetries, but rarely can it be stated with complete confidence that the coverage is adequate. The importance of addressing this aspect of the test program was increased when Drucker reported areas in which, potentially, the flow along the diffusers was stagnating. There was no accurate reference by which the locations of the areas could be determined with certainty. Yet, identification of such areas is a primary reason for conducting hot flow testing.

Temperature measurement by thermocouples suffers from two drawbacks. First, the thermocouple is a point device; it measures the temperature only at the point of the thermocouple junction. Second, the thermocouple wiring can produce both local disturbance in the flow field and a localized "fin cooling" of the surface. Both effects, if significant, would seriously impair the accuracy of the data collected in this research. In order to obtain data representing the entire surface temperature using a non-intrusive

device, thermal imagery was employed. This technique provided a photographic representation of the mixing stack, shroud, and diffuser surfaces from which temperature contours could easily be determined.

A. THE IMAGING EQUIPMENT

Infra-red photography cannot be used for this purpose because emulsions cannot be produced which are sensitive to radiation with a wavelength longer than 1.2 microns. Visible light has a wavelength of 0.4-0.8 microns. Conventional infra-red films are sensitive in the range 0.7-0.9 microns and in normal use the images recorded register only energy emitted by sources at temperatures above about 480° F, or the reflection of such energy by other bodies. The energy emitted by bodies at temperatures about 100° F is concentrated at a wavelength of 5 to 10 microns. Almost no energy is emitted in the range below 2 microns at this temperature. Figure (90) contains the curves for blackbody emission from various objects. The cross hatched area in this figure, from 2 to 5.6 microns, is the range of sensitivity for the thermal sensing camera used in this research. This equipment, an AGA Model 750, can resolve temperature differences as small as 0.4° F and is sensitive in the range from -4° F to 1650° F.

The AGA-750 system, shown in Figure (89), consists of an IR camera unit, a display unit with Polaroid camera

attachment, and a system power supply. The camera uses a liquid nitrogen cooled Indium antimonide detector and is provided with two lenses, one with a 20° x 20° field of vision, the other with a 7° x 7° field. The 20° x 20° lens was used in this research.

The display unit houses the system controls and the 2 x 1.75 inch black and white picture display. The display may be set to register warmer areas as either lighter or darker tones. The lighter-warmer/darker-cooler mode was used to produce Figures (91) and (92). It is also possible to highlight all areas within a given temperature band, producing an isothermal contour. The isotherm may be superimposed on the gray tone representation of the object, as in Figures (91) and (92), or the gray tones may be fully suppressed.

In the figures presented, the mixing stack assembly is shown horizontal with the gas flow from left to right. At the extreme left is the plenum forward sealing bulkhead. The warm exposed portion of the mixing stack prior to the shroud is seen extending from the bulkhead. The dark vertical bar over part of this area is the cooler support stand which obscures the mixing stack in this area. To the right of the exposed mixing stack is the cooler shroud surface which gradually grows warmer and hence becomes lighter along its length. Next is seen the two diffuser rings, again, cooler at the left (or inlet) side and growing warmer (lighter) toward the right. It is often difficult to

discern the transition from the first ring to the second due to the the fact the surface temperatures are nearly equal at that point. At the far right the hot gas flow leaving the eductor is clearly seen as a bright band.

B. ISOTHERM TEMPERATURE ESTIMATION

Several techniques are available for determining the temperatures represented in the isotherm display. At the top of the image the temperature range setting of the camera is shown in °C. The display unit can be set for any of 9 ranges from 2° C to 1000° C. The base temperature in the image is separately adjusted with a "level" control. On the left hand side of the display is a scale, each graduation representing 10 per cent of the total range in use. The width of the marker is adjustable and represents the range of temperature highlighted by a given isotherm. In this work a marker one unit, or 10 per cent, wide was used. Thus the temperature band covered by the isotherms shown in Figures (91) and (92) is 10 per cent of the display range or 5 for the Model A images and 50 for the Model B images. These bands do not translate directly into temperature, but must be adjusted based on the temperature level setting and the emissivity of the surface.

The system operating manual [Ref. 13] provides calibration curves and formulae for determining the actual temperature leavels represented by the isotherm markers.

The calibration must be corrected for the emissivity of the emitting surface and may be subject to false indications due to measurement of reflected solar energy. In order to provide a uniform surface emissivity and to reduce the possiblity of unwanted solar reflection, the models and the enclosure were sprayed with flat black paint. In this work, a surface emissivity of 0.92 has been assumed. Since direct temperature measurements of the surface are available, it is possible to calculate the actual emissivity. Such a technique is recommended in the future. Accurate knowledge of the emissivity will improve the quantitative value of the data obtained.

VI. EXPERIMENTAL RESULTS

Modifications to the gas generator and measurement plenums having been completed, data was taken on the performance of the two eductor models described above. The purpose of re-testing Model A was to validate data acquisition procedures and to ensure continuity with the results of previous researchers. Model B was the model of interest; the purpose of the hot flow testing being to confirm the results determined in cold flow testing.

A. MODEL A RESULTS

1. Pumping Performance

Figures (51) through (55) display the results of pumping coefficient measurements for Model A, Tables (VIII) through (XII). In each case except the first and last, the data is compared with that taken by Hill [Ref. 8] on the same model. Hill did not take low temperature data on this model, but does present such data for a solid walled mixing stack 2.5 diameters long. Hill's data for that configuration is compared to the data for Model A from the present research in Figure (51). Here, the strong correlation in pumping coefficient data that was obtained in all tests throughout the current research is seen. As expected from

previous cold flow work, the secondary pumping performance of the ported stack is seen to be somewhat better than the solid stack of identical length. The ported stack also induces additional tertiary flow which is not measured in this work, but which provides a further source of cooling flow.

Due to time constraints, the data taken by Hill at an uptake temperature of 550° F was not duplicated. Tests run at nominal uptake temperatures of 650° F, 750° F, and 850° F again show strong correlation in the present data, but an initial comparison with the results presented by Hill on the same model does not appear particulary favorable. At low flow rates P*/T* in Hill's data is consistently below the current results and, conversely, higher secondary flow rates were obtained by Hill as the vacuum in the plenum, and consequently P*/T*, was reduced. It is felt that both of these factors can adequately be accounted for by considering the differences in the way the models were installed for the two tests.

In Hill's testing, the mixing stack seal was at the exit end of the diffuser and the tertiary film cooling passages opened into the measurement plenum. Thus, his measured flow rate represents both secondary and tertiary flow. However, when flow into the plenum was restricted by closing the measurement nozzles, the resulting vacuum caused reverse flow through the film cooling passages into the

plenum, reducing the measured vacuum and causing the value of P*/T* obtained to be reduced. Such backflow was, in fact, observed and reported by Hill.

As the plenum vacuum was decreased by opening additional measurement nozzles, the pressure depression within the mixing stack again had effect and tertiary flow was reestablished; the total flow then measured exceeded secondary pumping capability alone. This hypothesis is supported by the results obtain by Drucker [Ref. 12], which give pumping coefficients for secondary flow on a similar but shorter stack of about 0.6 and total pumping coefficients (secondary plus tertiary flow) in the vicinity of 0.72. Considered in this light, the current results compare quite favorably with those obtained by Hill.

Figure (55) presents data taken at a uptake temperature of 955° F. This data corresponds well with that obtained at lower temperatures. Because of the interest in cooling of high temperature flows it was felt that extension of the data collection effort to this temperature level was warranted. Improvements in the gas generator range of operation previously discussed made collection of data at this, and higher, uptake temperatures possible.

The pumping coefficient results for all data runs in this series are presented in Figure (56) for comparison. The data is consistent and well grouped. The clear temperature dependence of pumping coefficient on temperature

observed in Welch's and Hill's data is not apparent here. This temperature dependence may have, in fact, been the result of a temperature dependent leak in the measurement plenum as postulated by Welch. Such a leak might well have been eliminated by the modifications to the plenum sealing system which have been performed.

2. Shroud and Diffuser Temperatures

Although Hill measured mixing stack wall as well as shroud and diffuser surface temperatures, the thermocouples have since been removed from the mixing stack. Because the intent here was to validate current procedures by comparison with previous data it was not considered essential to reinstall these sensors or duplicate all data taken before. The data taken on the external surface temperatures of the shroud and diffusers is presented in Table (XIII) Figures (57) through (60). Here, comparative data is available for nominal uptake temperatures of 650° F, 750° F, and 850° F plus an extension of the data base to 950° F. Low uptake temperature (i.e. inlet air temperature, about 175° F) data is not presented for these parameters because similar data was not available for comparison in Hill's work. In any event, the purpose of low temperature testing at the hot flow test facility is mainly to provide assurance of similarity with the cold flow facility results.

Hill obtained shroud and diffuser temperature measurement at two circumferential locations for most axial

positions. In this work, data was collected at only one location for each axial position. In each case the data is compared to the higher of the two temperatures recorded by Hill. No data was obtained at the X/D=1.75 position on the mixing stack due to failure of the thermocouple located there.

The comparison in results is quite favorable throughout. If the differences in ambient temperatures during data collection are taken into account, it is seen that the results are almost identical. The areas of highest temperature lie on the shroud before the start of the diffuser, and at the termination of the second diffuser ring. Maximum temperatures of 120° F, or about 60° F above ambient were recorded.

3. Exit Plane Temperatures

As with the other measures of performance presented, the exit plane temperature profile data obtained corresponds well with that of Hill. Figures (61), (63), and (65) present the raw data obtained. This data is tabulated in Table (XIV) In order to facilitate comparison of exit plane temperature data from a variety of mixing stack/diffuser configurations, it was decided to plot the data obtained in terms of a non-dimensional position factor, r/Rms, which is the ratio of the measurement point's radial distance from the center axis of the mixing stack to the interior radius of the mixing stack itself.

Figures (61) and (63) reveal highly acceptable correlation with the data obtain by Hill. There is a slight asymmetry in the profile which is probably due to a misalignment of the mixing stack. It is also possible that a small positional error has been introduced by the traversing mechanism. This device, shown in Figure (45), was originally constructed for use with the solid walled stacks and does not have sufficient range of motion to traverse the entire diffuser opening. It has, therefore, been necessary to take measurements from one edge to the center and then reposition the support stand and measure in from the opposite side. Modification of this device is recommended prior to any future research in the hot flow facility.

To further facilitate the comparison of data, the exit plane temperatures were referenced to the ambient temperature and normalized with respect to the uptake temperature reference to ambient. The value of this technique will become evident in later comparisons with Model B's data. The non-dimensional exit plane temperature coefficients for Model A are presented in Figures (62), (64), and (66). A comparison of these coefficients for all three nominal uptake temperatures is given in Figure (67). No explanation is immediately apparent for the difference observed in the curve for the 850° F uptake temperature. However, even with this variation, the data is considered to be very consistent.

In general, a 40 per cent reduction in maximum plume temperature can be said to have been achieved by this model. Further, the average plume temperature, by inspection, seems to be reduced about 55 to 60 per cent below the uptake temperature. Since the actual reduction in maximum plume temperature below the uptake temperature is, in all cases, more than 300° F, the performance of this model is considered to be quite good.

B. MODEL B RESULTS

Due to certain time constraints, only a limited number of data runs could be made on the second model. Therefore, in order to ensure both the validity of the testing and to obtain the most significant data, uptake temperatures were selected that would confirm the similarity with the cold flow model, allow direct comparison with previous hot flow work, and extend the range of the data base to the highest uptake temperature of interest.

1. Pumping Performance

The low temperature pumping coefficient performance of Model B is shown in Figure (68). Pumping coefficient data is tabulated in Tables (XV) through (XVII). The correspondence with the cold flow facility data obtained by Drucker [Ref. 12] on a geometrically similar model is reasonably good. A slight increase in performance over that obtained with Model A is also noted and was expected from a

comparison of the cold flow work of Drucker and Davis [Ref. 11]. Surprisingly, Figures (69) and (70) indicate a substantial increase in secondary pumping capability with the higher primary temperatures. At 950° F the secondary pumping coefficient approaches the total (secondary plus tertiary) pumping coefficient obtained in the cold flow facility. Although tertiary pumping was not measured here, data on shroud and diffuser temperatures presented later indicate that strong tertiary pumping is also present in this model. Since previous work has established that the pumping performance of the eductor generally declines as the length of the mixing stack in reduced, the enhancement in performance obtained by use of the tilted-angled nozzles in this shorter mixing stack assembly is seen to be significant. A comparison of the pumping coefficient performance of Model B at all temperatures tested is found in Figure (71).

2. Mixing Stack Temperatures

This model is equipped with a field of 12 type K thermocouples for measurement of mixing stack wall temperatures. The axial position of these thermocouples and the data obtained is given in Table (XIX). Due to a recording error, data for the two internal thermocouples located at the entrance of the mixing stack is not available. Four thermocouples were installed in pairs on the external surface to record the effects of one cooling port in the

first row and one in the last row. Data from the port in the first row indicates that film cooling air entering the mixing stack through the cooling ports reduces the external wall temperature immediately downstream of the port by approximately 35° F. Interestly, the external wall temperature just upstream of the cooling port is significantly (20-30° F) higher than the temperature of the wall between cooling ports at the same axial position. The results from the thermocouple pattern in the fourth row are more difficult to interpret, particularly since the thermocouple immediately upstream of the cooling port was providing clearly inaccurate results.

Figure (72) compares the mixing stack temperature data for the six thermocouples located between cooling ports with data obtained by Hill for Model A. It may be inferred from this limited data, that one effect of the tilted-angled nozzles in Model B is to mix the primary and secondary streams more rapidly, thereby increasing the temperatures of the mixing stack surface at any given axial position. The mixing stack temperatures for the locations between ports for all three uptake temperatures is found in Figure (73). The data is consistent, with maximum temperature of about 300° F being obtained in the 950° F uptake temperature run.

3. Mixing Stack Pressures

The data obtained for mixing stack pressures is presented in Figures (74) through (78) and in Table (XVIII).

Previous workers have presented mixing stack pressure data in a non-dimensionalized form, PMS*, which is a ratio of the pumping head available for tertiary flow to the driving head available from primary flow. It was noted when reducing this data, that PMS* is particularly sensitive to variation in the velocity of the primary jet. Since to maintain Mach number similarity, primary jet velocity must vary with the square root of the uptake temperature, and since PMS* varies with the square of the primary jet velocity, PMS* is directly dependent upon uptake temperature. This temperature dependence was not immediately apparent in cold flow results because the uptake temperature at that facility is fairly constant. Substantially reduced values of PMS* obtained in hot flow testing by Welch [Ref. 6] were largely unaccounted for. It was noted, however, that although the non-dimensionalized parameter varied widely, the actual values of the pressure depression with the various mixing stacks were reasonably constant or at least in the same order of magnitude. Because it is this pressure differential, in any event, which is the driving potential for induction of tertiary flow and because, in this case, the conditions obtained in the model directly represent the conditions expected in the prototype, the data plotted here is that actual data obtained. Values of PMS* were calculated and are tabulated in each table for reference.

Good correspondence between this data and the data taken by Drucker in cold flow testing is seen. In each case the value obtained from the position "A" tap at the 0.5 X/D axial position is substantially higher than all other data. It is suspected that this sensing line has a small leak, although a search was made for such a leak, and none was found. Figure (75) also displays two data points taken by Welch in hot flow testing of a solid walled mixing stack. Here the pressure depression obtained is less than in the ported stack for the same axial position. This is consistent with a comparision of the data obtained by Davis (solid walled stack) and Drucker (ported stack). The comparison of mixing stack pressures by position for the range of temperatures tested shown in Figures (77) and (78) does not reveal any significant effect of temperature.

It is noted that due to the small size of the pressure tap and the extremely long run of tubing (over 20 ft.) to the manometer, a substantial period of time was required for the manometer reading to reach its final value. Few oscillations were noted in these pressures and once a final value was reached it was found to be stable and repeatable. With the exception of the one point already noted, confidence in the values obtained is high. However, data taking would be greatly facilitated if the manometer installation were modified to place a manometer for measuring mixing stack pressures closer to the plenum.

4. Shroud and Diffuser Temperatures

The data obtained on shroud and diffuser temperatures may be found in Table (XX) and is presented in Figures (79) through (81). In each figure the film cooling effect can clearly be seen in the reduction of temperature at the last data point on the shroud. However, the temperatures achieved, both on the shroud and the second diffuser were substantially higher than the values obtained for Model A seen in Figures (59) and (60). This is felt to be the result of the more rapid and thorough mixing in Model B and the construction of this model which leaves a relatively long section of the shroud beyond the end of the mixing stack unshielded by the diffuser rings. In this area the performance of Model B is clearly inferior. The maximum exposed surface temperature in Model B being more than 80° F higher than in Model A. Extension of the first diffuser ring back to a point before the end of the mixing stack and addition of a third ring outside the second ring, but not extending beyond it, might improve the perforamance of this assembly.

5. Exit Plane Temperatures

Figures (82) through (88) display the exit plane temperature data found in Table (XXI). Here, again, both raw data and temperature coefficients are presented. Additionally, Figure (83) includes a non-dimensionalized velocity traverse taken from data presented by Drucker. The

non-dimensionalized velocity has been formed from the ratio of the exit plane velocity divided by the primary jet velocity. It is interesting to note in this figure that reductions in velocities and temperatures are very similar. This lends credence to the assumption that the diffusion of momentum and energy are similar under these flow conditions. This assumption underlies the rationale that permits use of the cold flow facility to characterize the high temperature performance of these eductor systems.

In the 850° F and 950° F runs it is seen that both the actual temperatures and the temperature coefficients are substantially reduced in this model. For an uptake temperature of 950° F the actual reduction is more than 380° F. Compared to Model A, Model B provides a maximum plume temperature which is 70° F cooler, reducing by an additional 14 percent the level of the maximum plume temperature compared to the ambient.

C. THERMAL IMAGERY

The results of thermal imagery of Model A at an uptake temperature of 950° F is seen in Figure (91). Athought difficult to discern in these reproductions of Polariod photographs, the temperature distribution of the mixing stack, shroud and diffuser surfaces is clearly evident in the display. The isotherms shown in this series confirm that the temperatures recorded by the thermocouples are

representative of the general surface condition. As expected from the thermocouple data, the hottest area of the shroud is found to be just before the beginning of the first diffuser ring. There is an area of similar temperature at the trailing edge of the second diffuser ring. Also noted is that the exposed portion of the mixing stack prior to the start of the shroud is at a temperature comparable with the hottest sections of the shroud and diffuser. The sensitivity of the equipment is evident in the third and fourth frames, where a hot spot created by a standoff between the shroud and the mixing stack is visible on the shroud surface just to the left of the warmer section.

Similar results are seen for Model B in Figure (92). Here the broader hot section in the shroud is clearly shown. There is also seen a definite curved pattern to the temperature contours on both the shroud and the diffuser. While some of the cooling indicated in the center of the view may be the result of fin cooling by the thermocouple field located there, similar cooler areas at the top and bottom of this view support the conclusion that the tertiary flow may, in fact, be stagnating as postulated by Drucker. The apparatus has been constructed in such way that the primary nozzle orientation may be rotated by 45 degrees in order to determine if such higher temperature zones are attributable to the action of the primary flow. Such an investigation should be conducted as the next step in the research program.

VII. CONCLUSIONS

Based on the data obtained and presented, the following conclusions are drawn:

1) The operational range and flexibility of the gas generator has been significantly improved. The facility is now fully capable of modeling a wide range of prototype uptake conditions.

2) The data obtained in testing the model designated Model A is found to be consistent with previous results for the same model.

3) Pumping coefficient data obtained in cold flow testing is representative of the performance of a similar system at actual operating temperatures.

4) Measurement of the exit plane velocity profile in cold flow testing does approximation provide a general approximation of the temperature profile for hot flow conditions.

5) The 15/20 tilted-angled primary nozzle geometry does provide superior pumping performance and a more uniformly mixed exit flow when combined with the short, slotted mixing stack.

6) The shroud and diffuser combination employed in Model B does permit the induction of substantial amounts of film cooling flow, however the geometry employed does not provide adequate shielding or make the most efficient use of film cooling potential. The surface temperatures for this assembly are substantially higher than those found in Model A.

VIII. RECOMMENDATIONS

Considering the experience gained in this research and in view of the results obtained, recommendations are offered both to improve further the research facility and to continue the current investigations.

A. IMPROVEMENTS TO THE TEST FACILITY

The following recommendations are made to make the operation of the gas generator more convenient or more reliable and to improve the speed and accuracy of data collection.

1) Replace the manual inlet air bypass globe valve with a valve which can be remotely operated from the control station. The current installation requires the operator to make numerous trips back and forth when setting test conditions, or to obtain the assistance of a second person.

2) Obtain a 12 inch oil manometer to display the pressure drop across the burner U-tube and mount it on the gauge board with the burner nozzle pressure gauge. This measurement is essential in lighting off the gas generator and can be used to monitor burner air fuel ratios during operation.

3) Relocate the 2 inch inclined water manometer currently used for measurement of the pressure drop across the burner U-tube to the side of the measurement plenum. Provide a new valve manifold and use this instrument to measure mixing stack pressures.

4) Redesign the traversing mechanism for exit plane temperature measurements with sufficient range to be used with any potential diffuser design.

B. RESEARCH RECOMMENDATIONS

Maintaining in mind the overall goal of this research program, the work should continue in the hot flow facility to confirm the present results, to define problem areas in the design and suggest promising avenues for further cold flow testing.

1) Realign Model B in the current installation and record a complete set of data to verify these results. Data should be taken at two or three additional intermediate uptake temperatures to completely characterize the model's performance.

2) Take duplicate temperature data, including thermal imagery, on Model B with the primary nozzle plate rotated 45 degrees.

3) Continue and expand the use of thermal imagery in order to characterize the surface temperature field.

4) Using the mixing stack from Model B, install a redesigned shroud and diffuser assembly. In this assembly the first diffuser ring should begin before the end of the mixing stack.

5) A smoke source which could be placed near the entrances to the film cooling clearances might be helpful in obtaining a qualitative appreciation for the strength of flow pattern being induced.

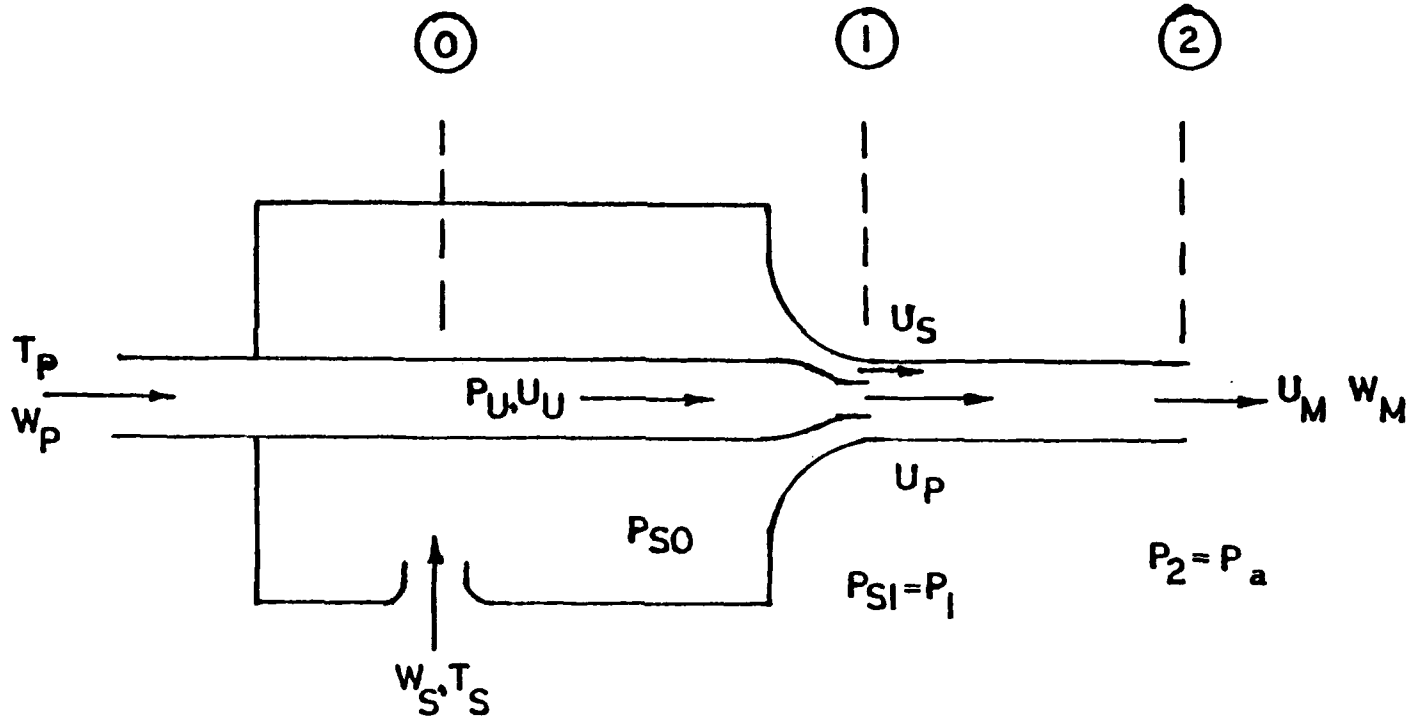

Figure 1, One Dimensional Eductor Model

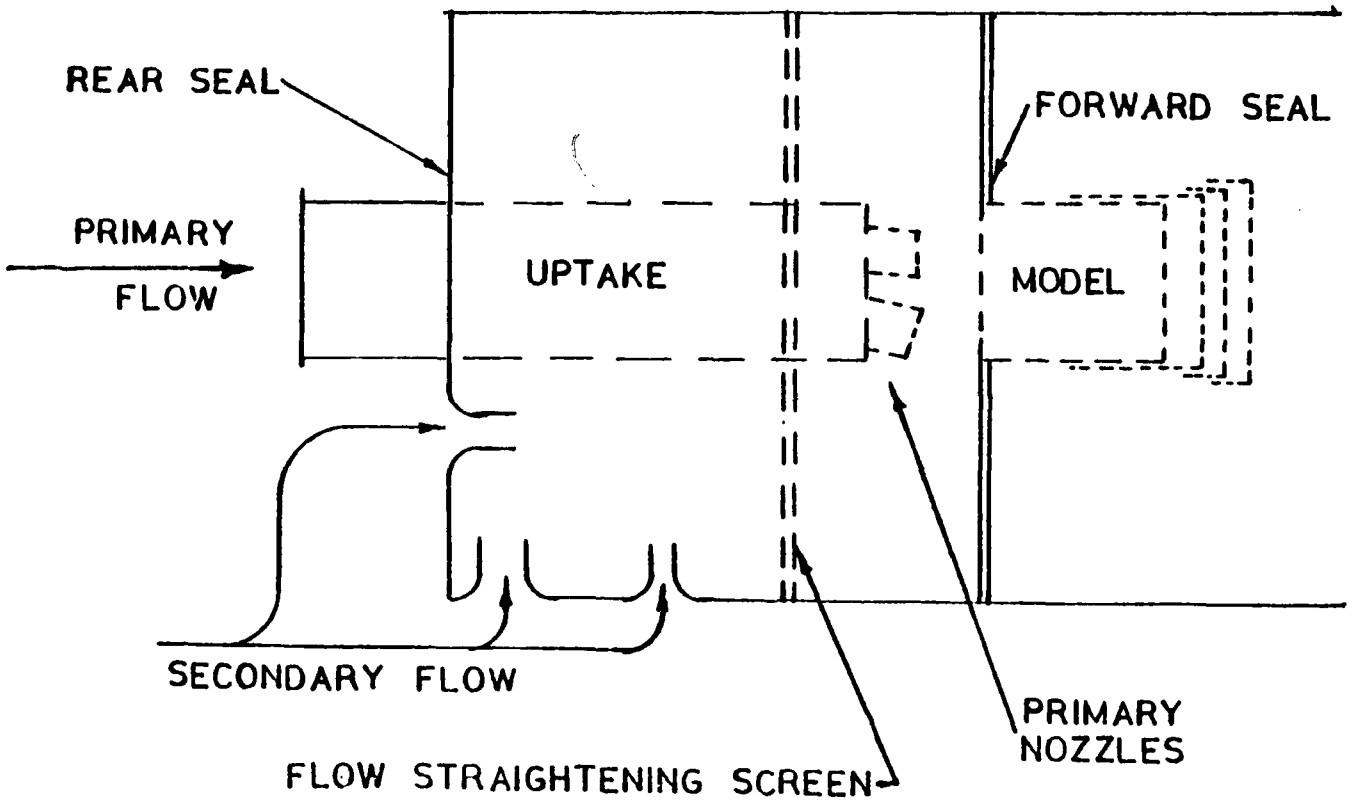

Figure 2, Plan of Uptake, Model, and Measurement Plenum

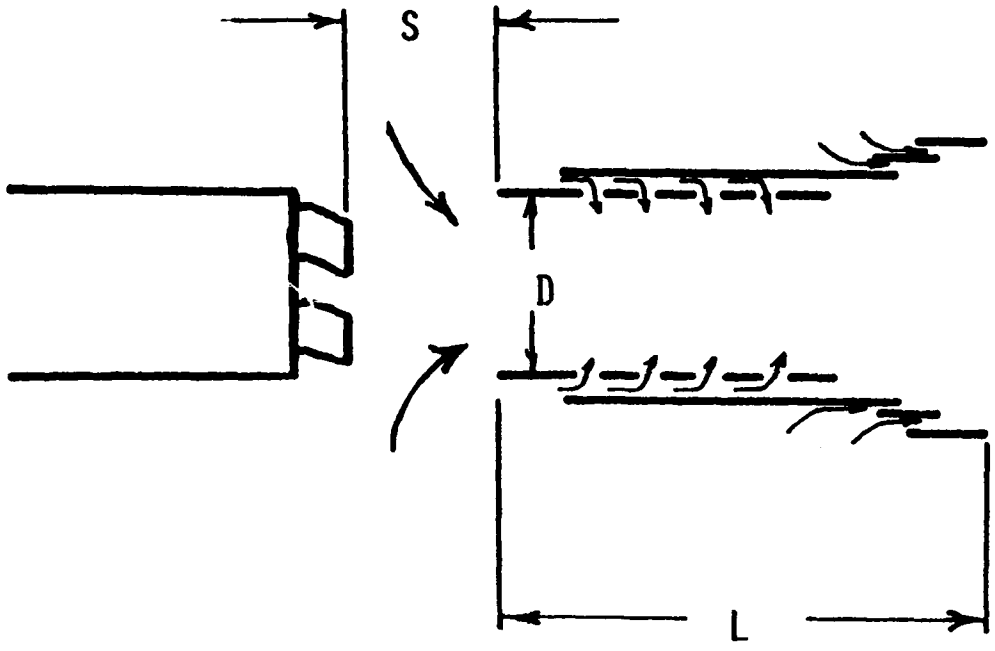

Figure 3, Characteristic Eductor Dimensions

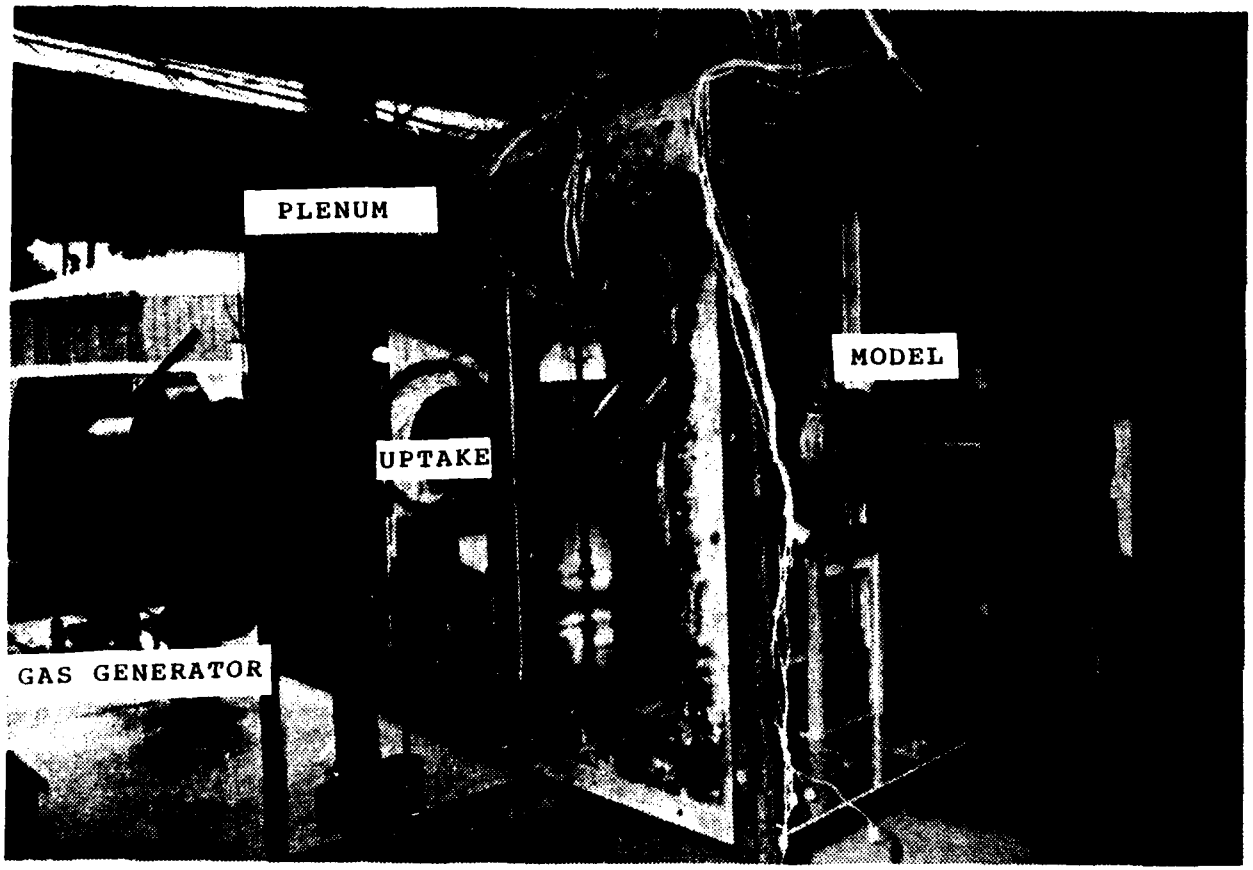

Figure 4, Hot Flow Test Facility

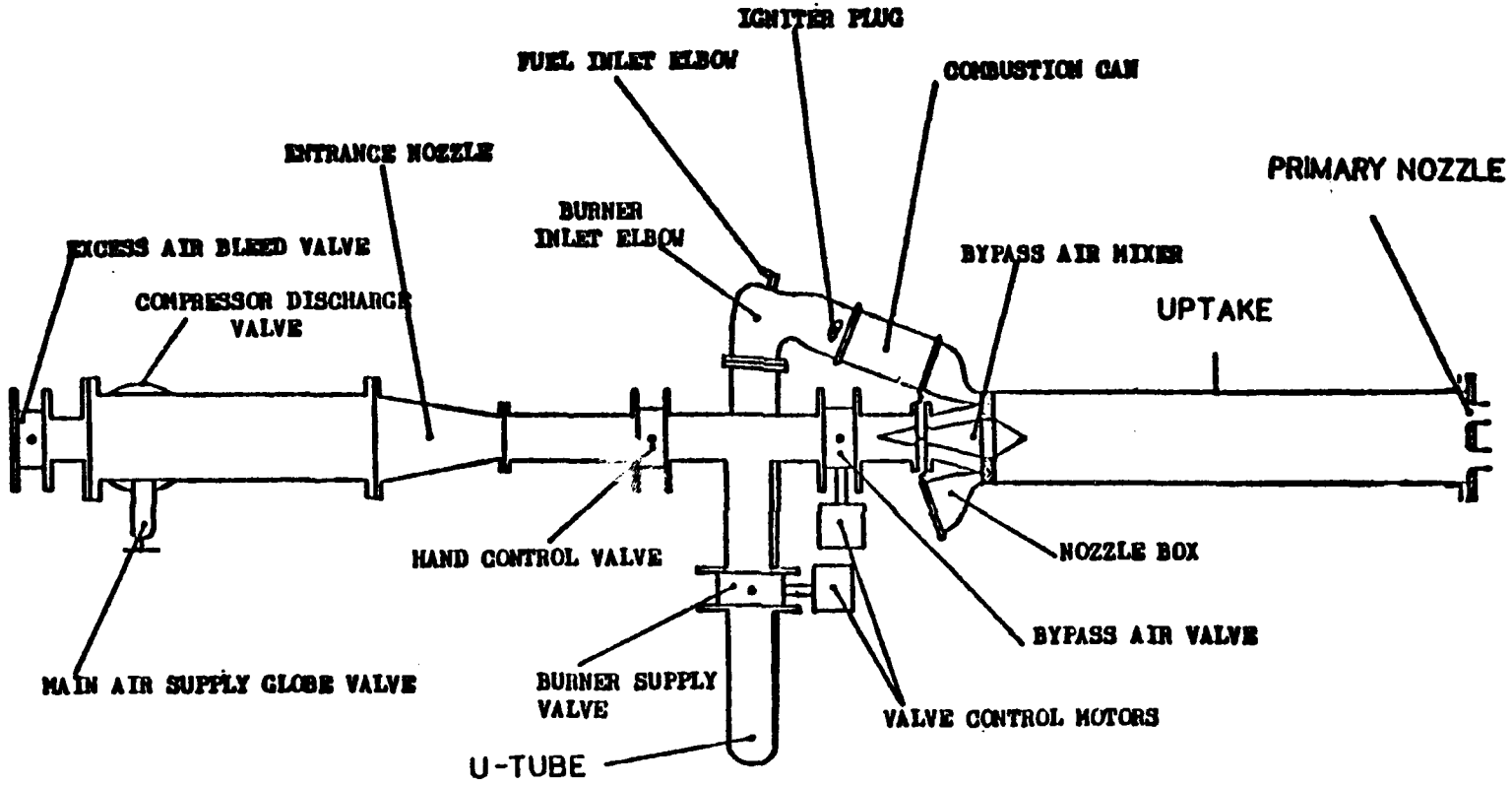

Figure 5, Gas Generator Arrangement

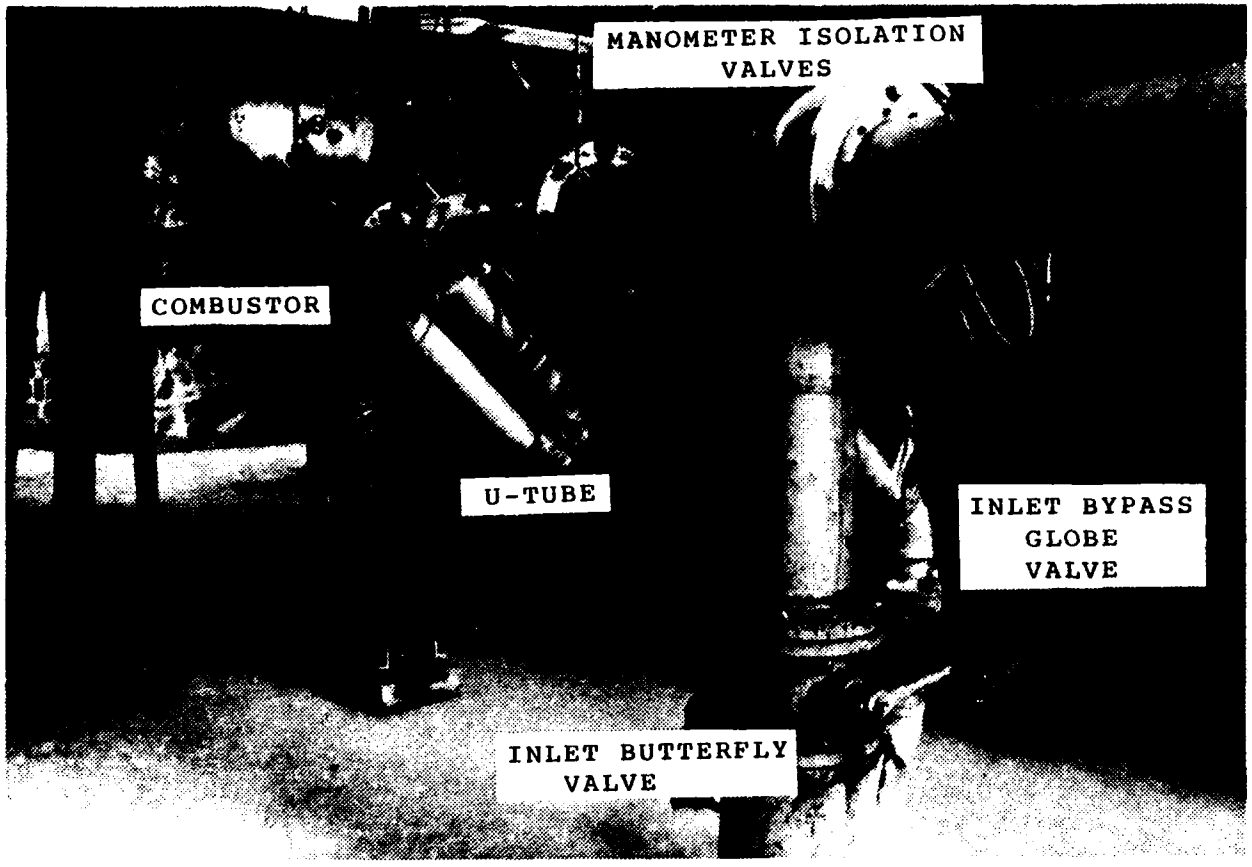

Figure 6, Air Supply Standpipe and Valving

AD-A123 776 TESTING OF A SHROUDED SHORT MIXING STACK GAS EDUCTOR MODEL USING HIGH TEMPERATURE PRIMARY FLOW(U) NAVAL POSTGRADUATE SCHOOL MONTEREY CA I J EICK OCT 82 2/3

UNCLASSIFIED F/G 21/2 NL

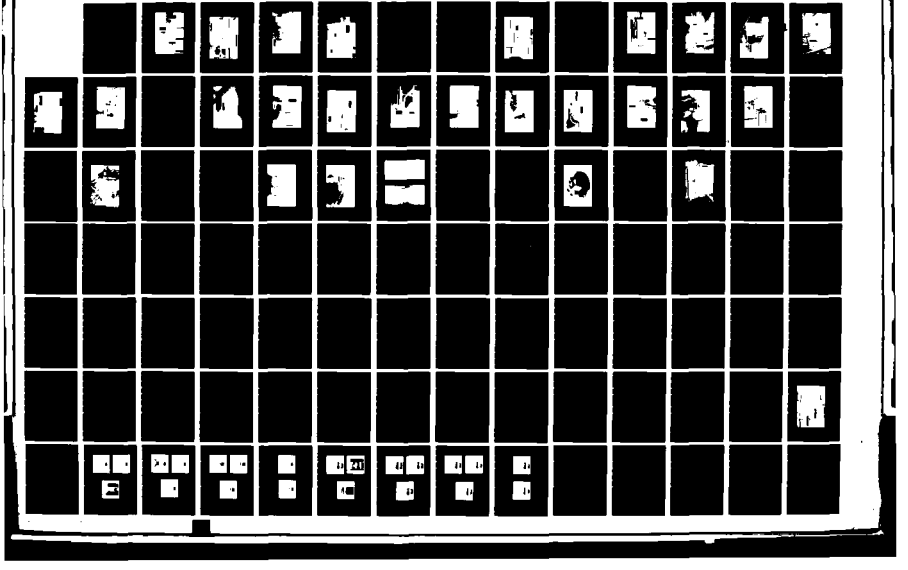

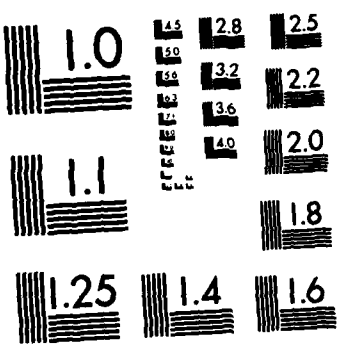

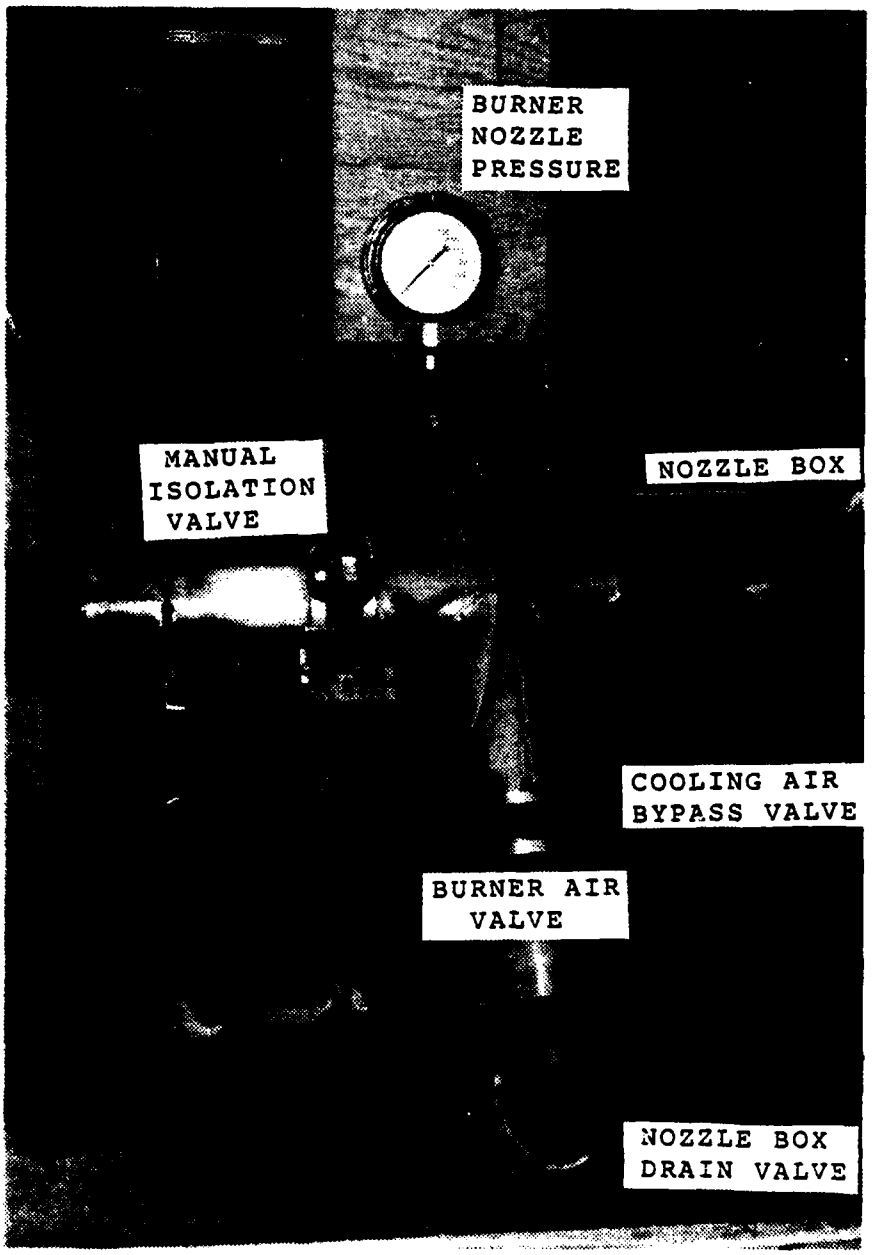

Figure 7, Combustion Air Piping

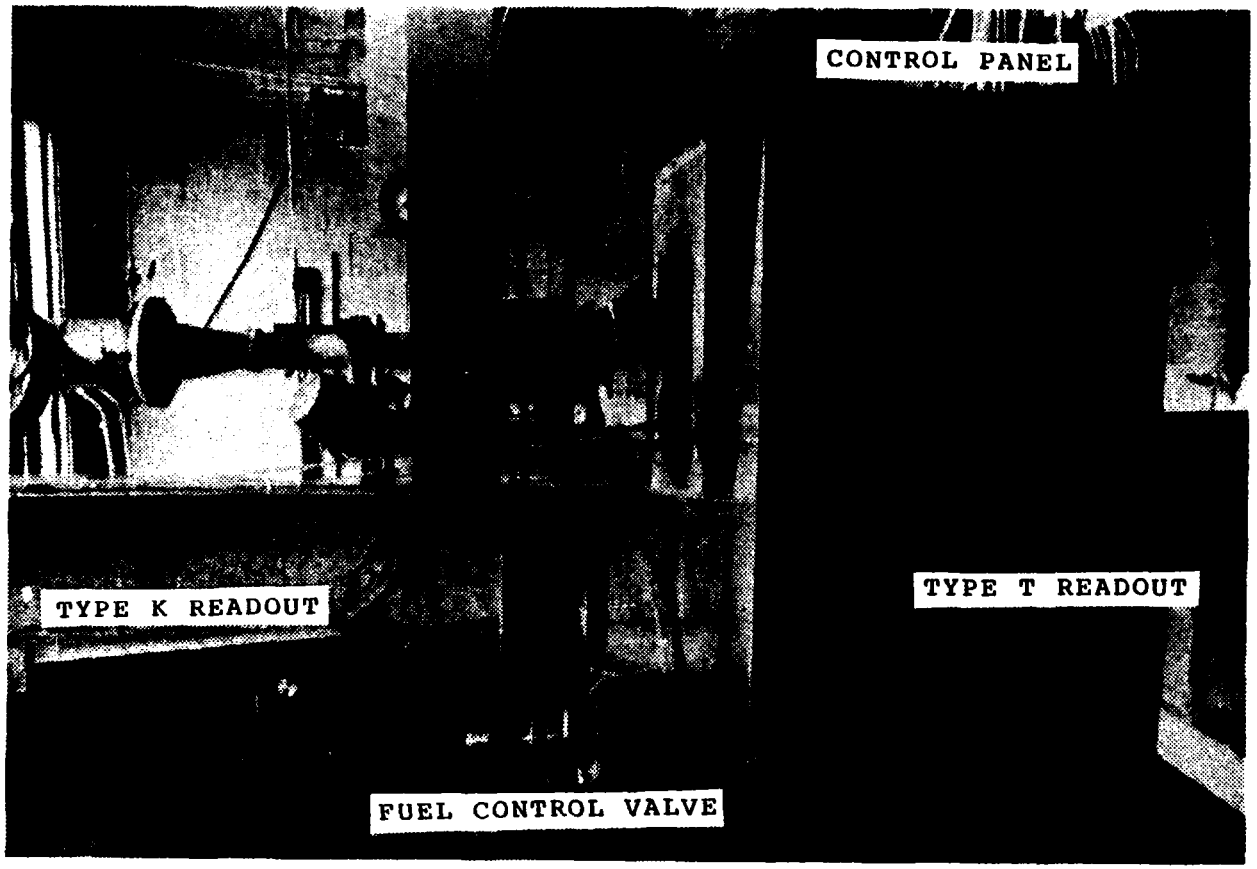

Figure 8, Gas Generator Control Station

Figure 9, Main Power Supply and Control Panel

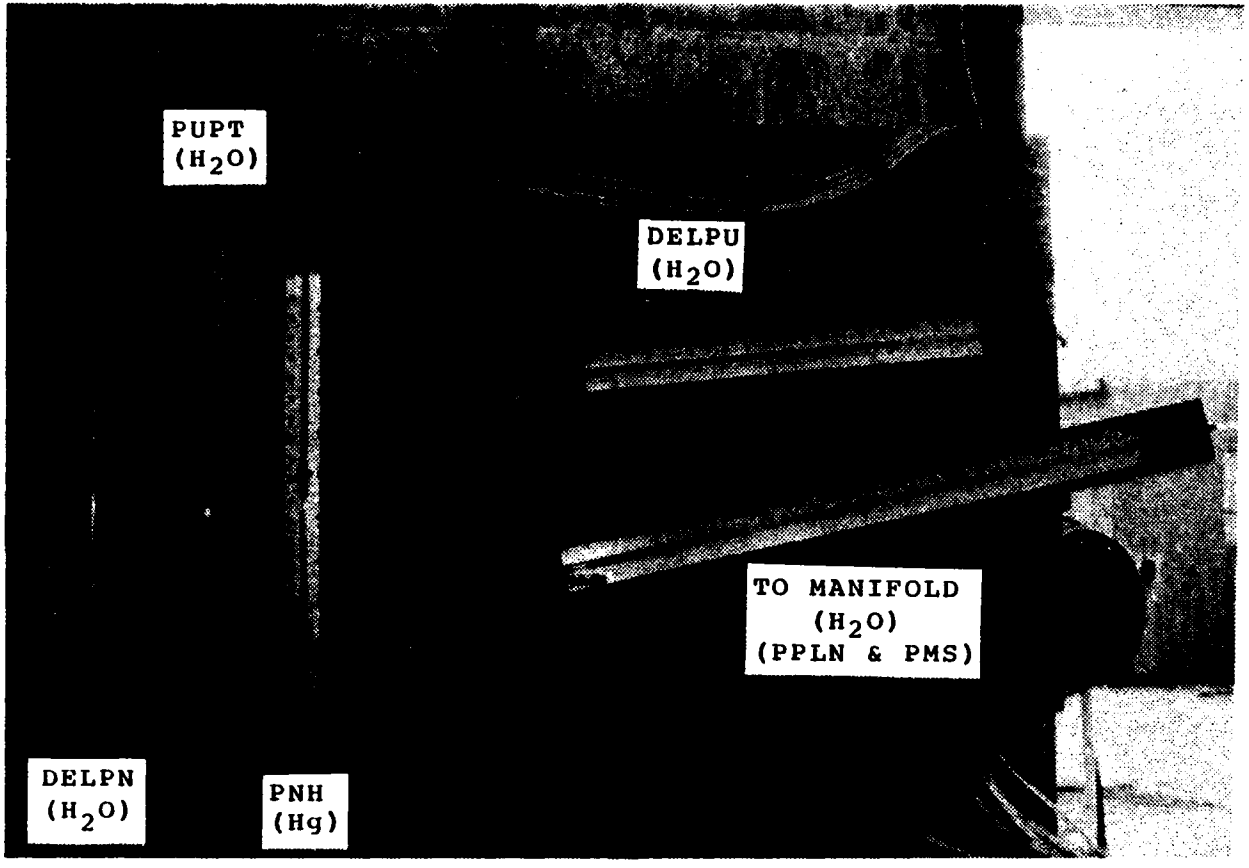

Figure 10, Manometer Installation

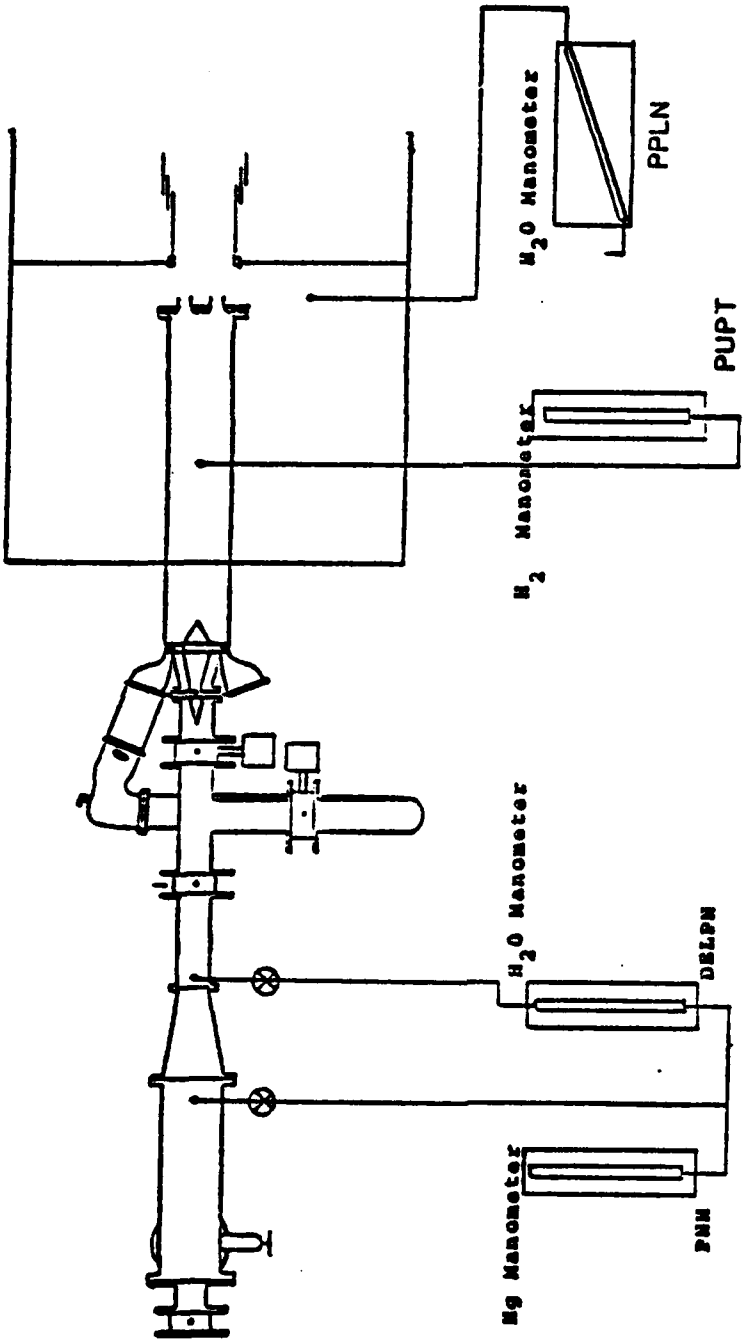

Figure 11, Schematic Diagram of Pressure Measurement System

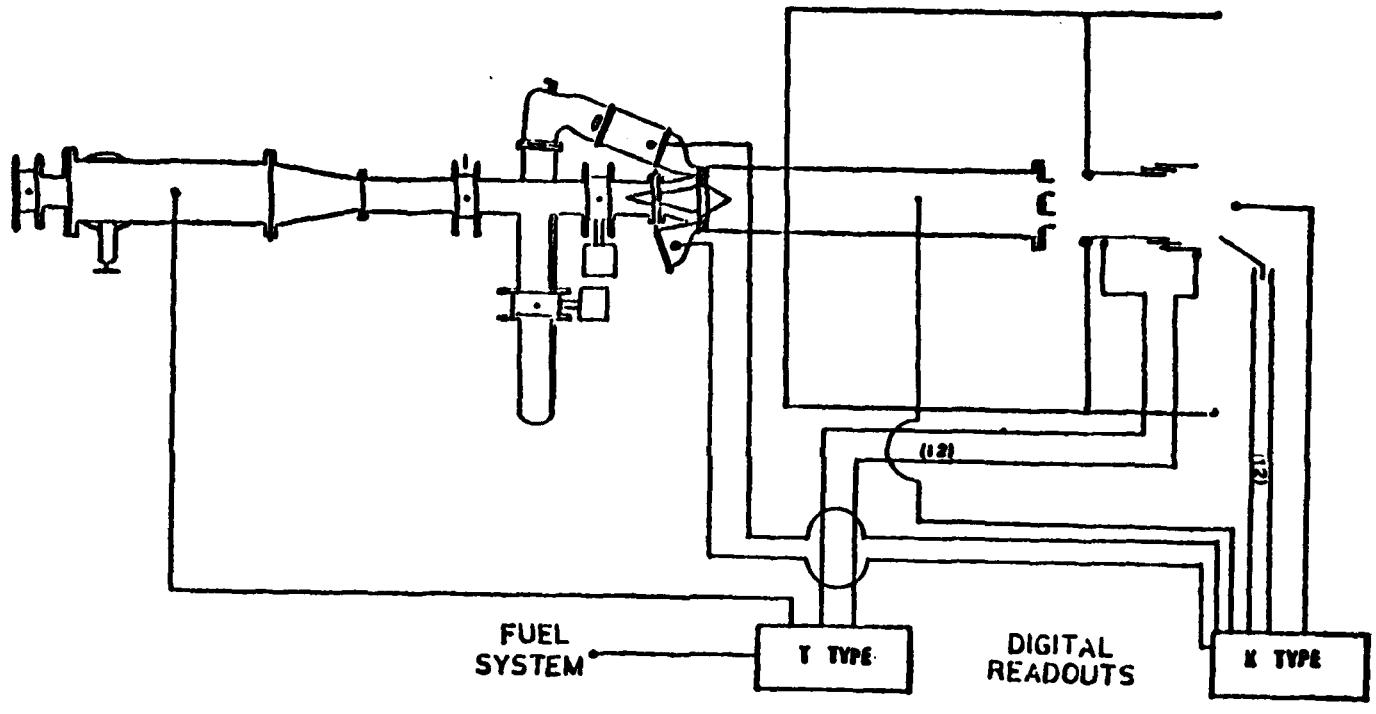

Figure 12, Schematic Diagram of Temperature Measurement System

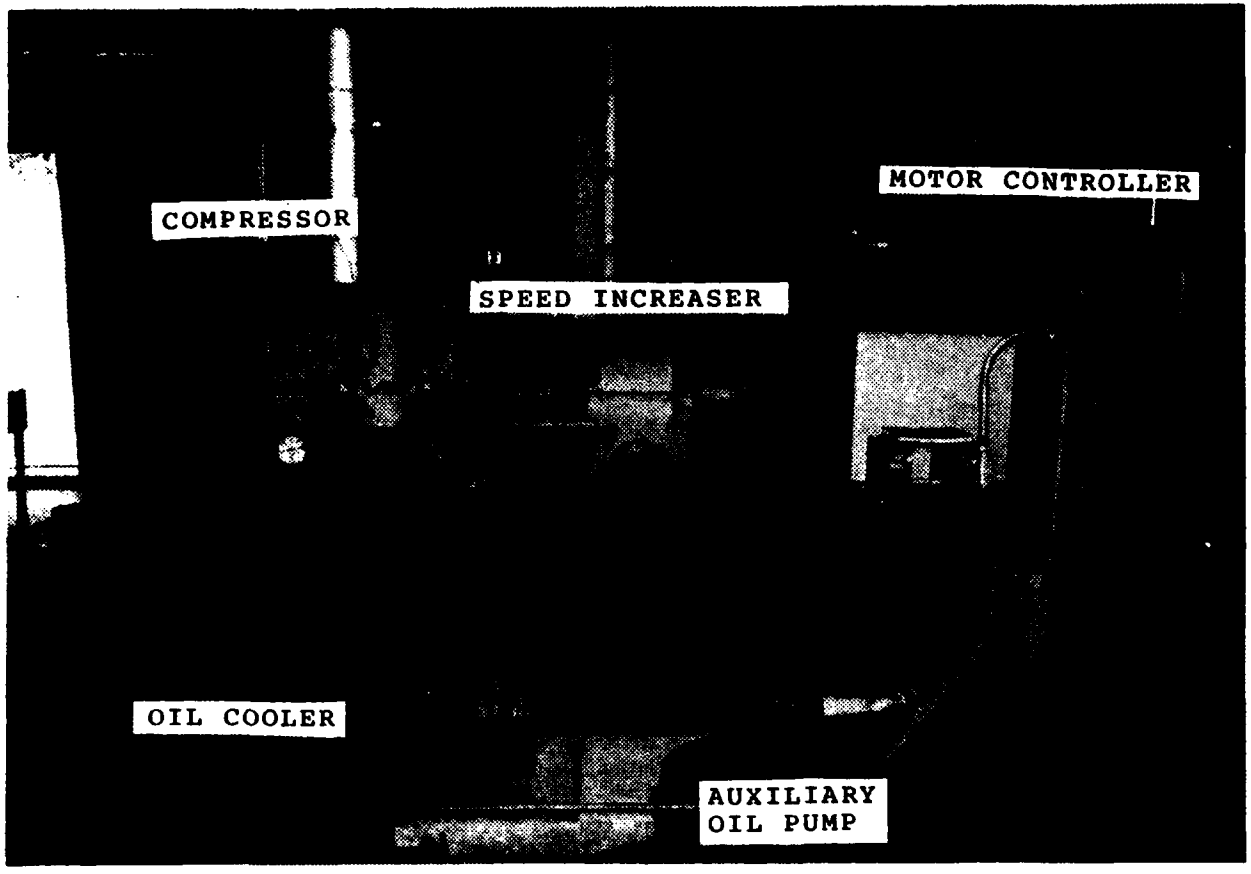

Figure 13, Carrier Air Compressor

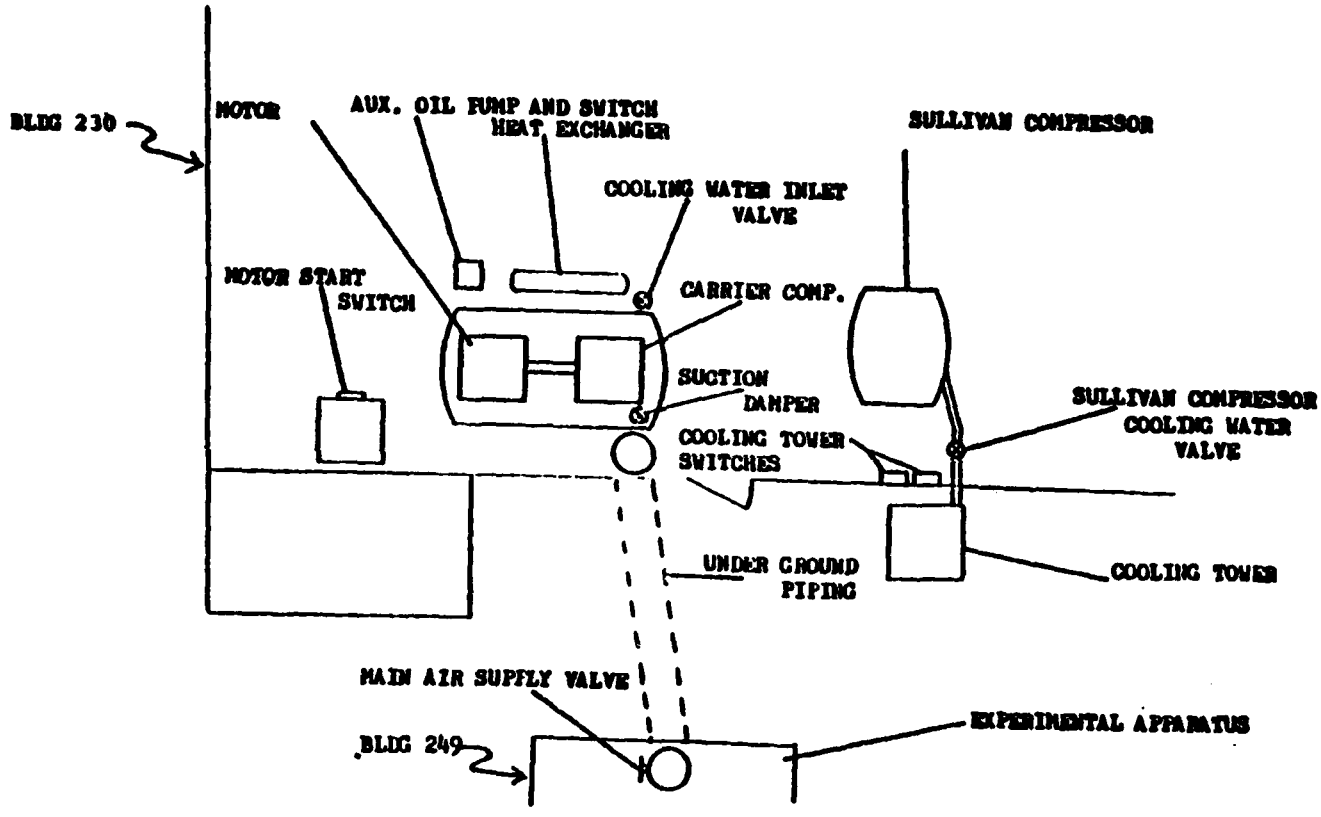

Figure 14, Compressor Layout

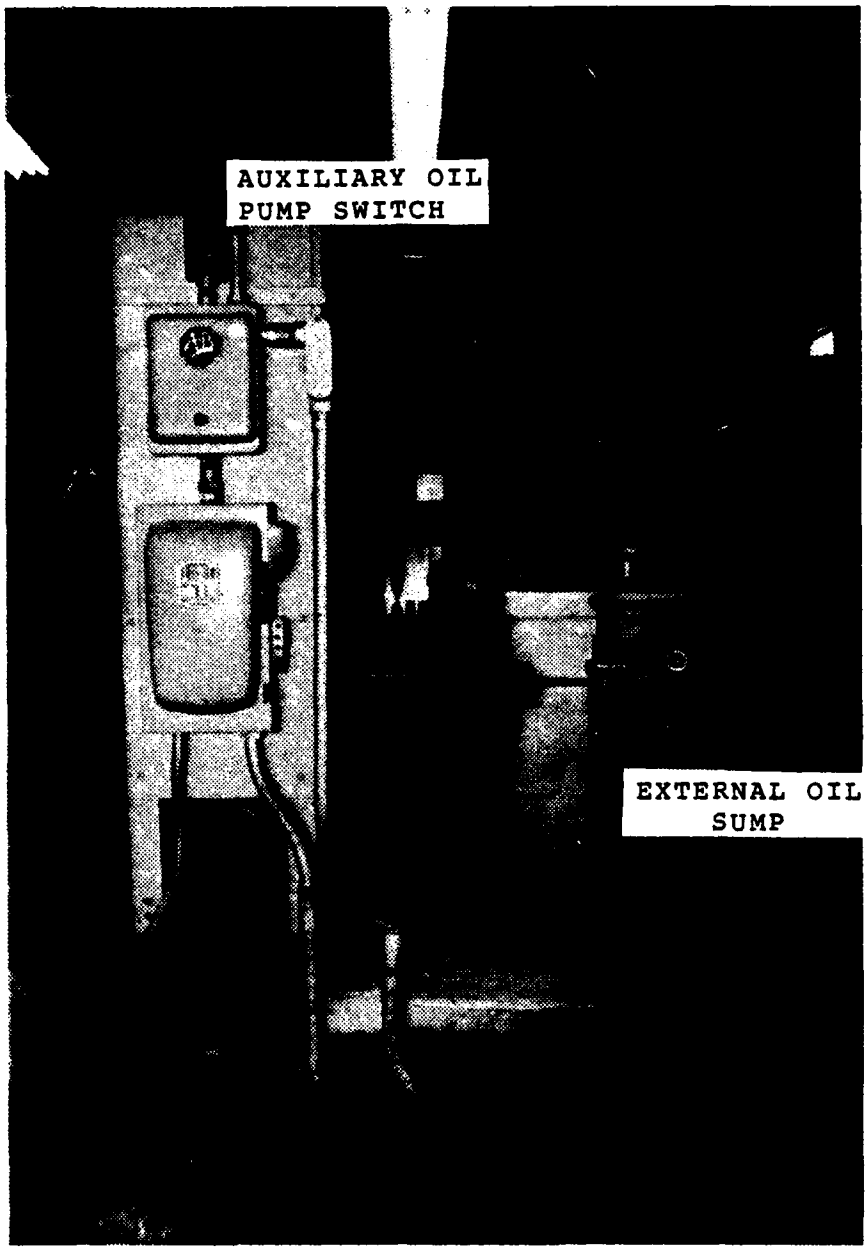

Figure 15, Auxiliary Oil Pump Control

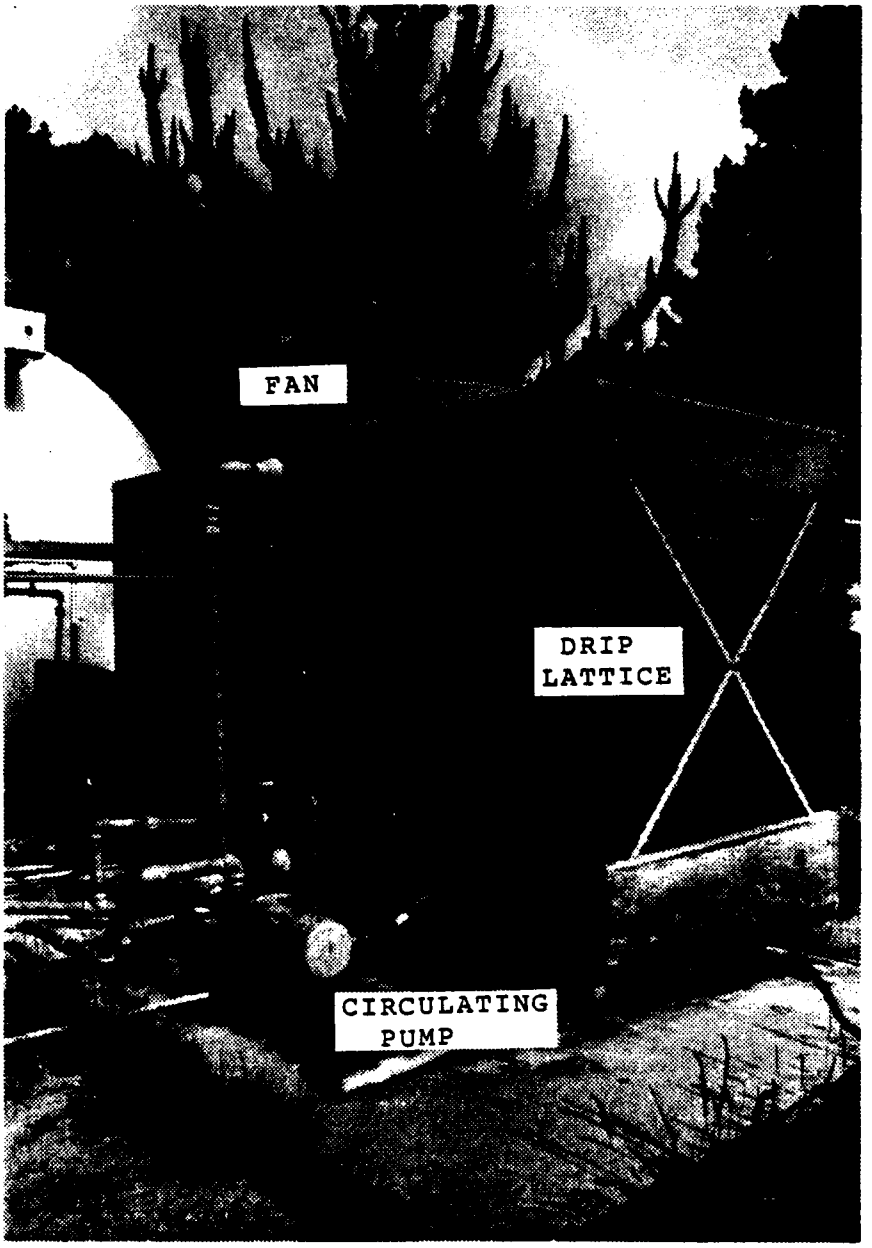

Figure 16, Cooling Tower and Pump

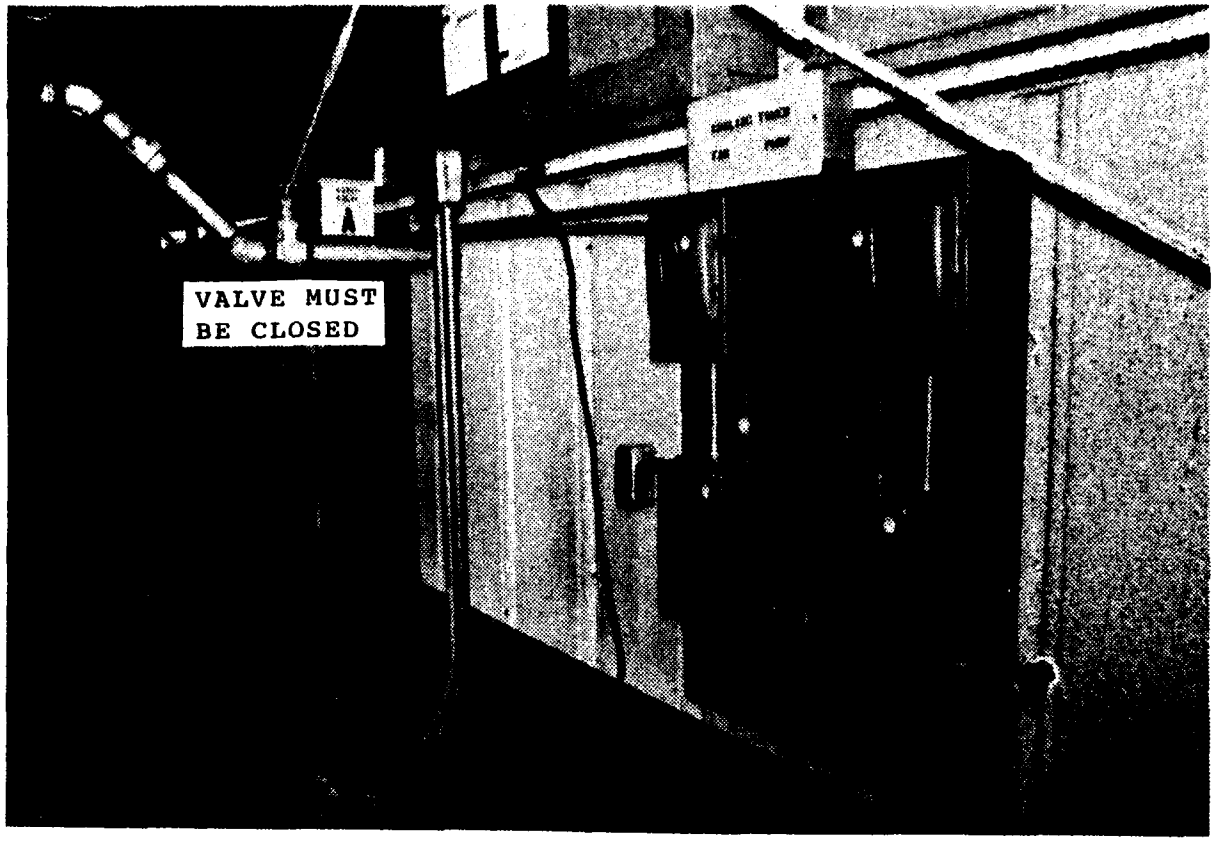

Figure 17, Cooling Water Pump and Tower Fan Controllers

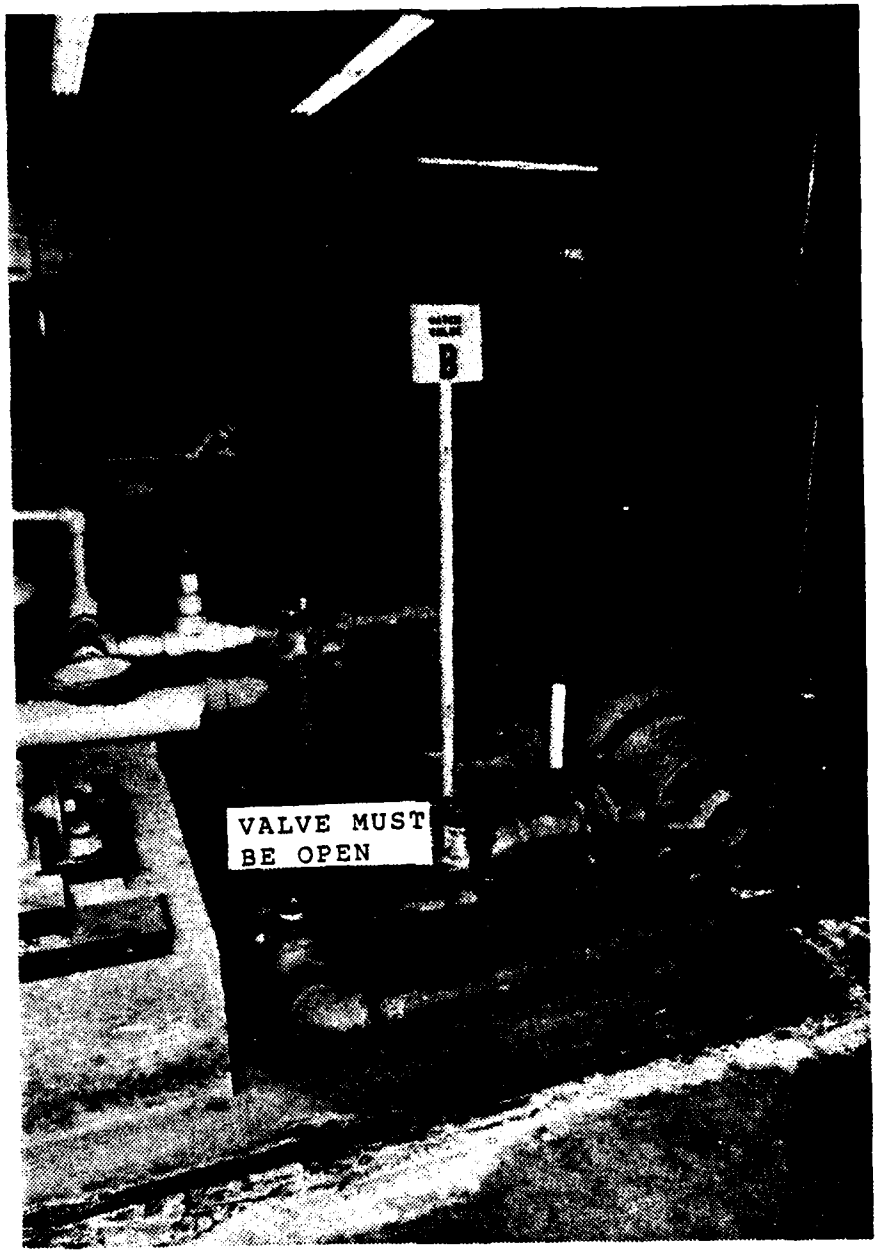

Figure 18, Cooling Water Inlet Valve

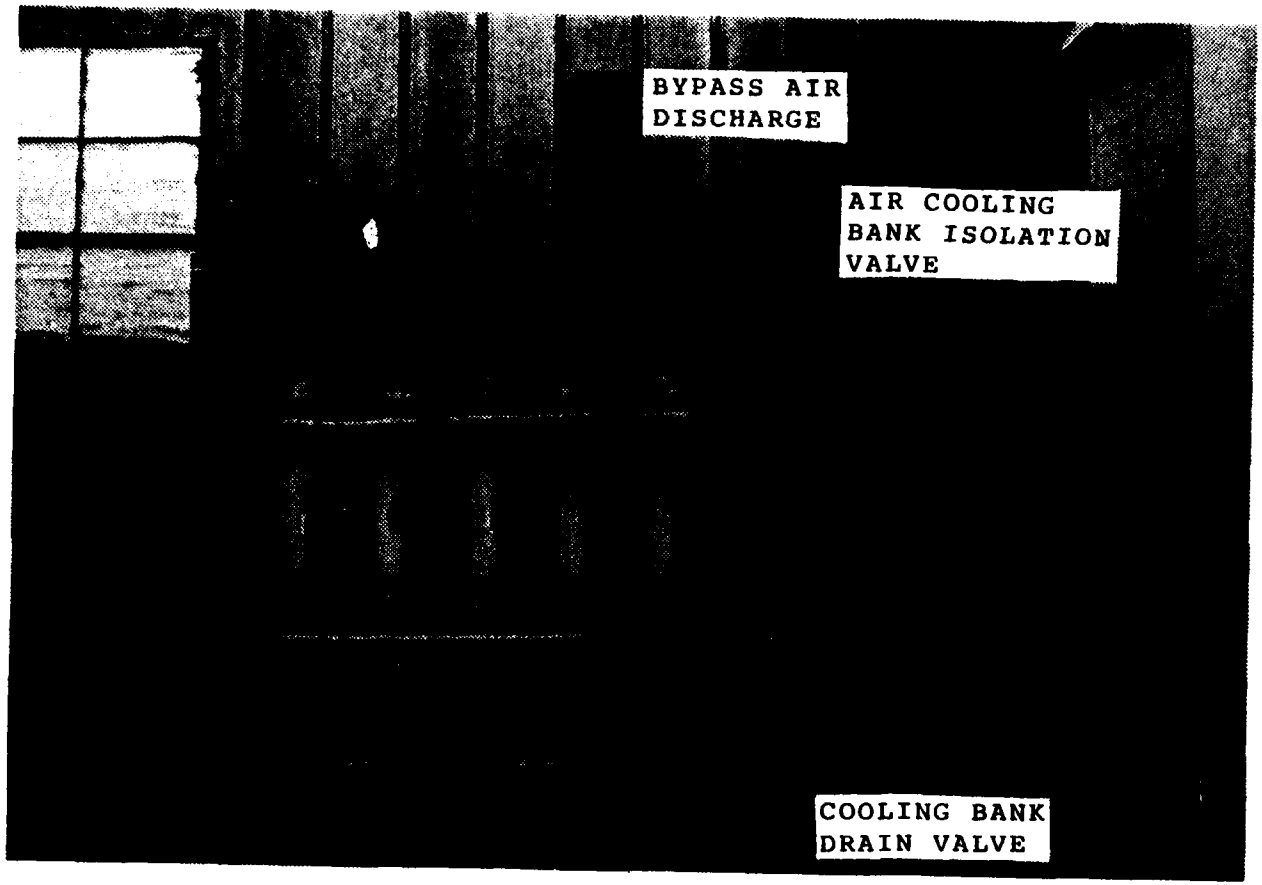

Figure 19, Air Cooling Bank and Bypass Discharge

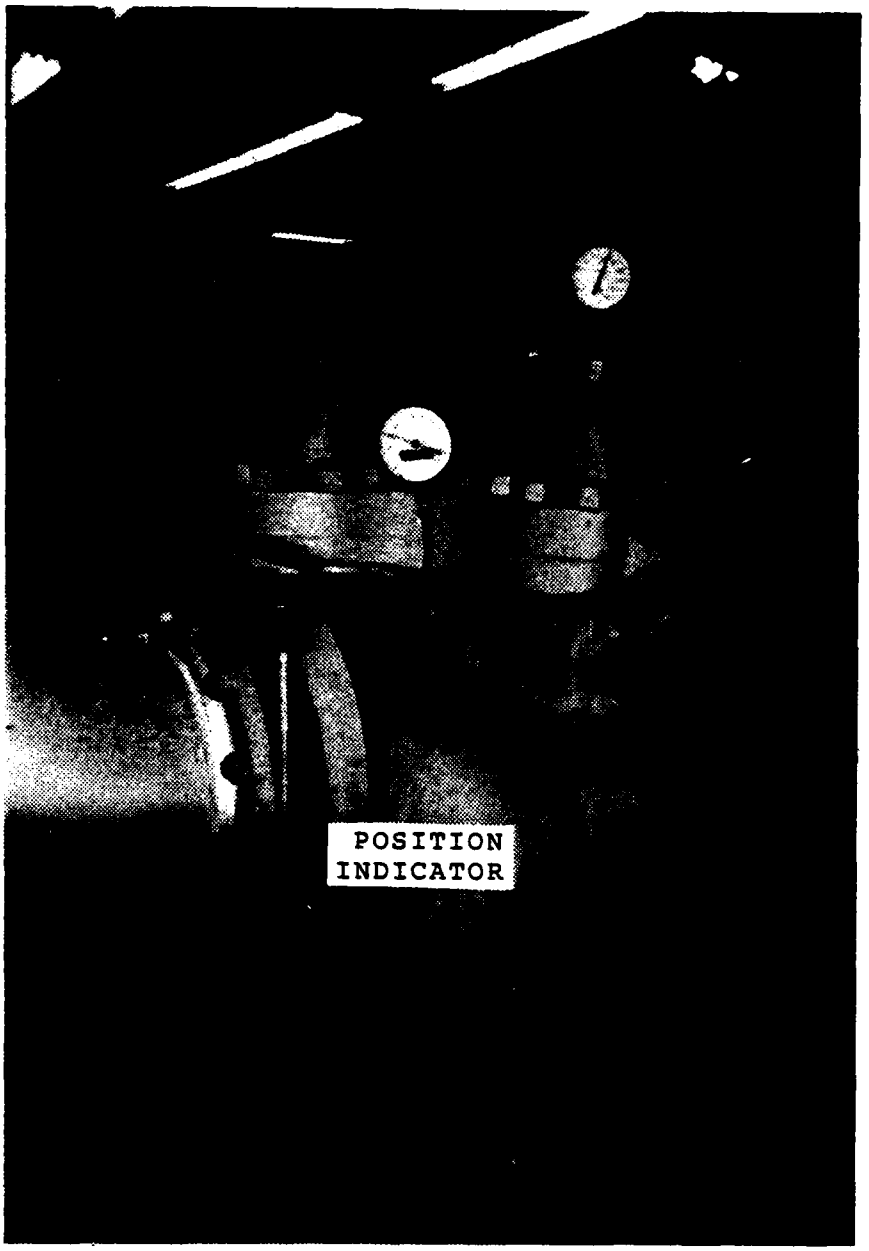

Figure 20, Air Compressor Suction Valve

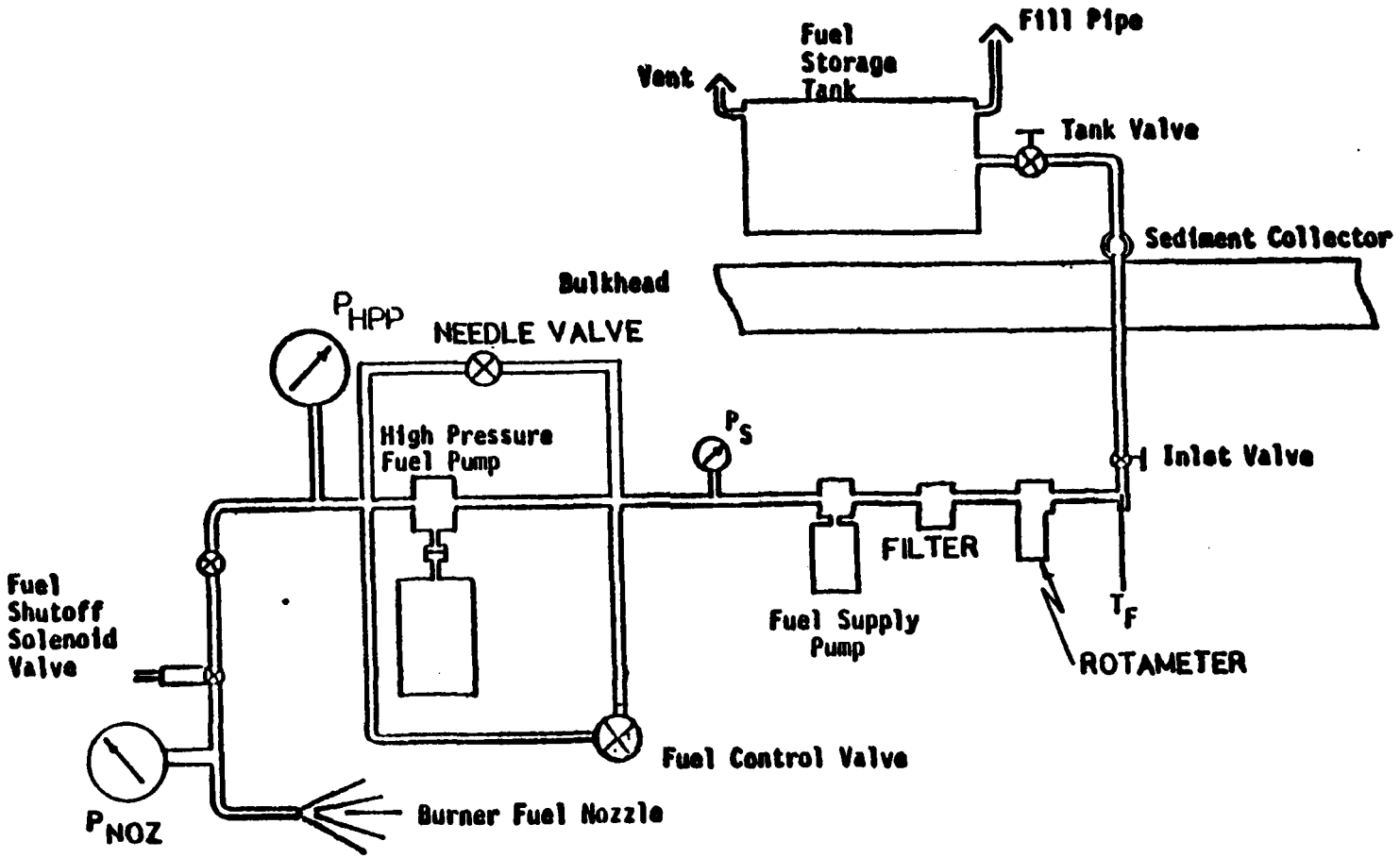

Figure 21, Gas Generator Fuel System

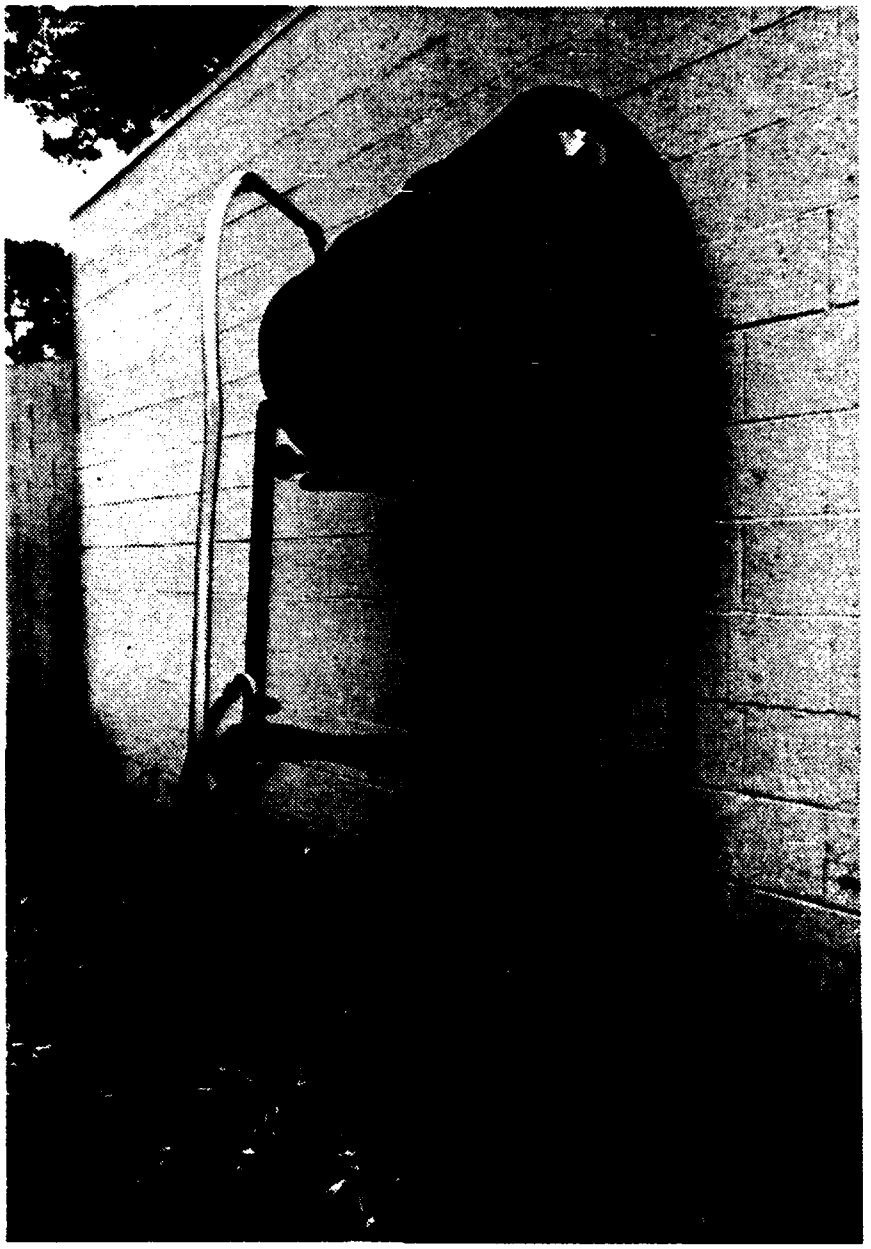

Figure 22, Fuel Service Tank

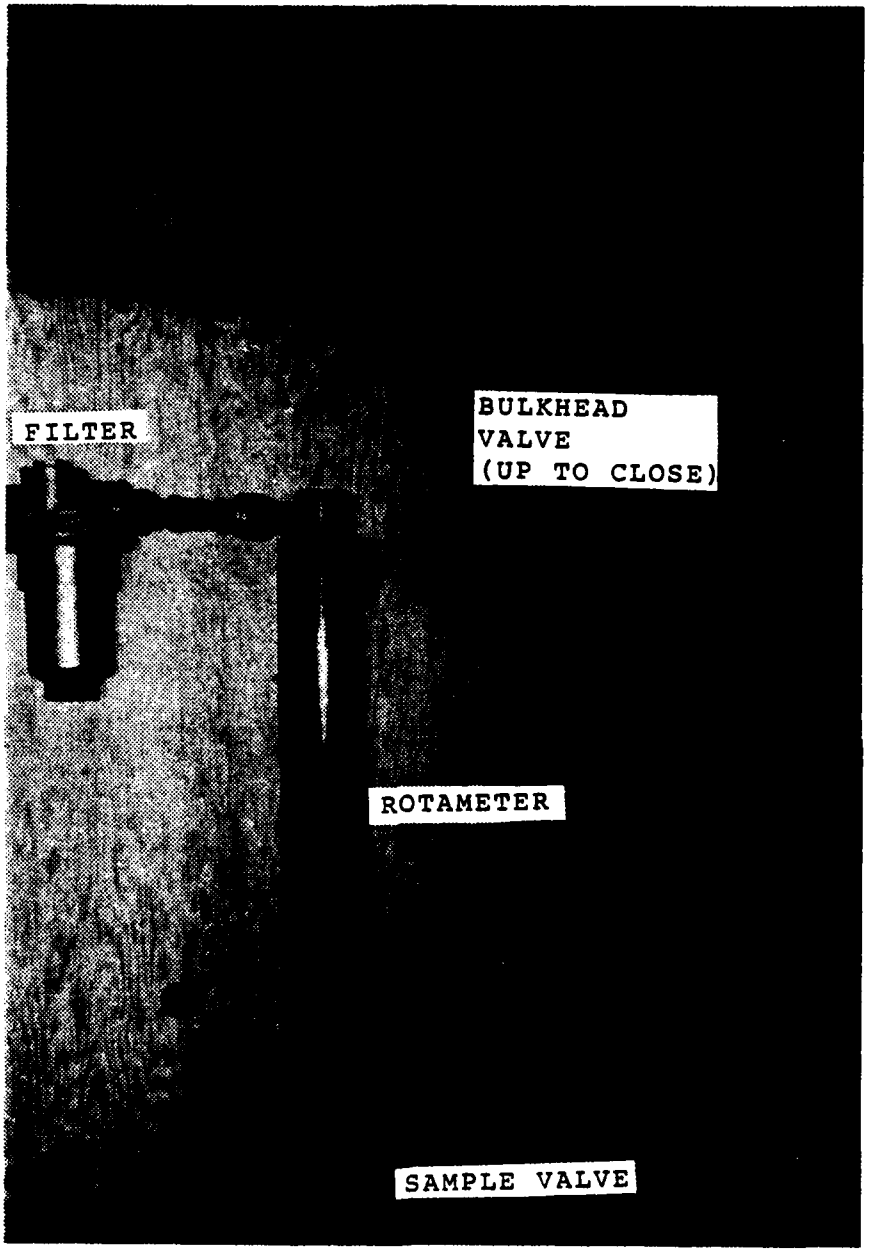

Figure 23, Fuel Measurement and Filtering

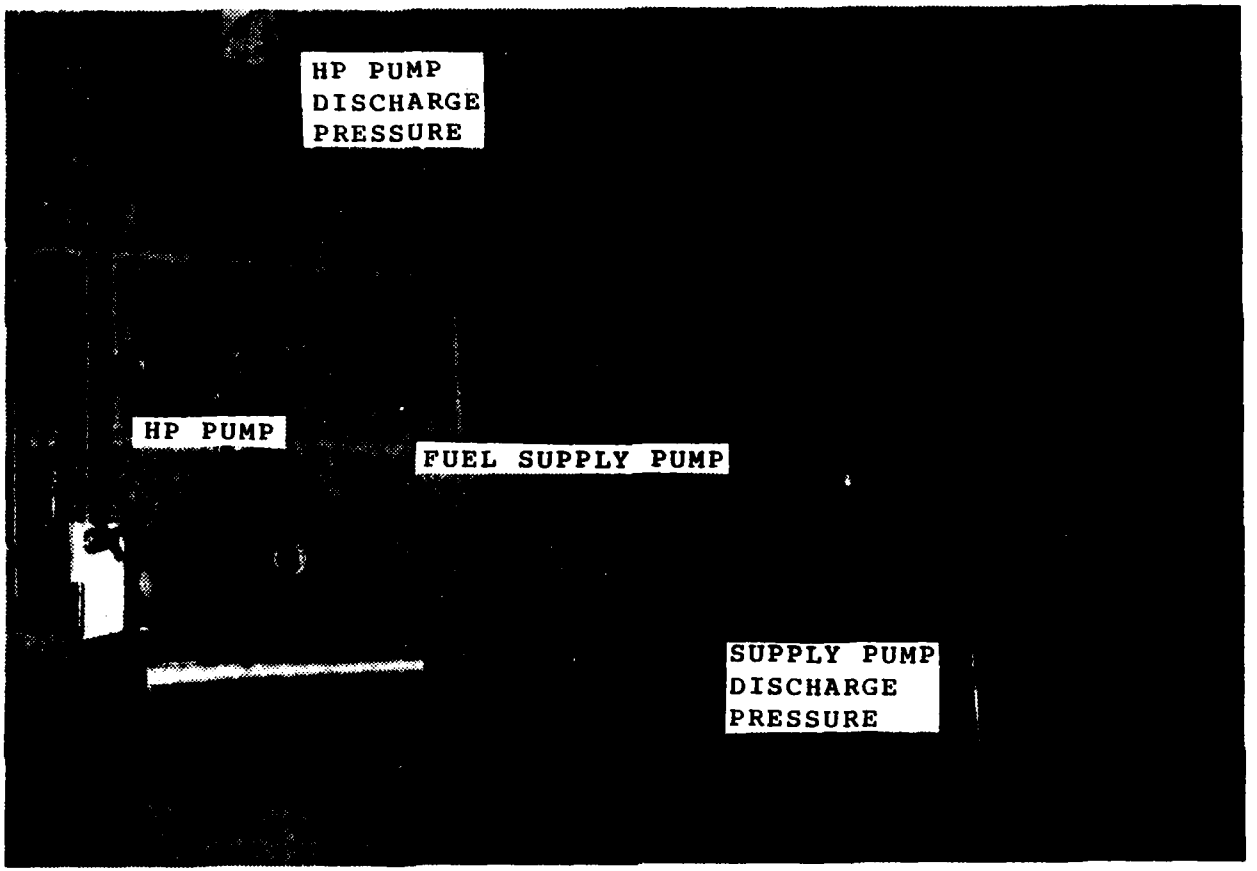

Figure 24, Fuel Pump Installation

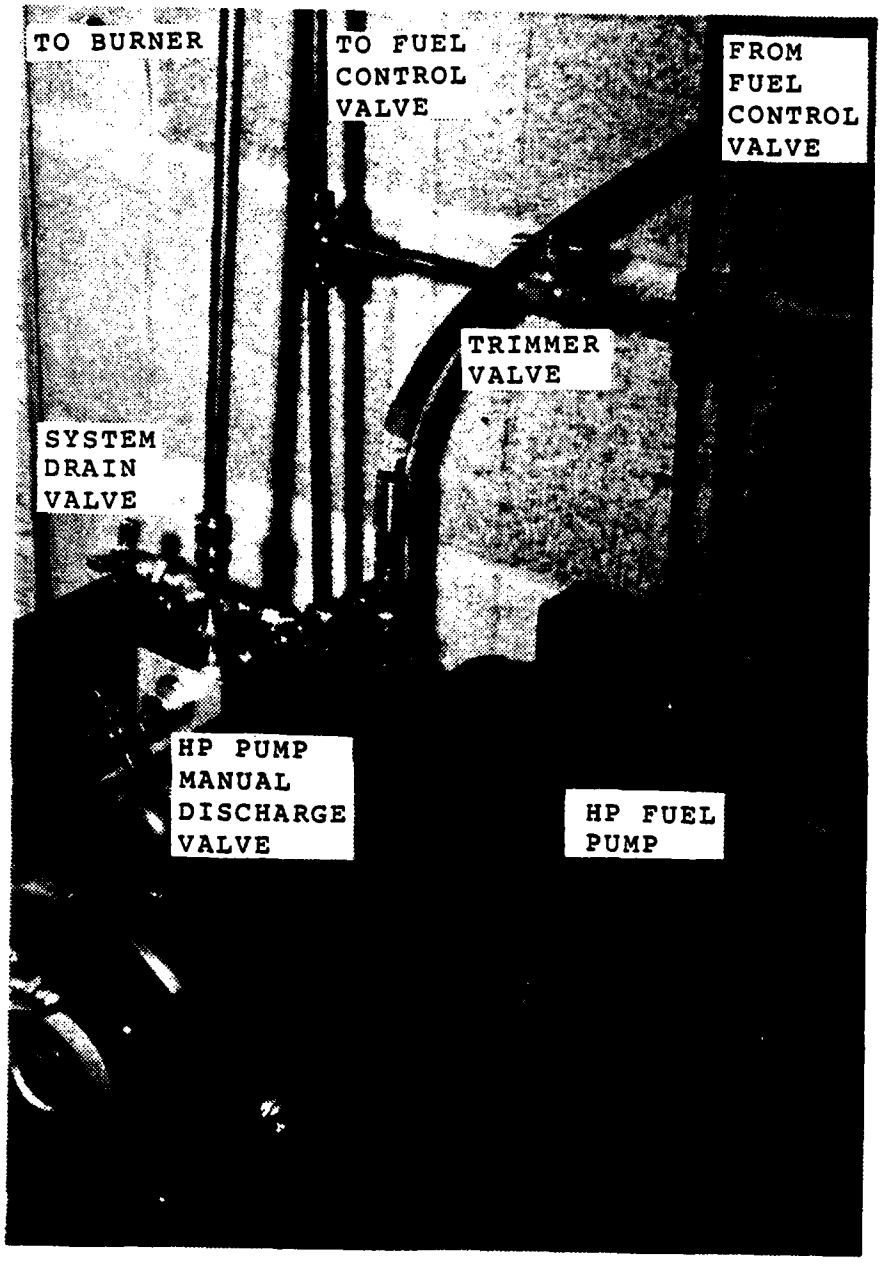

Figure 25, HP Fuel Piping and Valves

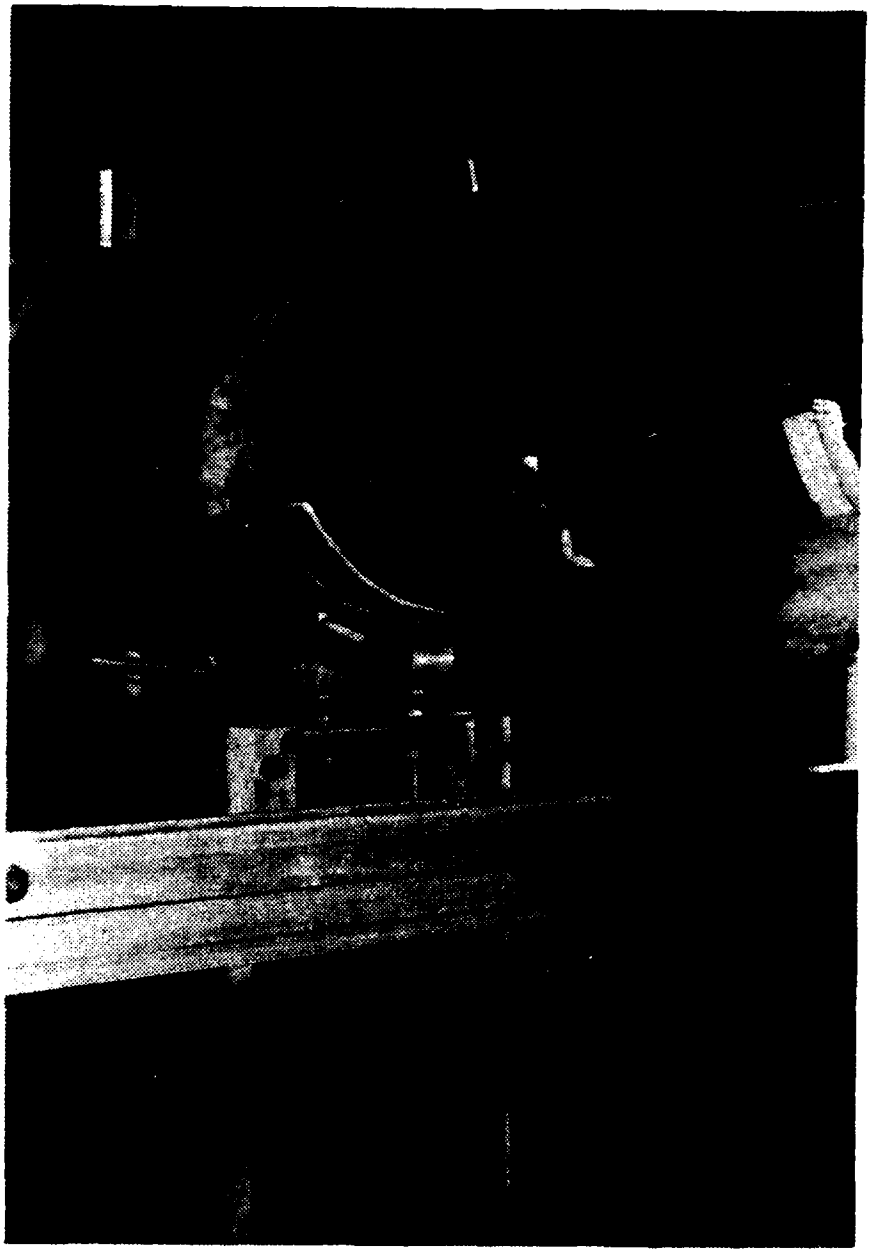

Figure 26, Uptake Piping Rear Support

Figure 27, Uptake Piping Forward Support

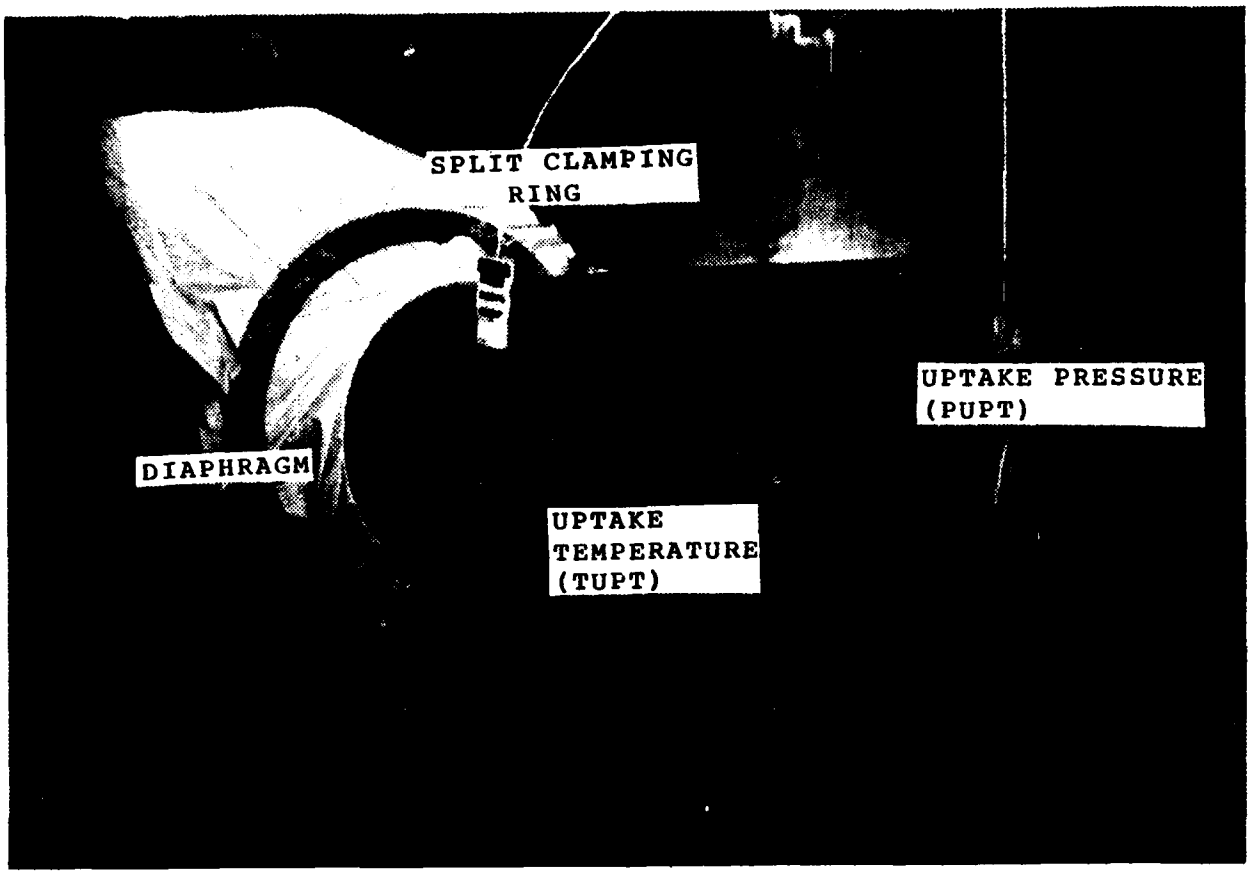

Figure 28, Finished Uptake Section

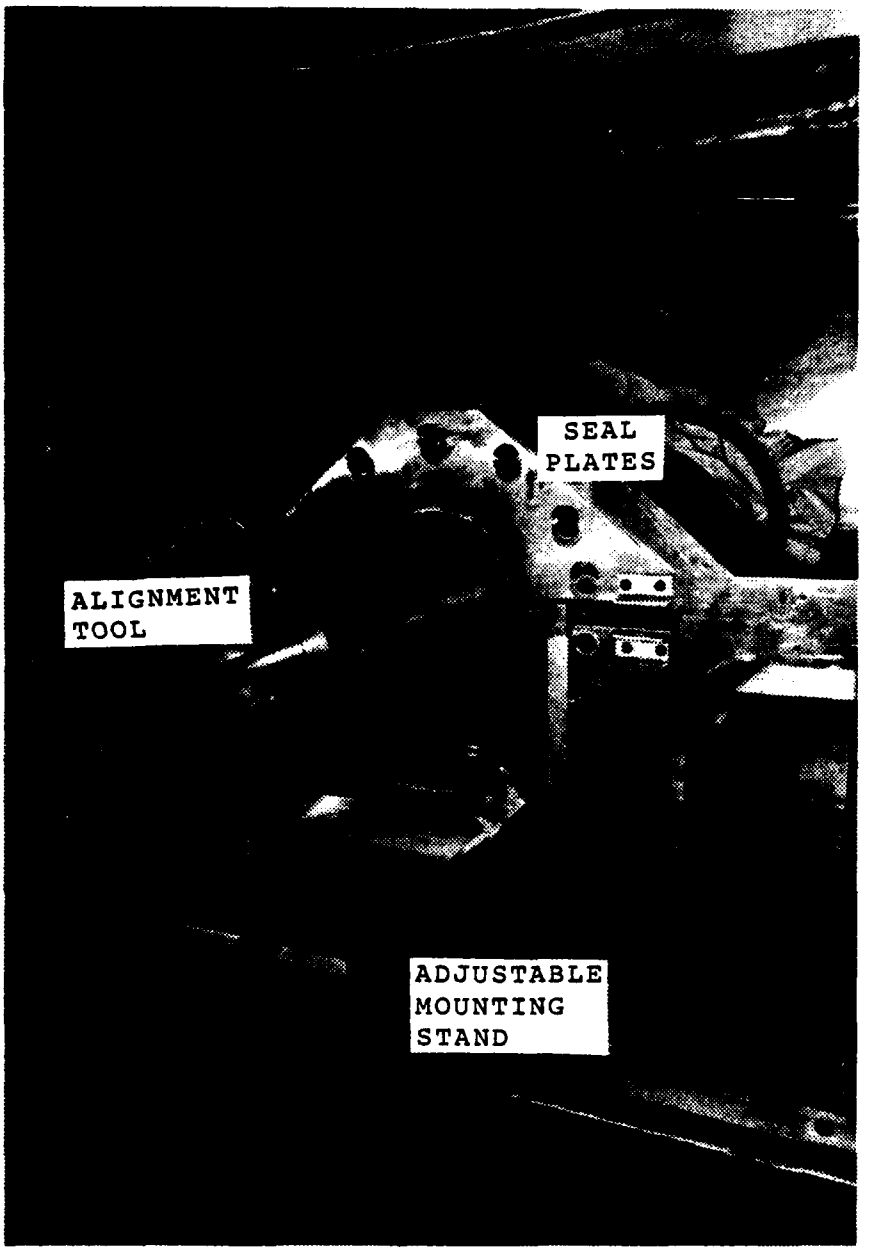

Figure 29, Model Installation

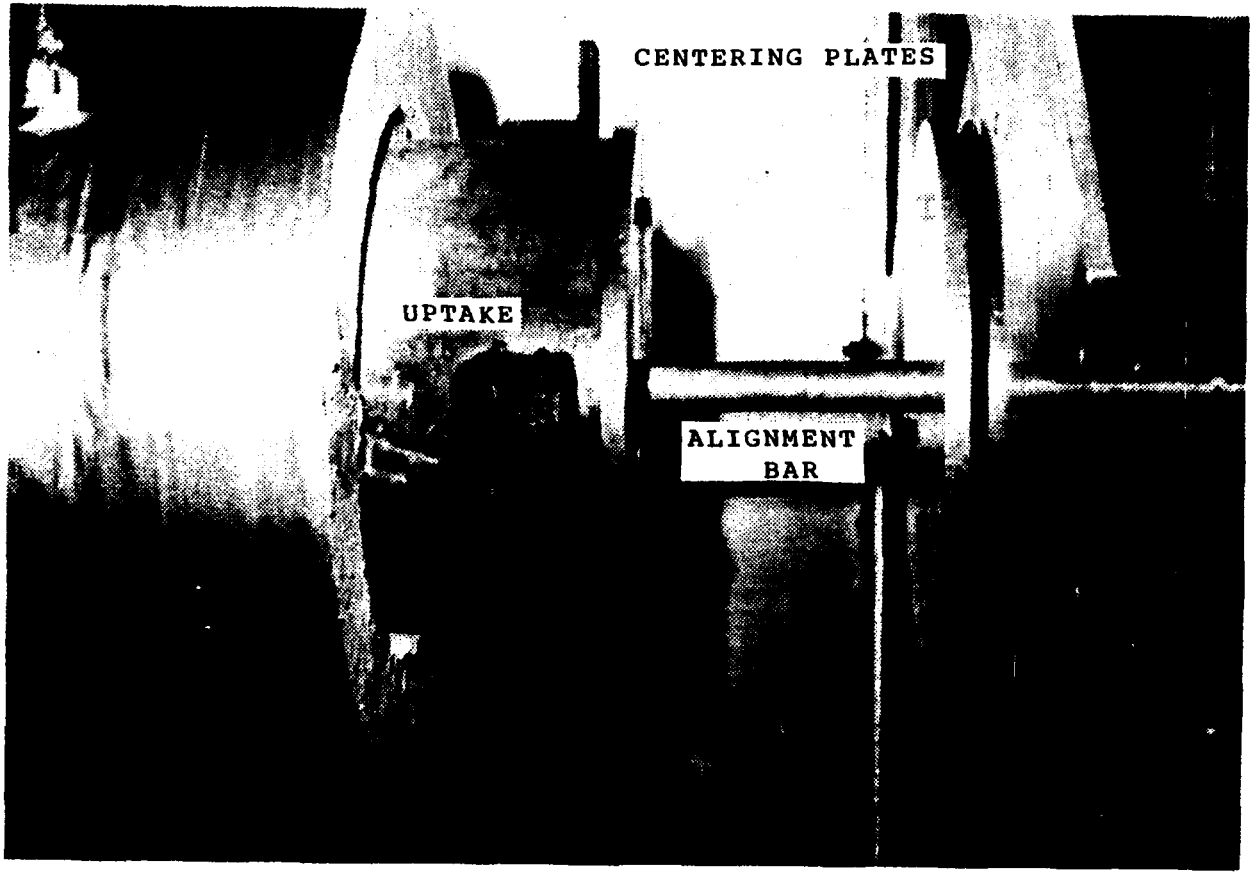

Figure 30, Model Alignment

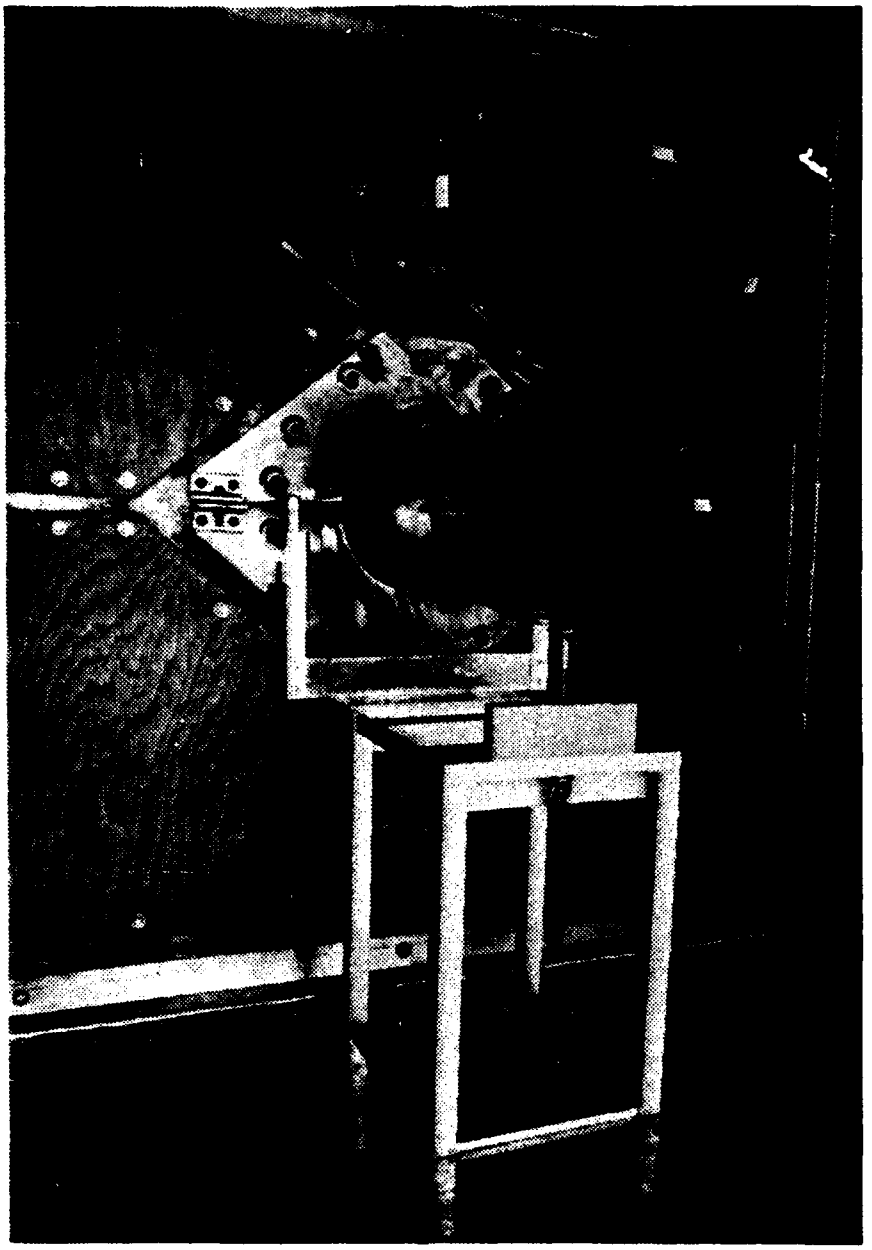

Figure 31, Model A Installed

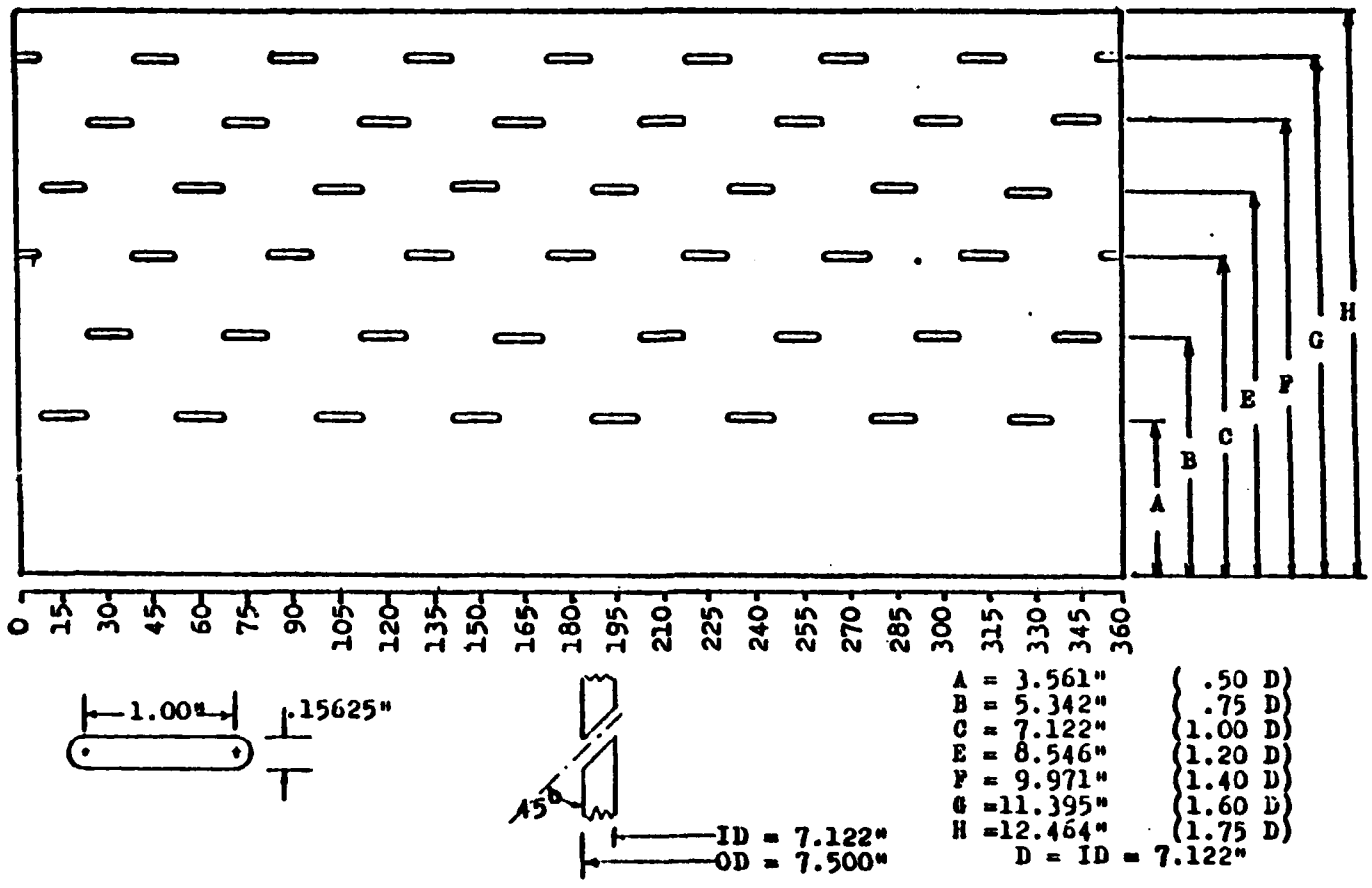

Figure 32, Dimensional Diagram of Slotted Mixing Stack (Model A)

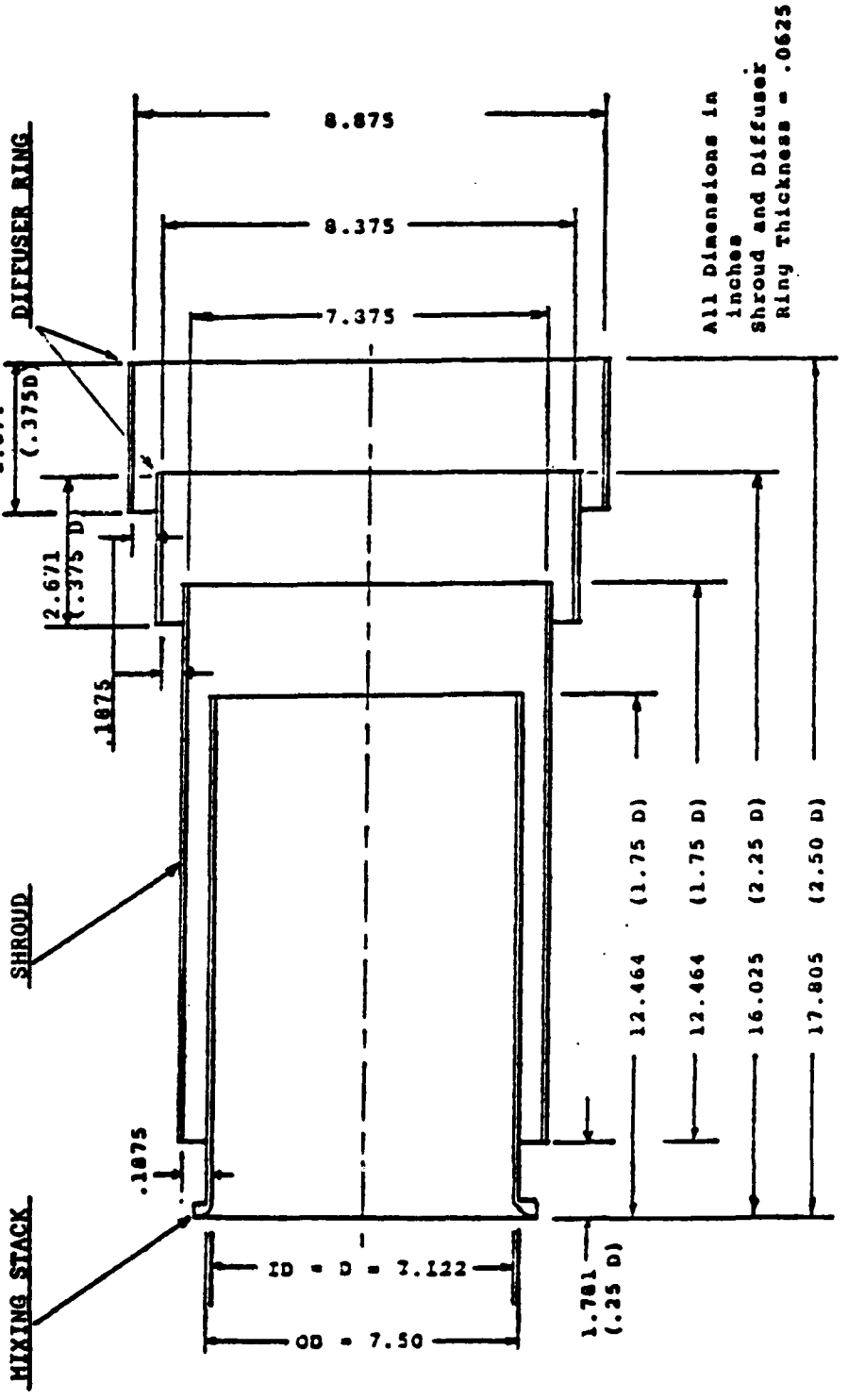

Figure 33, Mixing Stack with Shroud and Two Diffuser Rings (Model A)

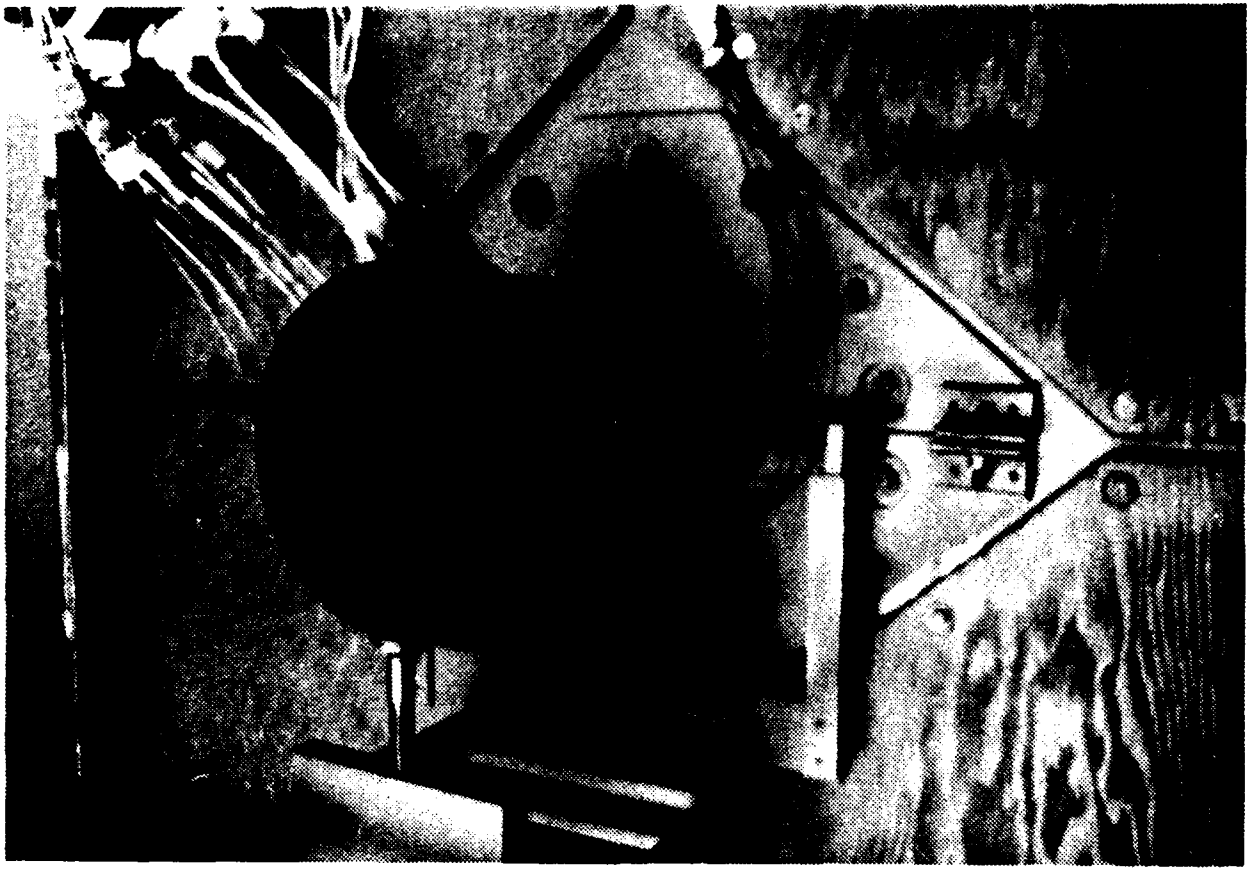

Figure 34, Model B Installed

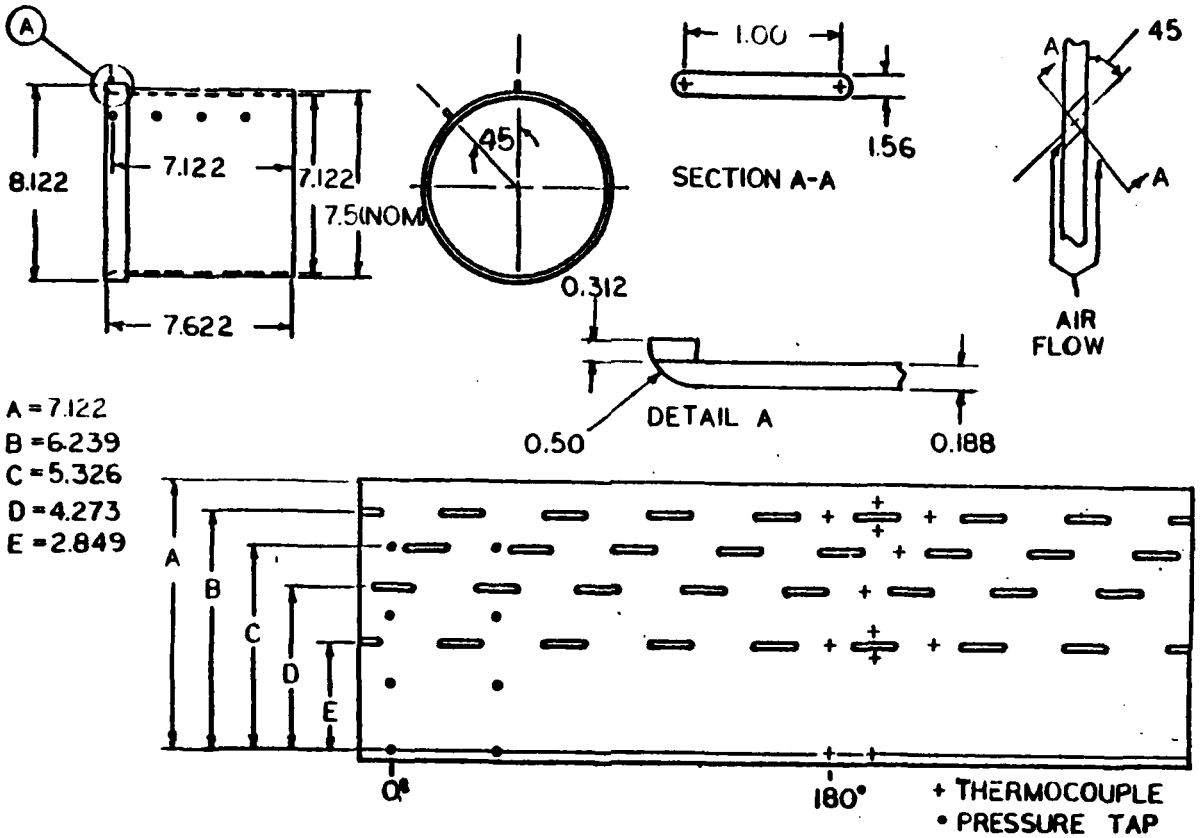

Figure 35, Dimensional Diagram of Slotted Mixing Stack (Model B)

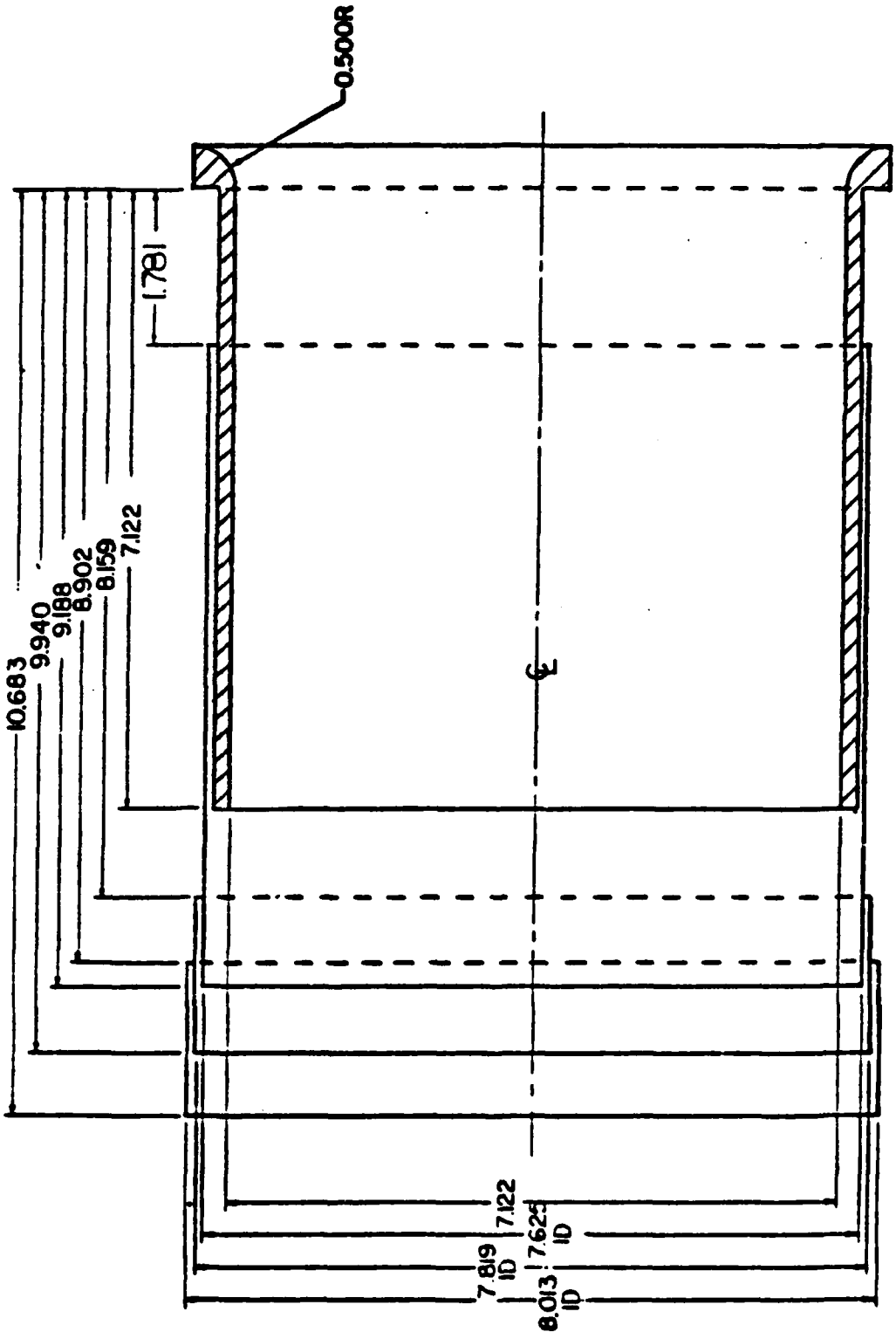

Figure 36, Mixing Stack with Shroud and Two Diffuser Rings (Model B)

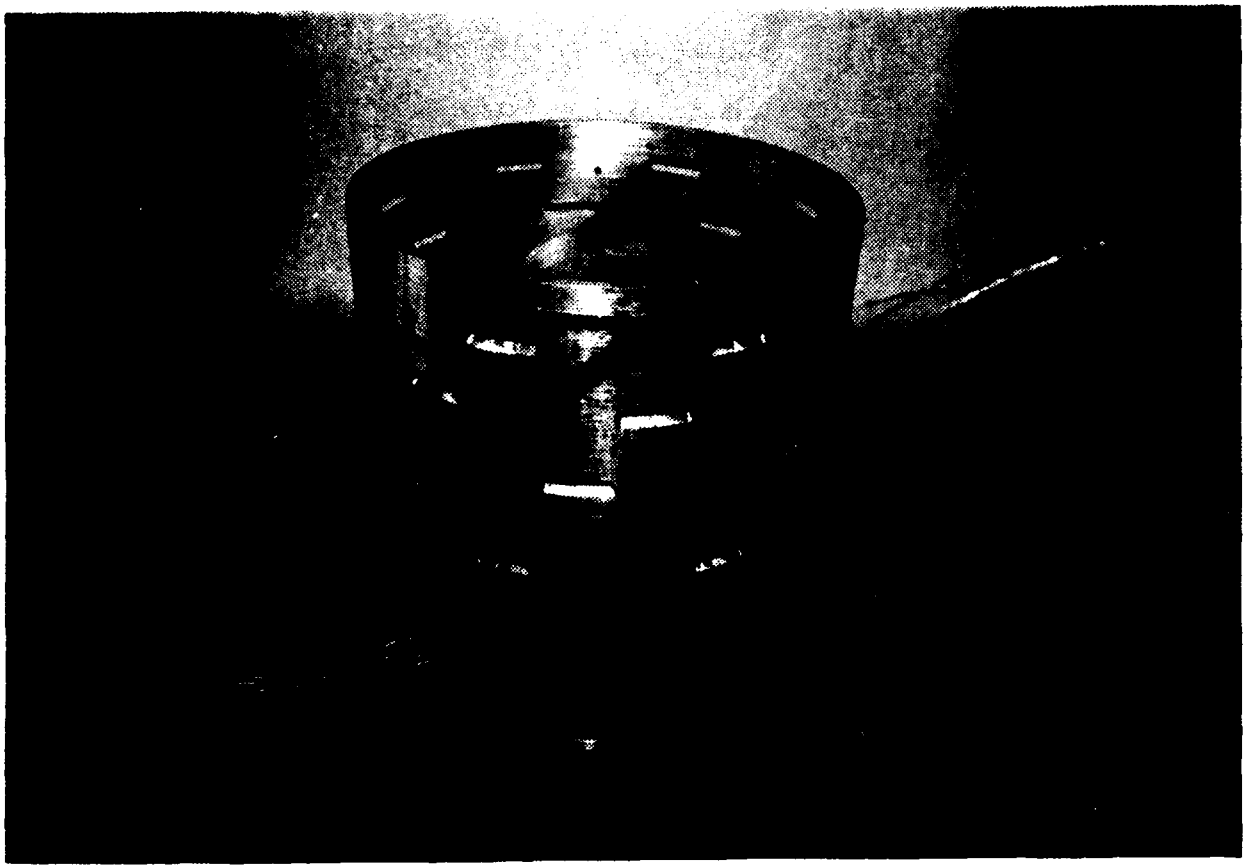

Figure 37, Mixing Stack for Model B

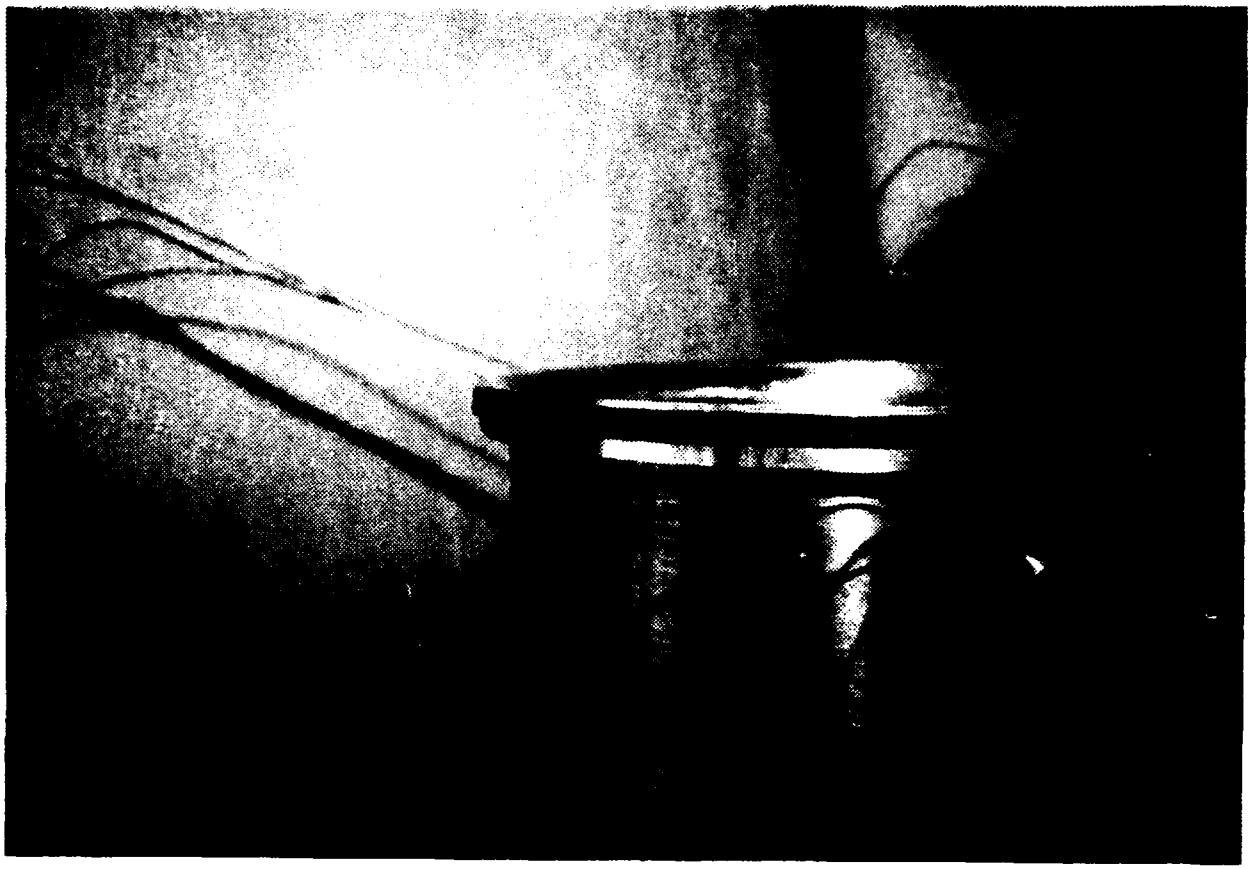

Figure 38, Mixing Stack Entrance O-ring Seal

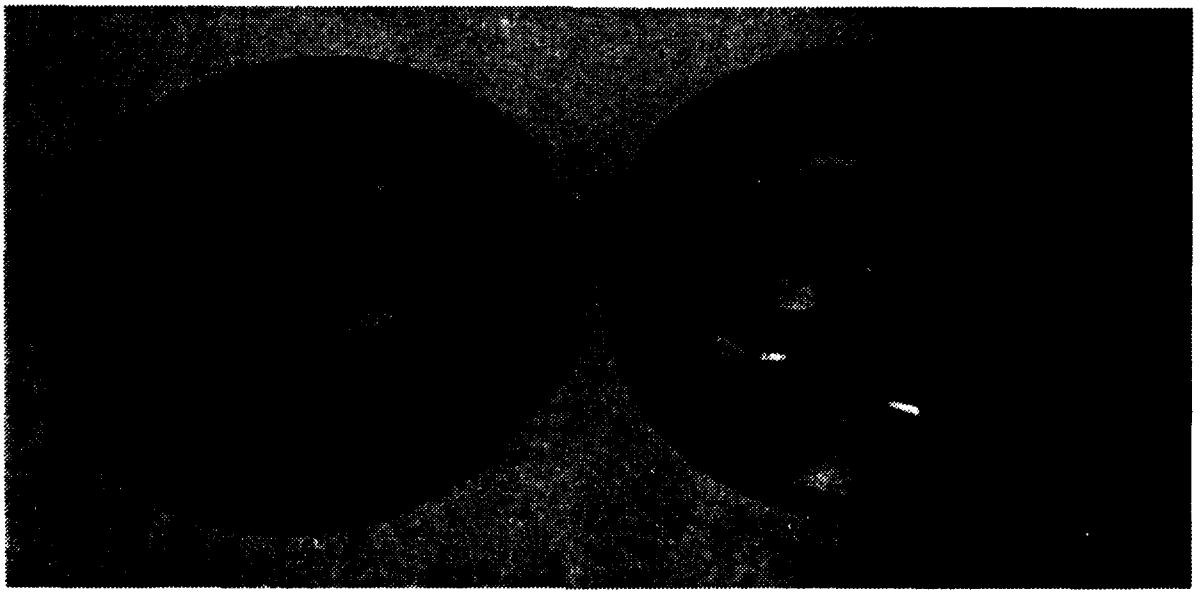

Figure 39, Straight and Tilted-angled
Primary Nozzle Plates

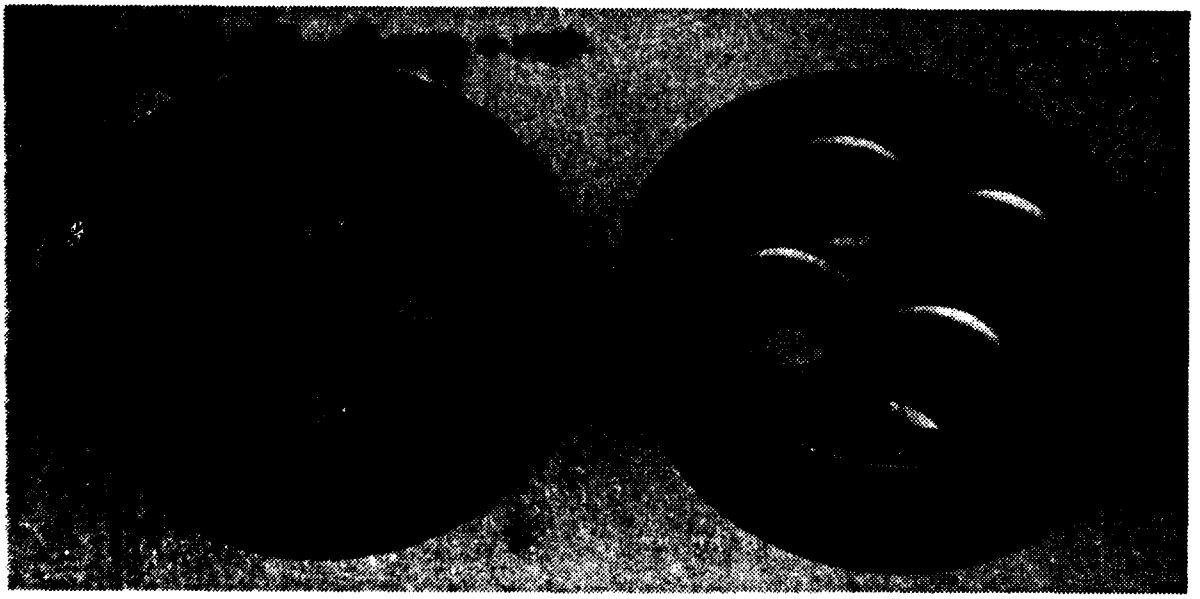

Figure 40, Primary Nozzle Plate Entrance
Configuration

All dimensions in inches

$A_m/A_p = 2.5$

A	10.000
B	45°
R_1	1.126
R_2	1.251

R_3	2.070
R_4	4.509
R_5	3.729
R_6	4.108

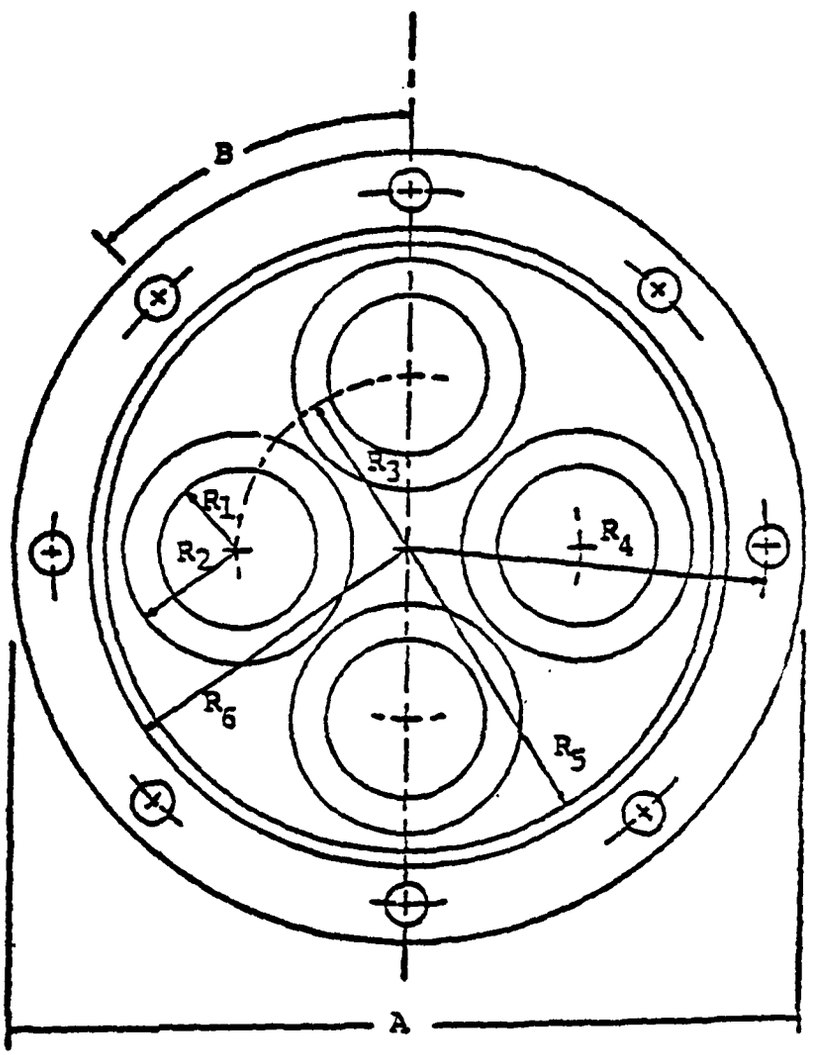

Figure 41, Dimensional Diagram of Primary Flow Nozzle Plate

	A_m/A_p = 2.5
A	1.251
B	1.126
C	1.770
D	2.520
E	.250
F	.125
G	.500

All dimensions in inches

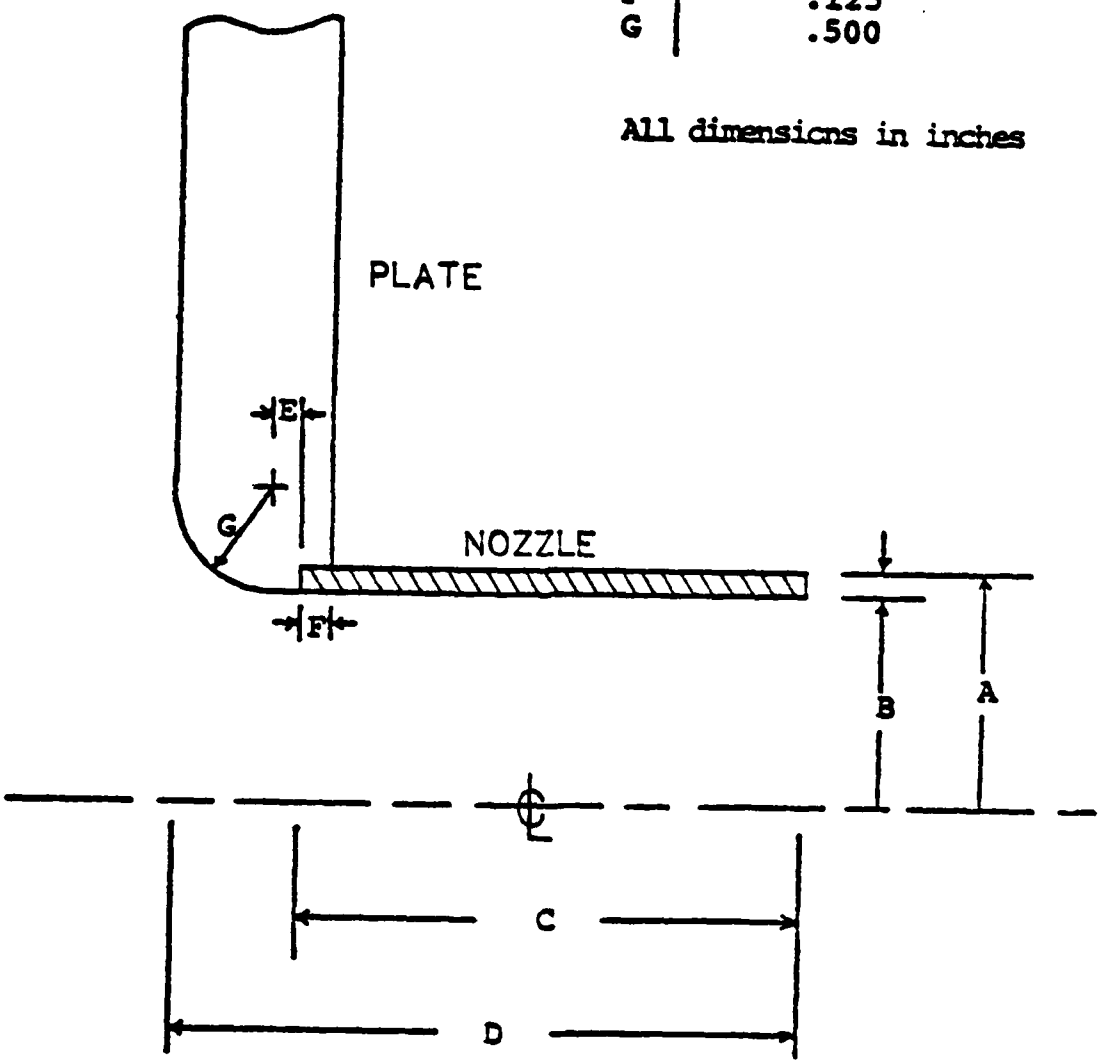

Figure 42, Dimensional Diagram of Straight Primary Nozzles (Model A)

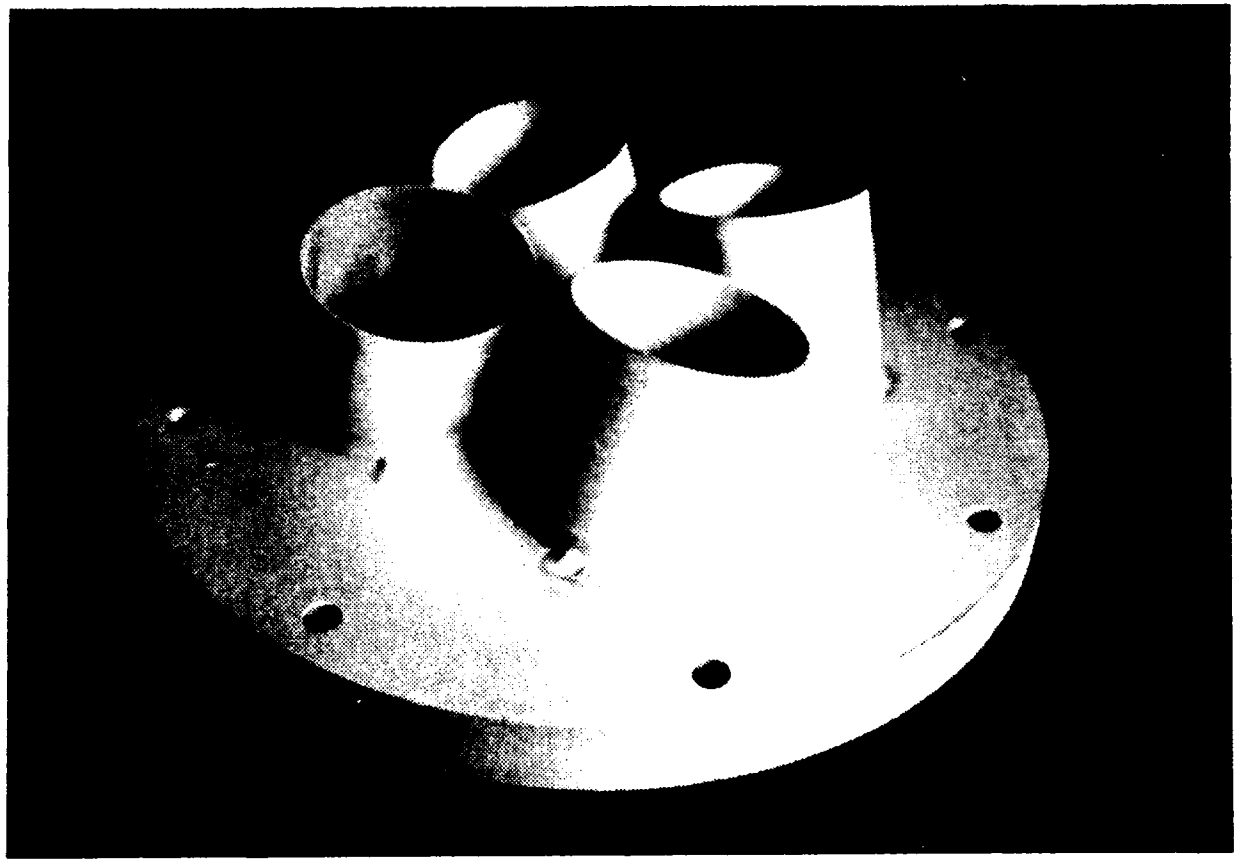

Figure 43, Tilted-angled Nozzle Plate

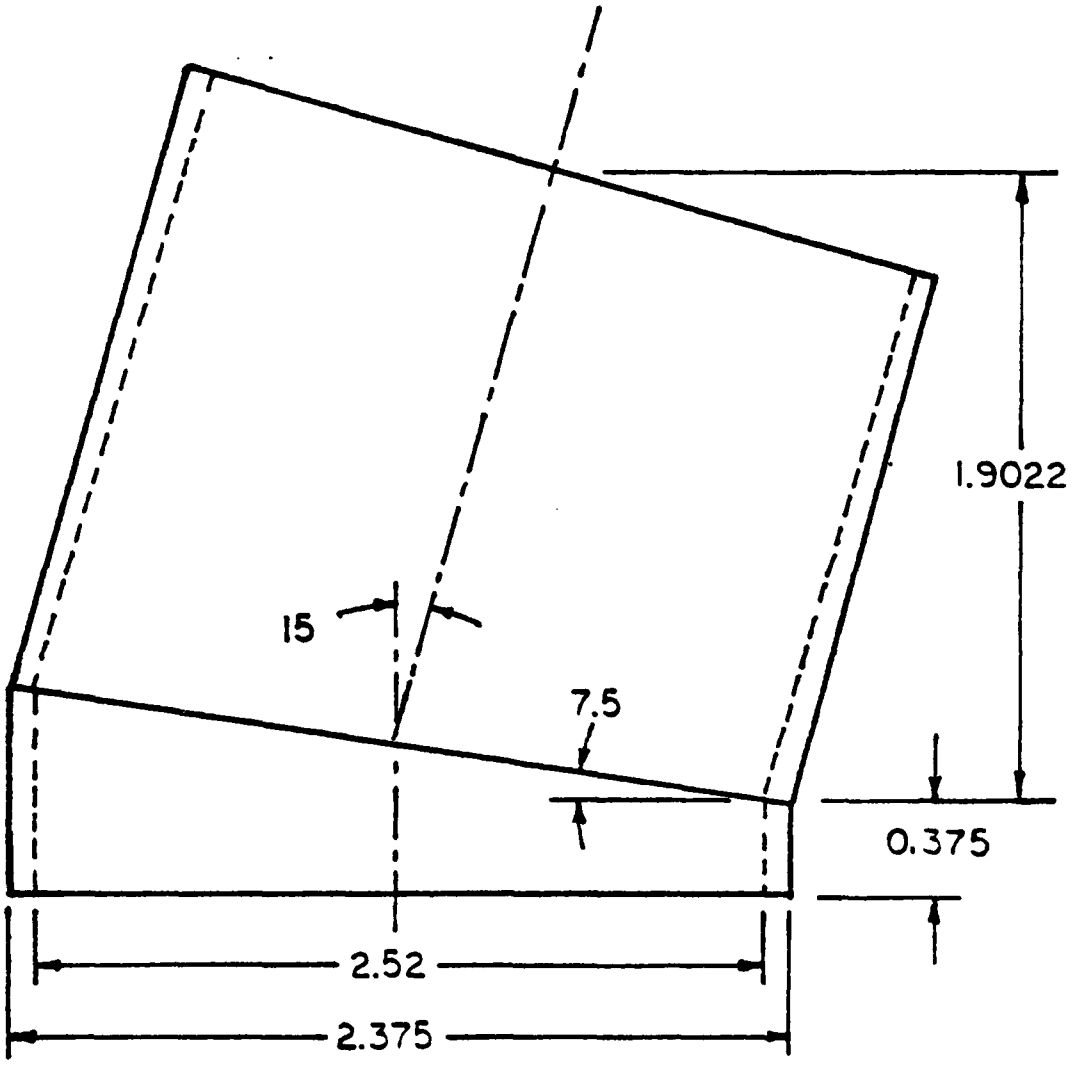

Figure 44, Tilted Nozzle Geometry

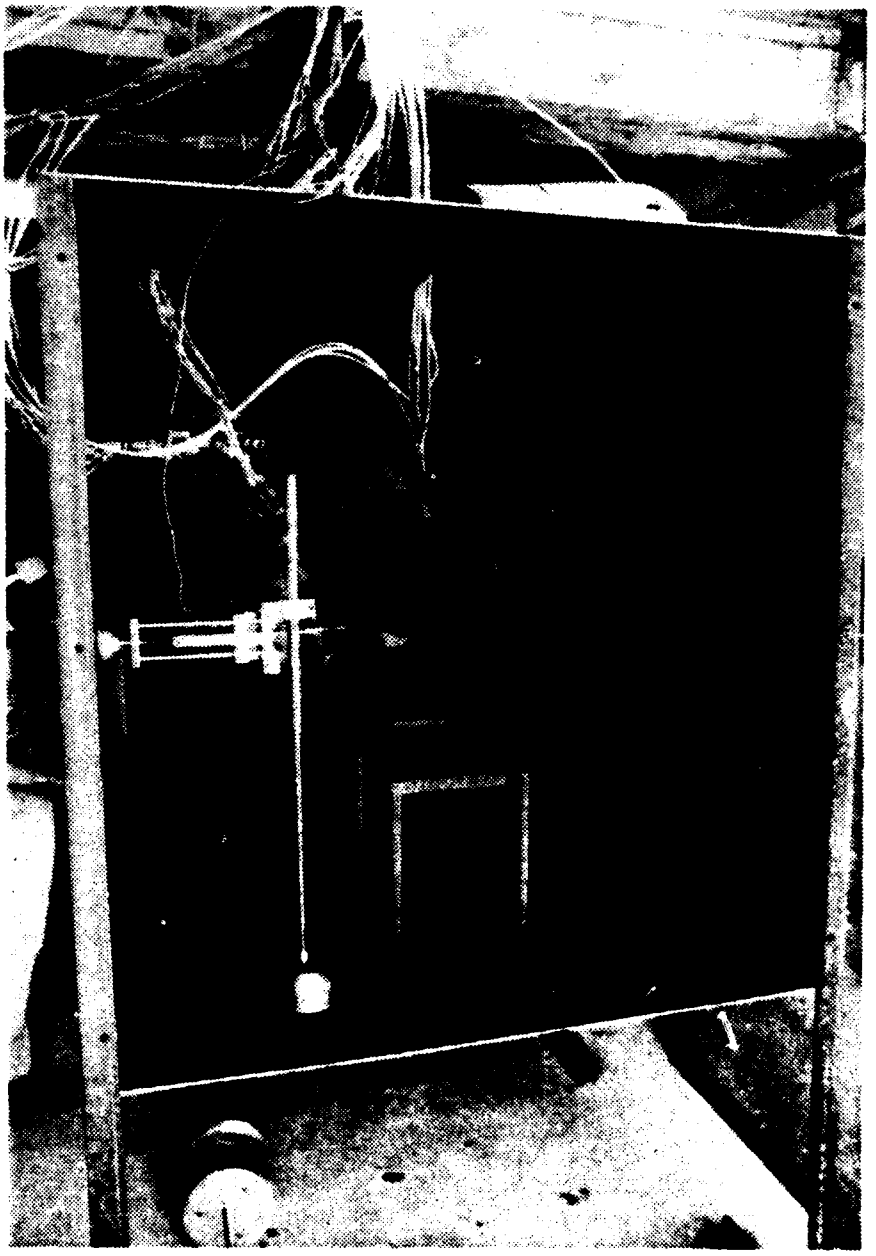

Figure 45, Exit Plane Temperature Measurement

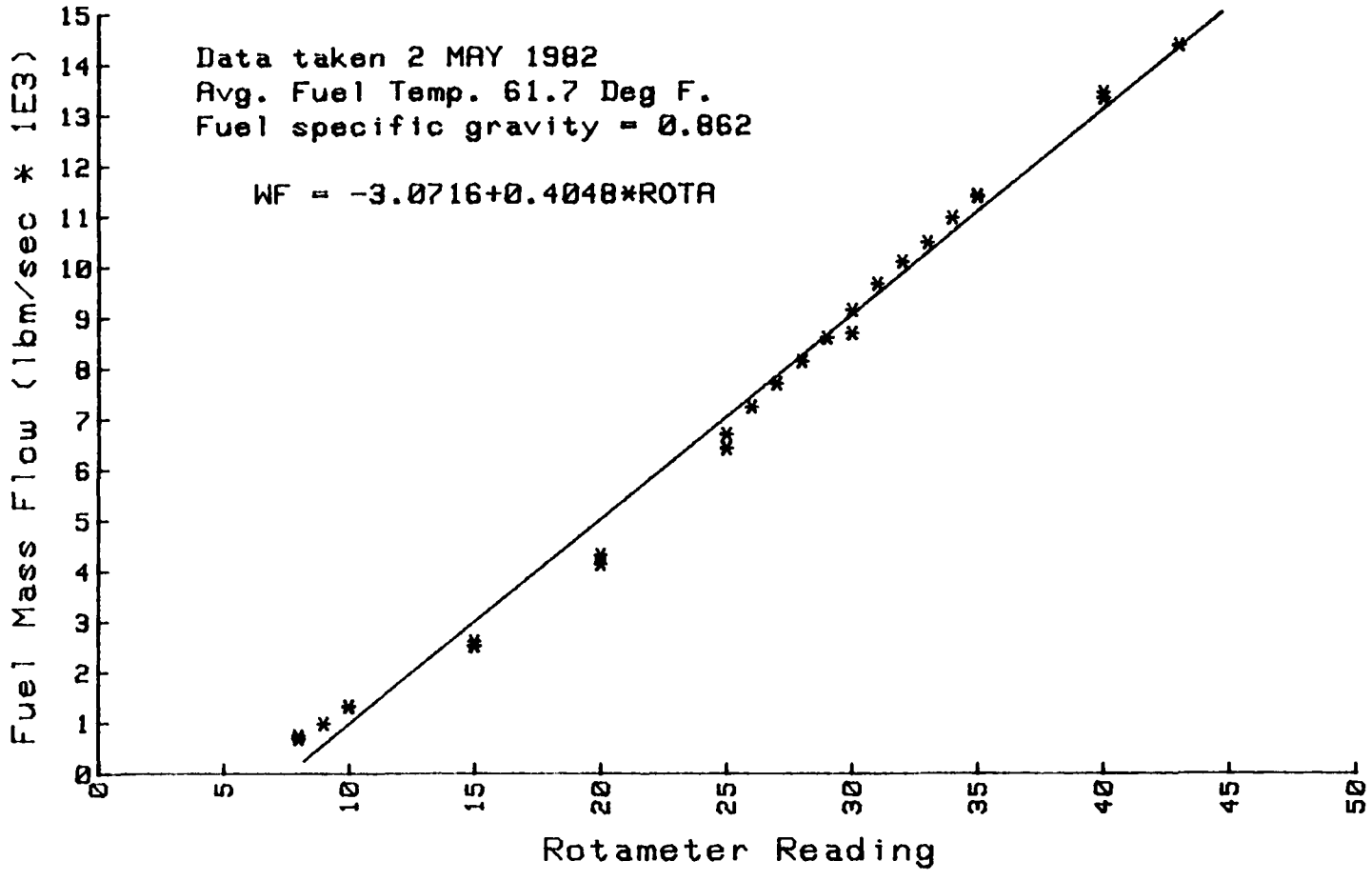

Figure 46, Rotameter Calibration Curve

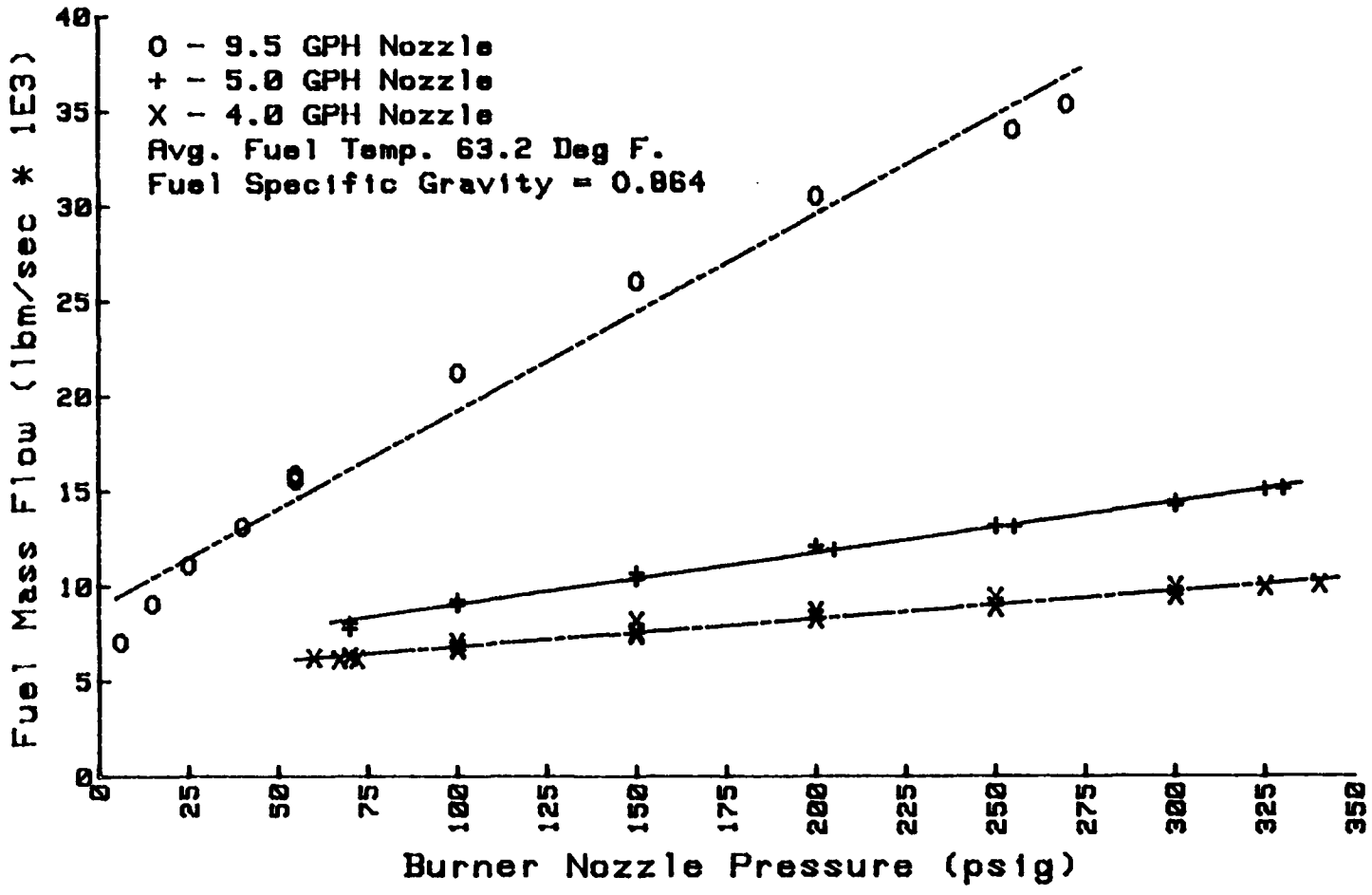

Figure 47, Fuel Mass Flow vs. Burner Nozzle Pressure Comparison

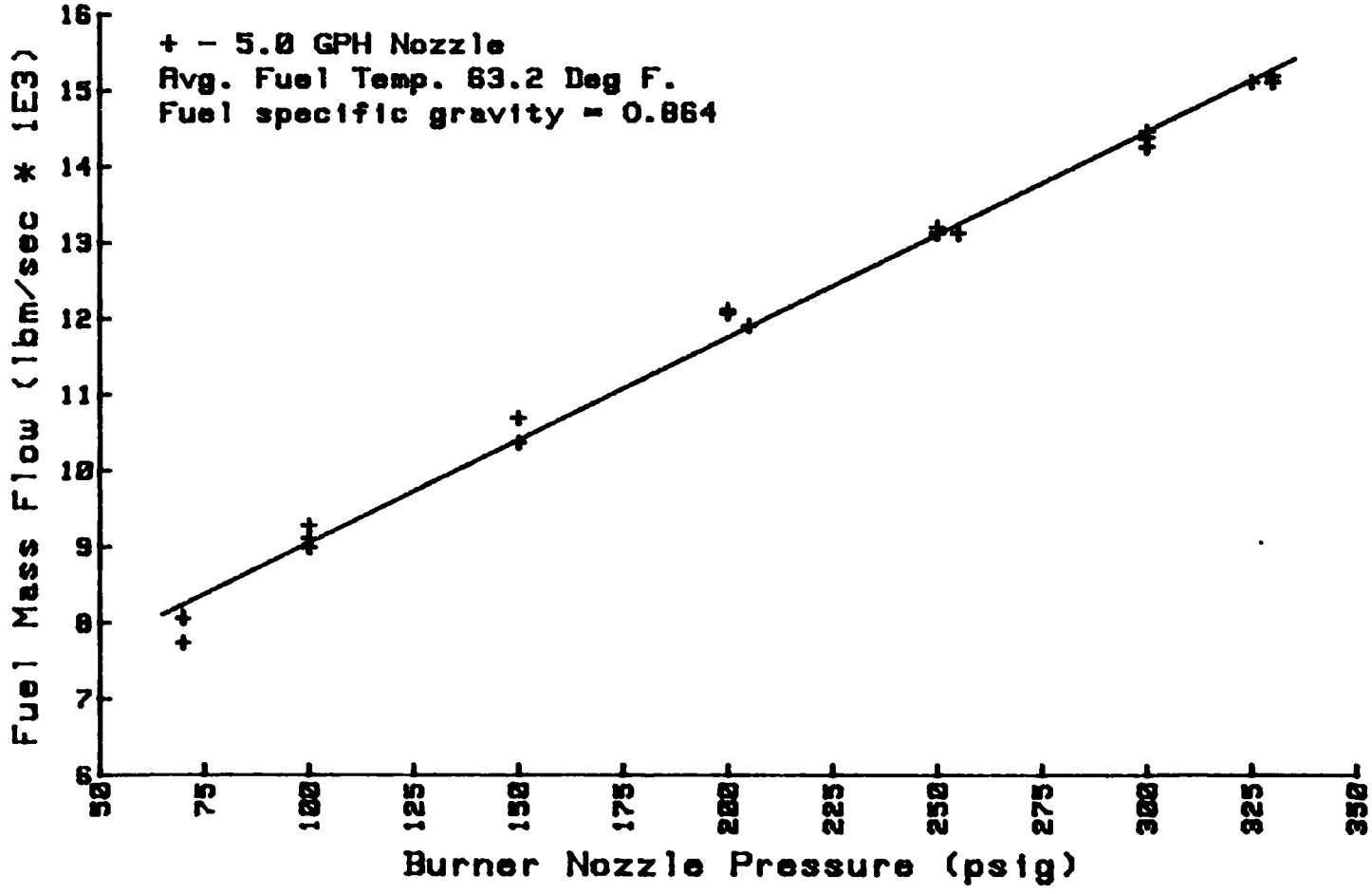

Figure 48, Performance of the 5.0 GPH Nozzle

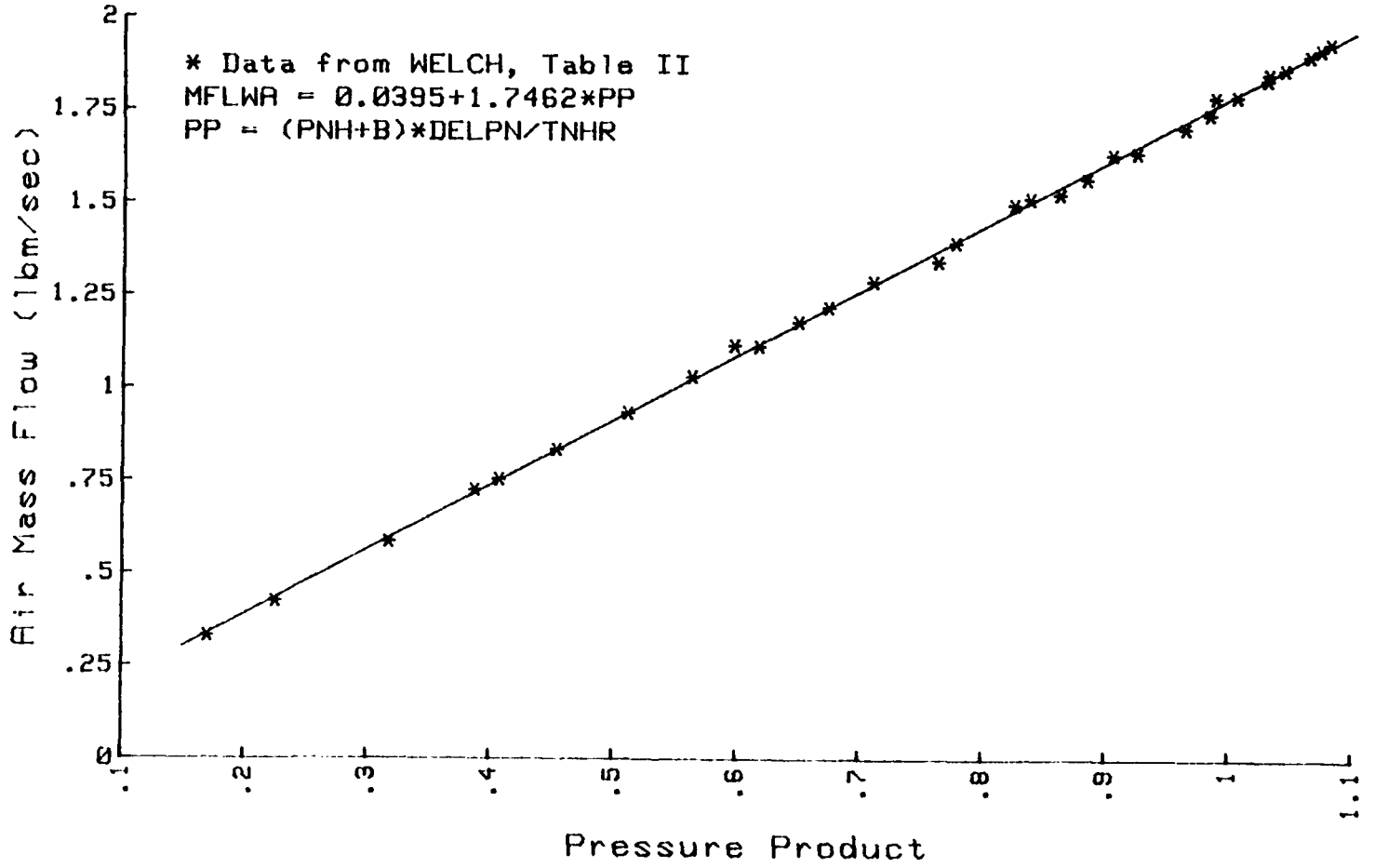

Figure 49, Total Air Mass Flow vs. Pressure Product

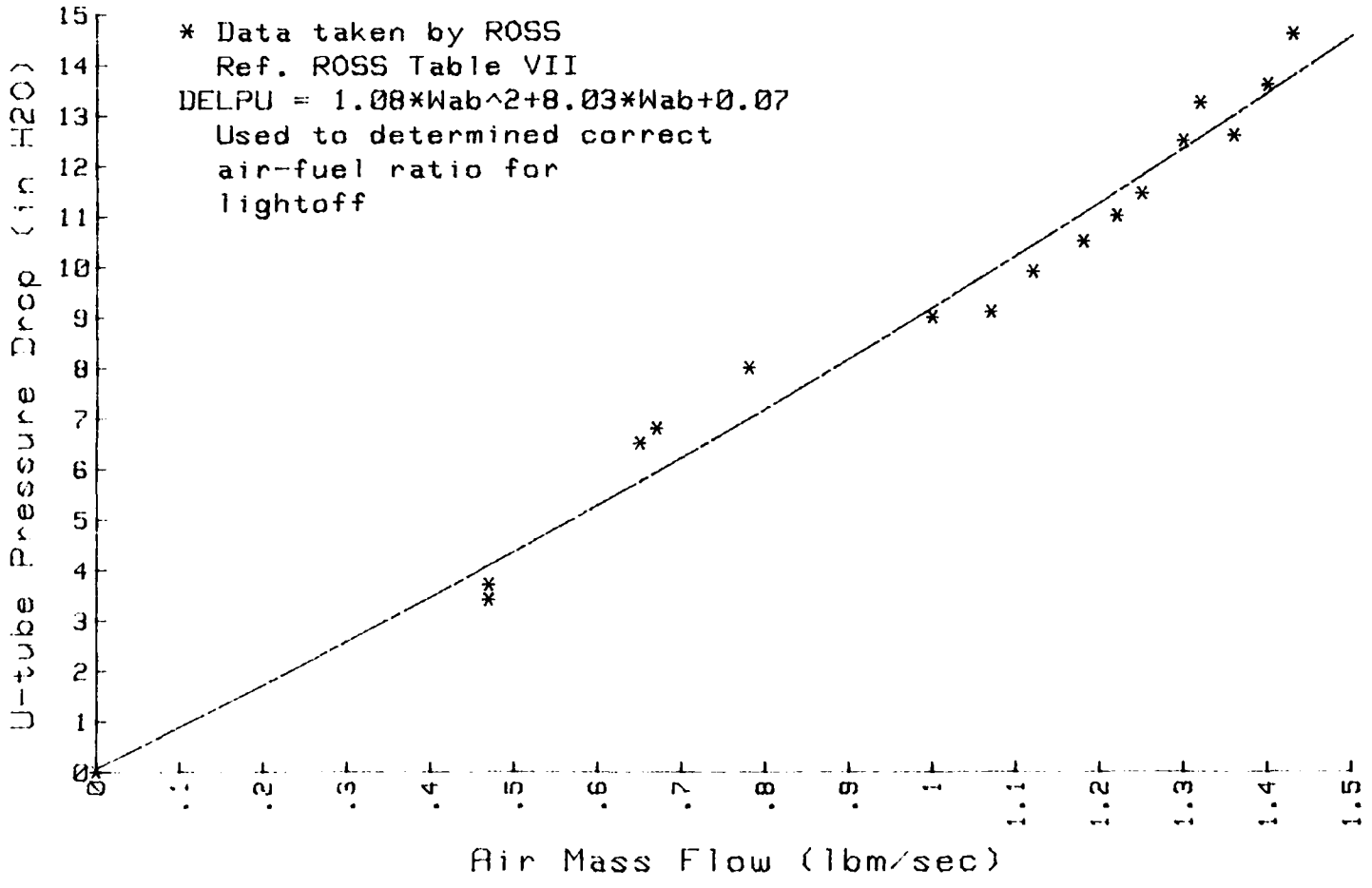

Figure 50, DELPU vs. Burner Air Flow

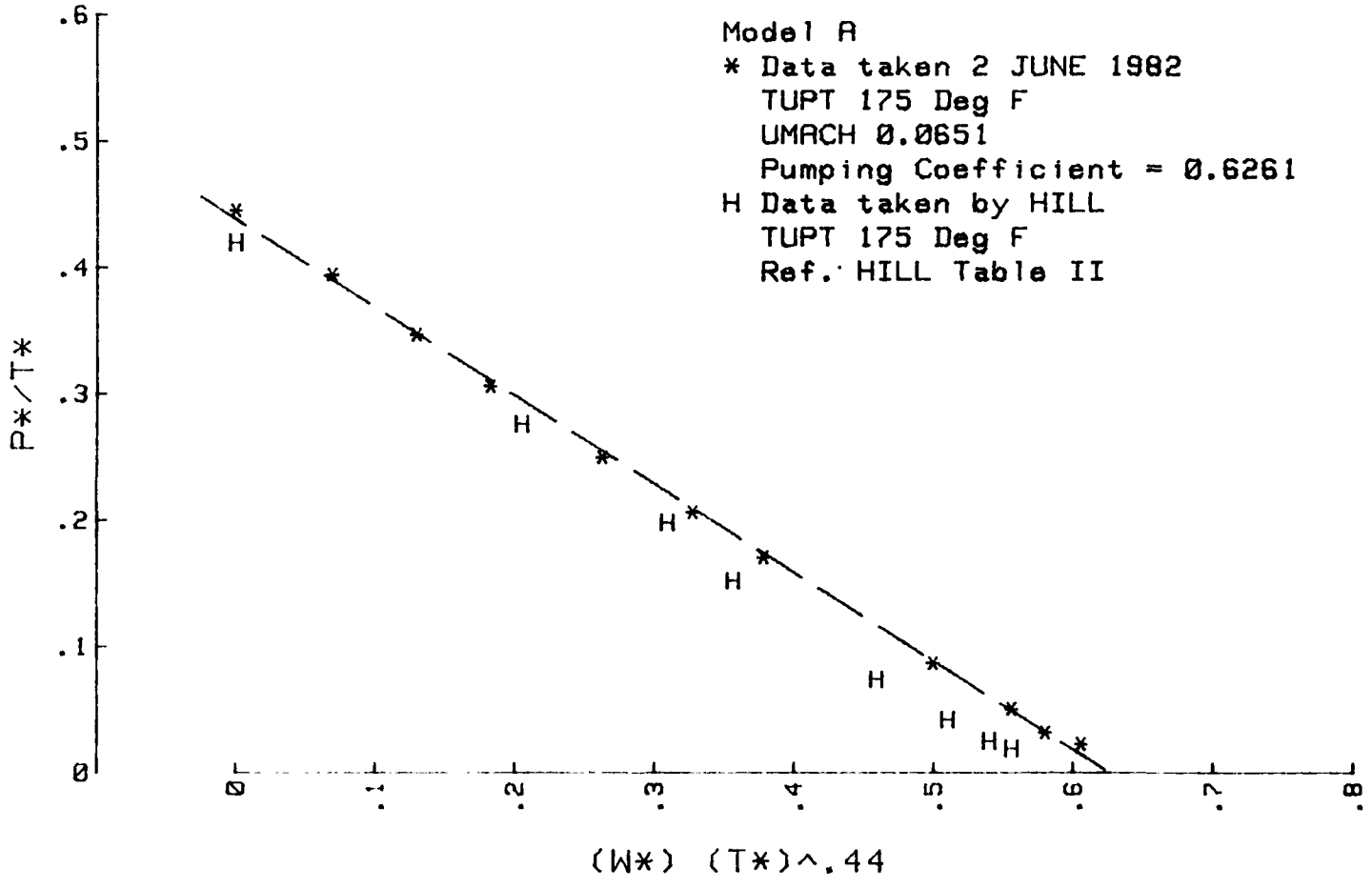

Figure 51, Pumping Coefficient, Model A (175° F)

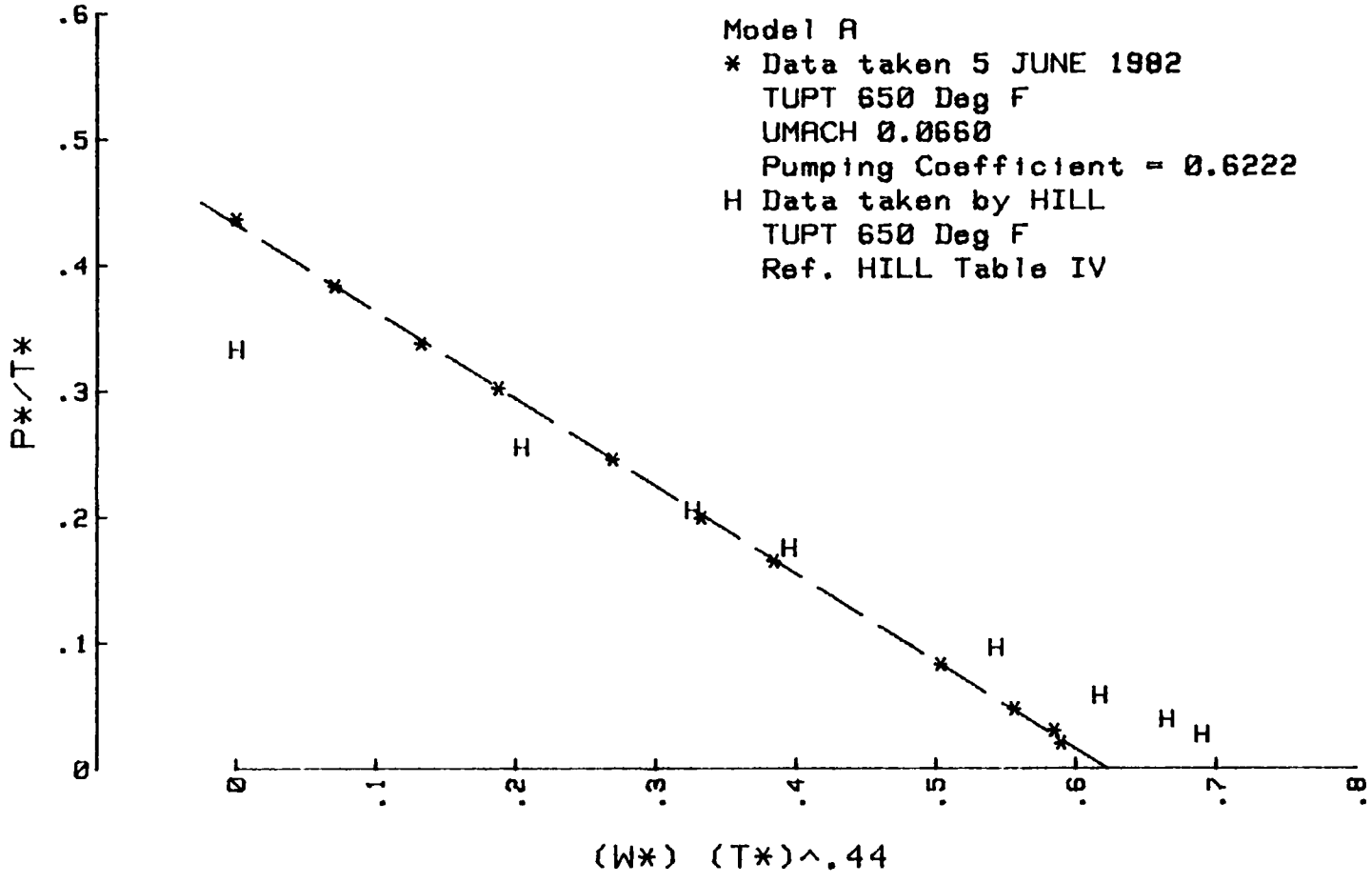

Figure 52, Pumping Coefficient, Model A (650° F)

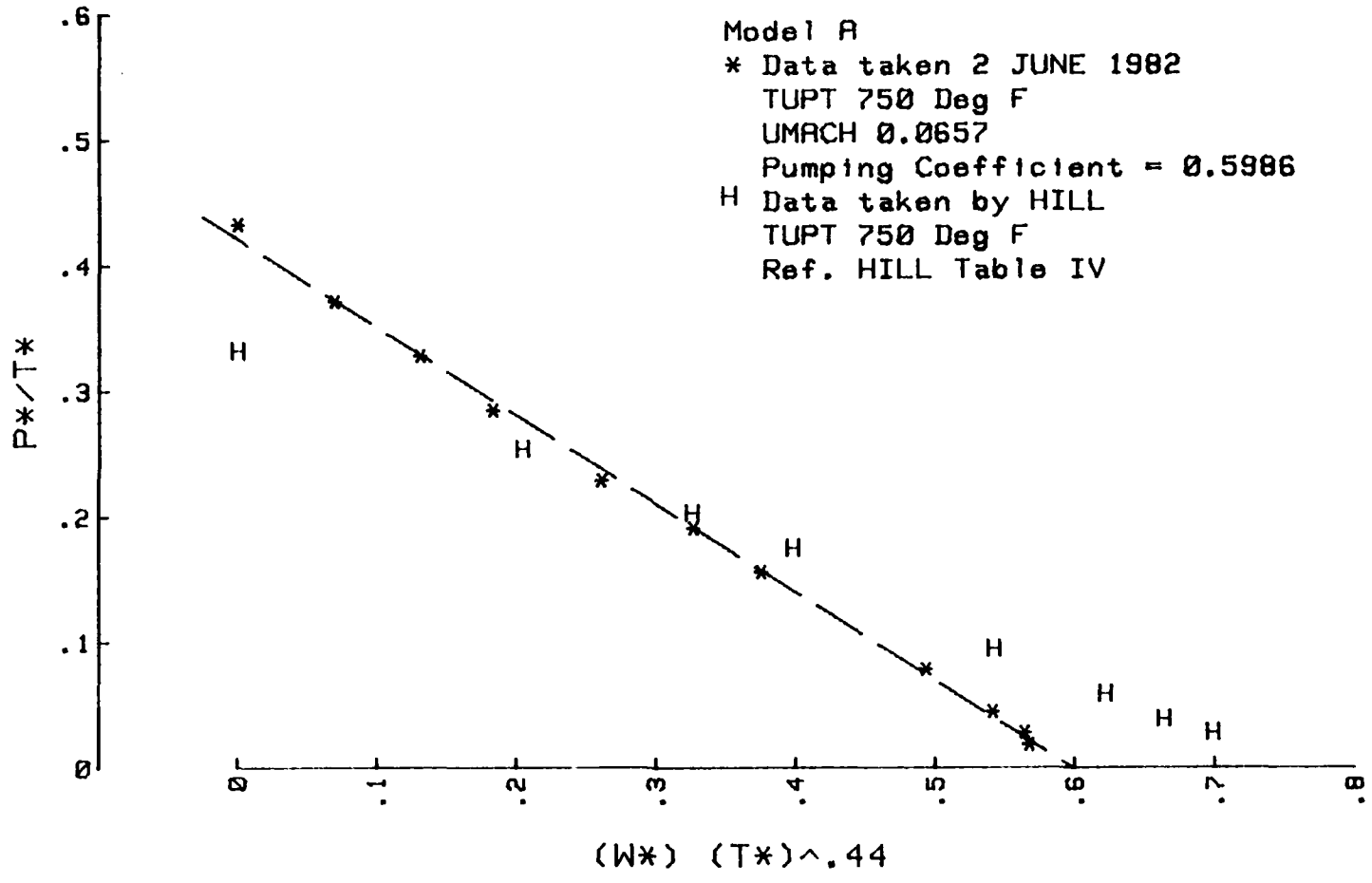

Figure 53, Pumping Coefficient, Model A (750° F)

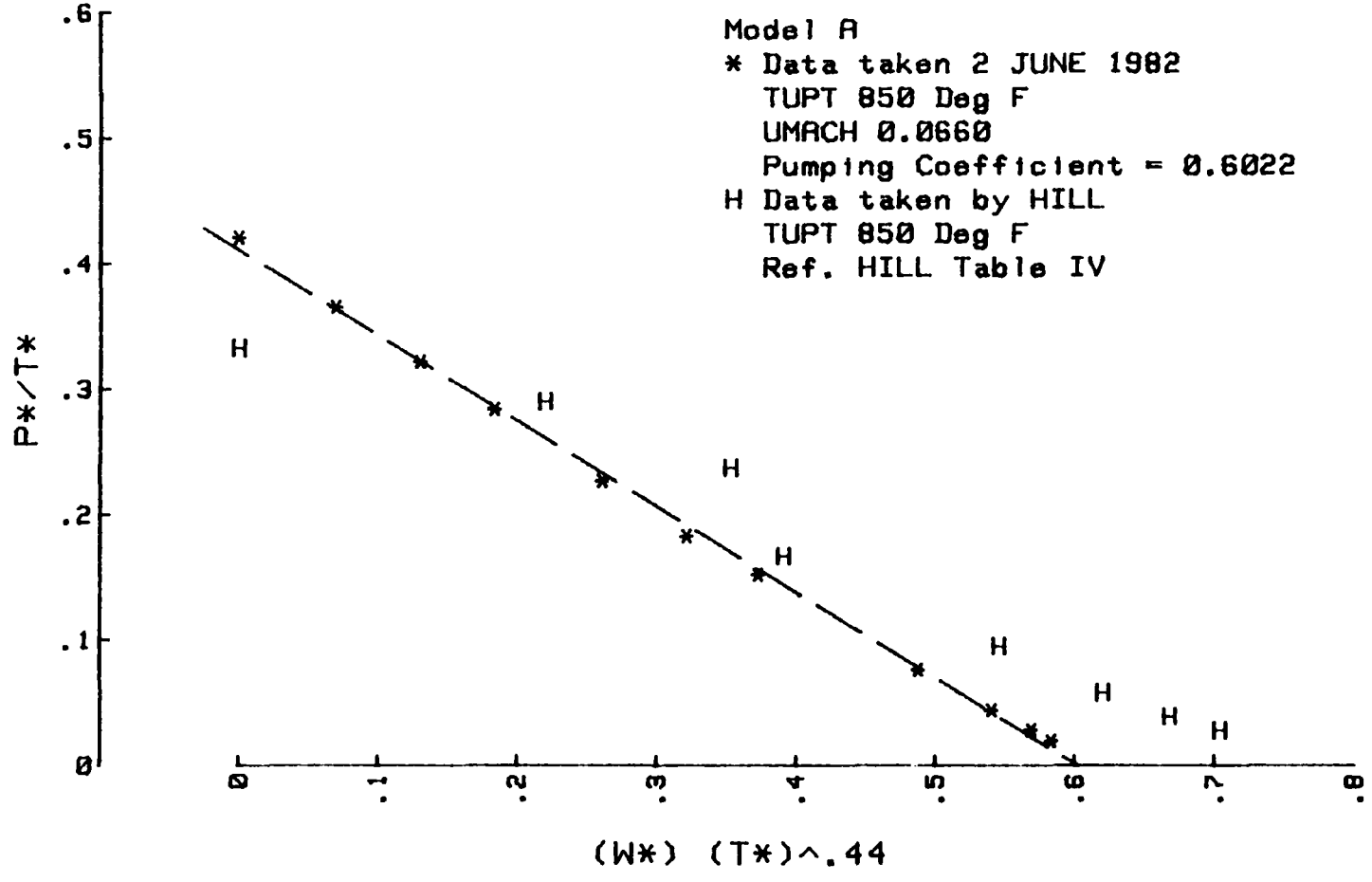

Figure 54, Pumping Coefficient, Model A (850° F)

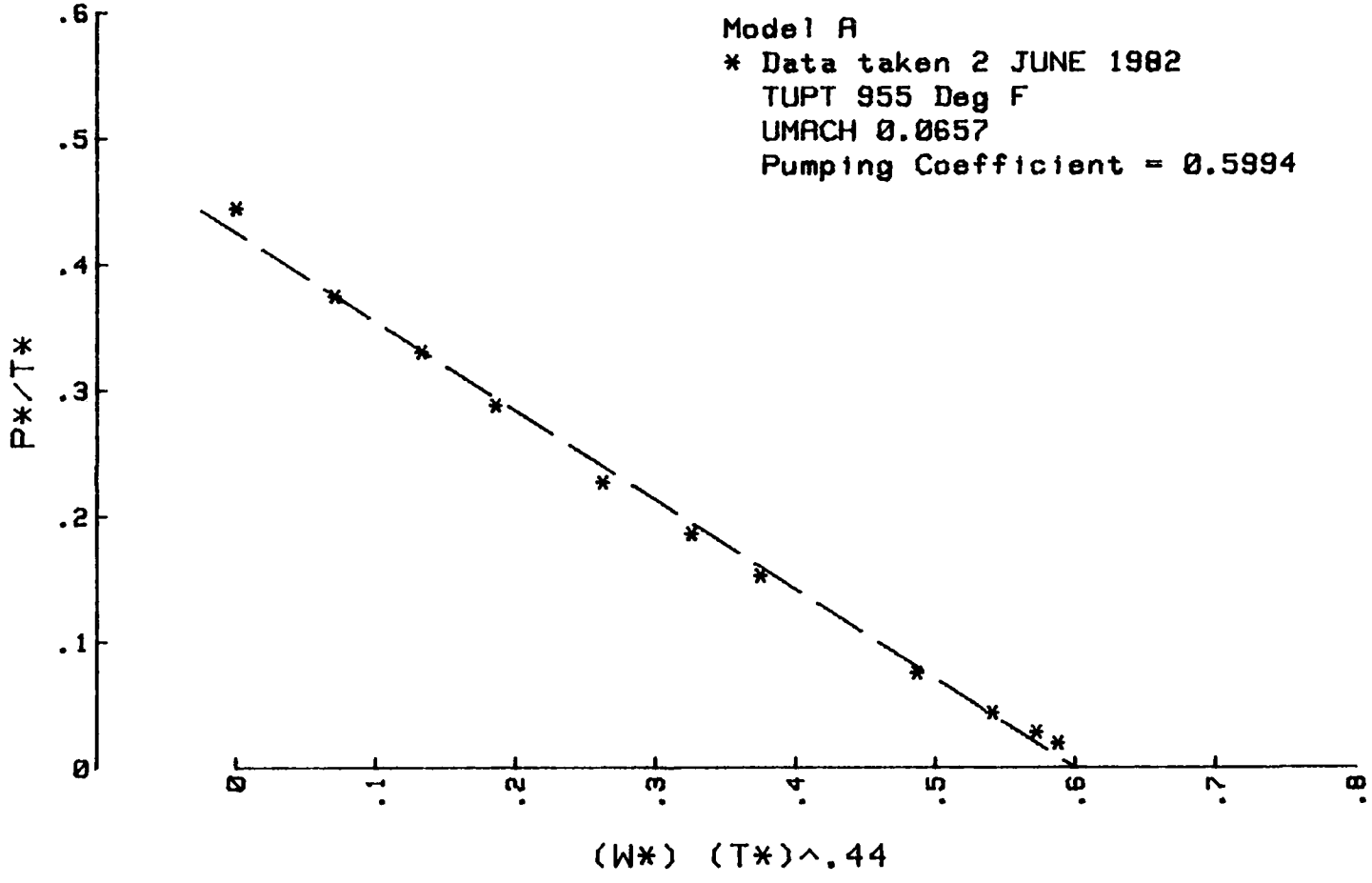

Figure 55, Pumping Coefficient, Model A (955° F)

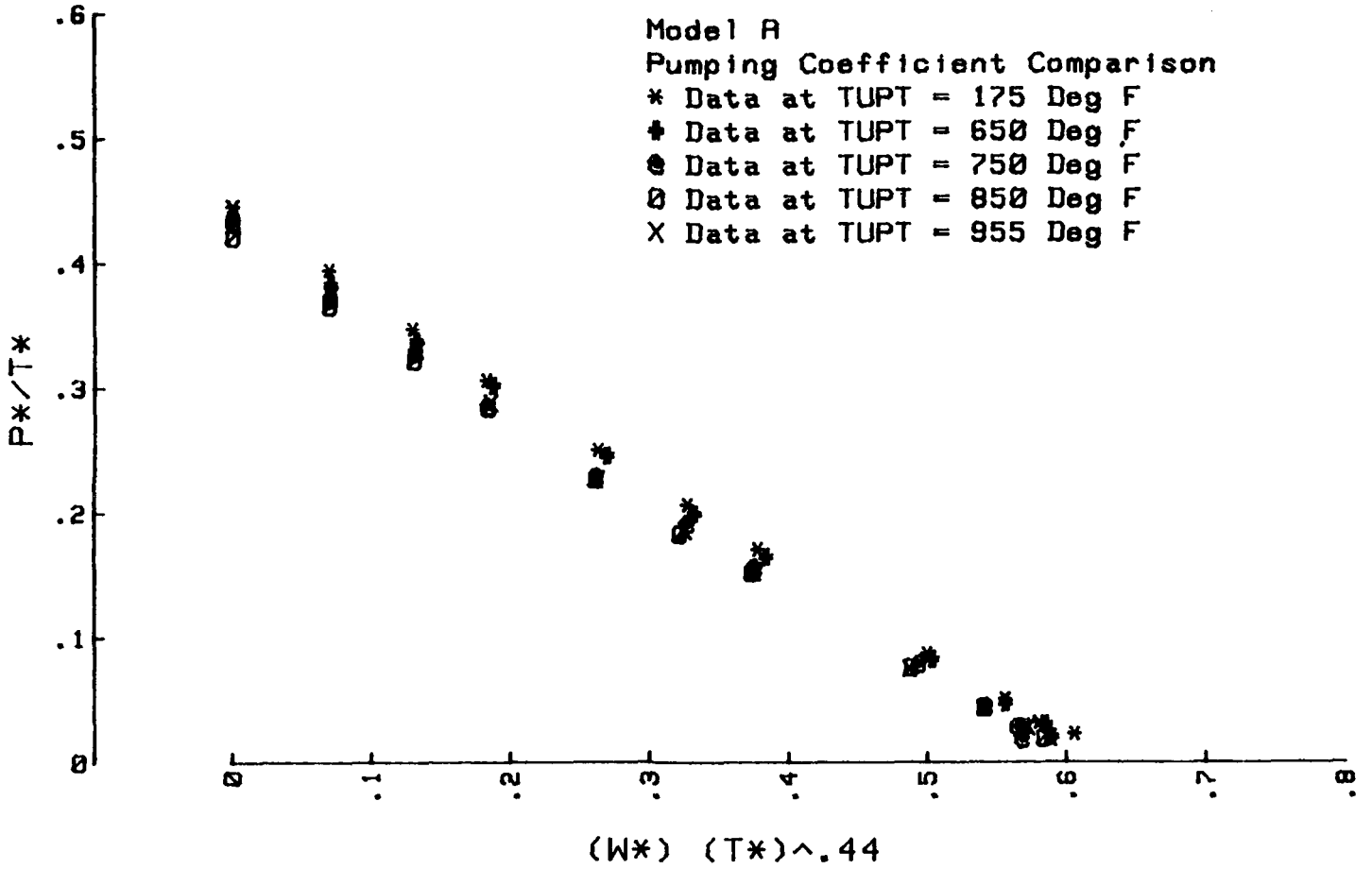

Figure 56, Pumping Coefficient Comparison, Model A

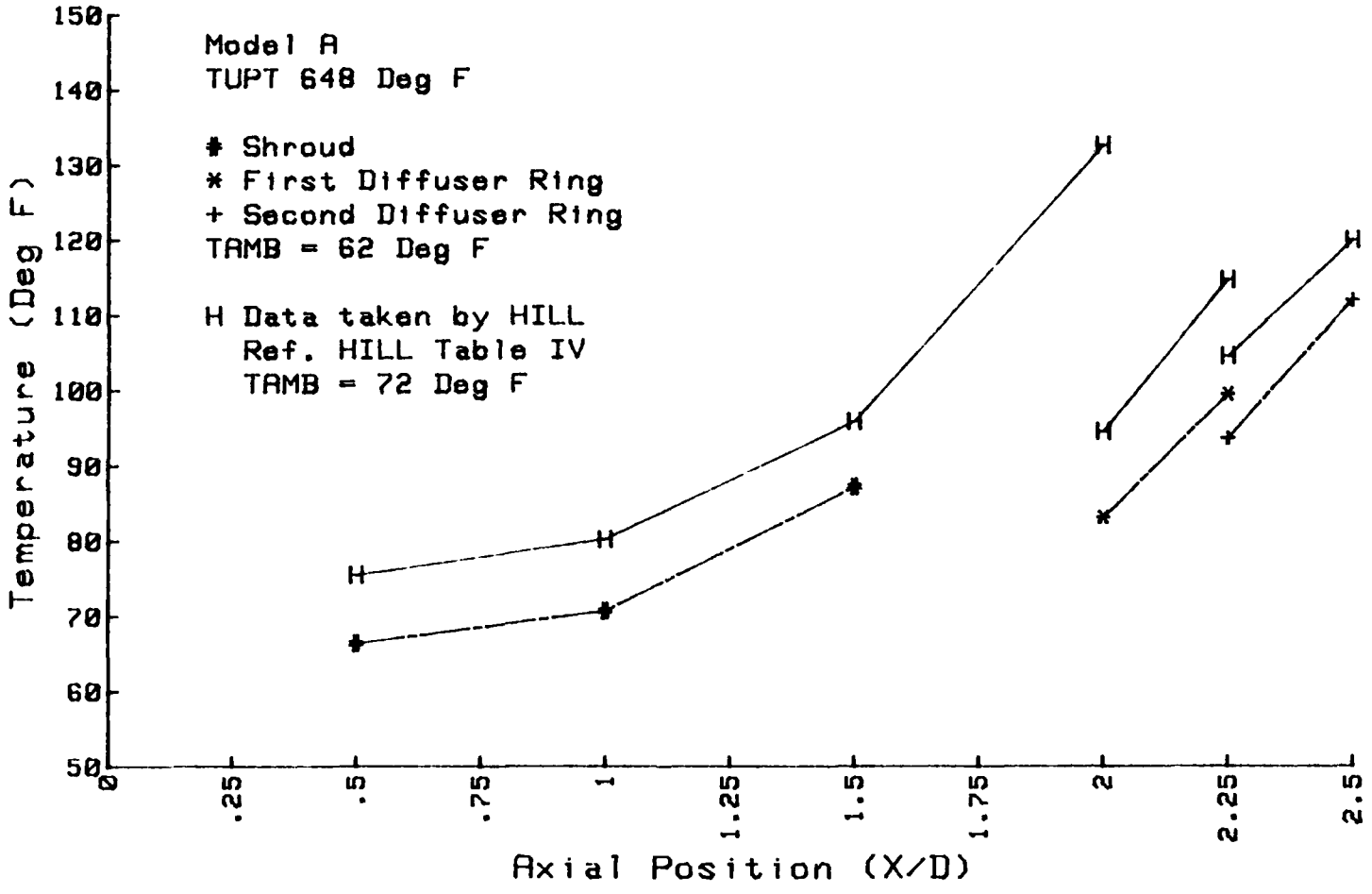

Figure 57, Shroud and Diffuser Temperatures,
Model A (648° F)

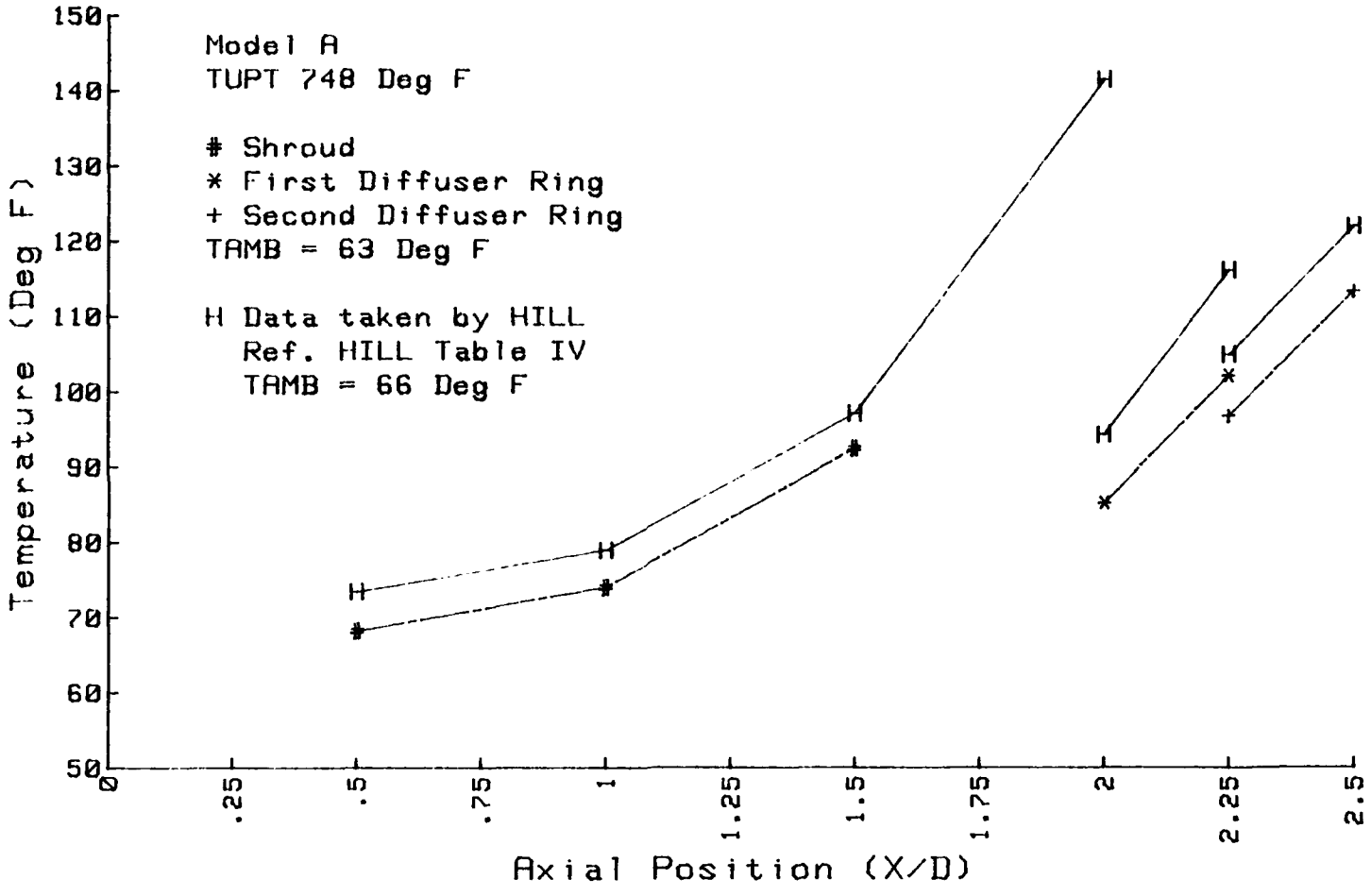

Figure 58, Shroud and Diffuser Temperatures,
Model A (748° F)

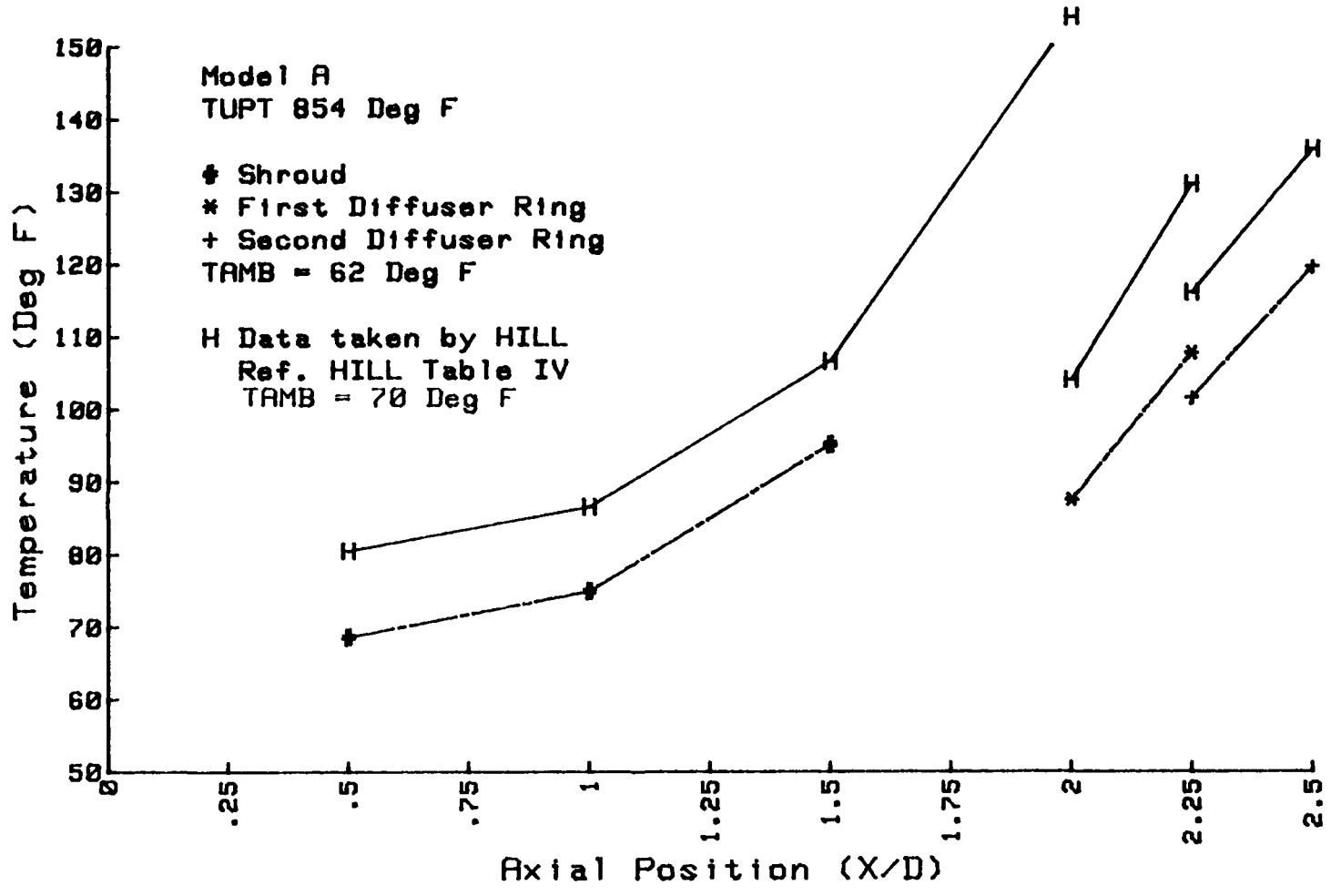

Figure 59, Shroud and Diffuser Temperatures, Model A (854° F)

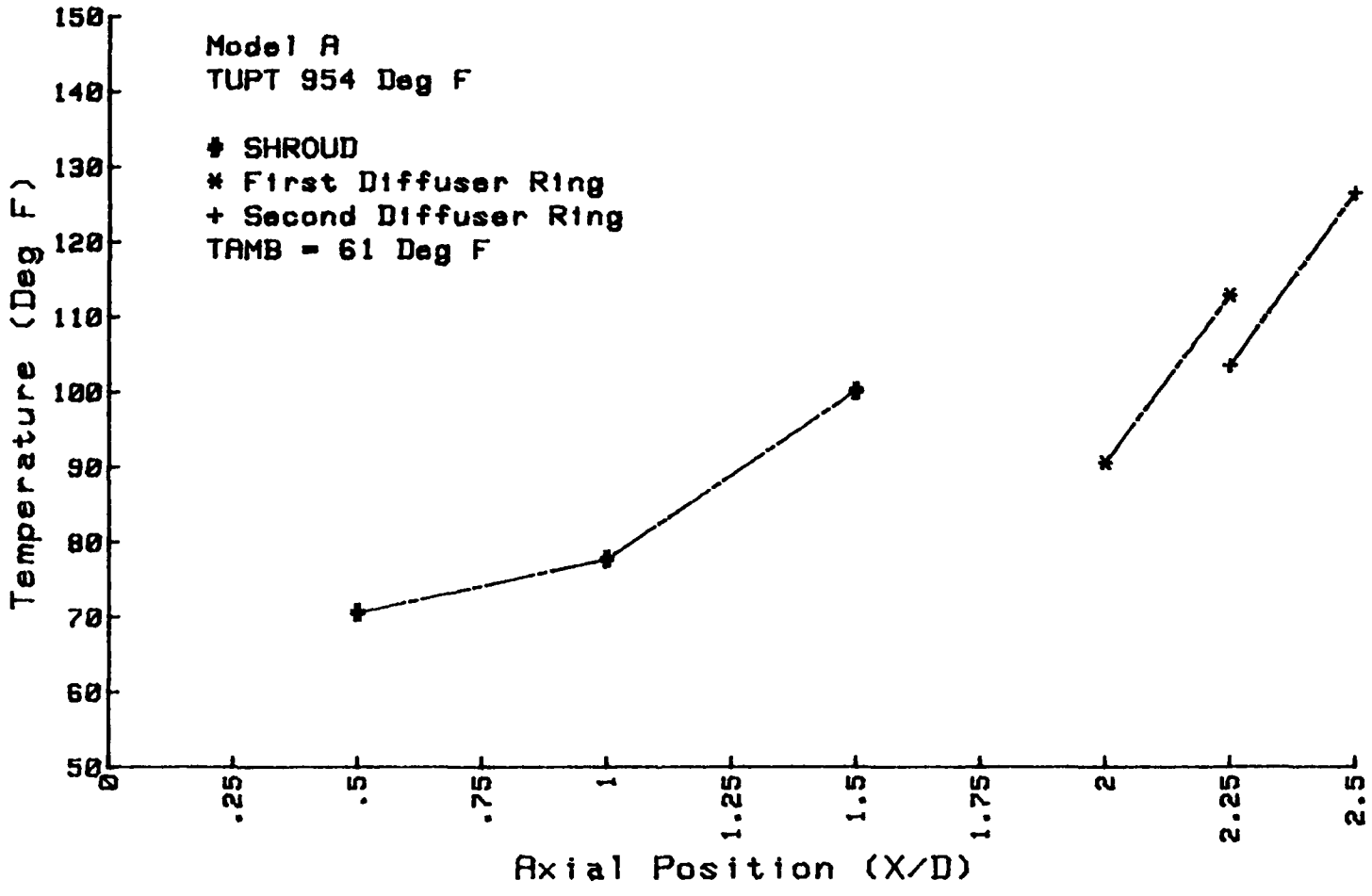

Figure 60, Shroud and Diffuser Temperatures, Model A (954° F)

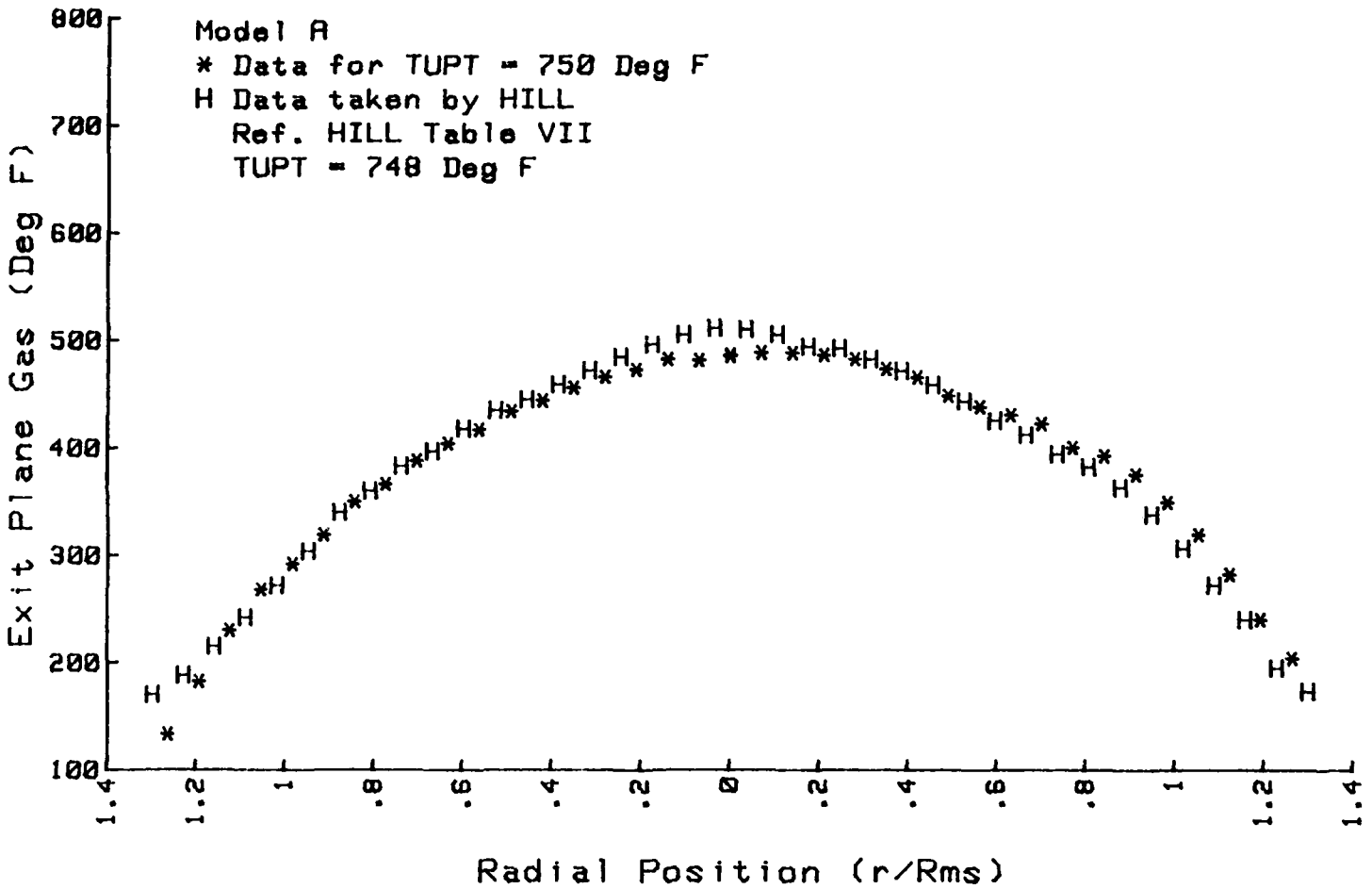

Figure 61, Exit Plane Temperatures Model A (750^{O} F)

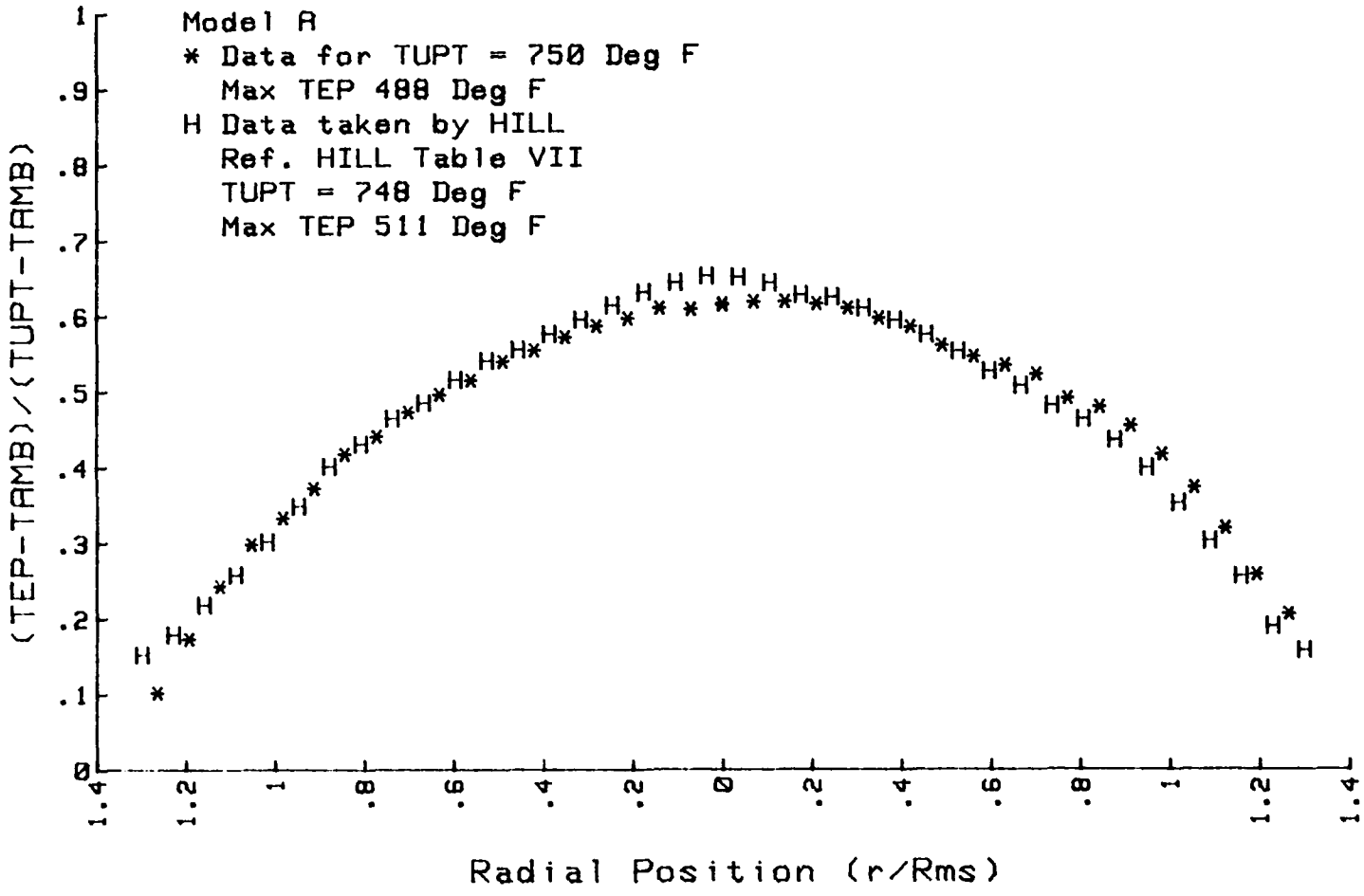

Figure 62, Exit Plane Coefficients, Model A (750° F)

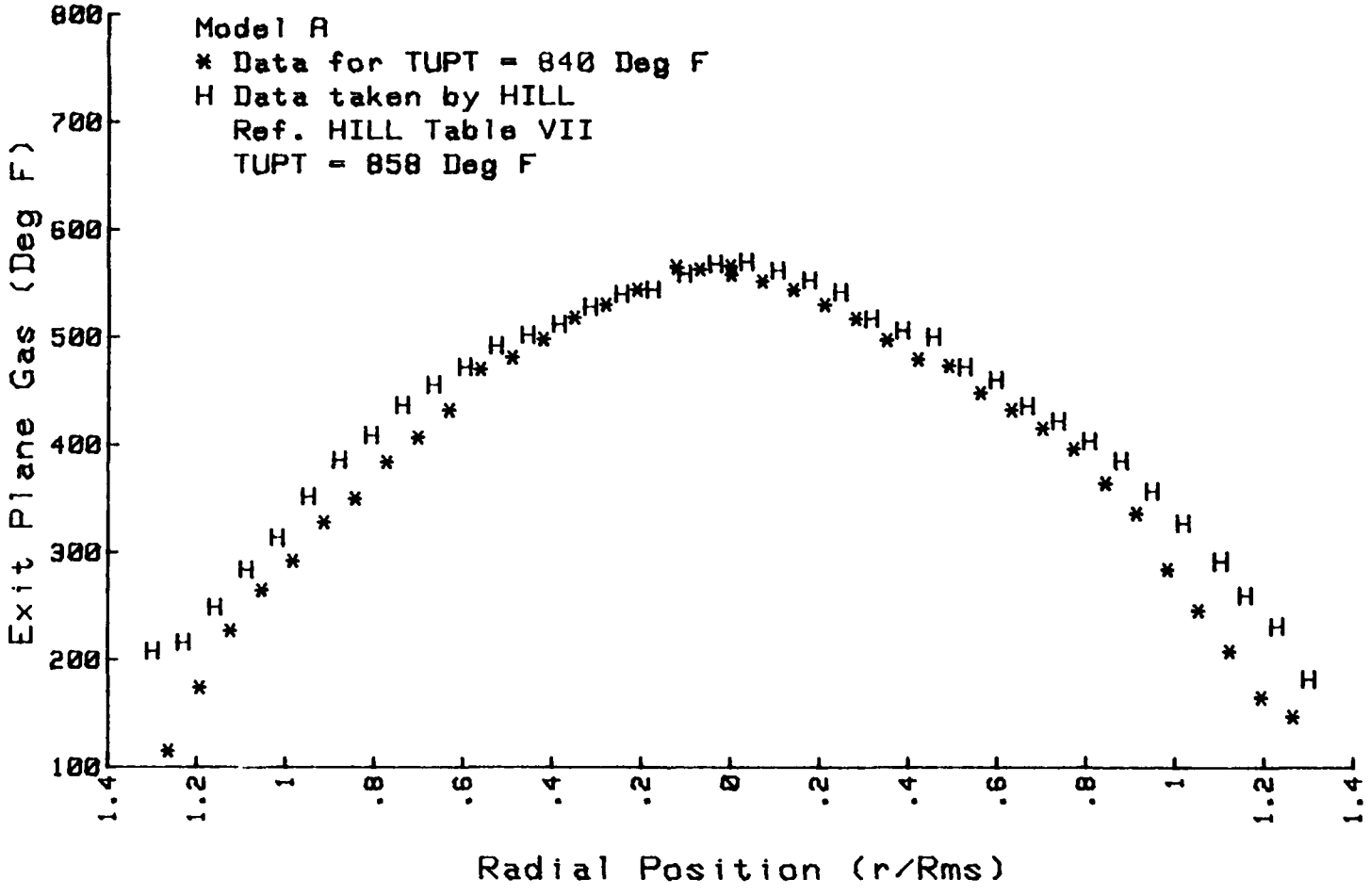

Figure 63, Exit Plane Temperatures, Model A (840^{O} F)

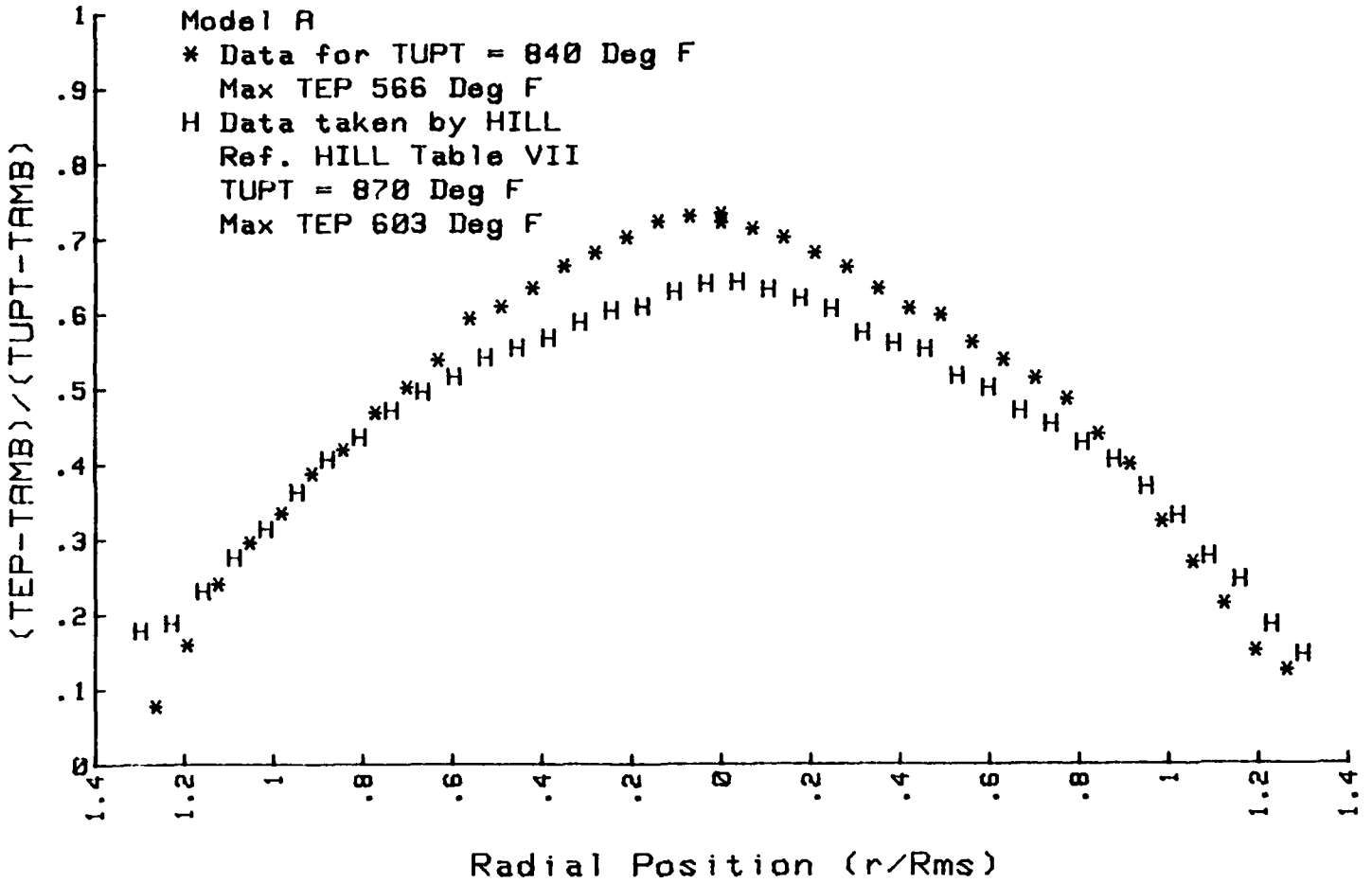

Figure 64, Exit Plane Coefficients, Model A (840° F)

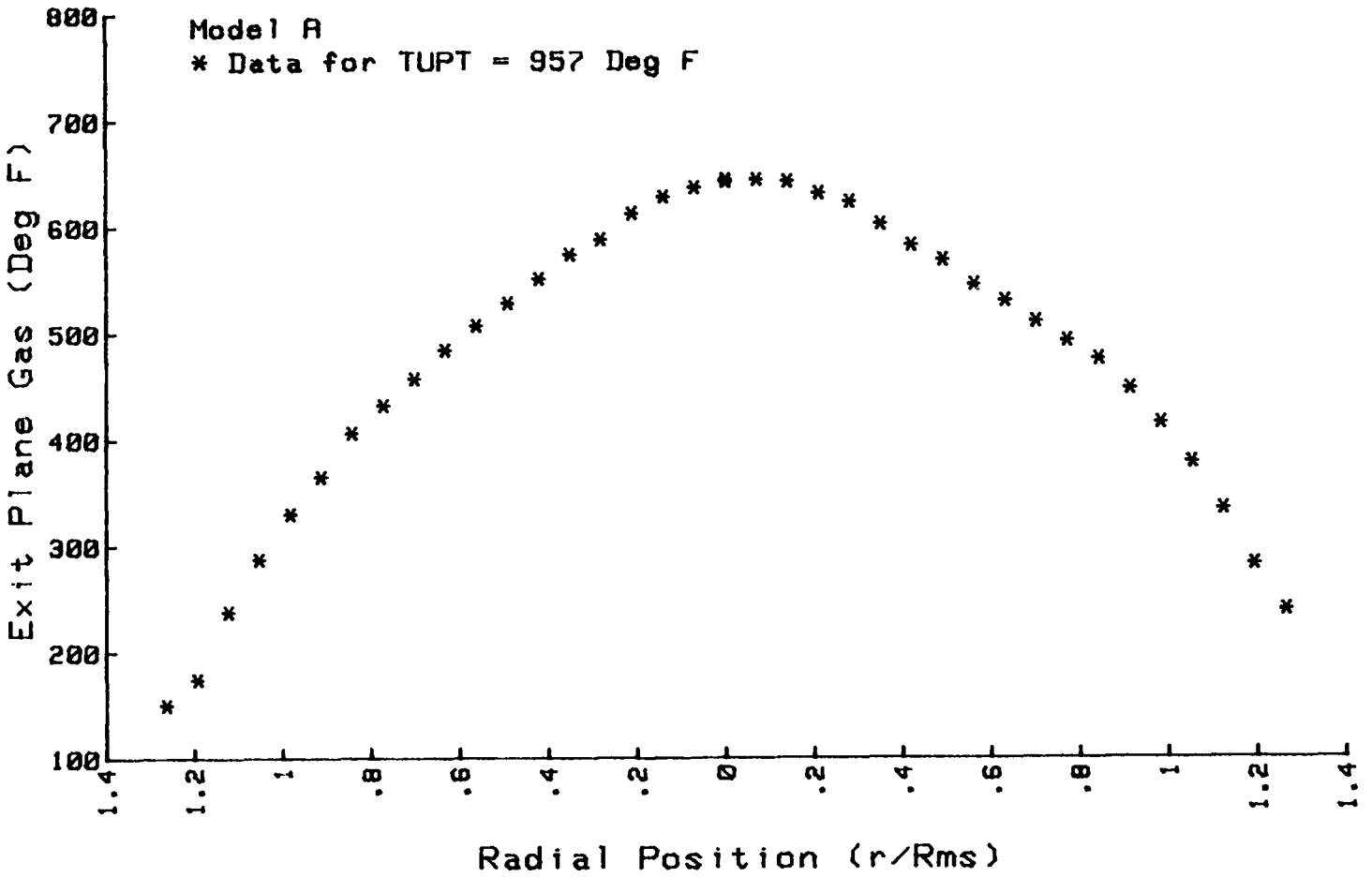

Figure 65, Exit Plane Temperatures, Model A (957^{O} F)

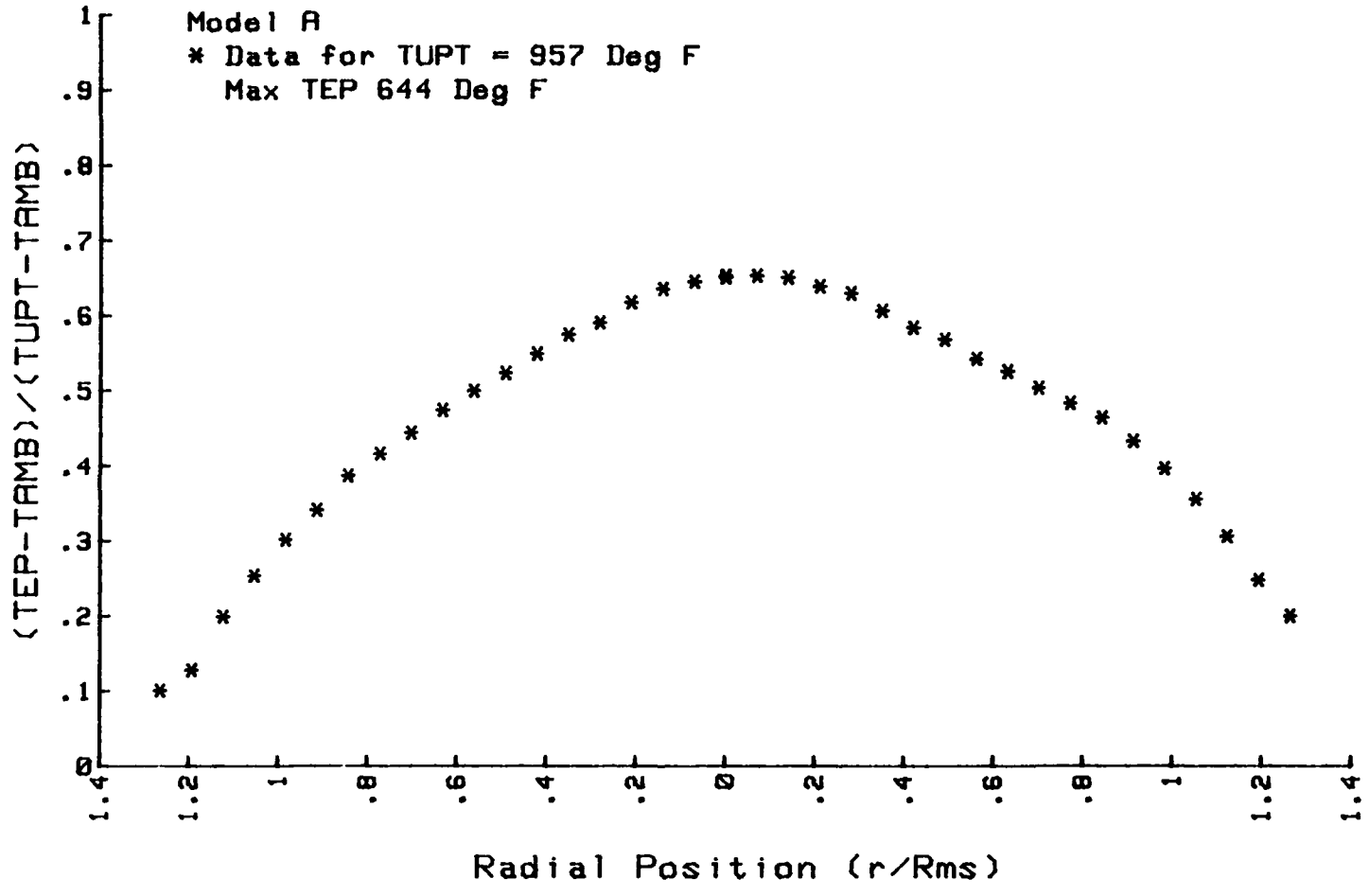

Figure 66, Exit Plane Coefficients, Model A (957^{O} F)

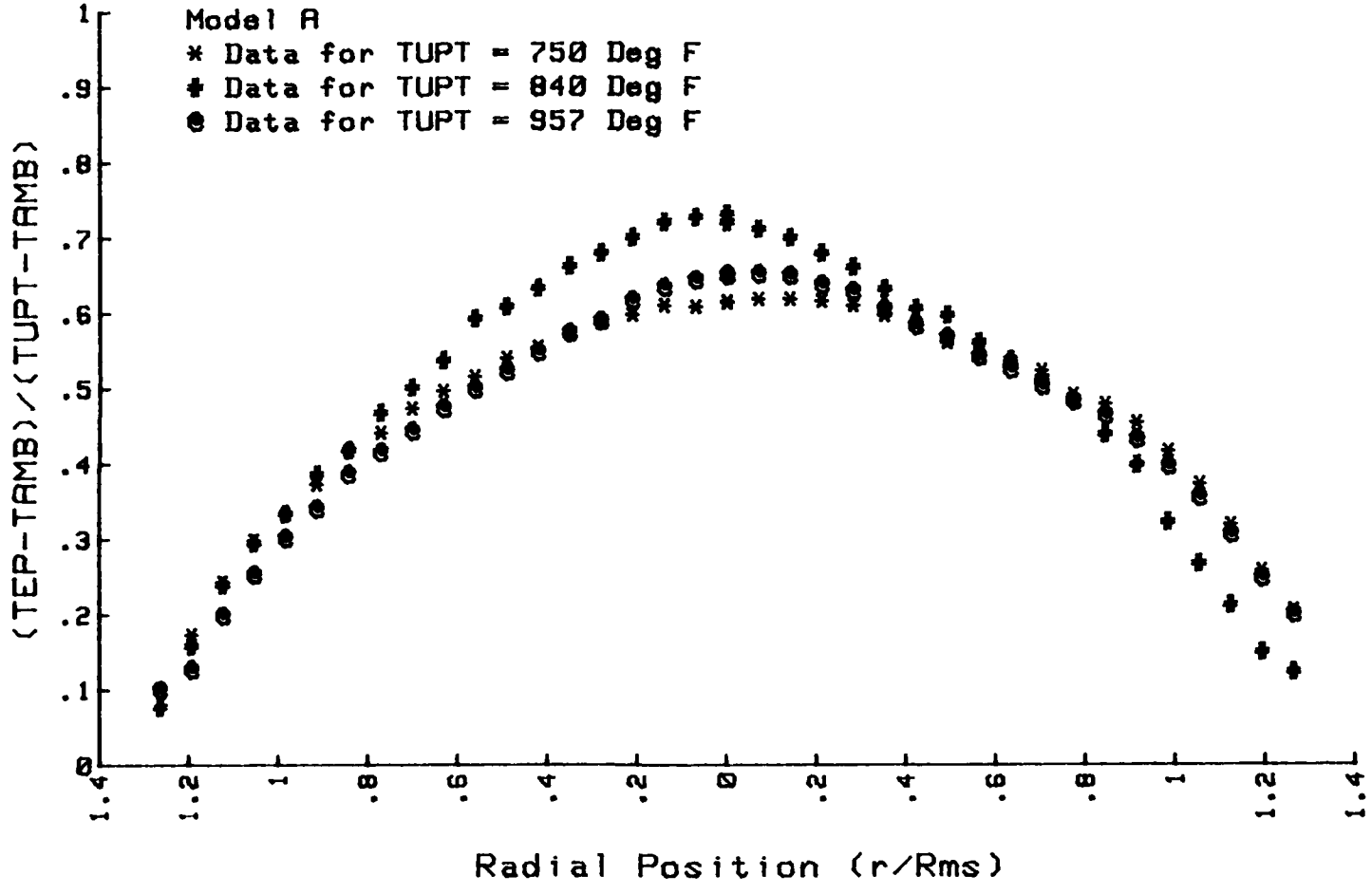

Figure 67, Exit Plane Coefficient Comparison, Model A

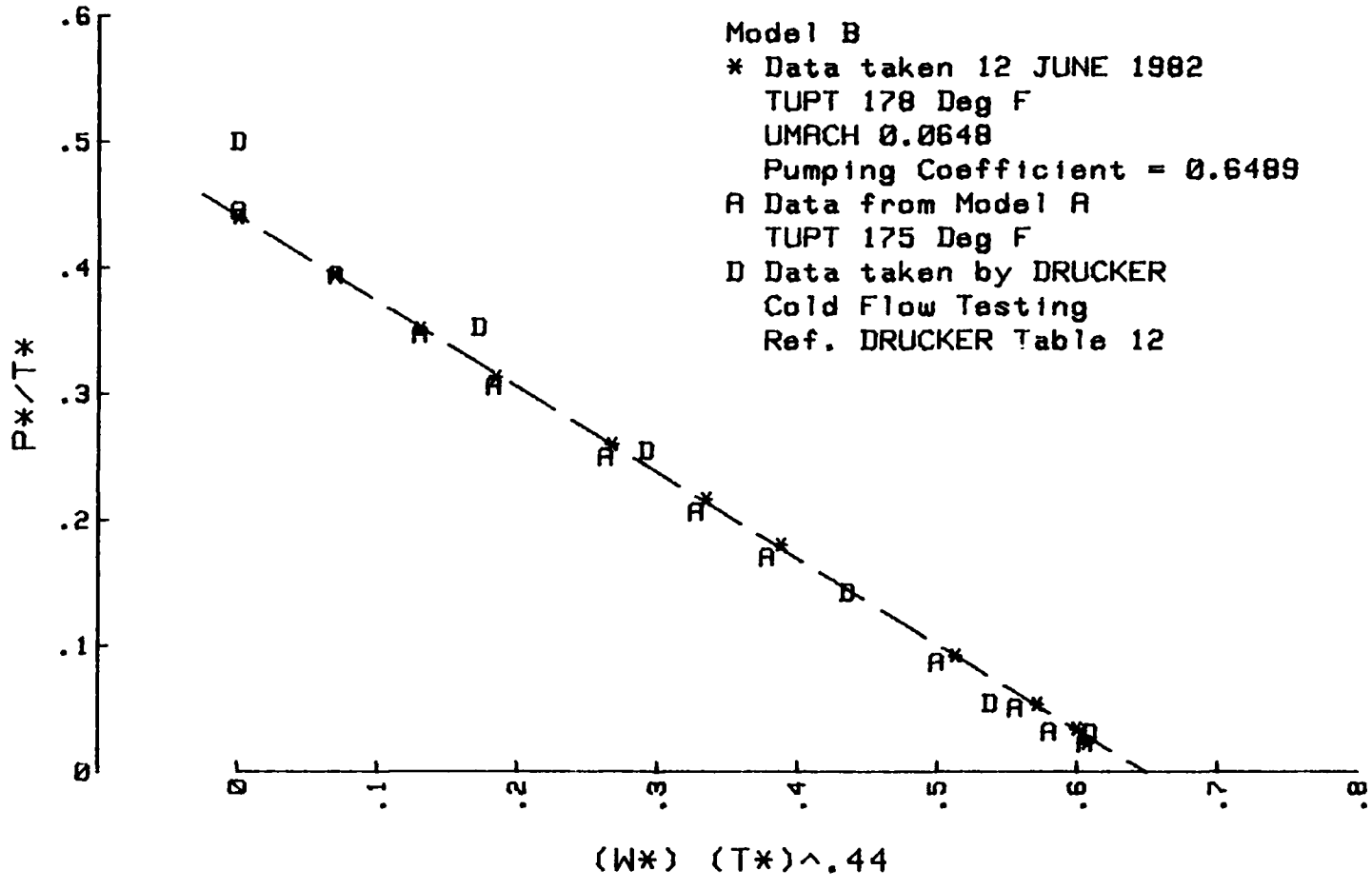

Figure 68, Pumping Coefficient, Model B (178° F)

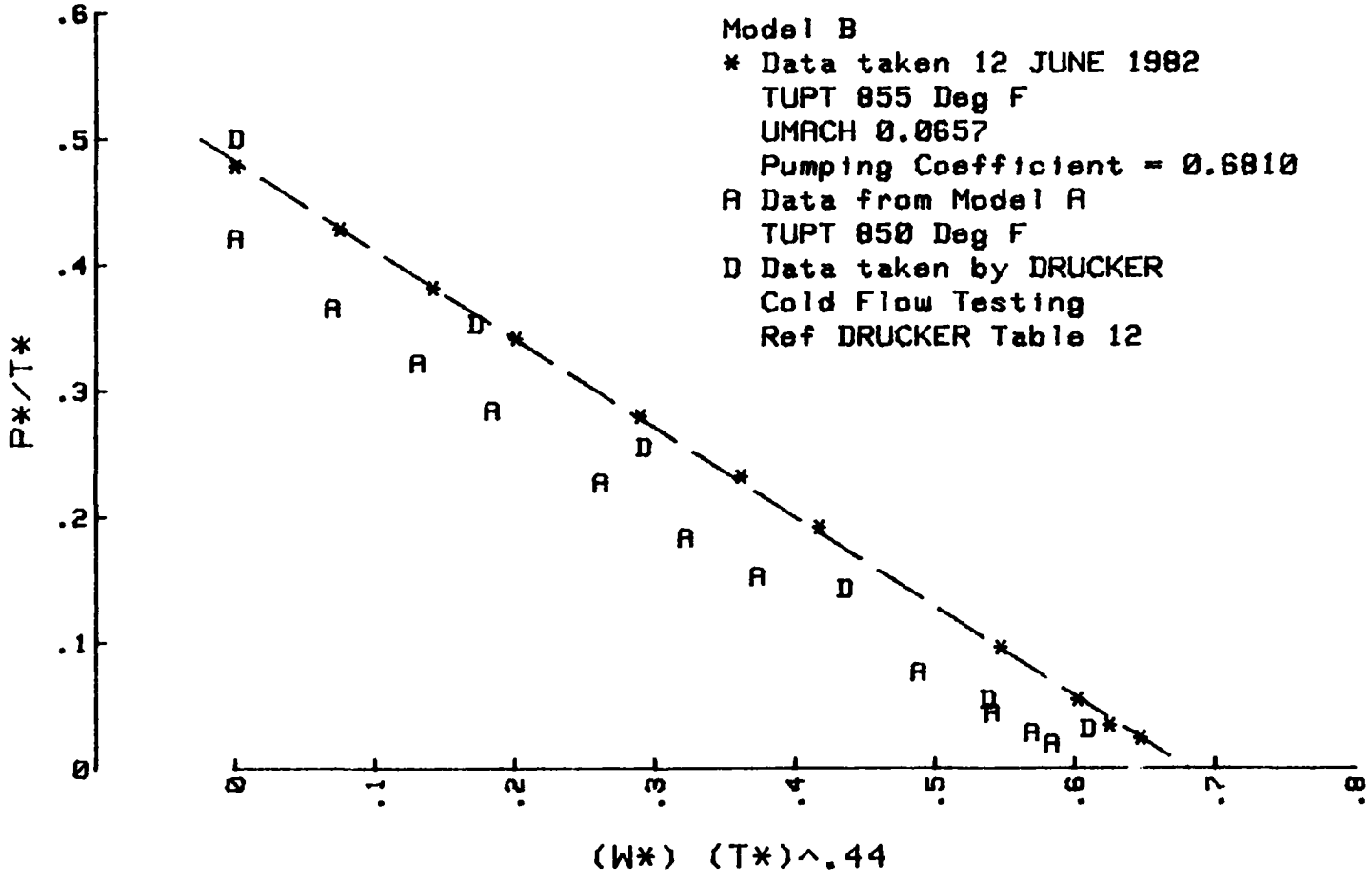

Figure 69, Pumping Coefficient, Model B (855° F)

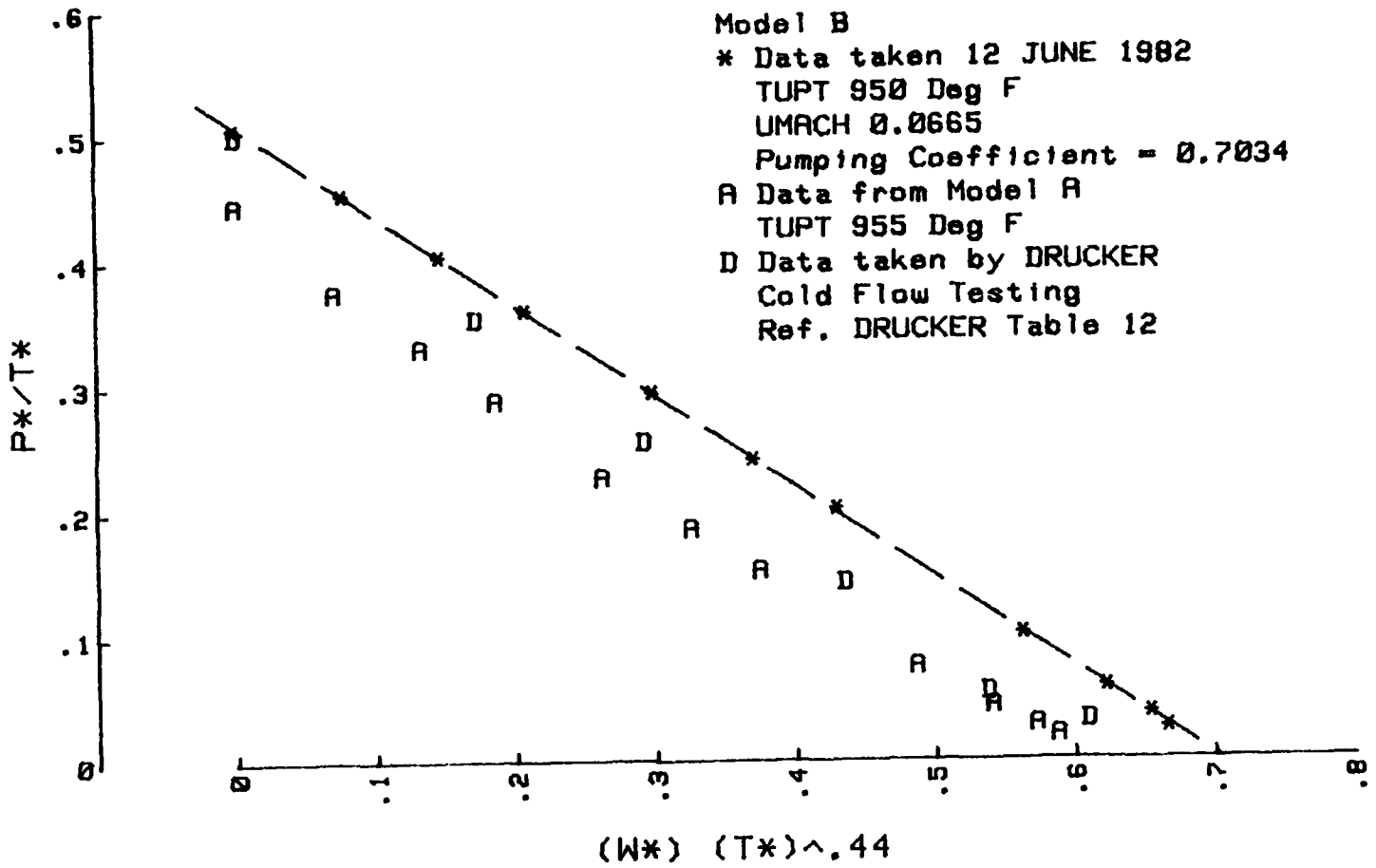

Figure 70, Pumping Coefficient, Model B (950° F)

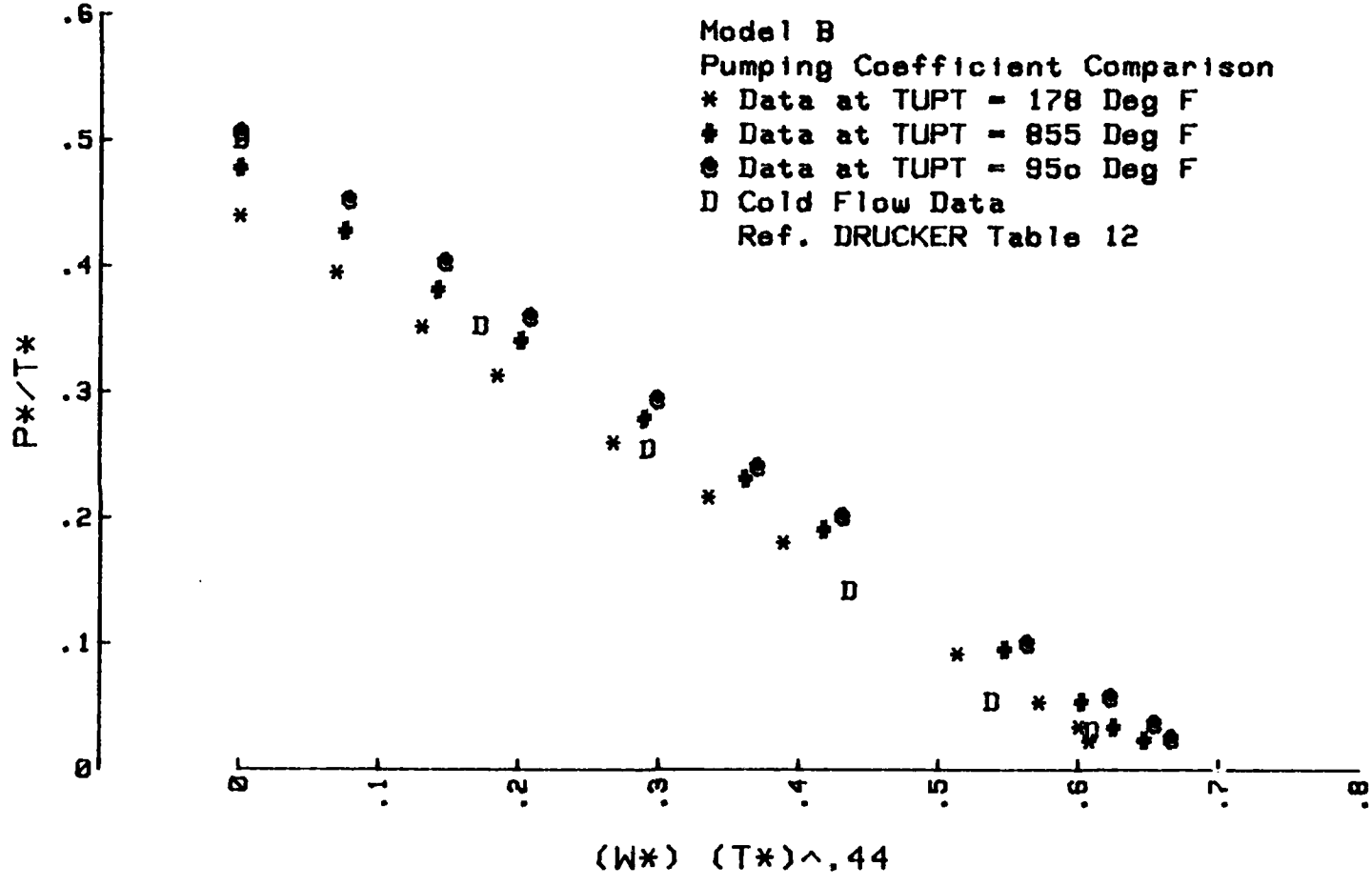

Figure 71, Pumping Coefficient Comparison, Model B

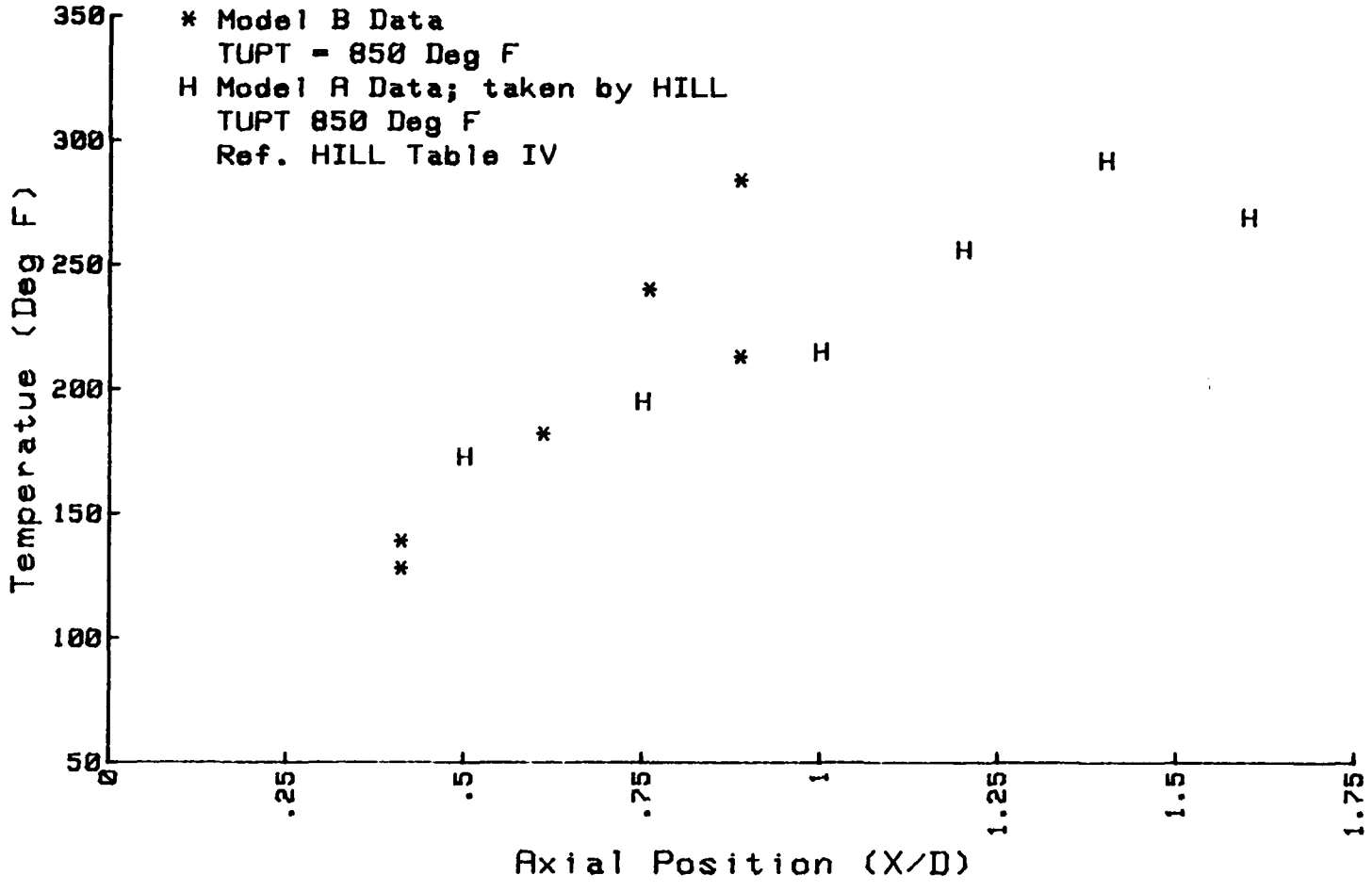

Figure 72, Mixing Stack Temperatures, Model B (850° F)

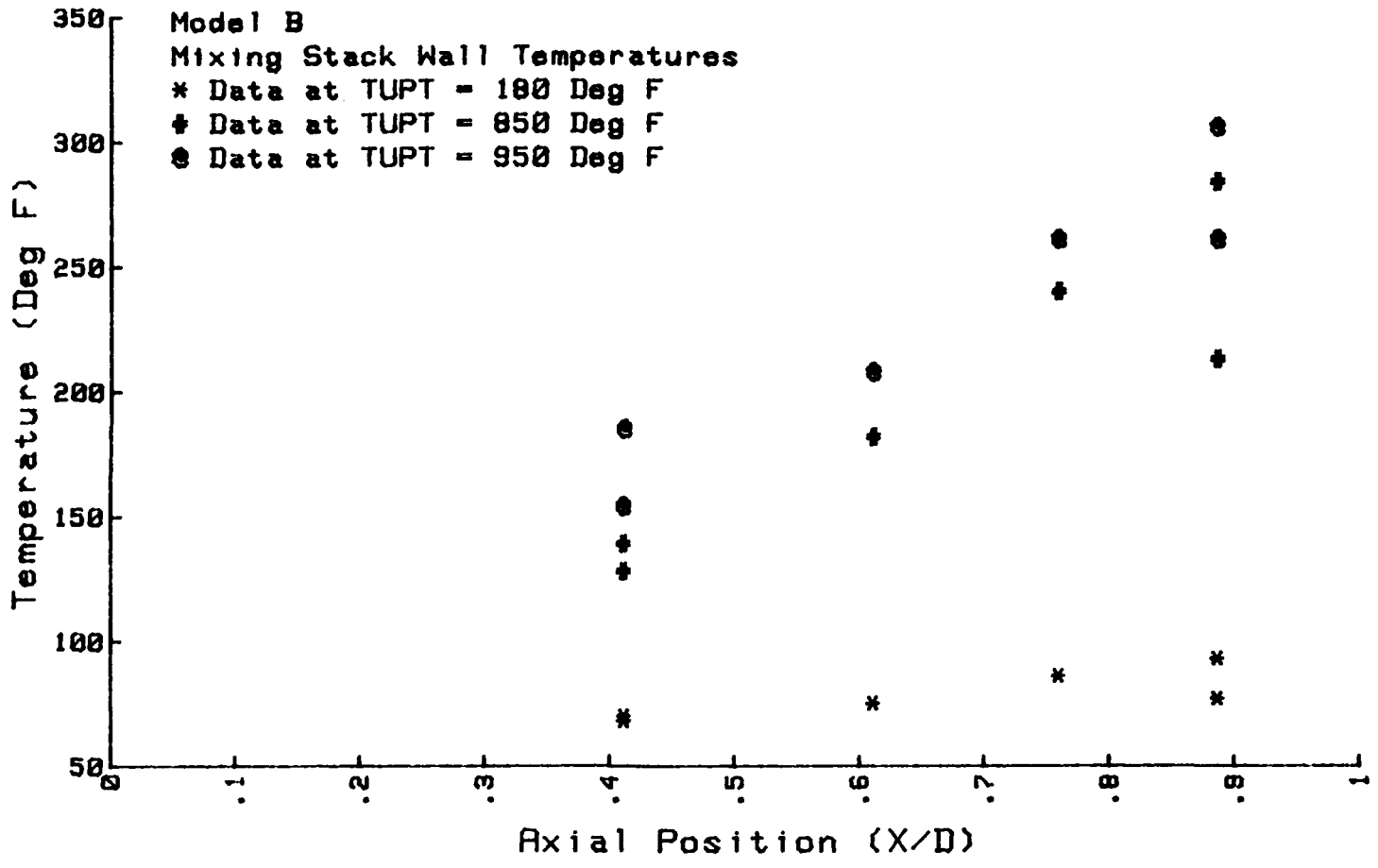

Figure 73, Mixing Stack Temperature Comparison, Model B

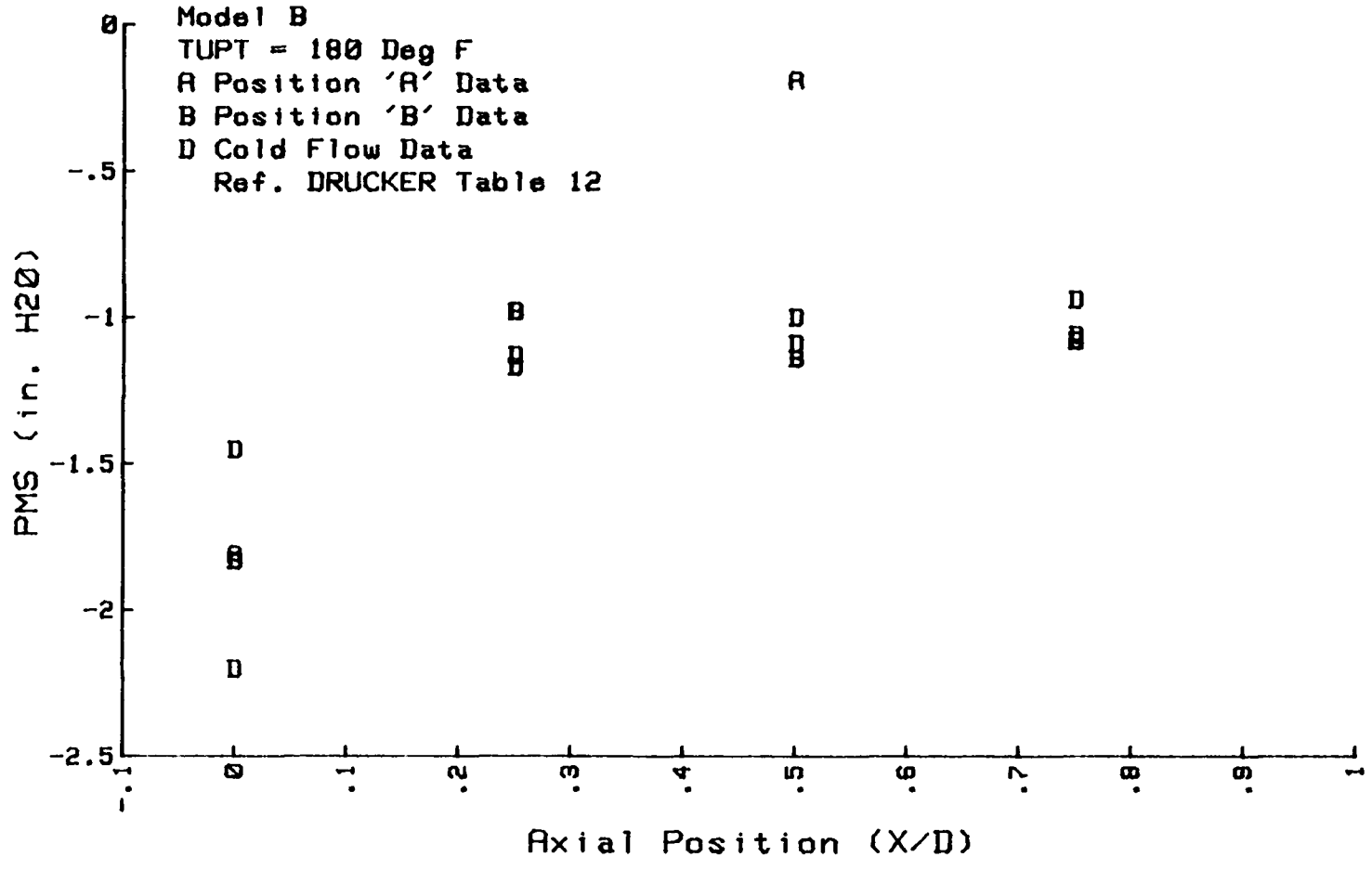

Figure 74, Mixing Stack Pressures, Model B (180° F)

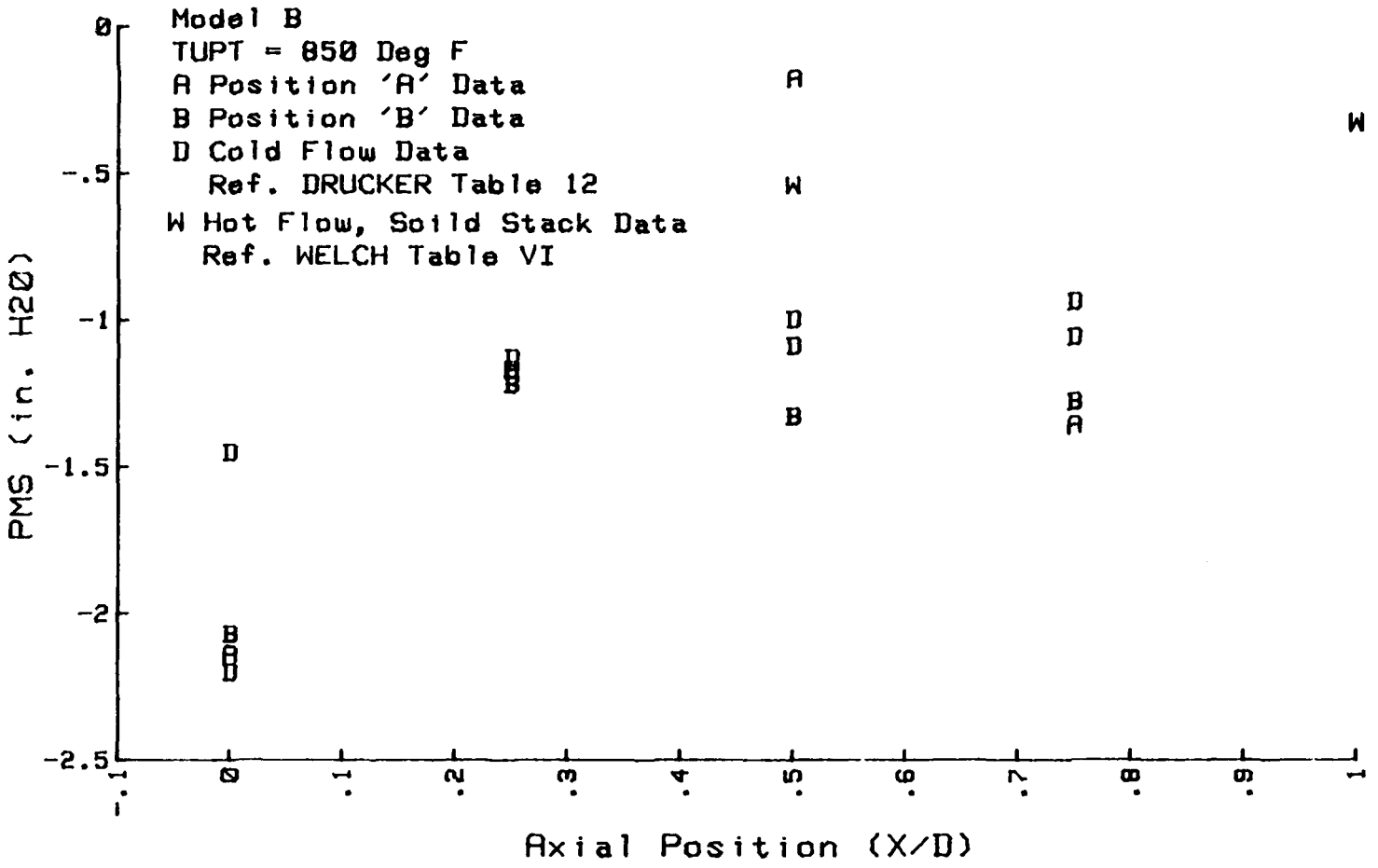

Figure 75, Mixing Stack Pressures, Model B (850° F)

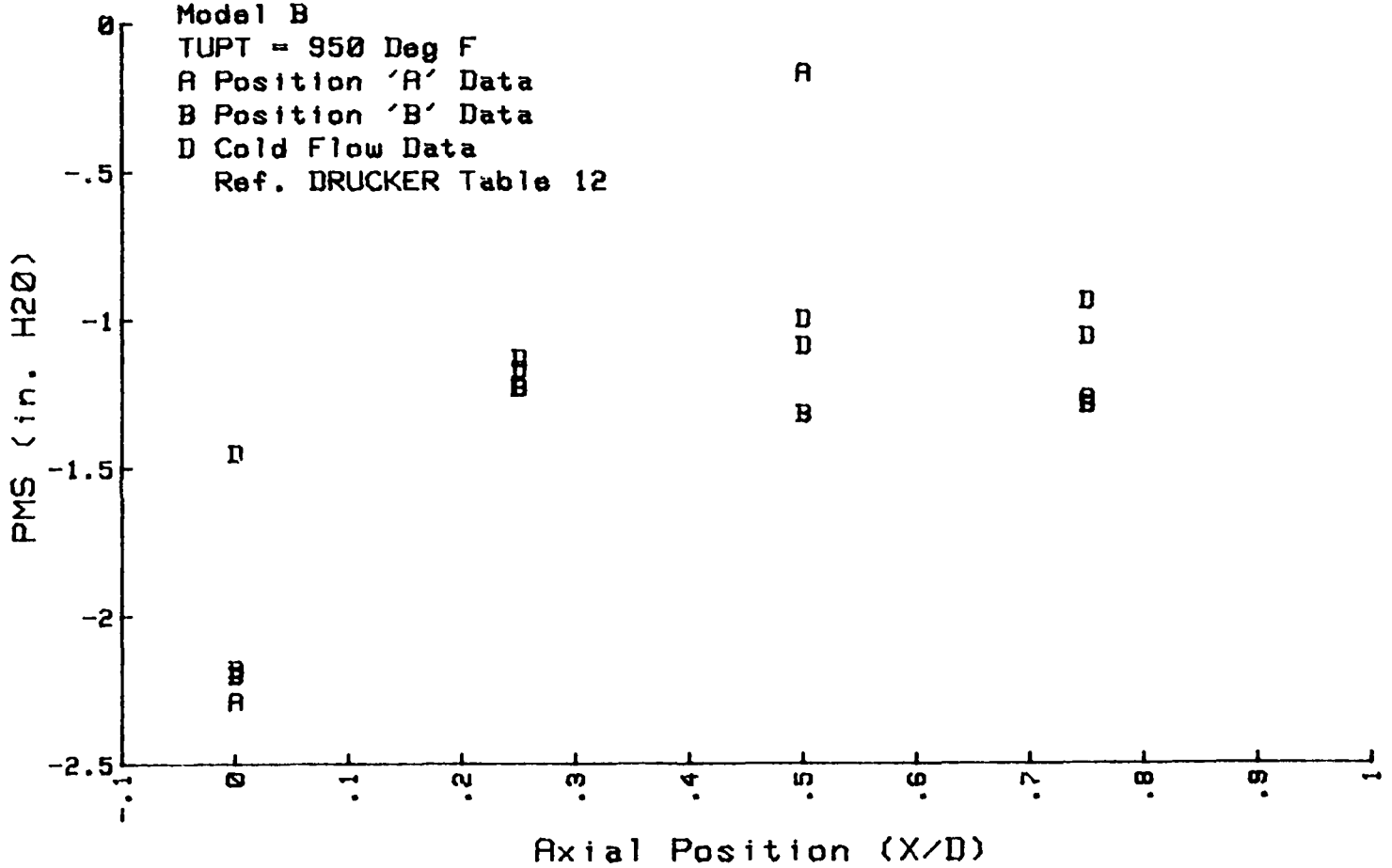

Figure 76, Mixing Stack Pressures, Model B (950° F)

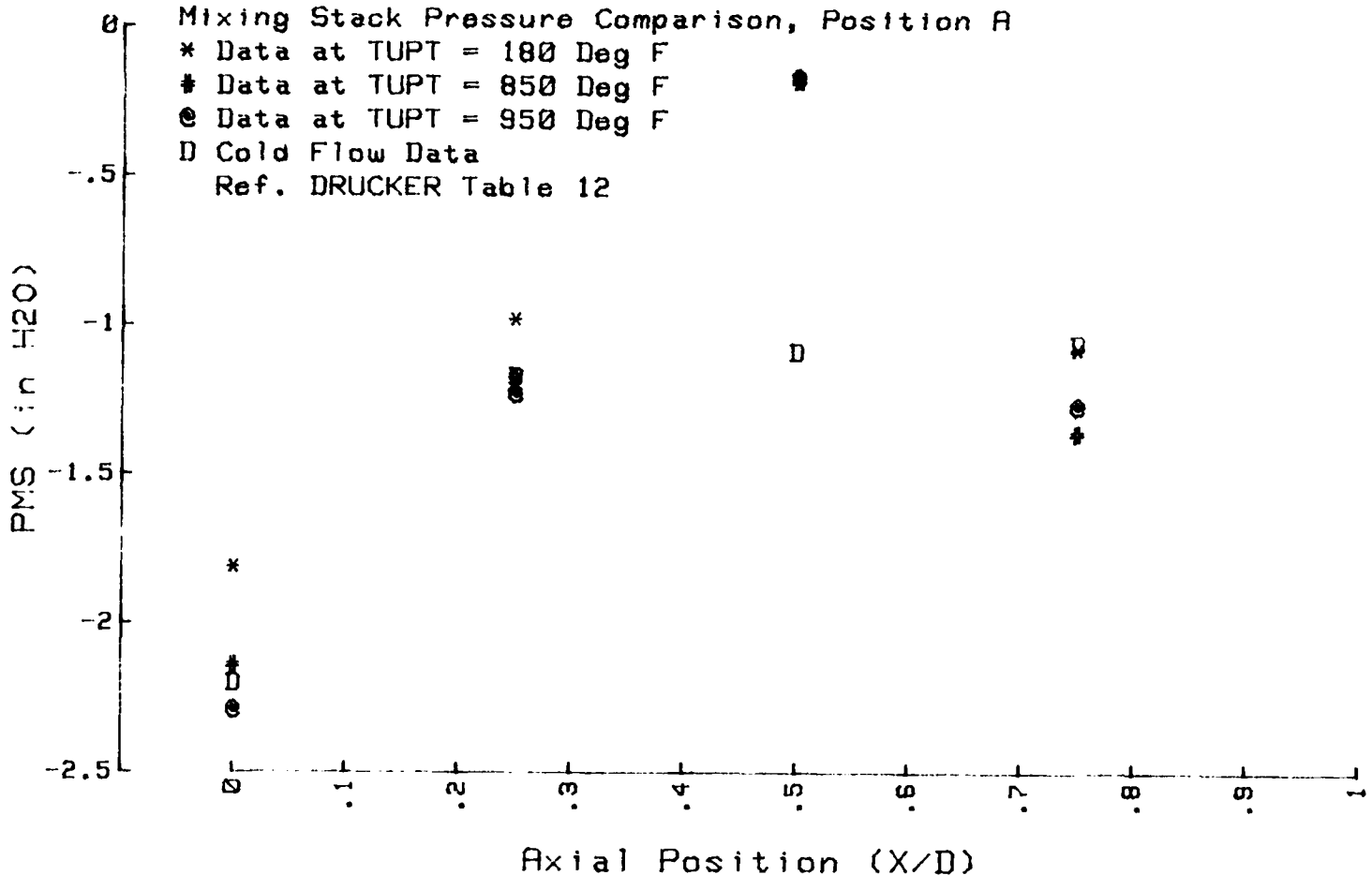

Figure 77, Mixing Stack Pressure Comparison,
Model B (Position A)

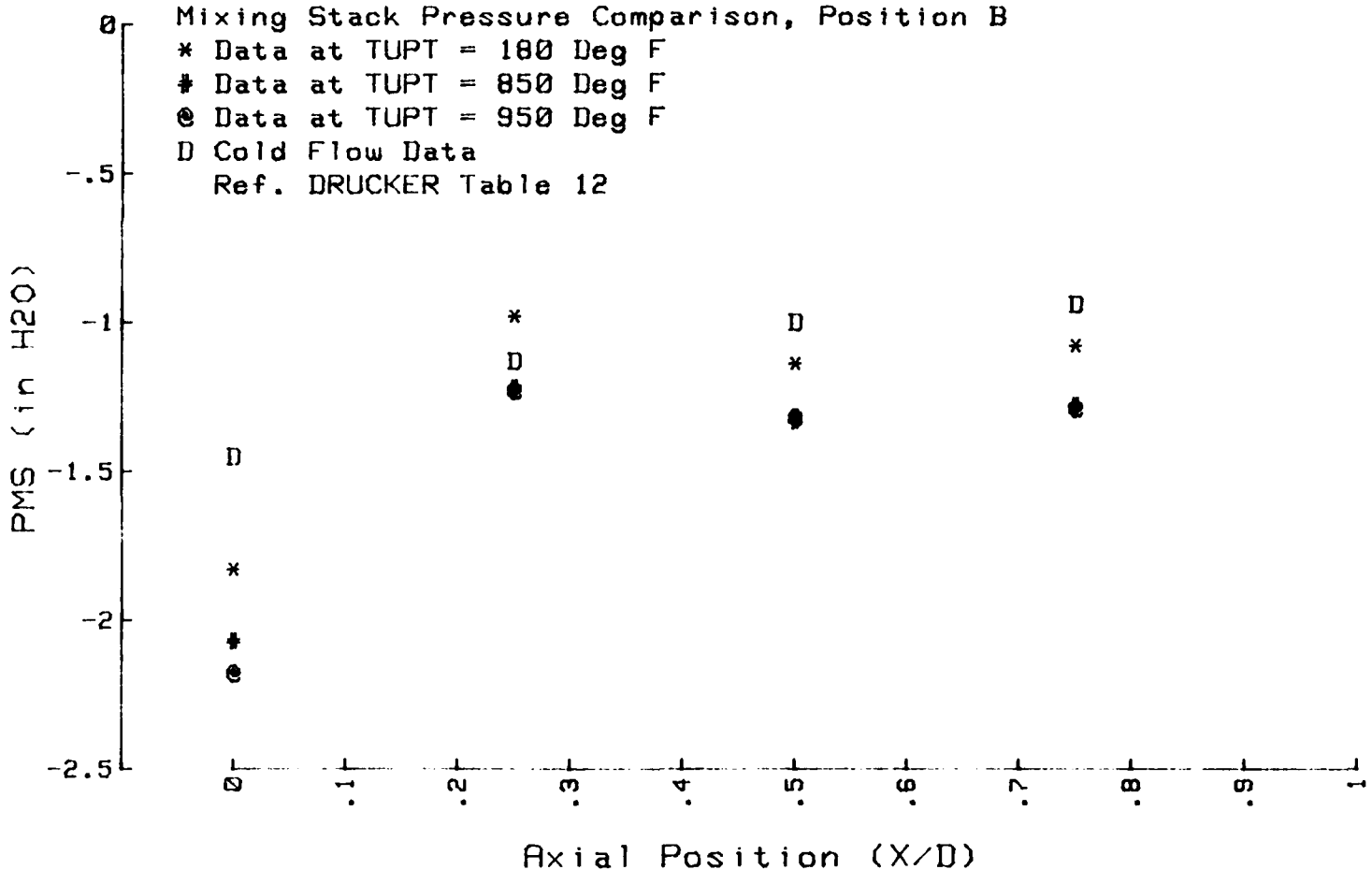

Figure 78, Mixing Stack Pressure Comparison,
Model B (Position B)

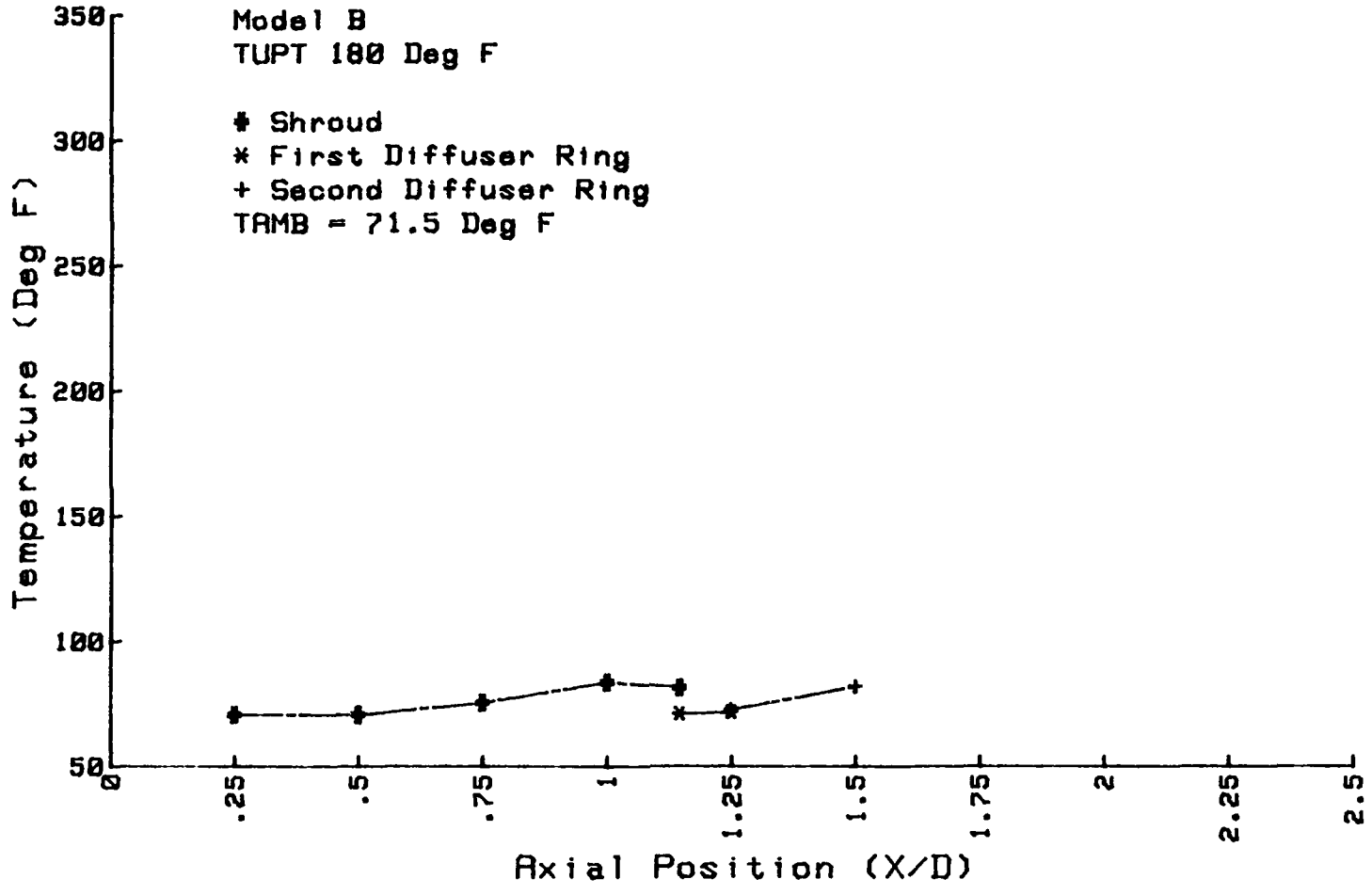

Figure 79, Shroud and Diffuser Temperatures, Model B (180° F)

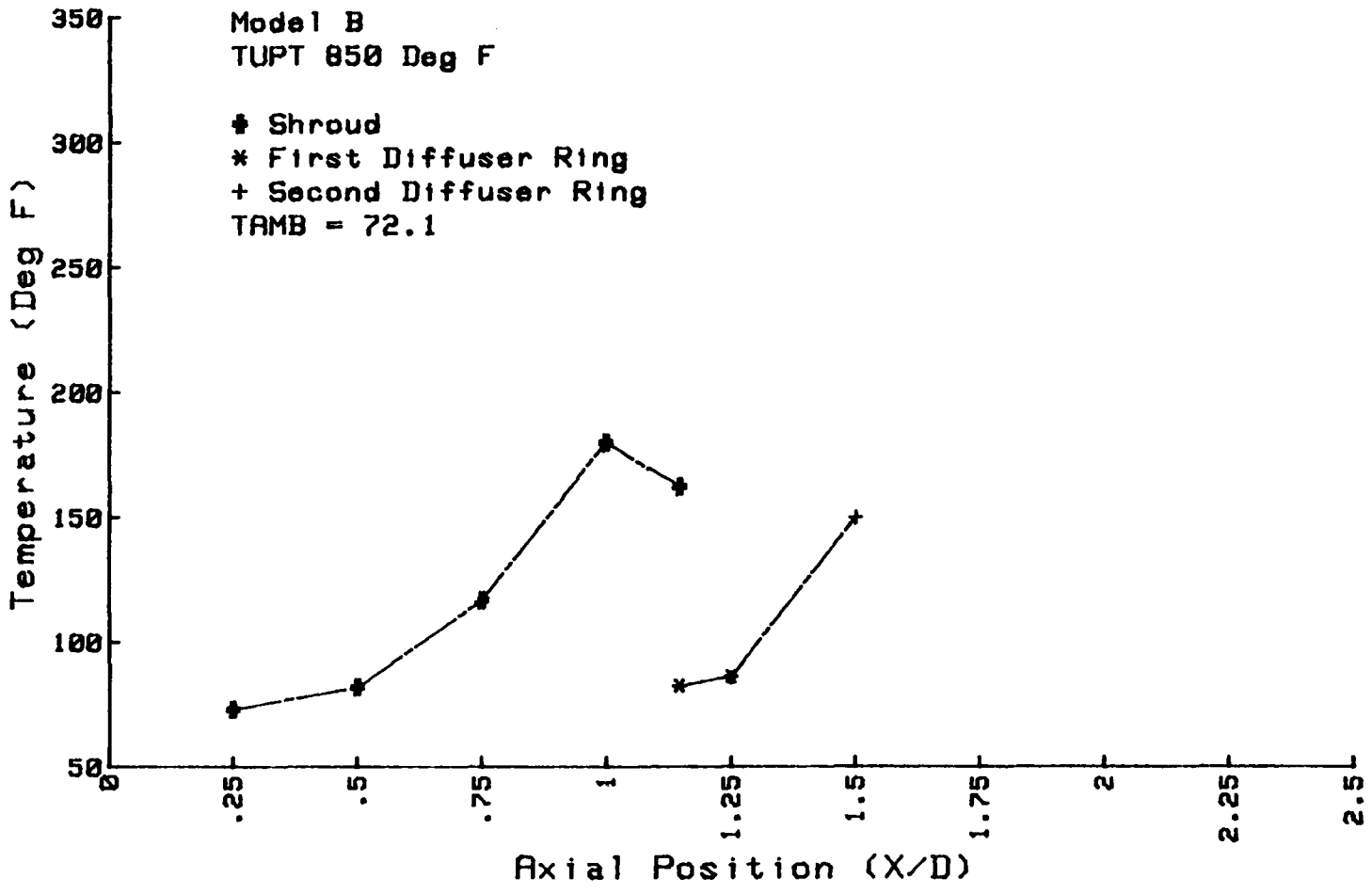

Figure 80, Shroud and Diffuser Temperatures,
Model B (850° F)

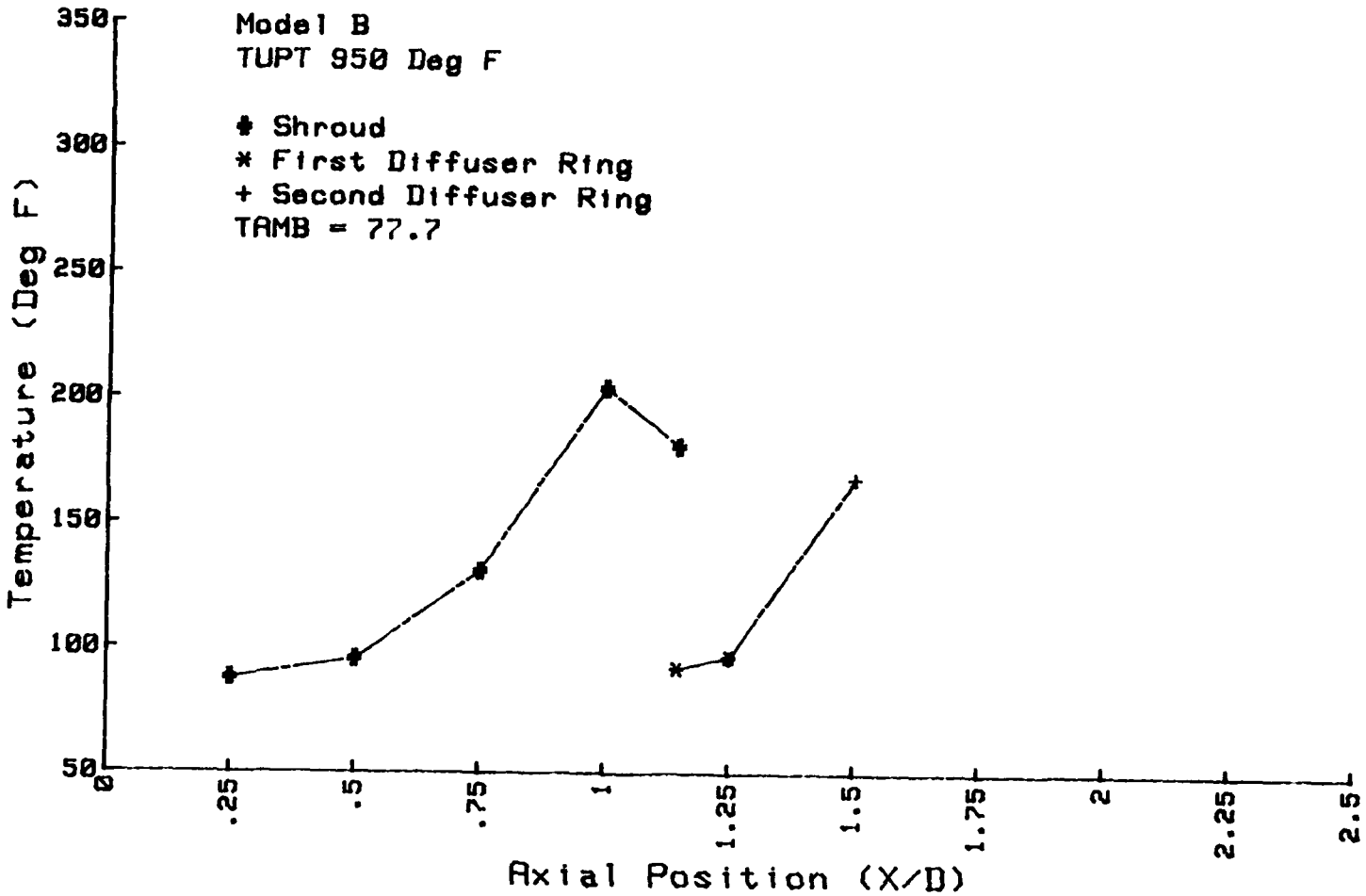

Figure 81, Shroud and Diffuser Temperatures,
Model B (950° F)

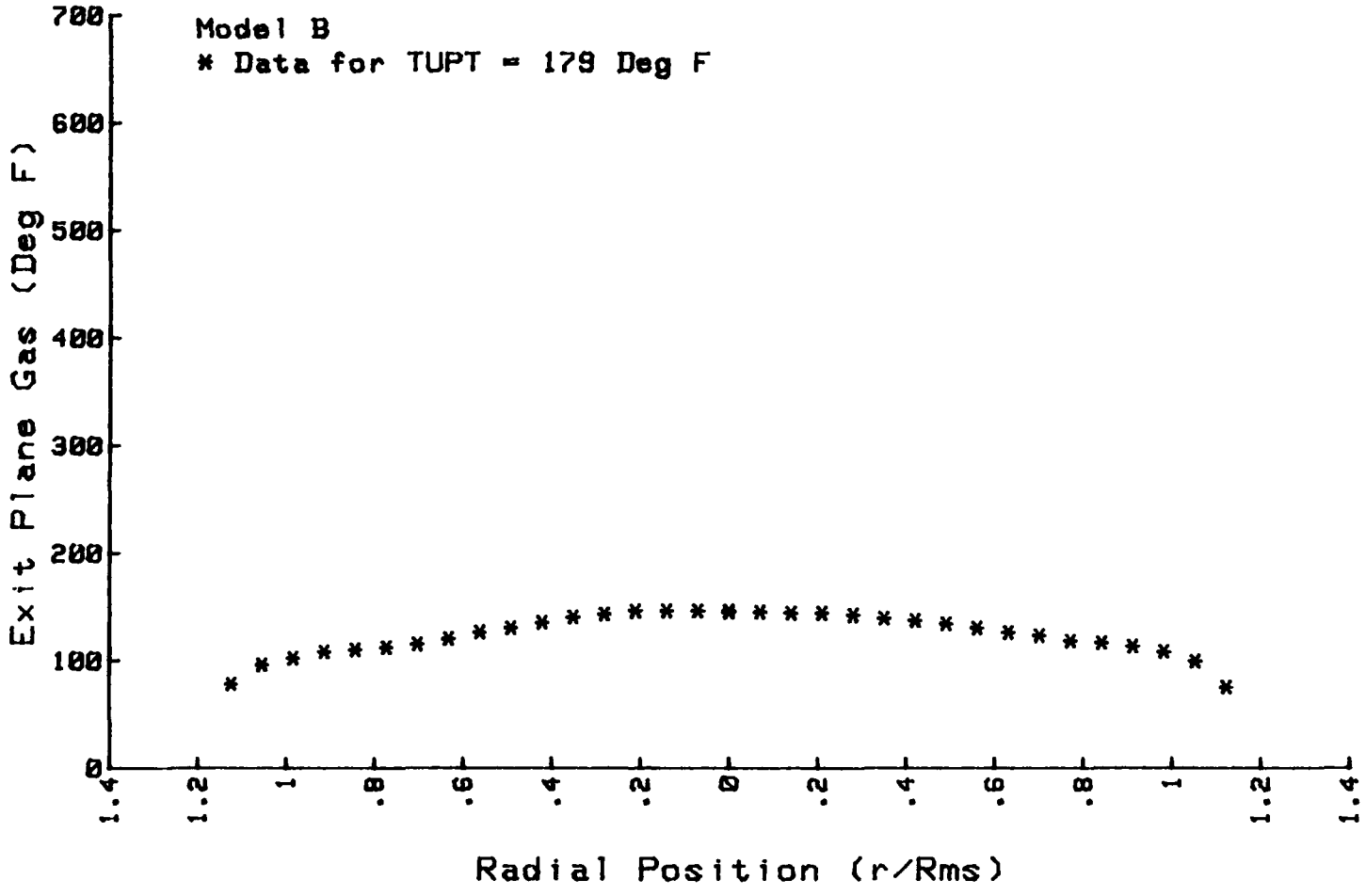

Figure 82, Exit Plane Temperature, Model B (179^{O} F)

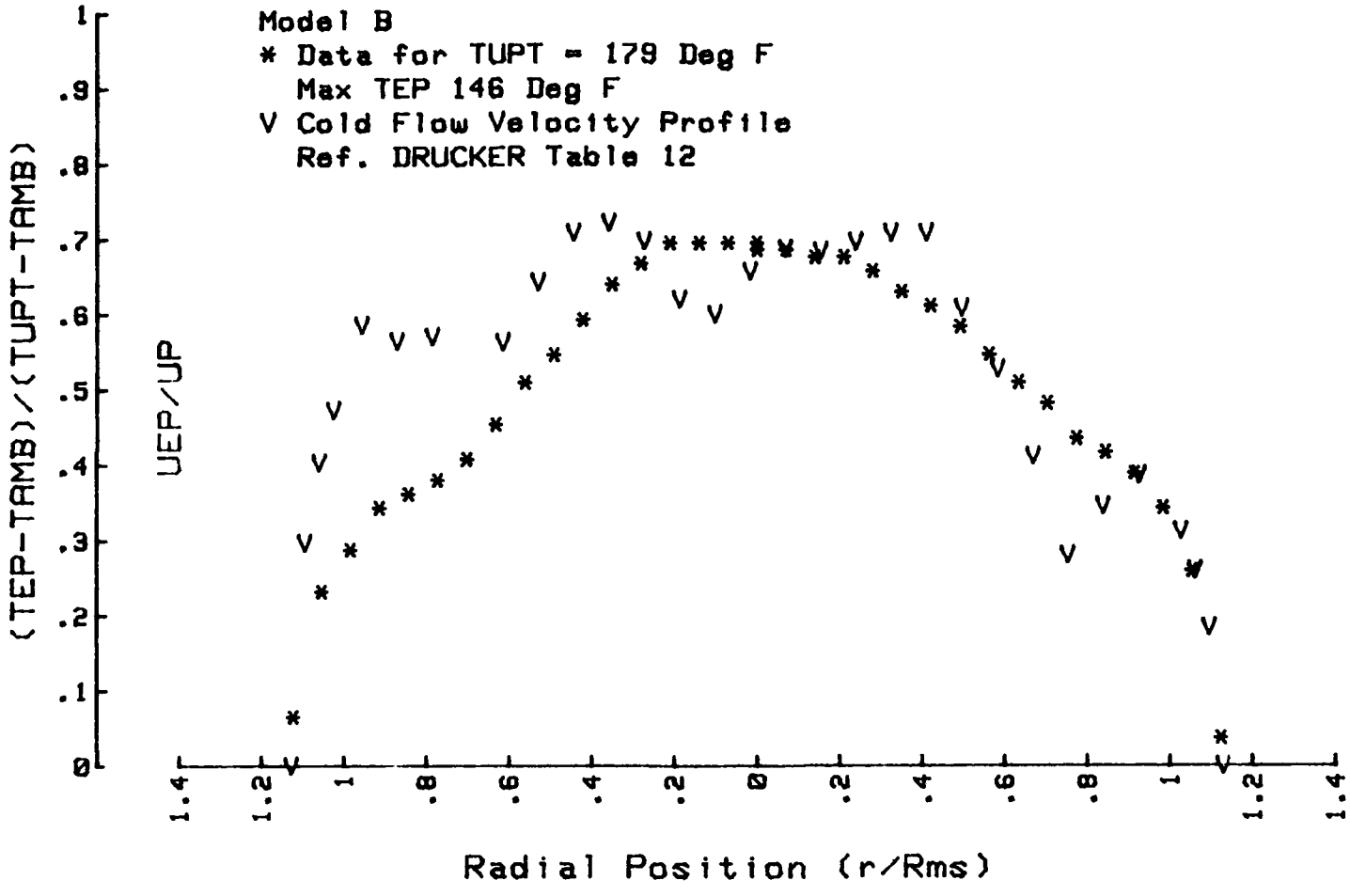

Figure 83, Exit Plane Coefficients, Model B (179° F)

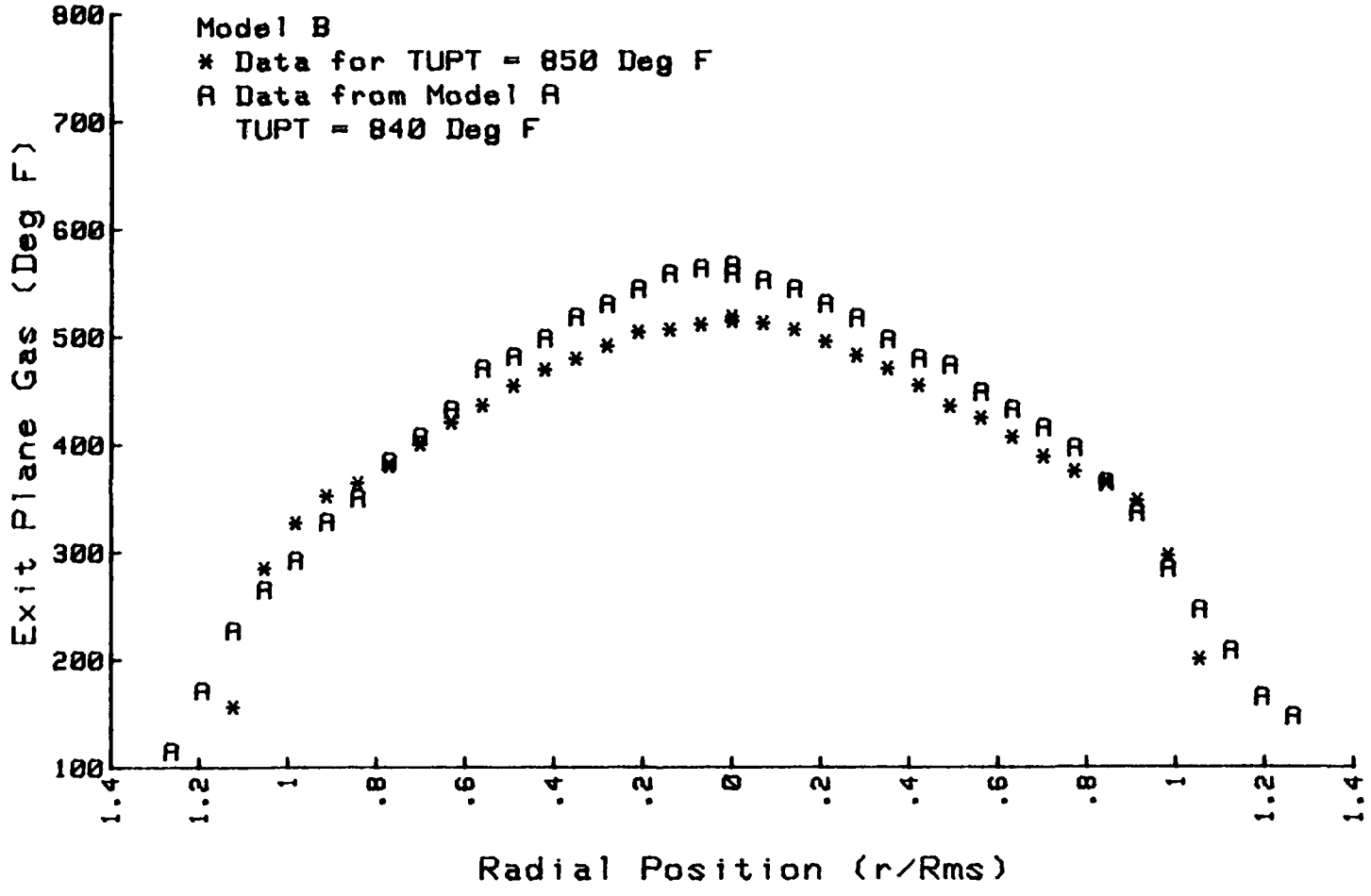

Figure 84, Exit Plane Temperatures, Model B (850° F)

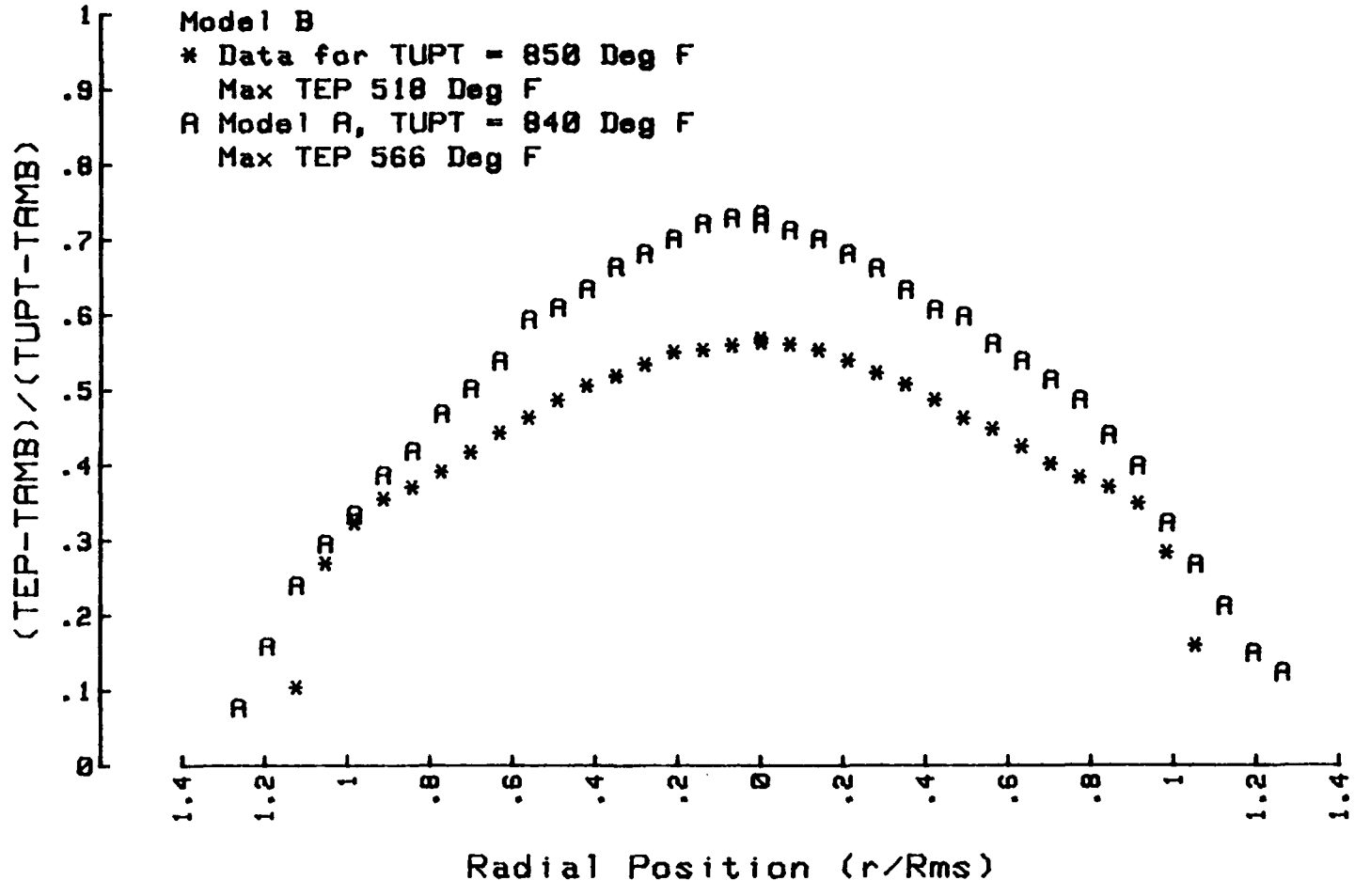

Figure 85, Exit Plane Coefficients, Model B (850° F)

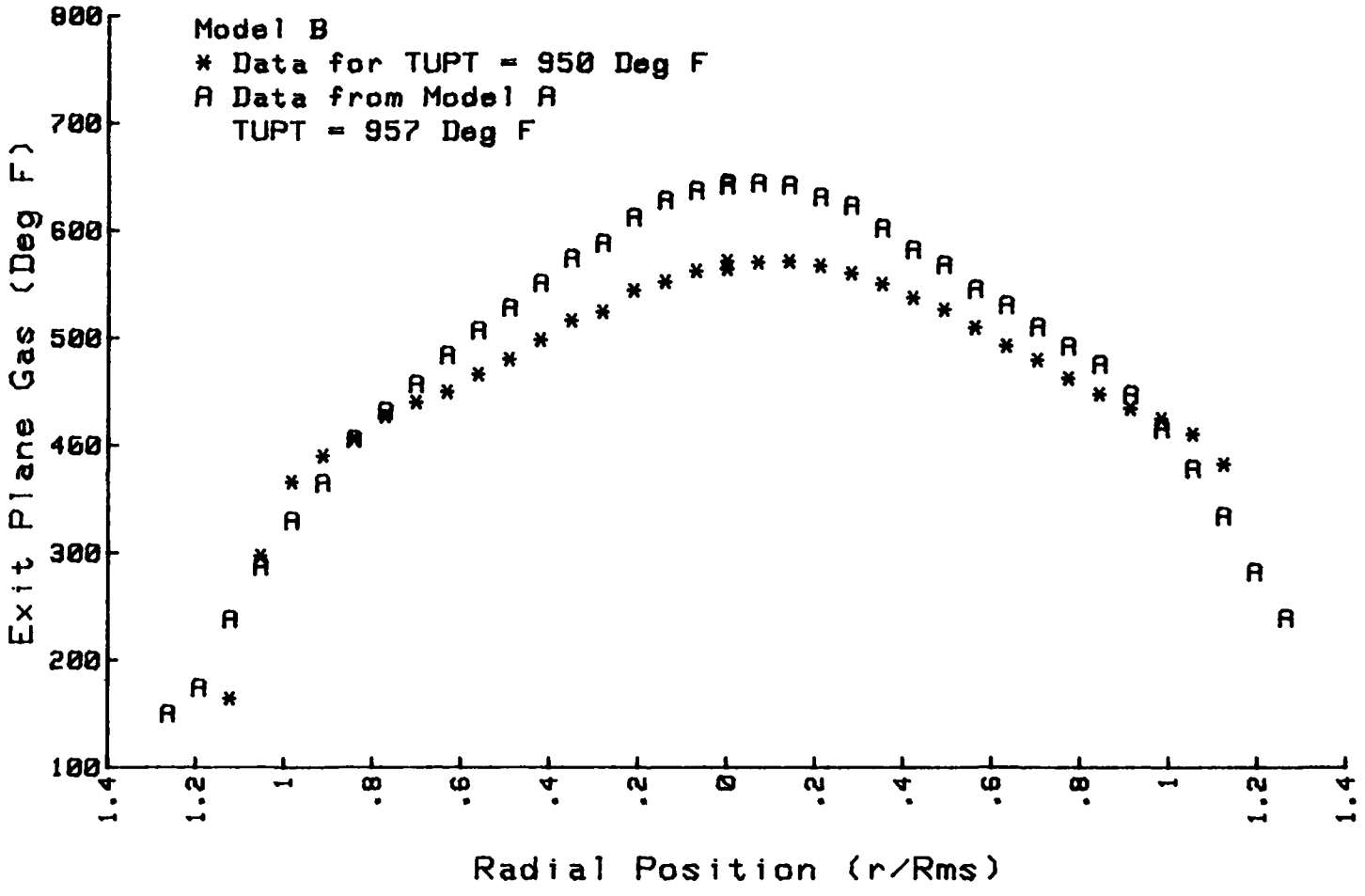

Figure 86, Exit Plane Temperatures, Model B (950° F)

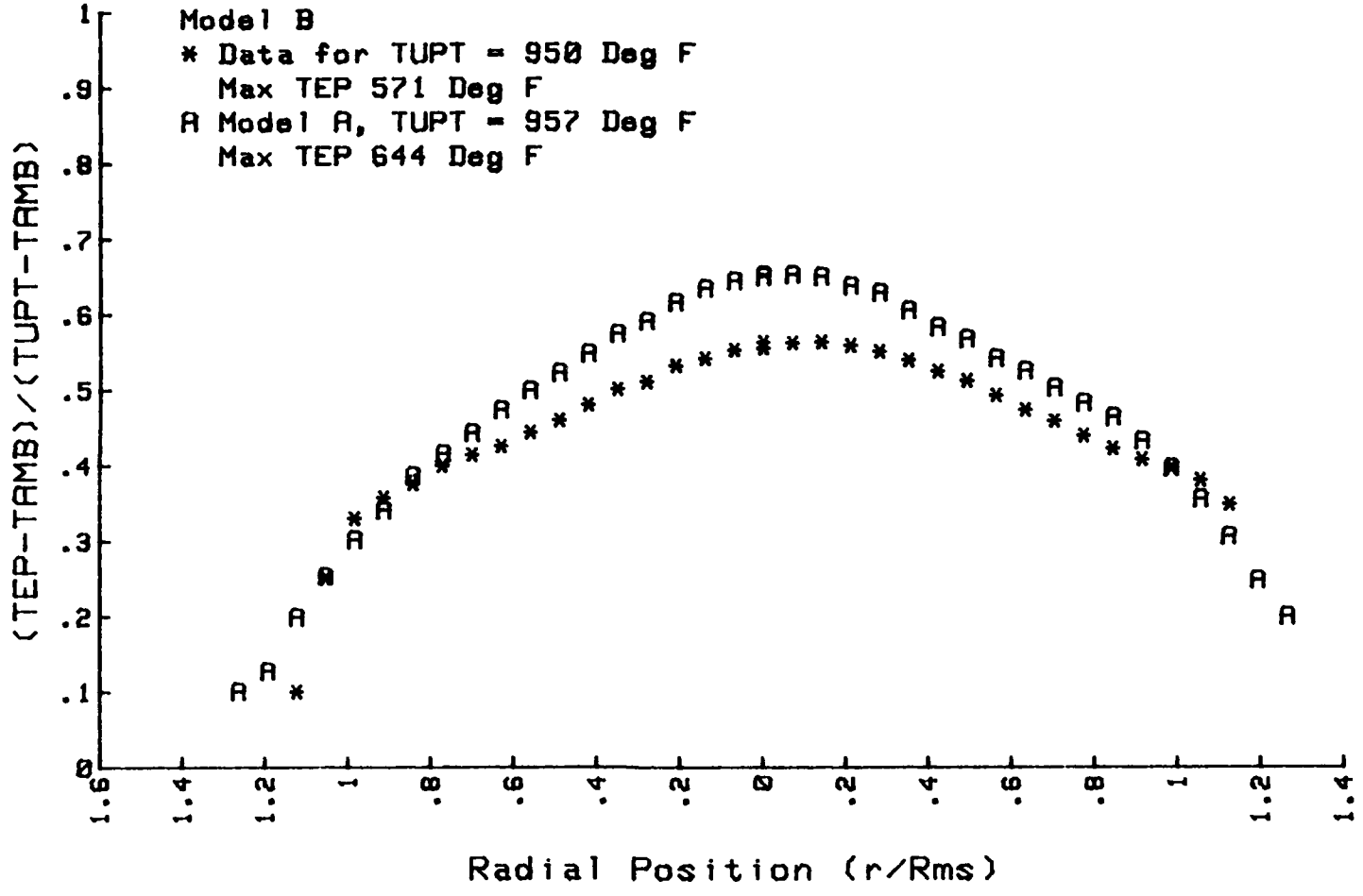

Figure 87, Exit Plane Coefficients, Model B (950° F)

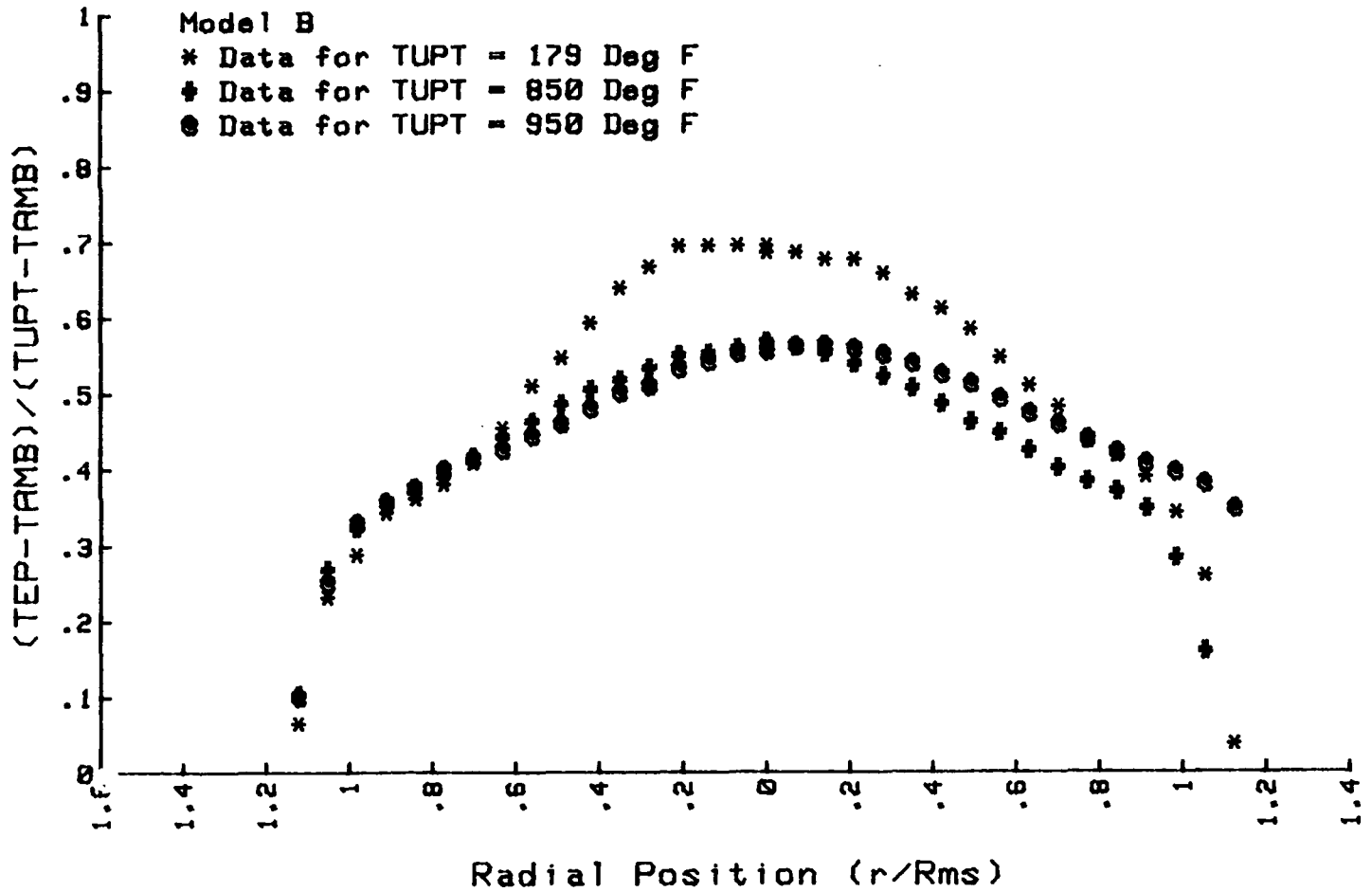

Figure 88, Exit Plane Coefficient Comparison, Model B

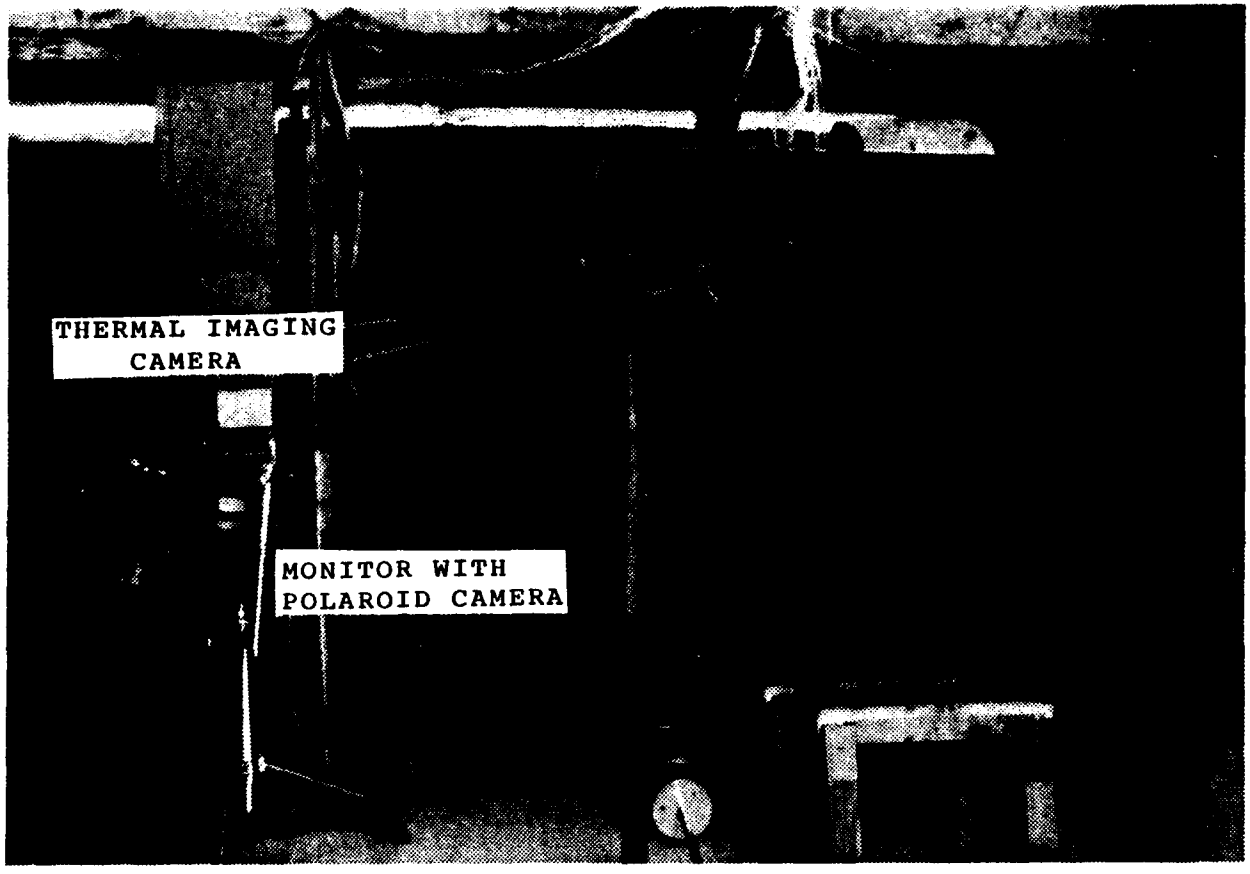

Figure 89, Model Thermal Imaging

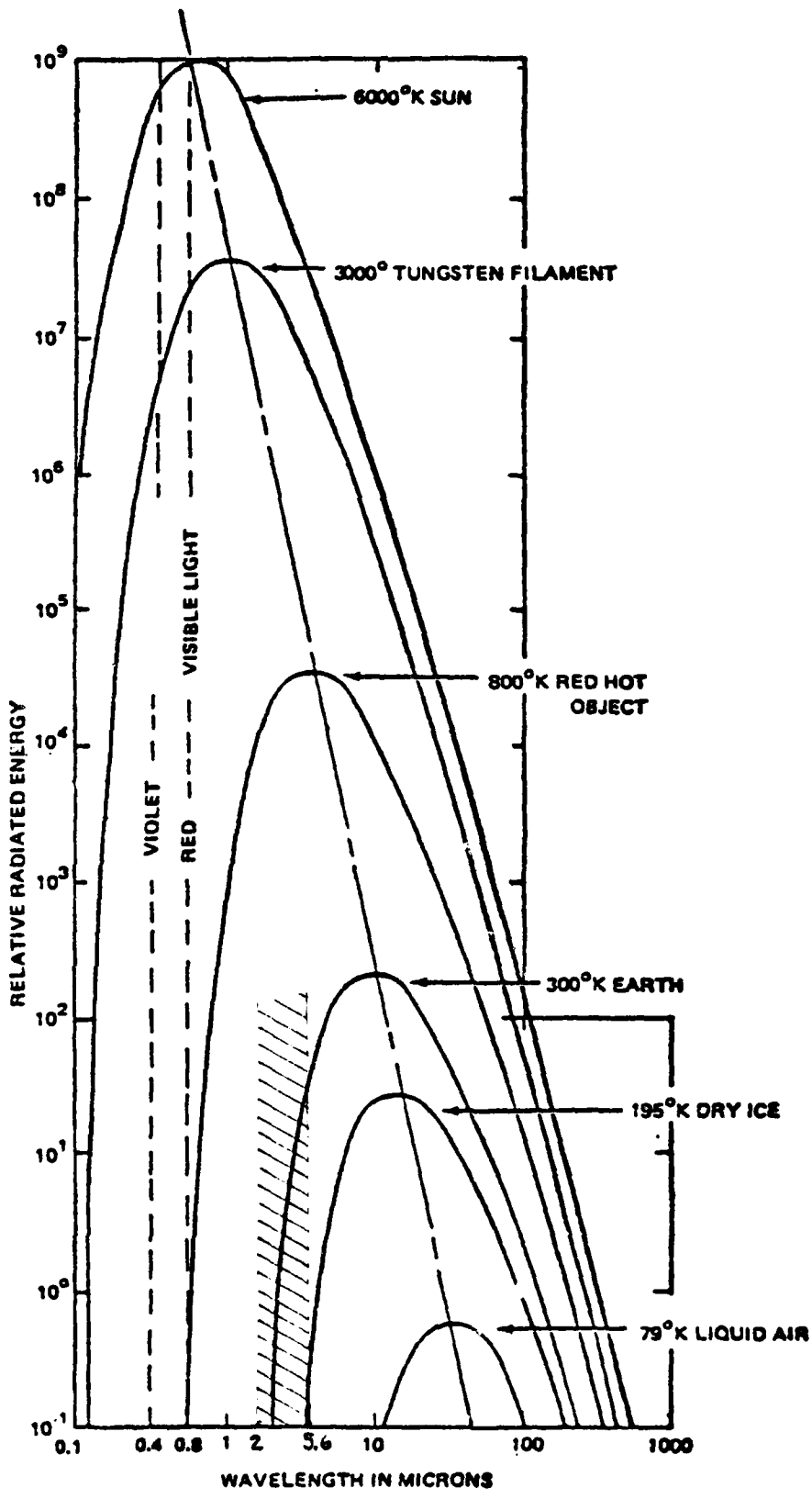

Figure 90, Blackbody Curves of Various objects

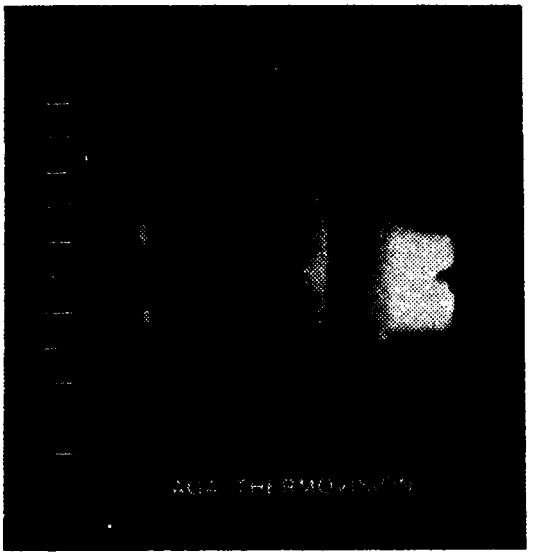

Range setting 100
Baseline

Range setting 50
Baseline

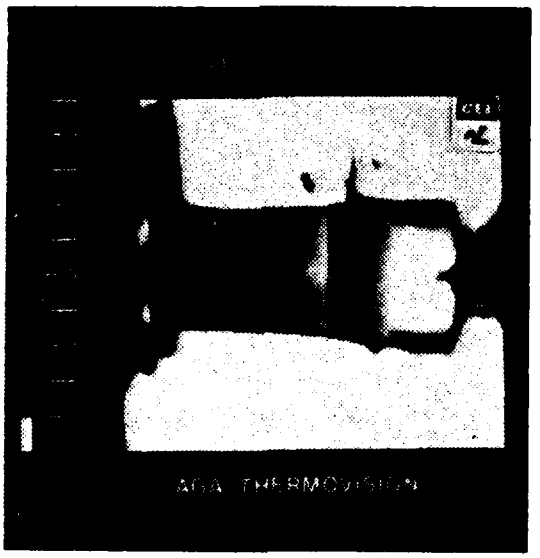

Range setting 50
Contour Marker 0.5

Figure 91, Thermal Imagery, Model A
(955° F)

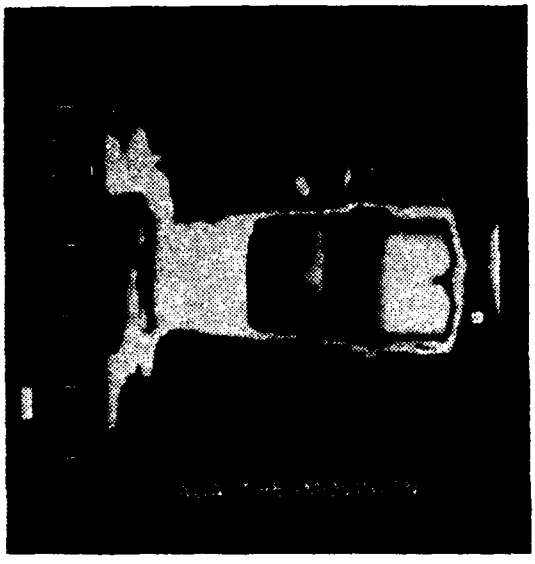

Range setting 50
Contour Marker 1.5

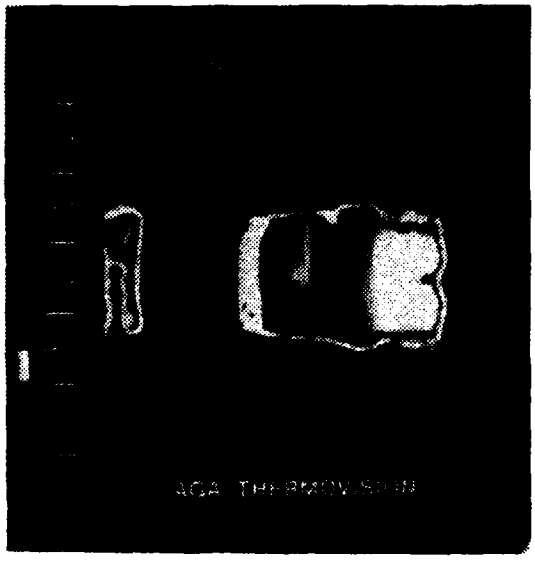

Range setting 50
Contour Marker 2.5

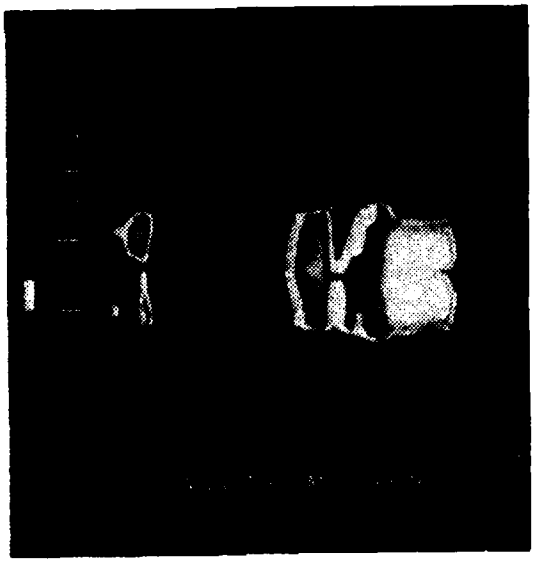

Range setting 50
Contour Marker 4.5

Figure 91, continued

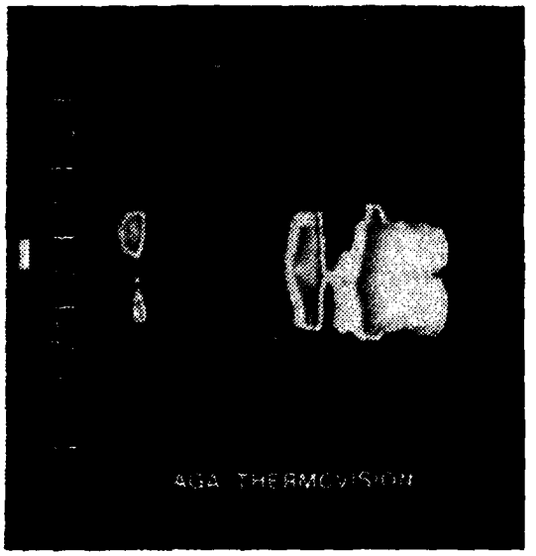

Range setting 50
Contour Marker 5.5

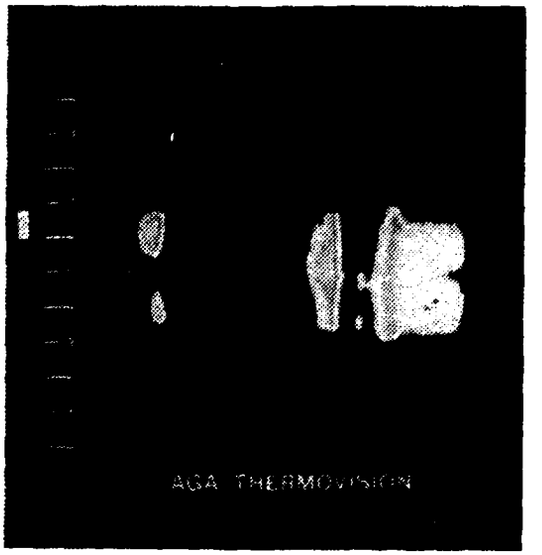

Range setting 50
Contour Marker 6.5

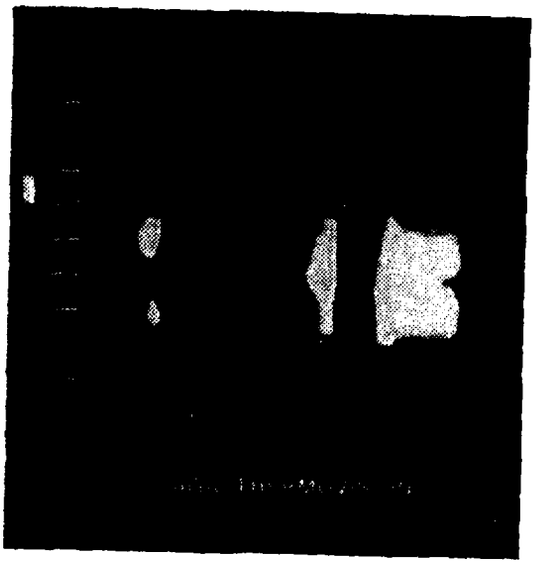

Range setting 50
Contour Marker 7.5

Figure 91, continued

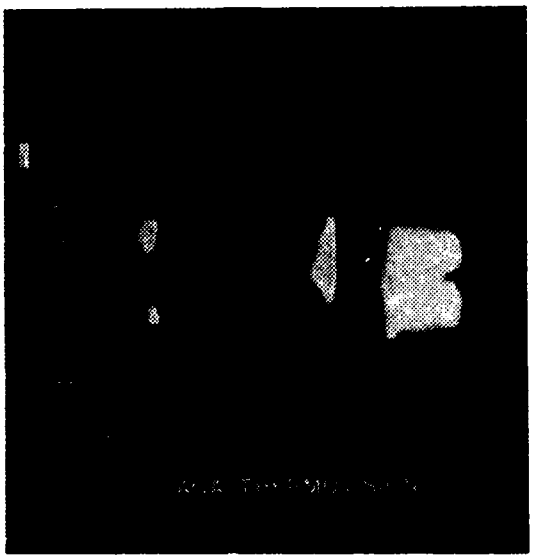

Range setting 50
Contour Marker 8.5

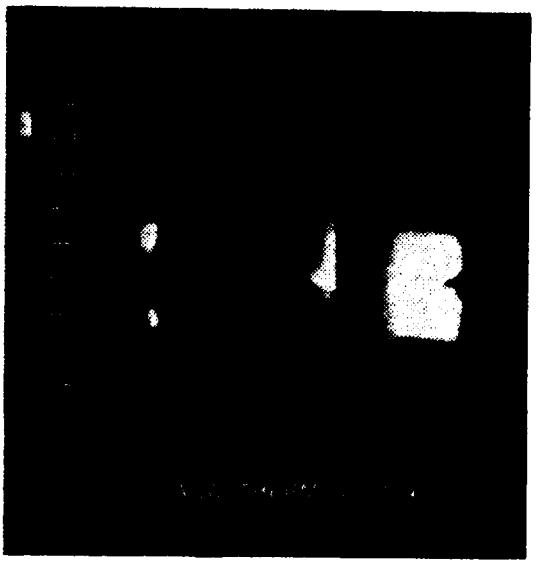

Range setting 50
Contour Marker 9.5

Figure 91, continued

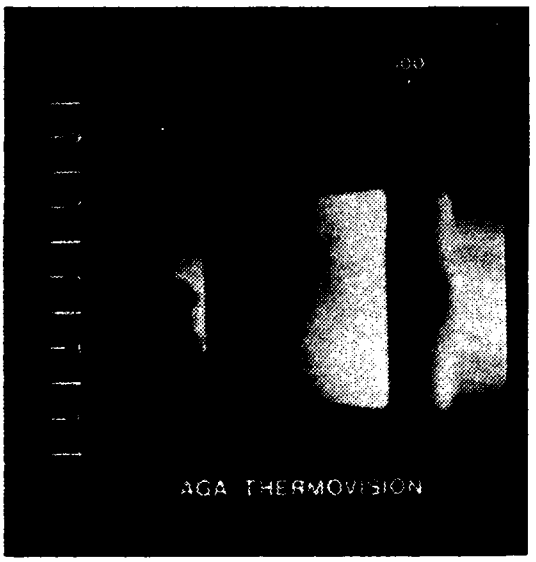

Range setting 500
Baseline

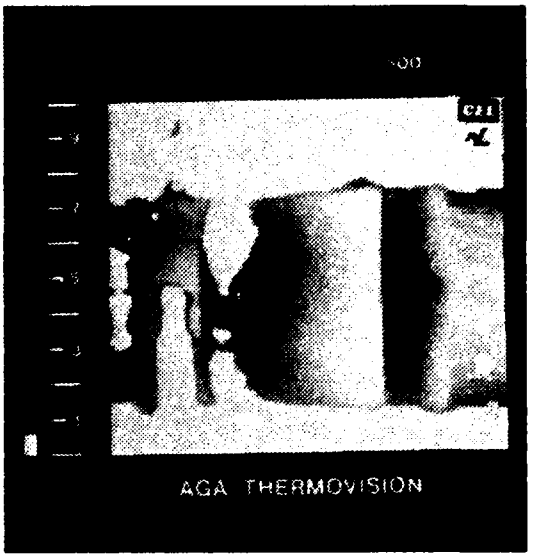

Range setting 500
Contour Marker 0.0

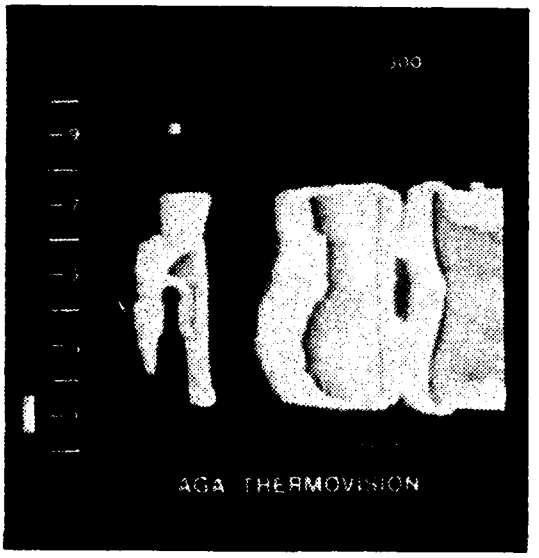

Range setting 500
Contour Marker 1.0

Figure 92, Thermal Imagery, Model B
(950° F)

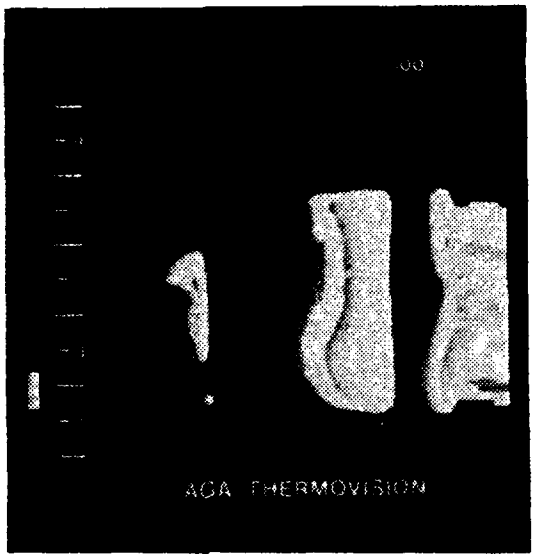

Range setting 500
Contour Marker 2.0

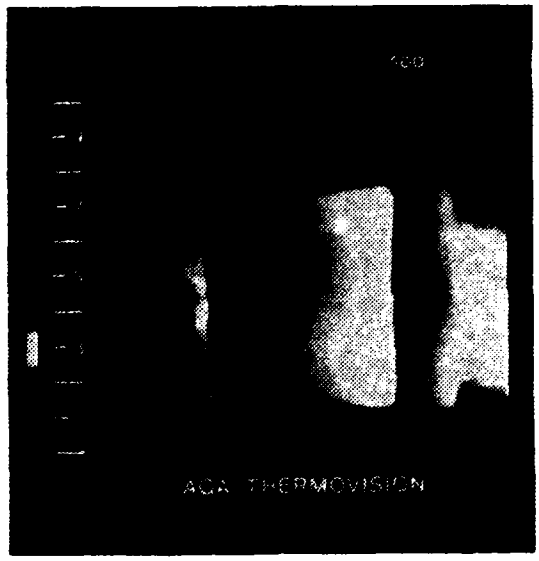

Range setting 500
Contour Marker 3.0

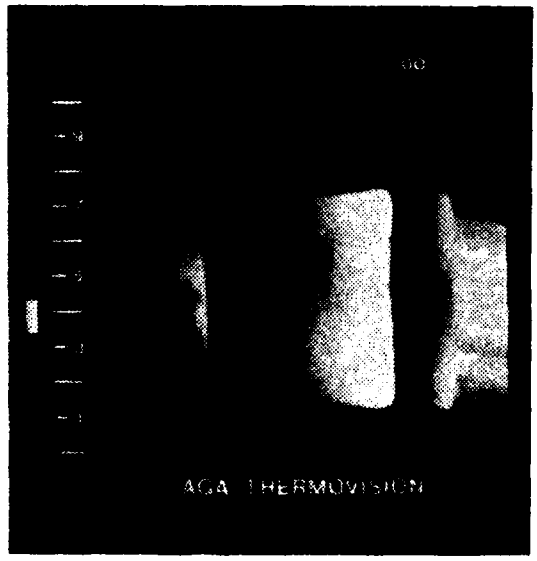

Range setting 500
Contour Marker 4.0

Figure 92, continued

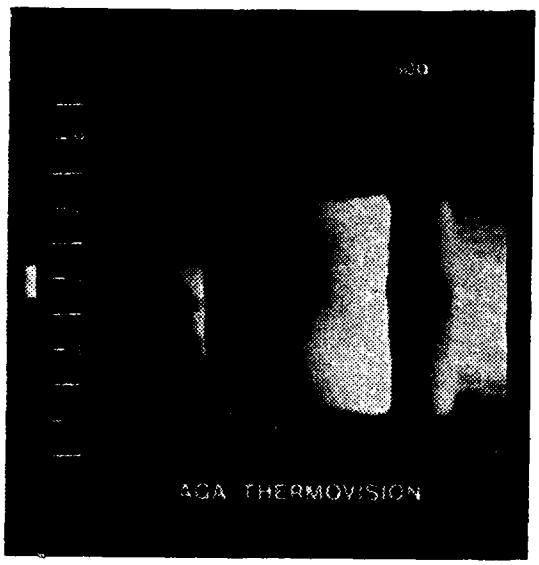

Range setting 500
Contour Marker 5.0

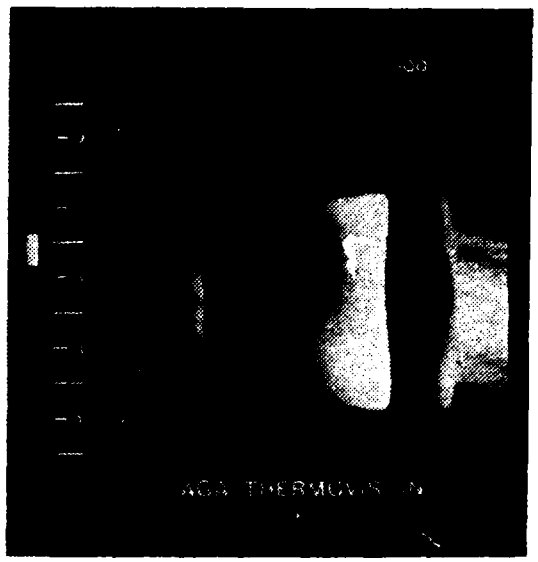

Range setting 500
Contour Marker 6.0

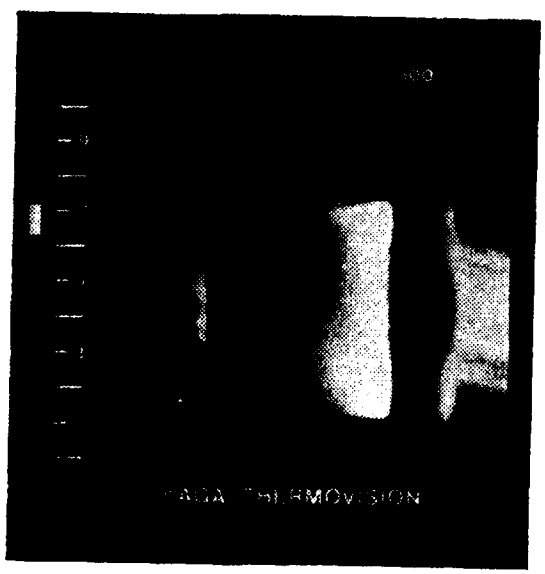

Range setting 500
Contour Marker 7.0

Figure 92, continued

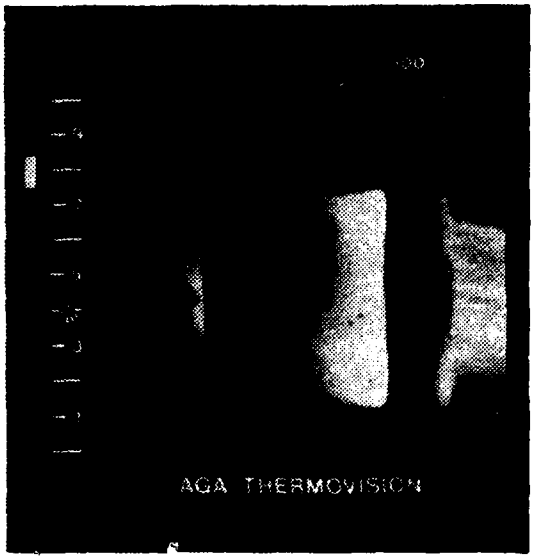

Range setting 500
Contour Marker 8.0

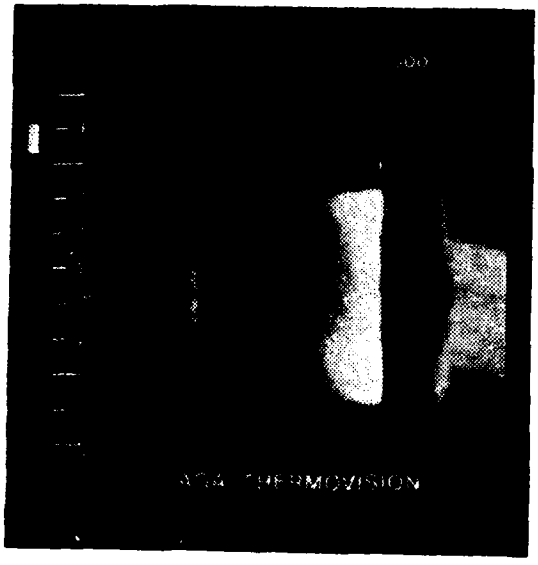

Range setting 500
Contour Marker 9.0

Figure 92, continued

TABLE I

Rotameter Calibration Data

Rotometer Reading	Weight Empty (gr.)	Weight Full (gr.)	Net Weight (gr.)	Time (sec.)	Mass Flow lbm/sec	Flow Rate GPH
08	67.0	29.5	37.5	120	0.689	0.345
09	84.0	30.7	53.3	120	0.979	0.490
10	103.3	31.8	71.5	120	1.314	0.657
15	173.1	31.1	142.0	120	2.609	1.306
20	256.7	31.6	225.1	120	4.136	2.070
25	381.4	31.9	349.5	120	6.421	3.214
30	520.0	31.8	488.2	120	8.696	4.489
35	342.9	32.4	310.5	60	11.41	5.710
40	397.8	32.1	365.7	60	13.44	6.725
43	423.3	32.1	391.2	60	14.37	7.194
40	757.7	32.4	725.3	120	13.33	6.669
35	651.5	31.5	620.0	120	11.39	5.701
34	629.3	32.1	597.2	120	10.97	5.491
33	603.2	32.8	570.4	120	10.48	5.245
32	582.5	32.4	550.1	120	10.11	5.058
31	558.8	32.3	526.5	120	9.613	4.841
30	530.0	32.0	498.0	120	9.149	4.579
29	500.8	32.3	468.5	120	8.607	4.308
28	475.4	32.2	443.2	120	8.142	4.075
27	450.5	31.4	419.1	120	7.700	3.854
26	426.5	32.4	394.1	120	7.240	3.624
25	395.9	31.2	364.7	120	6.700	3.353
20	267.1	32.2	234.9	120	4.316	2.160
15	169.0	31.9	137.1	120	2.519	1.261
10	104.6	31.9	72.7	120	1.336	0.669
08	72.1	31.6	40.5	120	0.744	0.372

NOTES

1) Average fuel temperature 61.7° F
2) Fuel: Number two diesel; specific gravity = 0.862

TABLE II

Burner Calibration Data, 4.0 GPH Nozzle

Supply Pump Pressure (PSIG)	High Pressure Pump (PSIG)	Nozzle Pressure (PSIG)	Rotameter	Mass Flow Rate x 10^3 lbm/sec
16.0	60	60	23.0	6.239
16.0	70	70	23.1	6.278
16.0	110	100	25.0	7.047
16.0	160	150	27.8	8.181
16.0	70	67	22.8	6.157
16.0	105	100	24.2	6.724
15.5	160	150	26.3	7.574
15.3	210	200	29.0	8.666
15.3	260	250	38.0	9.395
15.2	310	300	32.2	9.962
15.1	335	324	32.2	9.962
15.8	75	72	22.8	6.157
15.5	105	100	24.0	6.643
15.4	160	150	26.0	7.452
15.3	210	200	28.0	8.262
15.3	260	250	29.5	8.868
15.2	310	300	31.0	9.476
15.1	350	340	32.5	10.083

NOTES

1) Nozzle 60° HARSCH, 4.0 GPH
2) Average fuel temperature 54° F
3) Fuel: Number two diesel; specific gravity 0.864
4) Mass flow determined from equation:

$$WF = 0.404759 * ROTA - 3.071594$$

where

WF = Fuel Mass Flow Rate (lbm/sec)
ROTA = Rotameter reading

TABLE III

Burner Calibration Data, 5.0 GPH Nozzle

Supply Pump Pressure (PSIG)	High Pressure Pump (PSIG)	Nozzle Pressure (PSIG)	Rotameter	Mass Flow Rate x 10^3 lbm/sec
15.5	75	70	26.7	7.734
15.4	110	100	29.8	8.990
15.3	160	150	33.3	10.366
15.3	215	205	37.0	11.904
15.1	270	255	40.0	13.119
15.1	315	300	42.8	14.252
15.0	350	330	44.9	15.102
15.5	75	70	27.5	8.059
15.4	110	100	30.1	9.112
15.5	160	150	34.0	10.690
15.2	215	200	37.5	12.107
15.1	265	250	40.0	13.119
15.0	320	300	43.1	14.374
15.0	340	325	44.9	15.102
15.5	75	70	27.5	8.059
15.4	110	100	30.5	9.274
15.4	160	150	34.0	10.690
15.3	215	200	37.4	12.066
15.2	265	250	40.2	13.198
15.0	320	300	33.3	14.454
15.0	350	330	45.1	15.183

NOTES

1) Nozzle 60° MONARCH, 5.0 GPH
2) Average fuel temperature 53° F
3) Fuel: Number two diesel; specific gravity 0.864
4) Mass flow determined from equation:

$$WF = 0.404759 * ROTA - 3.071594$$

where

WF = Fuel Mass Flow Rate (lbm/sec)
ROTA = Rotameter reading

TABLE IV

Burner Calibration Data, 9.5 GPH Nozzle

Supply Pump Pressure (PSIG)	High Pressure Pump (PSIG)	Nozzle Pressure (PSIG)	Rotameter _____	Mass Flow Rate x 10^3 lbm/sec
15.3	70	55	46.8	15.871
15.0	125	100	60.0	21.214
14.7	185	150	71.8	25.990
14.5	250	200	82.9	30.4829
14.4	310	255	91.5	33.964
14.3	335	270	94.8	35.300
15.2	70	55	46.1	15.589
The following values were obtained by placing the fuel control valve at minimum setting and throttling the high pressure pump discharge valve.				
15.3	70	40	40.0	13.119
15.3	75	25	35.0	11.095
15.5	75	15	30.0	9.071
15.5	75	6	25.0	7.047

NOTES

1) Nozzle 60° MONARCH, 9.5 GPH
2) Average fuel temperature 53° F
3) Fuel: Number two diesel; specific gravity 0.864
4) Atomization was poor below 50 PSIG nozzle pressure and ceased below 37 PSIG.
5) Mass flow determined from equation:

$$WF = 0.404759 * ROTA - 3.071594$$

where
WF = Fuel Mass Flow Rate (lbm/sec)
ROTA = Rotameter reading

TABLE V

Thermocouple Display Channel Assignments, Type K

Channel	Assignment
1	Exit Plane (TEP)
2	Plenum Ambient
3	Uptake (TUPT)
4	Burner (TBURN)
5	Nozzle Box at the postition of the removed burner
6	Mixing Stack, thermocouple 5
7	Mixing Stack, thermocouple 10
8	Mixing Stack, thermocouple 8
9	Mixing Stack, thermocouple 12
10	Mixing Stack, thermocouple 11
11	Mixing Stack, thermocouple 7
12	Mixing Stack, thermocouple 4
13	Mixing Stack, thermocouple 6
14	Mixing Stack, thermocouple 3
15	Mixing Stack, thermocouple 9
16	Mixing Stack, thermocouple 2
17	Mixing Stack, thermocouple 1
18	unused

AD-A123 776 TESTING OF A SHROUDED SHORT MIXING STACK GAS EDUCTOR MODEL USING HIGH TEMPERATURE PRIMARY FLOW(U) NAVAL POSTGRADUATE SCHOOL MONTEREY CA I J EICK OCT 82 3/3

UNCLASSIFIED F/G 21/2 NL

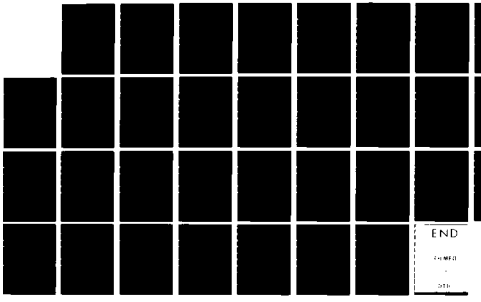

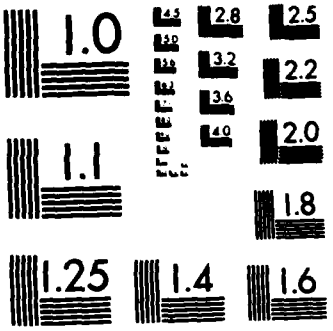

TABLE VI

Thermocouple Display Channel Assignments, Type T

Channel	Assignment
1	Fuel Supply
2	Ambient Air (TAMB)
3	Inlet Air Supply (TNH)
4	unused
5	Model B Shroud, X/D=0.25
6	Model B Shroud, X/D=0.5
7	Model B Shroud, X/D=0.75
8	Model B Shroud, X/D=1.0
9	Model B Shroud, X/D=1.15
10	Model B First Diffuser Ring X/D=1.15
11	Model B First Diffuser Ring X/D=1.25
12	Model B Second Diffuser Ring X/D=1.25
13	Model B Second Diffuser Ring X/D=1.5
14-18	unused

TABLE VII

Model Characteristics

	MODEL A	MODEL B
Mixing Stack Assembly L/D (overall)	2.5	1.5
Mixing Stack		
Inside Diameter (D)	7.122"	7.122"
L/D	1.75	1.0
Rows of Film Cooling Slots	6	4
Shroud Start Position (X/D)	.25	.25
Diffuser		
Number of Rings	2	2
Ring Length (l/D)	.25	.25
Half Angle	9.3°	7.3°
Film Cooling Clearance	0.1875"	0.076"
Stand-off Distance (S/D)	0.5	0.5
Primary Nozzles		
Number	4	4
Type	Straight (0/0)	Tilted-angled (15/20)
Am/Ap	2.5	2.5

*** HOT RIG PERFORMANCE *** TUPT: 175
2 RING DIFFUSER

DATE: 2 JUNE 1982

DATA TAKEN BY I J EICK

NUMBER OF PRIMARY NOZZLES: 4
PRIMARY NOZZLE DIAMETER: 2.25 INCHES
UPTAKE DIAMETER: 7.510 INCHES
AREA RATIO, AP/AP: 2.50
GAMMA: 1.3953

MIXING STACK LENGTH: 17.81 INCHES
MIXING STACK DIAMETER: 7.122 INCHES
MIXING STACK L/D: 2.50
STANDOFF RATIO: 0.50
AMBIENT PRESSURE: 29.93 INCHES HG

NR	PNH IN HG	CELPN IN H2O	TNH DEG F	ROTA	TBURN DEG F	TUPT DEG F	TAMB DEG F	PUPT IN H2O	PPLN IN H2O	SEC AREA SQ IN
1	3.70	14.80	183.2	0.0	168.0	175.0	60.4	4.70	4.40	0.000
2	3.80	14.80	183.5	0.0	168.0	175.0	60.0	5.20	3.90	1.767
3	3.80	14.90	183.4	0.0	168.0	175.0	59.4	5.60	3.45	3.534
4	3.80	14.90	183.2	0.0	168.0	175.0	60.8	6.00	3.04	5.301
5	3.80	14.80	183.5	0.0	168.0	175.0	59.2	6.50	2.46	8.443
6	3.80	14.80	183.5	0.0	168.0	175.0	60.4	6.95	2.03	11.585
7	3.90	14.80	183.8	0.0	168.0	175.0	60.4	7.30	1.68	14.726
8	3.90	14.70	184.1	0.0	169.0	176.0	61.2	8.00	0.85	27.293
9	3.90	14.60	184.6	0.0	170.0	176.0	62.5	8.30	0.49	39.859
10	3.95	14.65	184.3	0.0	169.0	176.0	60.8	8.50	0.31	52.425
11	3.95	14.65	184.9	0.0	170.0	177.0	62.6	8.60	0.22	64.992
12	4.00	14.65	185.1	0.0	170.0	177.0	61.5	8.80	0.00	******

NR	WPA LBM/S	WF LBM/S	WP LBM/S	WS LBM/S	W*	P*	T*	P*/T*	W*T**.44	UP FT/S	UM FT/S	UU FT/S	UMACH
1	1.576	0.000	1.576	0.000	0.000	0.365	0.819	0.445	0.000	231.5	92.4	81.3	0.0658
2	1.578	0.000	1.578	0.119	0.076	0.323	0.819	0.394	0.069	231.5	98.1	81.3	0.0658
3	1.583	0.000	1.583	0.224	0.142	0.284	0.818	0.347	0.130	232.0	103.3	81.5	0.0660
4	1.583	0.000	1.583	0.315	0.199	0.251	0.820	0.306	0.183	231.8	107.6	81.4	0.0659
5	1.578	0.000	1.578	0.453	0.287	0.204	0.818	0.250	0.263	230.6	113.7	81.0	0.0656
6	1.578	0.000	1.578	0.564	0.357	0.169	0.819	0.206	0.327	230.4	118.9	80.9	0.0655
7	1.580	0.000	1.580	0.652	0.413	0.140	0.819	0.170	0.378	230.5	123.1	80.9	0.0656
8	1.574	0.000	1.574	0.858	0.545	0.071	0.819	0.087	0.500	229.5	132.6	80.7	0.0653
9	1.568	0.000	1.568	0.951	0.606	0.041	0.821	0.050	0.556	228.5	136.6	80.3	0.0650
10	1.573	0.000	1.573	0.996	0.634	0.026	0.819	0.032	0.580	229.0	138.8	80.5	0.0651
11	1.572	0.000	1.572	1.039	0.661	0.018	0.820	0.023	0.606	229.2	141.1	80.5	0.0651
12	1.573	0.000	1.573	0.000	0.000	0.000	0.819	0.000	0.000	229.2	91.5	80.5	0.0651

Table VIII, Pumping Coefficient Data,
Model A (175° F)

*** MOI BIG PERFORMANCE *** TUPT: 650
2 RING DIFFUSER

DATE: 5 JUNE 1982

DATA TAKEN BY I J EICK

NUMBER OF PRIMARY NOZZLES: 4
PRIMARY NOZZLE DIAMETER: 2.25 INCHES
UPTAKE DIAMETER: 7.510 INCHES
AREA RATIO, AM/AP: 2.50
GAMMA: 1.3741

MIXING STACK LENGTH: 17.81 INCHES
MIXING STACK DIAMETER: 7.122 INCHES
MIXING STACK L/D: 2.50
STANDOFF RATIO: 0.50
AMBIENT PRESSURE: 29.90 INCHES HG

NR	PNH IN HG	CELPN IN H2O	TNH DEG F	ROTA	TBURN DEG F	TUPT DEG F	TAMB DEG F	PUPT IN H2O	PPLN IN H2O	SEC AREA SQ IN
1	4.00	8.30	185.4	27.4	1162.0	652.0	63.1	5.40	4.39	0.000
2	4.00	8.30	185.7	27.5	1154.0	650.0	61.4	5.90	3.84	1.767
3	4.10	8.30	185.4	27.5	1156.0	650.0	64.3	6.30	3.39	3.534
4	4.10	8.20	185.5	27.5	1157.0	649.0	62.5	6.70	2.99	5.301
5	4.10	8.20	185.6	27.5	1156.0	650.0	62.0	7.20	2.43	8.443
6	4.15	8.20	185.5	27.6	1159.0	650.0	63.7	7.60	1.97	11.585
7	4.15	8.25	185.6	27.5	1162.0	651.0	62.9	7.90	1.64	14.726
8	4.20	8.25	185.7	27.5	1158.0	649.0	62.3	8.15	0.82	27.293
9	4.25	8.25	185.3	27.5	1152.0	648.0	62.6	9.00	0.47	39.859
10	4.25	8.25	185.5	27.5	1156.0	648.0	63.0	9.15	0.30	52.425
11	4.25	8.25	185.4	27.5	1154.0	648.0	63.3	9.20	0.20	64.992
12	4.25	8.20	185.5	27.5	1163.0	647.0	61.1	9.40	0.00	******

NR	WPA LBM/S	WF LBM/S	WP LBM/S	WS LBM/S	W*	P*	T*	P*/T*	W*T**.44	UP FT/S	UM FT/S	UL FT/S	UMACH
1	1.193	0.008	1.201	0.000	0.000	0.205	0.470	0.436	0.000	309.2	123.4	108.4	0.0669
2	1.192	0.008	1.201	0.118	0.098	0.180	0.470	0.383	0.071	308.2	128.7	108.0	0.0668
3	1.194	0.008	1.202	0.221	0.184	0.159	0.472	0.338	0.132	308.3	133.8	108.1	0.0668
4	1.187	0.008	1.195	0.312	0.261	0.142	0.471	0.302	0.188	305.9	137.2	107.3	0.0663
5	1.187	0.008	1.195	0.448	0.375	0.115	0.470	0.245	0.269	305.8	143.6	107.2	0.0663
6	1.188	0.008	1.196	0.553	0.462	0.094	0.472	0.199	0.332	305.7	148.6	107.2	0.0663
7	1.192	0.008	1.200	0.642	0.535	0.077	0.470	0.165	0.384	306.5	153.2	107.5	0.0664
8	1.192	0.008	1.200	0.842	0.701	0.039	0.471	0.083	0.503	305.6	162.3	107.3	0.0664
9	1.194	0.008	1.202	0.931	0.774	0.022	0.472	0.047	0.556	305.3	166.4	107.1	0.0663
10	1.193	0.008	1.201	0.977	0.814	0.014	0.472	0.030	0.585	305.2	168.6	107.1	0.0662
11	1.193	0.008	1.202	0.989	0.823	0.010	0.472	0.020	0.592	305.1	169.2	107.1	0.0662
12	1.190	0.008	1.198	0.000	0.000	0.000	0.471	0.000	0.000	303.8	121.3	106.6	0.0660

Table IX, Pumping Coefficient Data,
Model A (650° F)

*** HOT RIG PERFORMANCE *** TUPT: 750
2 RING DIFFUSER

DATE: 2 JUNE 1982

DATA TAKEN BY I J EICK

NUMBER OF PRIMARY NOZZLES: 4
PRIMARY NOZZLE DIAMETER: 2.25 INCHES
UPTAKE DIAMETER: 7.510 INCHES
AREA RATIO: AM/AP: 2.50
GAMMA: 1.3677

MIXING STACK LENGTH: 17.81 INCHES
MIXING STACK DIAMETER: 7.122 INCHES
MIXING STACK L/D: 2.50
STANDOFF RATIO: 0.50
AMBIENT PRESSURE: 29.93 INCHES HG

NR	PNH IN HG	CELPN IN H2O	TNH DEG F	ROTA	TBURN DEG F	TUPT DEG F	TAMB DEG F	PUPT IN H2O	PPLN IN H2O	SEC AREA SQ IN
1	4.50	7.35	186.4	24.0	1130.0	744.0	63.2	6.15	4.23	0.000
2	4.55	7.45	186.6	24.0	1141.0	751.0	62.3	6.70	3.70	1.767
3	4.60	7.40	186.3	24.0	1131.0	740.0	61.1	7.50	3.22	3.534
4	4.80	7.40	186.5	24.0	1076.0	746.0	61.6	7.85	2.82	5.301
5	4.85	7.40	186.6	24.1	1088.0	750.0	62.9	8.40	2.27	8.443
6	4.90	7.20	186.8	24.0	1090.0	753.0	61.5	8.75	1.85	11.585
7	4.90	7.30	186.8	24.1	1087.0	753.0	64.2	9.05	1.53	14.726
8	4.95	7.20	187.1	24.0	1087.0	753.0	62.5	9.76	0.76	27.293
9	4.95	7.20	187.1	24.0	1088.0	754.0	66.1	10.00	0.43	39.859
10	5.00	7.20	187.5	23.9	1088.0	754.0	64.6	10.20	0.27	52.425
11	5.00	7.30	187.5	23.9	1086.0	754.0	62.0	10.30	0.18	64.992
12	5.00	7.30	187.5	24.0	1080.0	749.0	63.5	10.40	0.00	******

NR	WPA LBM/S	WF LBM/S	WP LBM/S	WS LBM/S	W*	P*	T*	P*/T*	W*T**.44	UP FT/S	UM FT/S	UU FT/S	UMACH
1	1.132	0.007	1.139	0.000	0.000	0.188	0.434	0.432	0.000	317.1	126.6	111.0	0.0660
2	1.140	0.007	1.147	0.116	0.101	0.160	0.431	0.371	0.070	320.8	133.6	112.3	0.0666
3	1.138	0.007	1.144	0.216	0.189	0.142	0.434	0.328	0.131	316.8	136.8	110.8	0.0660
4	1.141	0.007	1.147	0.304	0.265	0.123	0.432	0.285	0.183	318.5	141.9	111.5	0.0663
5	1.141	0.007	1.148	0.433	0.377	0.099	0.432	0.228	0.261	319.7	148.4	111.8	0.0664
6	1.127	0.007	1.134	0.537	0.474	0.082	0.430	0.191	0.327	316.1	151.9	110.6	0.0656
7	1.135	0.007	1.141	0.620	0.543	0.067	0.432	0.156	0.375	318.0	156.7	111.3	0.0659
8	1.128	0.007	1.134	0.811	0.715	0.034	0.431	0.078	0.493	315.4	164.7	110.4	0.0654
9	1.128	0.007	1.134	0.888	0.783	0.019	0.433	0.044	0.542	315.4	168.6	110.4	0.0654
10	1.126	0.007	1.135	0.926	0.816	0.012	0.432	0.028	0.564	315.4	170.3	110.4	0.0654
11	1.136	0.007	1.142	0.940	0.823	0.008	0.430	0.018	0.568	317.4	171.6	111.1	0.0658
12	1.136	0.007	1.142	0.000	0.000	0.000	0.433	0.000	0.000	316.0	126.2	110.6	0.0657

Table X, Pumping Coefficient Data,
Model A (750° F)

*** HOT RIG PERFORMANCE *** TUPT: 850
2 RING DIFFUSER

DATE: 2 JUNE 1982

DATA TAKEN BY I J EICK

NUMBER OF PRIMARY NOZZLES: 4
PRIMARY NOZZLE DIAMETER: 2.25 INCHES
UPTAKE DIAMETER: 7.510 INCHES
AREA RATIO, AM/AP: 2.50
GAMMA: 1.3614

MIXING STACK LENGTH: 17.81 INCHES
MIXING STACK DIAMETER: 7.122 INCHES
MIXING STACK L/D: 2.50
STANDOFF RATIO: 0.50
AMBIENT PRESSURE: 29.93 INCHES HG

NR	PNH IN HG	CELPN IN H2O	TNH DEG F	ROTA	TBURN DEG F	TUPT DEG F	TAMB DEG F	PUPT IN H2O	PPLN IN H2O	SEC AREA SQ IN
1	4.50	6.90	184.9	26.2	1180.0	850.0	62.2	6.95	4.28	0.000
2	4.90	6.90	185.1	26.1	1180.0	850.0	62.5	7.50	3.71	1.767
3	4.90	6.85	185.1	26.2	1182.0	850.0	63.9	7.95	3.24	3.534
4	4.55	6.85	185.3	26.0	1185.0	851.0	63.2	8.30	2.86	5.301
5	5.00	6.85	185.4	26.1	1183.0	850.0	64.3	8.80	2.28	8.[illegible]3
6	5.00	6.90	185.4	26.1	1183.0	851.0	60.8	9.25	1.85	11.585
7	5.05	6.85	185.2	26.1	1180.0	850.0	60.5	9.50	1.53	14.726
8	5.10	6.90	185.2	26.2	1180.0	850.0	60.1	10.20	0.77	27.293
9	5.10	6.85	185.2	26.1	1178.0	850.0	62.8	10.50	0.44	39.859
10	5.10	6.80	185.2	26.2	1176.0	850.0	62.5	10.65	0.28	52.425
11	5.15	6.75	185.5	26.1	1176.0	849.0	61.1	10.70	0.19	64.992
12	5.15	6.70	185.6	26.0	1180.0	852.0	63.1	10.90	0.00	******

AR	WFA LBM/S	WF LBM/S	WP LBM/S	WS LBM/S	W*	P*	T*	P*/T*	W*T**.44	UP FT/S	UM FT/S	UL FT/S	UMACH
1	1.106	0.008	1.113	0.000	0.000	0.168	0.398	0.421	0.000	337.3	134.7	117.8	0.0673
2	1.106	0.007	1.113	0.116	0.104	0.146	0.399	0.365	0.070	336.8	140.0	117.6	0.0672
3	1.102	0.008	1.109	0.216	0.195	0.129	0.400	0.322	0.130	335.2	144.3	117.1	0.0669
4	1.102	0.007	1.110	0.305	0.275	0.113	0.399	0.284	0.184	335.3	148.6	117.1	0.0669
5	1.103	0.007	1.110	0.434	0.391	0.091	0.400	0.226	0.261	334.8	154.5	117.0	0.0669
6	1.107	0.007	1.114	0.538	0.483	0.072	0.397	0.182	0.321	335.8	159.8	117.4	0.0671
7	1.104	0.007	1.111	0.622	0.560	0.060	0.397	0.152	0.373	334.4	163.2	116.9	0.0668
8	1.109	0.008	1.116	0.818	0.733	0.030	0.397	0.076	0.488	335.2	172.8	117.2	0.0670
9	1.105	0.007	1.112	0.901	0.810	0.017	0.399	0.044	0.541	333.8	176.3	116.7	0.0667
10	1.101	0.008	1.108	0.945	0.853	0.011	0.399	0.028	0.569	332.5	177.9	116.2	0.0665
11	1.097	0.007	1.105	0.967	0.875	0.008	0.398	0.019	0.583	331.1	178.2	115.8	0.0662
12	1.093	0.007	1.101	0.000	0.000	0.000	0.399	0.000	0.000	330.5	131.9	115.6	0.0660

Table XI, Pumping Coefficient Data,
Model A (850° F)

*** HOT RIG PERFORMANCE *** TUPT: 955
2 RING DIFFUSER

DATE: 2 JUNE 1982

DATA TAKEN BY I J EICK

NUMBER OF PRIMARY NOZZLES: 4
PRIMARY NOZZLE DIAMETER: 2.25 INCHES
UPTAKE DIAMETER: 7.510 INCHES
AREA RATIO, AM/AP: 2.50
GAMMA: 1.3556

MIXING STACK LENGTH: 17.81 INCHES
MIXING STACK DIAMETER: 7.122 INCHES
MIXING STACK L/D: 2.50
STANDOFF RATIO: 0.50
AMBIENT PRESSURE: 29.93 INCHES HG

NR	PNH IN HG	DELPN IN H2O	TNH DEG F	ROTA	TBURN DEG F	TUPT DEG F	TAMB DEG F	PUPT IN H2O	PPLN IN H2O	SEC AREA SQ IN
1	5.80	6.20	185.6	30.0	1208.0	953.0	61.1	8.75	4.52	0.000
2	5.80	6.30	185.6	30.0	1208.0	957.0	63.4	8.90	3.87	1.767
3	5.90	6.20	185.6	29.9	1197.0	955.0	61.7	9.50	3.36	3.534
4	5.95	6.20	185.6	30.0	1197.0	955.0	62.0	9.90	2.93	5.301
5	6.00	6.30	185.4	30.0	1198.0	955.0	59.3	10.45	2.34	8.443
6	6.00	6.20	185.0	30.0	1199.0	956.0	59.8	10.90	1.89	11.585
7	6.00	6.20	184.6	30.0	1199.0	956.0	58.0	11.20	1.55	14.726
8	6.10	6.15	184.4	30.0	1206.0	959.0	61.8	12.00	0.76	27.293
9	6.10	6.15	184.9	30.0	1208.0	962.0	60.9	12.65	0.44	39.859
10	6.40	6.00	184.8	30.0	1164.0	959.0	61.4	12.80	0.28	52.425
11	6.40	6.00	184.9	30.0	1165.0	959.0	60.7	12.90	0.19	64.992
12	6.60	5.90	184.7	30.0	1145.0	954.0	62.4	13.20	0.00	******

NR	WFA LBM/S	WF LBM/S	WP LBM/S	WS LBM/S	W*	P*	T*	P*/T*	W*T**.44	UP FT/S	UN FT/S	UU FT/S	UMACH
1	1.063	0.009	1.072	0.000	0.000	0.164	0.369	0.444	0.000	350.4	139.9	121.8	0.0672
2	1.071	0.009	1.080	0.118	0.110	0.138	0.369	0.374	0.071	353.6	146.9	123.0	0.0678
3	1.064	0.009	1.073	0.221	0.206	0.122	0.369	0.330	0.133	350.4	150.5	121.9	0.0672
4	1.065	0.009	1.074	0.309	0.288	0.106	0.369	0.288	0.186	350.3	154.7	121.9	0.0672
5	1.074	0.009	1.083	0.441	0.408	0.083	0.367	0.226	0.262	352.7	161.9	122.8	0.0677
6	1.066	0.009	1.075	0.544	0.506	0.068	0.367	0.185	0.326	350.0	165.7	121.8	0.0671
7	1.066	0.009	1.075	0.627	0.583	0.056	0.366	0.152	0.375	349.8	169.4	121.8	0.0671
8	1.064	0.009	1.073	0.811	0.756	0.028	0.368	0.075	0.487	349.0	178.1	121.5	0.0669
9	1.063	0.009	1.072	0.902	0.841	0.016	0.366	0.043	0.541	349.4	182.4	121.5	0.0668
10	1.055	0.009	1.064	0.946	0.889	0.010	0.367	0.028	0.572	345.8	183.1	120.3	0.0662
11	1.055	0.009	1.064	0.967	0.909	0.007	0.367	0.019	0.585	345.7	184.0	120.2	0.0662
12	1.045	0.009	1.058	0.000	0.000	0.000	0.369	0.000	0.000	342.5	136.7	119.1	0.0657

Table XII, Pumping Coefficient Data,
Model A (950° F)

TABLE XIII

Shroud and Diffuser Temperature Data, Model A

Uptake Temperature	Axial Position	Temperature (° F) 177	648	748	854	954
				(° F)		
Shroud	0.5	61.6	66.4	68.2	68.6	70.6
	1.0	62.1	70.7	74	74.9	77.7
	1.5	65.6	87.2	92.4	95.1	100.1
First	2.0	67.5	83.1	85.1	87.4	90.5
Diffuser	2.0	66.9	81.3	82.5	85.5	86.2
Ring	2.25	70.2	99.4	102.0	107.6	112.7
Second	2.25	69.5	93.6	96.7	101.5	103.4
Diffuser	2.25	69.6	93.4	95.6	99.9	100.3
Ring	2.5	72.0	108.3	111.9	118.8	126.4
	2.5	73.3	111.9	113.2	119.5	120.4
Ambient		62	62	63	62	61

TABLE XIV

Exit Plane Temperature Data, Model A

Axial Position	r/Rms	Temperature (° F)			
Uptake Temperature		177	750	840	957
		(° F)			
0.0	1.264	63	133	115	150
0.25	1.193	70	185	171	174
0.5	1.123	77	230	227	238
0.75	1.053	82	268	265	287
1.0	0.983	87	292	292	330
1.25	0.913	92	319	328	365
1.5	0.843	98	350	350	406
1.75	0.772	102	366	384	432
2.0	0.702	109	388	407	457
2.25	0.632	112	404	432	484
2.5	0.562	118	417	470	507
2.75	0.491	122	434	481	528
3.0	0.421	127	444	498	551
3.25	0.351	130	456	518	574
3.5	0.281	131	466	530	588
3.75	0.211	132	473	544	612
4.0	0.140	134	482	558	628
4.25	0.070	135	481	563	637
4.5	0.0	136	485	566	644
4.5	0.0	136	486	558	642
4.25	0.070	136	488	552	649
4.0	0.140	135	488	544	642
3.75	0.211	133	486	530	631
3.5	0.281	133	482	517	623
3.25	0.351	127	473	497	602
3.0	0.421	126	465	479	582
2.75	0.491	121	448	473	568
2.5	0.562	120	438	448	545

(continued)

Table (XIV) (continued)

Axial Position	r/Rms	Temperature (° F)			
Uptake Temperature		177	750	840	957
		(° F)			
2.25	0.632	110	430	432	530
2.0	0.702	110	422	415	510
1.75	0.772	106	400	396	492
1.5	0.843	102	392	364	475
1.25	0.913	95	375	336	447
1.0	0.983	89	349	284	415
0.75	1.053	84	319	246	378
0.5	1.123	78	282	208	334
0.25	1.193	73	240	165	282
0.0	1.264	69	204	147	239
Ambient		62	63	62	61

*** HOT RIG PERFORMANCE *** TUPT: 178
2 RING DIFFUSER

DATE: 12 JUNE 1982

NUMBER OF PRIMARY NOZZLES: 4
PRIMARY NOZZLE DIAMETER: 2.25 INCHES
UPTAKE DIAMETER: 7.510 INCHES
AREA RATIO, AM/AP: 2.50
GAMMA: 1.3951

DATA TAKEN BY I J EICK

MIXING STACK LENGTH: 7.12 INCHES
MIXING STACK DIAMETER: 7.122 INCHES
MIXING STACK L/D: 1.50
STANDOFF RATIO: 0.50
AMBIENT PRESSURE: 29.82 INCHES HG

NR	PNH IN HG	CELPN IN H2O	TNH DEG F	ROTA	TBURN DEG F	TUPT DEG F	TAMB DEG F	PUPT IN H2O	PPLN IN H2O	SEC AREA SQ IN
1	3.60	14.70	184.6	0.0	172.0	177.0	71.5	5.60	4.31	0.000
2	3.60	14.70	184.7	0.0	172.0	178.0	71.8	6.05	3.87	1.767
3	3.60	14.70	185.0	0.0	173.0	178.0	72.1	6.50	3.44	3.534
4	3.60	14.70	185.2	0.0	173.0	178.0	71.5	6.90	3.06	5.301
5	3.65	14.70	185.1	0.0	173.0	178.0	70.6	7.40	2.54	8.443
6	3.70	14.60	185.3	0.0	173.0	178.0	70.8	7.80	2.10	11.585
7	3.70	14.60	185.3	0.0	173.0	178.0	72.0	8.10	1.75	14.726
8	3.70	14.60	185.5	0.0	173.0	178.0	71.6	8.40	0.89	27.293
9	3.80	14.60	185.5	0.0	173.0	179.0	71.8	9.30	0.52	39.859
10	3.80	14.55	185.6	0.0	173.0	179.0	71.1	9.45	0.33	52.425
11	3.80	14.55	185.8	0.0	174.0	179.0	71.5	9.50	0.22	64.992
12	3.80	14.55	186.1	0.0	174.0	179.0	71.1	9.75	0.00	******

NR	WPA LBM/S	WF LBM/S	WP LBM/S	WS LBM/S	W*	P*	T*	P*/T*	W*T**.44	UP FT/S	UM FT/S	UL FT/S	UMACH
1	1.564	0.000	1.564	0.000	0.000	0.367	0.834	0.440	0.000	231.3	92.3	81.0	0.0655
2	1.564	0.000	1.564	0.117	0.075	0.329	0.833	0.395	0.069	231.4	98.1	81.1	0.0655
3	1.564	0.000	1.564	0.221	0.141	0.293	0.834	0.351	0.130	231.1	103.1	81.0	0.0654
4	1.564	0.000	1.564	0.313	0.200	0.261	0.833	0.313	0.185	230.8	107.5	80.9	0.0654
5	1.565	0.000	1.565	0.454	0.290	0.216	0.832	0.260	0.268	230.7	114.3	80.8	0.0653
6	1.561	0.000	1.561	0.567	0.363	0.180	0.832	0.216	0.335	229.8	119.5	80.5	0.0651
7	1.561	0.000	1.561	0.657	0.421	0.150	0.834	0.180	0.388	229.6	123.8	80.5	0.0650
8	1.560	0.000	1.560	0.868	0.556	0.077	0.833	0.092	0.513	229.1	133.9	80.4	0.0650
9	1.563	0.000	1.563	0.969	0.620	0.045	0.832	0.054	0.572	229.6	139.0	80.5	0.0650
10	1.560	0.000	1.560	1.016	0.651	0.028	0.831	0.034	0.600	229.1	141.0	80.3	0.0648
11	1.560	0.000	1.560	1.028	0.659	0.019	0.832	0.023	0.608	229.0	141.5	80.3	0.0648
12	1.555	0.000	1.559	0.000	0.000	0.000	0.831	0.000	0.000	228.8	91.3	80.2	0.0648

Table XV, Pumping Coefficient Data,
Model B (178° F)

*** HOT RIG PERFORMANCE *** TUPT: 855
2 RING DIFFUSER

DATE: 12 JUNE 1982

DATA TAKEN BY I J EICK

NUMBER OF PRIMARY NOZZLES: 4
PRIMARY NOZZLE DIAMETER: 2.25 INCHES
UPTAKE DIAMETER: 7.510 INCHES
AREA RATIO, AM/AP: 2.50
GAMMA: 1.3614

MIXING STACK LENGTH: 7.12 INCHES
MIXING STACK DIAMETER: 7.122 INCHES
MIXING STACK L/D: 1.50
STANDOFF RATIO: 0.50
AMBIENT PRESSURE: 29.82 INCHES HG

NR	PNH IN HG	CELPN IN H2O	TNH DEG F	ROTA	TBURN DEG F	TUPT DEG F	TAMB DEG F	PUPT IN H2O	PPLN IN H2O	SEC AREA SQ IN
1	4.30	6.80	189.7	31.2	1289.0	845.0	74.8	6.90	4.69	0.000
2	4.35	6.75	189.6	31.6	1302.0	854.0	75.9	7.95	4.20	1.767
3	4.40	6.75	198.6	31.6	1302.0	853.0	75.7	7.90	3.74	3.534
4	4.40	6.70	189.6	31.6	1303.0	854.0	75.6	8.30	3.32	5.301
5	4.40	6.70	189.7	31.6	1301.0	853.0	75.5	8.80	2.71	8.448
6	4.50	6.70	189.7	31.6	1303.0	854.0	76.6	9.30	2.25	11.589
7	4.50	6.70	189.7	31.6	1303.0	856.0	75.4	9.60	1.86	14.726
8	4.50	6.70	189.8	31.6	1301.0	855.0	74.8	10.45	0.93	27.293
9	4.60	6.70	189.6	31.6	1302.0	856.0	74.6	10.80	0.53	39.859
10	4.60	6.70	189.7	31.6	1300.0	856.0	74.0	11.00	0.33	52.425
11	4.60	6.70	189.5	31.6	******	855.0	74.5	11.05	0.23	64.992
12	4.60	6.70	189.6	31.6	1309.0	858.0	73.0	11.30	0.00	******

NR	WPA LBM/S	WF LBM/S	WP LBM/S	WS LBM/S	W*	P*	T*	P*/T*	W*T**.44	UP FT/S	UM FT/S	UU FT/S	UMACH
1	1.083	0.010	1.093	0.000	0.000	0.196	0.410	0.478	0.000	331.4	132.3	115.6	0.0662
2	1.080	0.010	1.090	0.122	0.112	0.174	0.408	0.428	0.075	332.4	138.7	115.8	0.0661
3	1.074	0.010	1.084	0.230	0.212	0.158	0.408	0.386	0.143	329.8	143.1	115.1	0.0657
4	1.077	0.010	1.087	0.325	0.299	0.139	0.407	0.341	0.201	330.7	148.1	115.4	0.0659
5	1.077	0.010	1.087	0.467	0.430	0.114	0.408	0.279	0.290	330.0	154.8	115.2	0.0658
6	1.079	0.010	1.088	0.583	0.536	0.094	0.408	0.231	0.361	330.3	160.7	115.3	0.0658
7	1.079	0.010	1.088	0.675	0.620	0.078	0.407	0.191	0.417	330.5	165.2	115.4	0.0658
8	1.078	0.010	1.088	0.885	0.813	0.039	0.407	0.096	0.547	329.4	175.0	115.0	0.0656
9	1.080	0.010	1.090	0.976	0.895	0.022	0.406	0.054	0.602	329.9	179.6	115.2	0.0657
10	1.080	0.010	1.090	1.013	0.930	0.014	0.406	0.034	0.625	329.7	181.3	115.1	0.0657
11	1.080	0.010	1.090	1.048	0.962	0.010	0.406	0.024	0.647	329.4	182.9	115.1	0.0657
12	1.080	0.010	1. 90	0.000	0.000	0.000	0.404	0.000	0.000	329.9	131.7	115.2	0.0657

Table XVI, Pumping Coefficient Data,
Model B (855° F)

*** HOT RIG PERFORMANCE *** TUPT: 950
2 RING DIFFUSER

DATE: 12 JUNE 1982

DATA TAKEN BY I J EICK

NUMBER OF PRIMARY NOZZLES: 4
PRIMARY NOZZLE DIAMETER: 2.25 INCHES
UPTAKE DIAMETER: 7.510 INCHES
AREA RATIO, AM/AP: 2.50
GAMMA: 1.3556

MIXING STACK LENGTH: 7.12 INCHES
MIXING STACK DIAMETER: 7.122 INCHES
MIXING STACK L/D: 1.50
STANDOFF RATIO: 0.50
AMBIENT PRESSURE: 29.82 INCHES HG

NR	PNH IN HG	CELPN IN H2O	TNH DEG F	ROTA	TBURN DEG F	TUPT DEG F	TAMB DEG F	PUPT IN H2O	PPLN IN H2O	SEC AREA SQ IN
1	5.65	6.30	188.3	28.0	1214.0	950.0	78.5	8.90	5.18	0.000
2	5.70	6.30	188.2	28.0	1213.0	949.0	79.0	9.40	4.63	1.767
3	5.70	6.30	188.2	28.3	1217.0	952.0	77.0	9.90	4.13	3.534
4	5.70	6.25	188.1	28.0	1219.0	952.0	77.6	10.30	3.65	5.301
5	5.75	6.25	188.0	28.0	1223.0	952.0	76.7	10.90	2.98	8.443
6	5.80	6.25	188.1	28.0	1221.0	952.0	76.6	11.40	2.44	11.585
7	5.80	6.25	188.2	28.0	1222.0	952.0	77.8	11.75	2.04	14.726
8	5.90	6.25	188.2	28.0	1224.0	954.0	76.2	12.20	1.02	27.293
9	5.90	6.20	188.1	28.0	1227.0	953.0	76.7	13.10	0.58	39.859
10	5.90	6.20	188.4	28.0	1225.0	954.0	75.5	13.30	0.37	52.425
11	5.90	6.20	188.1	28.0	1226.0	954.0	77.6	13.35	0.25	64.992
12	5.90	6.20	188.4	28.0	1227.0	955.0	76.1	13.60	0.00	******

NR	WPA LBM/S	WF LBM/S	WP LBM/S	WS LBM/S	W*	P*	T*	P*/T*	W*T**.44	UP FT/S	UM FT/S	UU FT/S	UMACH
1	1.065	0.008	1.073	0.000	0.000	0.193	0.382	0.506	0.000	352.1	140.6	122.1	0.0674
2	1.066	0.008	1.074	0.127	0.119	0.173	0.382	0.453	0.078	351.6	146.7	122.0	0.0674
3	1.066	0.008	1.074	0.241	0.224	0.153	0.380	0.403	0.147	352.0	152.5	122.1	0.0674
4	1.062	0.008	1.070	0.340	0.317	0.137	0.381	0.360	0.207	350.2	156.7	121.5	0.0670
5	1.063	0.008	1.071	0.489	0.457	0.112	0.380	0.294	0.298	349.9	163.9	121.4	0.0670
6	1.063	0.008	1.071	0.607	0.567	0.091	0.380	0.240	0.370	349.6	169.6	121.3	0.0670
7	1.063	0.008	1.071	0.705	0.658	0.077	0.381	0.201	0.430	349.2	174.4	121.2	0.0669
8	1.065	0.008	1.073	0.925	0.863	0.038	0.379	0.100	0.563	349.3	185.1	121.4	0.0670
9	1.060	0.008	1.069	1.019	0.953	0.022	0.380	0.058	0.622	347.4	188.9	120.6	0.0665
10	1.060	0.008	1.069	1.071	1.003	0.014	0.379	0.037	0.654	347.4	191.3	120.6	0.0665
11	1.060	0.008	1.069	1.090	1.020	0.009	0.380	0.025	0.666	347.3	192.4	120.7	0.0665
12	1.060	0.008	1.069	0.000	0.000	0.000	0.379	0.000	0.000	347.3	138.6	120.6	0.0665

Table XVII, Pumping Coefficient Data,
Model B (950° F)

TABLE XVIII

Mixing Stack Pressure Data, Model B

	Axial Position	Mixing Stack Pressure (in. H_2O referenced to B)		
Uptake Temperature		180	850 (° F)	950
Position A	0.0	-1.81	-2.14	-2.29
	0.25	-0.98	-1.17	-1.23
	0.5	-0.19	-0.18	-0.17
	0.75	-1.08	-1.36	-1.27
Position B	0.0	-1.83	-2.07	-2.18
	.25	-0.98	-1.22	-1.23
	0.5	-1.14	-1.33	-1.32
	0.75	-1.08	-1.28	-1.29
			PMS*	
Position A	0.0	-0.030	-0.017	-0.017
	0.25	-0.016	-0.009	-0.009
	0.5	-0.003	-0.001	-0.001
	0.75	-0.019	-0.011	-0.009
Position B	0.0	-0.030	-0.016	-0.015
	0.25	-0.016	-0.010	-0.009
	0.5	-0.019	-0.011	-0.010
	0.75	-0.017	-0.010	-0.009
Ambient Temperature (° F)		71.5	75.0	77.0
Primary Nozzle Velocity (ft/sec)		228.80	329.94	347.29

TABLE XIX

Mixing Stack Temperature Data, Model B

Thermocouple Number	Axial Position	Mixing Stack Temperature (° F)		
Uptake Temperature		180	850	950
			(° F)	
5	0.0	xxx	xxx	xxx
10	0.0	xxx	xxx	xxx
8	0.41	68	128	154
12	0.41	70	139	185
11	0.36	72	160	193
7	0.46	70	125	143
4	0.61	75	182	208
6	0.76	86	240	261
3	0.89	77	213	261
9	0.89	93	284	306
2	0.84	66	77	70
1	0.94	86	231	255
Ambient		71	73	77

TABLE XX

Shroud and Diffuser Temperature Data, Model B

Uptake Temperature	Axial Position	Temperature (° F) 180	850	950
Shroud	0.25	70.7	73.1	88.0
	0.5	70.6	81.9	95.5
	0.75	75.4	116.6	130.8
	1.0	83.5	179.9	204.0
	1.15	81.3	162.0	181.0
First Diffuser Ring	1.15	70.9	82.4	92.0
	1.25	71.6	86.0	96.8
Second Diffuser Ring	1.25	72.6	85.8	96.3
Ambient		71	72	77

TABLE XXI

Exit Plane Temperature Data, Model B

Axial Position	r/Rms	Temperature (° F)		
Uptake Temperature		182	852 (° F)	953
0.0	1.123	78	156	164
0.25	1.053	96	285	297
0.5	0.983	102	327	366
0.75	0.913	108	352	390
1.0	0.843	110	364	406
1.25	0.772	112	380	422
1.5	0.702	115	400	440
1.75	0.632	120	420	450
2.0	0.562	126	436	466
2.25	0.491	130	454	480
2.5	0.421	135	469	498
2.75	0.351	140	479	516
3.0	0.281	143	491	524
3.25	0.211	146	504	544
3.5	0.140	146	506	552
3.75	0.070	146	511	562
4.0	0.0	146	514	564
4.0	0.0	145	518	571
3.75	0.070	145	512	570
3.5	0.140	144	506	571
3.25	0.211	144	495	567
3.0	0.281	142	482	560
2.75	0.351	139	470	550
2.5	0.421	137	454	537
2.25	0.491	134	435	526
2.0	0.562	130	424	509
1.75	0.632	126	406	492
1.5	0.702	123	388	479
1.25	0.772	118	374	462
1.0	0.843	116	364	447
0.75	0.913	113	347	434
0.5	0.983	108	296	424
0.25	1.053	99	200	410
0.0	1.123	75	xxx	382
Ambient		71	72	77

APPENDIX A

GAS GENERATOR OPERATION

I. PRIMARY AIR COMPRESSOR OPERATION The primary air flow for the gas generator is supplied by a Carrier Model 18P352 three stage centrifugal air compressor located in Building 230. The compressor is driven through a Western Gear Model 95HSA speed increasing gearbox by a 300 horsepower General Electric induction motor. The compressor serves various other experiments both in building 230 and 249. Figure (14) is a schematic of the compressor system layout. The cooling water system serves both the Carrier compressor and the Sullivan compressor for the supersonic wind tunnel in building 230.

Lube oil for the compressor and speed increaser bearings is supplied from an external sump by either an attached pump or an electrically driven auxiliary pump. The lube oil is cooled in a closed loop oil to fresh water heater exchanger. Cooling water circulates within its own loop and is cooled in an evaporative cooling tower which stands between buildings 230 and 249. Makeup is automatically provided to the fresh water loop by a float operated valve in the cooling tower.

It is recommended that the lube oil system for the compressor be started approximately one hour prior to

compressor lightoff. This ensures adequate pre-lubrication and warms the oil to some degree, decreasing starting loads. This is critical, as the compressor operates at near the capacity of the breaker in the supplying substation. Should this breaker trip out during the starting sequence it will be necessary to call the trouble desk and have base electricians reset it.

During periods when operations are being conducted daily or when it is desired to operate early in the morning, it is permissable to leave the auxiliary oil pump running overnight with the cooling water system secured. This will maintain the lube oil at a temperature suitable for lightoff and eliminate this delay.

When fully warmed up the compressor supplies air to the gas generator at 170-190° F. It normally takes the compressor about one hour to reach stable operation at this temperature. Although it is possible to obtain a gas generator lightoff with a lower air supply temperature, stable operation enhances data taking and reduces the number of control adjustments required during data runs. It is, therefore, desirable to allow the system to fully stabilize prior to lighting off the gas generator or collecting data. The following lightoff sequence is recommended:

A) Check the oil level in the compressor's external sump. Oil should be within four inches of the top of the sight glass.

B) Start the auxiliary oil pump by positioning the "hand-off-automatic" switch (Figure 15) in the "hand" position. The electric pump will start and oil pressure should register approximately 30 PSIG. Inspect the system for leaks and note the level in the external sump.

C) Wait 45 minutes to one hour. During this period the compressor bearing temperatures should rise to approximately 70° F.

D) Line up the combustion gas generator for operation.

1) Open the two manometer isolation valves at the pressure taps on either side of the inlet reducing section (Figure 5). Reconnect manometer tubing at the manometers if it has previously been disconnected.

2) Ensure the main air supply butterfly valve is fully closed (Figure 6).

3) Open the air supply bypass globe valve two and one quarter turns (Figure 6).

4) Open the manually operated 4 inch butterfly isolation valve (Figure 5).

5) Energize the main power panel (Figure 9) and open the electrically operated burner air supply and cooling air bypass valves fully.

6) Ensure the gas generator exhaust area is clear.

E) Start the air compressor fresh water cooling system:

1) Check the water level in the cooling tower, it should be at the level of the inlet line.

2) Vent the cooling water pump casing. Open the petcock on the suction side of the pump casing until all air in the suction line is expelled.

3) Ensure valve "A" to the Sullivan compressor is closed.

4) Open valve "B" to the Carrier compressor.

5) Start the cooling water pump and cooling tower fan (Figure 17). The fan is interlocked with the pump and will not start unless the pump is running.

6) Inspect the cooling tower drip lattice to ensure water is circulating.

F) Open the drain on the air compressor air cooling bank (Figure 19).

G) Ensure the compressor air suction valve is fully closed (indicator vertical) (Figure 20).

> **WARNING** When in operation the compressor produces hazardous noise. Ensure all personnel in the vicinity are wearing adequate hearing protection prior to starting the compressor.

H) Start the air compressor motor (Figure 13), the controller uses an automatic two stage start circuit.

I) When the compressor is fully up to speed, switch the auxiliary lube oil pump to the "automatic" position. Lube oil pressure should remain about 24-30 PSIG. Oil is now being supplied by the attached pump driven by the speed increasing gearbox. If the oil pressure should fall to 12 PSIG, the auxiliary pump will start automatically.

J) When compressor operation has stabilized, slowly open the suction valve until the indicator is in the full open (horizontal) position. Air is now being supplied to the gas generator. Bypass air from the supply to other experiments will also be discharged outside the rear of building 230. Normally it is not necessary to secure this bypass flow, but in unusual circumstances it may be stopped by closing the isolation valve on the cooling bank (Figure 19).

K) Operation of the air compressor should be monitored periodically.

1) Normal oil pressure from the attached pump is 24 PISG. Specified bearing pressures are 20-25 PSIG.

2) Normal oil pressure from the auxiliary electric pump is 30 PSIG.

3) Normal oil temperature at the outlet of the lube oil cooler is 100-105° F (135° F maximum).

4) Normal Bearing temperatures for the compressor are 140-160° F. Speed increaser oil temperature is normally 120-130° F.

5) Do not allow any bearing temperature to exceed 200° F. In the event bearing temperatures rise above 180° F during normal operation, the oil cooler should be inspected for proper water temperature and flow rate.

II. GAS GENERATOR LIGHT OFF Allow the air compressor to operate for approximately one hour in order for air inlet temperature to the gas generator to stabilize.

A) Approximately 15 minutes prior to gas generator light off, line up the fuel system and place it in operation.

1) Open the fuel tank suction valve (Figure 22) and bulkhead isolation valve (Figure 21).

2) Ensure the solenoid operated emergency fuel cutoff valve is closed and close the HP pump manual discharge valve.

3) Open the nozzle box drain valve.

4) If this is the first time the system is being placed in operation, open both the fuel control valve (Figure 8) and the needle trimmer valve (Figure 24) fully. If the trimmer valve is known to be properly set, it need not be adjusted as described in this and following steps.

5) Start the fuel supply pump. Fuel supply pressure will be 14-16 PSIG.

6) Start the HP pump. With both trimmer and fuel control valves fully open the discharge pressure

will be 25-30 PSIG. With the trimmer valve properly set and the fuel control valve fully open, the HP pump discharge pressure will be 80 PSIG.

7) If the trimmer valve is to be adjusted, close the fuel control valve with the trimmer valve fully open. Observing the HP pump discharge pressure, slowly close the trimmer valve until the HP pump pressure reaches 350 PSIG. The trimmer valve is now set and the fuel control valve should provide smooth control over a range of 80-350 PSIG HP pump discharge pressure. All subsequent fuel control adjustments will be made using the fuel control valve.

8) Using the fuel control valve, set the HP pump discharge pressure at 200 PSIG and allow the system to recirculate for 10-15 minutes to warm the fuel. This facilitates combustion and ensures a clean lightoff.

B) When the inlet air temperature reaches 170-180° F, the gas generator may be lighted off.

1) Adjust inlet air bypass valve to obtain a pressure of approximately 4.0 in Hg at the upstream side of the inlet reducing section (PNH).

2) Ensure the burner air valve is fully open. Adjust the bypass cooling air valve to obtain a pressure drop across the U-tube of 1.60 inches H_2O. In some cases it may be necessary to leave the cooling air bypass valve fully open and reduce the inlet air pressure (PNH) slightly to obtain this setting. The pressure drop across the inlet reducing section (DELPN) will be about 15 inches H_2O. This provides the recommended lightoff air fuel ratio of 20.

3) Open the HP pump manual discharge valve fully.

4) Set the high temperature (Type K) readout to monitor burner temperature (TBURN). Set the low temperature (Type T) readout to monitor air inlet temperature (TNH).

5) Ensure the gas generator exhaust area is clear.

6) Adjust the HP pump discharge pressure to 150 PSIG.

7) Depress and hold down the spring loaded ignitor switch for 10 seconds.

8) While continuing to hold the ignitor switch depressed, open the solenoid operated emergency fuel cutoff valve. Ignition should be observed in 6-12 seconds. If the gas generator fails to light, close the emergency fuel cutoff valve and release the ignitor switch. Allow the system to

purge for 5 minutes or until no raw fuel is being expelled from the primary nozzle. If the gas generator fails to light, raw fuel will be expelled from the primary nozzles and will collect in the base of the secondary plenum. This should be wiped up prior to continuing.

9) When ignition is observed, release the ignitor switch.

10) Observe the burner temperature. When the burner temperature reaches 1000° F begin reducing fuel pressure toward minimum (70-75 PSIG at the burner nozzle, (PNOZ)) to stabilize burner temperature between 1000 and 1300° F.

> WARNING Do not allow burner temperature to exceed 1500° F.

It will be necessary to close the cooling air bypass valve to about 50 per cent open to achieve stable operation at the desired burner temperature.

CAUTION Do not allow burner temperature to fall below 1000° F. The gas generator will begin to emit white smoke when the burner temperature falls to about 950° F and combustion will cease at a burner temperature of about 800° F. If combustion ceases there will be a noticable change in sound intensity accompanied by quantities of white smoke and rapidly falling burner temperature; immediately close the emergency fuel cutoff valve. Readjust fuel and air controls to lightoff settings and reinitiate the lightoff sequence.

The prescribed lightoff sequence usually leads to stable operation with an uptake temperature of 400-500° F and an uptake Mach number of about 0.07.

WARNING Do not allow uptake temperature to exceed 1200° F at any time.

11) When stable operation has been established, close the nozzle box drain valve prior to attempting to adjust the uptake Mach number.

III. TEMPERATURE/MACH NUMBER CONTROL

The control process consists of a iterative sequence of adjustments in the uptake temperature (TUPT), inlet air pressure (PNH), and bypass cooling air mass flow. Some practice is necessary to achieve reasonable accuracy in the adjustment process. It must be kept in mind that effect of the bypass cooling air valve varies depending on the valve's initial position. When the bypass valve is more than 50 per cent open, opening the valve reduces air flow through the burner, increasing burner temperature (TBURN), however, the increase in the proportion of cool bypass air mixing with the combustion gas results in a lower uptake temperature. When a majority of the air flow is already passing through the combustion chamber, that is, when the bypass valve is

less than 50 per cent open, and particularly when it is less than 25 per cent open, the increase in burner temperature resulting from opening the bypass valve more than offsets the increased proportion of cooling air and the uptake temperature will raise when the bypass valve is opened. With these cautions in mind, the following adjustment procedure is recommended:

A) Adjust the fuel control valve to obtain the desired uptake temperature. Do not allow burner temperature to fall below 1000° F or to exceed 1300° F during this process.

B) As burner temperature approaches one of the limits, change air flow through the burner either by adjusting the bypass valve or the inlet globe valve. Choice of control device depends on the prior operating state. If the system has been stablized at the desired Mach number it is usually best to control burner temperature during transitions by using the inlet globe valve. The key operating parameters are uptake temperature (TUPT) and uptake pressure (PUPT). Burner temperature is monitored to ensure safe combustion is maintained. For operation with uptake an Mach number of approximately 0.065, the values in Table XXII are recommended:

TABLE XXII

Recommended Initial Control Settings

TUPT (° F)	PUPT (inches H O)
950	13.3
850	11.1
750	10.5
650	9.6
550	9.0
175	8.8

C) Compute the uptake Mach number (UMACH) using the formula:

$$UMACH = 1.037 \times 10^{-4} (TUPTR/\gamma)^{0.5} \times ((((PNH + B) \times DELPN / TNHR)^{0.5} + (2.318 \times 10^{-4} \times ROTA) + 2.085 \times 10^{-4}) / (B + (PUPT / 13.5717)))$$

(eqn A.1)

where:

UMACH = Uptake Mach number

TUPTR = Absolute uptake temperature (R)

γ = Ratio of specific heats for air

TABLE XXIII

Values of the Ratio of Specific Heats for Air

TUPT (° F)	γ
175	1.3991
550	1.3805
650	1.3741
750	1.3677
850	1.3614
950	1.3556

PNH = Air pressure before the inlet reducing section (inches Hg)

B = Corrected atmospheric pressure (inches Hg)

DELPN = Pressure drop across the inlet reducing section (inches H_2O)

TNHR = Absolute air temperature before the inlet reducing section (R)

ROTA = Fuel mass flow rotameter reading

PUPT = Gas pressure in the uptake section (inches H_2O)

D) Adjust the uptake temperature and pressure as necessary using a combination of inlet globe valve, cooling air bypass valve, and fuel control valve changes until the desired test Mach number is obtained.

E) If inlet air temperature has been allowed to stablize prior to gas generator operation, it will be found that, once the desired uptake temperature and Mach number have been set, no adjustments to the system will be required during data runs. Uptake temperature will be maintained within plus or minus four degrees and uptake Mach number will vary less than 0.001 under most circumstances. The largest variations in uptake Mach number observed have been during pumping coefficient runs when changes in secondary flow induce large changes in uptake pressure. If the gas generator is at the operating point prior to closing the plenum, it will be unnecessary to make adjustments for the slight increase (0.0005 to 0.0010) in Mach number which occurs when secondary flow is shut off.

IV. SECURING THE SYSTEM

A) When data runs are complete , shut down the gas generator by reducing the fuel pressure to minimum and immediately closing the solenoid operated emergency fuel cutoff valve.

1) Shut off the high pressure fuel pump.
2) Shut off the fuel supply pump.
3) Open the cooling air bypass valve fully.
4) Open the inlet bypass globe valve until an inlet pressure (PNH) of 4.0-5.0 inches Hg is obtained.
5) Allow the gas generator to run in this manner until the uptake temperature drops to approximately the inlet air temperature.
6) Close the fuel system bulkhead and tank isolation valves. It is good practice to refill the fuel service tank at the end of each operating period. Keeping the tank full of fuel reduces moisture buildup from condensation. Any water or sediment which might enter the tank during filling will have time to settle out and can be removed through the stripping connection prior to the next lightoff.

B) When the gas generator has cooled sufficiently, the air compressor may be shut down.

1) Close the compressor suction butterfly valve.
2) Stop the electric motor.
3) When the compressor oil pressure falls below 20 PSIG, switch the auxiliary oil pump control from the "automatic" to the "hand" position.
4) Allow the lube oil system to run for one hour or until the compressor bearing temperatures are less than 80° F.
5) Stop the auxiliary lube oil pump.
6) Stop the cooling tower fan and cooling water pump.

C) Close the 4 inch butterfly manual isolation valve.

D) Close the inlet bypass globe valve.

E) Open the nozzle box drain valve.

F) Close the manometer isolation valves. It is also good practice to disconnect the inlet air pressure (PNH) and reducing section pressure drop (DELPN) manometers at the manometer. Other users of the compressor operate at pressures sufficient to over-pressurize these instruments. Over-pressurization

of the mercury manometer which measures the inlet pressure could result in a hazardous mercury spill.

G) De-energize the main power panel and shut off the thermocouple readouts.

APPENDIX B

UNCERTAINTY ANALYSIS

The determination of the uncertainties in the experimentally determined pressure coefficients and pumping coefficients was made using the methods described by Kline and McClintock [Ref. Kline]. The basic uncertainty anylysis for the cold flow eductor model test facility was conducted by Ellin [Ref. Ellin]. Hill [Ref. Hill] follows this development in analysis of the hot flow facility. Hill's analysis has been corrected for changes in the measured uncertainties resulting from the installation of new fuel flow measuring equipement. The uncertainties obtained using the second order equation suggested by Kline and McClintock were applicable to the experimental work conducted during the present research and are listed here.

UNCERTAINTY IN MEASURED VALUES

Parameter	Value	Uncertainty
TAMB	537 R	±1
TUPT	1415 R	±1
B	29.83 in Hg	±0.005
DELPN	6.20 in H_2O	±0.05
PUPT	13.6 in H_2O	±0.05
ROTA	28.0	±0.2
PNH	5.9 in Hg	±0.05
TNH	649 R	±0.2
PPLN	5.18 in H_2O	±0.01

UNCERTAINTY IN CALCULATED VALUES

P*/T*	1.7%
W*T*0.44	1.4%

```
C   J A HILL                    23 MAY 79,  REVISED 6 AUG 79                RIG00040
C   I J EICK                    REVISED 26 JUN 82                           RIG00050
C   THIS PROGRAM READS RAW DATA FROM THE HOTRIG EXPERIMENT, PERFORMS THE    RIG00060
C   DATA REDUCTION AND YIELDS TABULAR OUTPUT FOR PUMPING COEFFICIENT        RIG00070
C   DETERMINATION.                                                          RIG00080
C                                                                           RIG00090
C                                                                           RIG00100
C   **************************                                              RIG00110
C   VARIABLE NAMES                                                          RIG00120
C                                                                           RIG00130
C   AM     AREA OF MIXING STACK, SQ FT                                      RIG00140
C   AMAP   AM/AP                                                            RIG00150
C   AP     AREA OF PRIMARY NOZZLES, SQ FT                                   RIG00160
C   AUP    AREA OF UPTAKE, SQ FT                                            RIG00170
C   B      BAROMETER READING, IN HG                                         RIG00180
C   C1     CONVERSION OF P/RT TO DENSITY                                    RIG00190
C   C2     CONVERSION OF INCH WATER TO INCH HG                              RIG00200
C   C3     CONVERSION OF DEG F TO DEG R                                     RIG00210
C   C4     CONVERSION OF IN H2O TO LBF/SQ FT                                RIG00220
C   DATE   DATE OF RUN                                                      RIG00230
C   DELPN  PRESSURE DROP ACROSS ENTRANCE NOZZLE, IN H2O                     RIG00240
C   DM     DIAMETER OF MIXING STACK, IN                                     RIG00250
C   DP     DIAMETER OF PRIMARY NOZZLES, IN                                  RIG00260
C   DU     DIAMETER OF UPTAKE, IN                                           RIG00270
C   GAMMA  RATIO OF AIR SPECIFIC HEATS                                      RIG00280
C   LD     LENGTH TO DIAMETER RATIO OF MIXING STACK                         RIG00290
C   LMS    LENGTH OF MIXING STACK, IN                                       RIG00300
C   MUPT   NOMINAL UPTAKE TEMPERATURE FOR THE RUN                           RIG00310
C   MR     NUMBER OF DIFFUSER RINGS                                         RIG00320
C   NNOZ   NUMBER OF PRIMARY NOZZLES                                        RIG00330
C   NR     NUMBER OF RUNS                                                   RIG00340
C   PPLN   PRESSURE DROP ACROSS SECONDARY NOZZLES, IN H2O                   RIG00350
C   PNH    PRESSURE UPSTREAM OF ENTRANCE NOZZLE, IN HG                      RIG00360
C   PRTR   P*/T*                                                            RIG00370
C   PSTR   NON DIMENSIONAL PRESSURE, P*                                     RIG00380
C   PUPT   UPTAKE PRESSURE, IN H2O                                          RIG00390
C   RHOA   DENSITY OF AMBIENT AIR, LBM/CU FT                                RIG00400
C   RHOM   DENSITY IN MIXING STACK, LBM/CU FT                               RIG00410
C   RHOP   DENSITY AT PRIMARY NOZZLE, LBM/CU FT                             RIG00420
C   RHOS   DENSITY OF SECONDARY AIR, LBM/CU FT                              RIG00430
C   RHOUP  DENSITY IN UPTAKE, LBM/CU FT                                     RIG00440
C   ROTA   FUEL GAS FLOW ROTAMETER READING                                  RIG00450
C   SD     STANDOFF RATIO                                                   RIG00460
C   TAMB   AMBIENT TEMPERATURE, DEG F                                       RIG00470
C   TAMBR  AMBIENT TEMPERATURE, DEG R                                       RIG00480
C   TBURN  BURNER TEMPERATURE, DEG F                                        RIG00490
C   TNH    ENTRANCE NOZZLE TEMPERATURE, DEG F                               RIG00500
C   TNHR   ENTRANCE NOZZLE TEMPERATURE, DEG R                               RIG00510
```

```
C   TSTR   NON DIMENSIONAL TEMPERATURE, T*                                  RIG00520
C   TUPT   UPTAKE TEMPERATURE, DEG F                                        RIG00530
C   TUPTR  UPTAKE TEMPERATURE, DEG R                                        RIG00540
C   UM     VELOCITY IN MIXING STACK, FT/SEC                                 RIG00550
C   UMACH  UPTAKE MACH NUMBER                                               RIG00560
C   UP     VELOCITY IN PRIMARY NOZZLES, FT/SEC                              RIG00570
C   UU     VELOCITY IN UPTAKE, FT/SEC                                       RIG00580
C   WF     MASS FLOW OF FUEL, LBM/SEC                                       RIG00590
C   WPA    MASS FLOW OF PRIMARY AIR, LBM/SEC                                RIG00600
C   WP     MASS FLOW THROUGH PRIMARY NOZZLES, LBM/SEC                       RIG00610
C   WS     MASS FLOW OF SECONDARY AIR, LBM/SEC                              RIG00620
C   WSTR   NON DIMENSIONAL MASS FLOW RATE, W*                               RIG00630
C   WSTR44 EMPIRICAL PUMPING COEFFICIENT                                    RIG00640
C                                                                           RIG00650
C                                                                           RIG00660
C                                                                           RIG00670
C   ************************************                                    RIG00680
C     INPUT AND INITIAL DATA                                                RIG00690
C                                                                           RIG00700
      IMPLICIT REAL*8(A-H,O-W)                                              RIG00710
      REAL*4 LD,LMS                                                         RIG00720
C                                                                           RIG00730
      DIMENSION DATE(2)                                                     RIG00740
      DIMENSION PNH(13),DELPN(13),TNH(13),ROTA(13), TBURN(13),TUPT(13),     RIG00750
     *PUPT(13),PPLN(13),TAMB(13),SECAIR(13)                                 RIG00760
      DIMENSION WPA(13),WF(13),WP(13),WS(13),WSTR(13),PSTR(13),TSTR(13),RIG00770
     *PRTR(13),WSTR44(13),UP(13),UM(13),UU(13),UMACH(13)                    RIG00780
C                                                                           RIG00790
      DATA NNOZ/4/,DP/2.25D0/,DU/7.51D0/,AMAP/2.50D0/,AP/.1104466D0/        RIG00800
     *,DM/7.122D0/,SD/.5D0/,AM/.2766504D0/,                                 RIG00810
     *AUP/.3076148D0/                                                       RIG00820
      DATA C1/1.321566D0/,C2/13.5717D0/,C3/459.67D0/,C4/5.19408D0/          RIG00830
      DATA SECAIR/0.0D0,1.767146D0,3.534292D0,5.301438D0,8.44303D0,         RIG00840
     *11.584623D0,14.726216D0,27.292583D0,39.858957D0,52.425327D0,          RIG00850
     *64.991698D0,2*1004.0D13/                                              RIG00860
      READ (5,80) NR,LMS,LD                                                 RIG00870
80    FORMAT(I2,F6.3,F4.2)                                                  RIG00880
      DO 555 JJK=1,NR                                                       RIG00890
      READ (5,100) DATE,B,GAMMA,MR,MTUPT                                    RIG00900
100   FORMAT(2A8,F5.2,F6.4,I1,I3)                                           RIG00910
C                                                                           RIG00920
C                                                                           RIG00930
      DO 90 I=1,12                                                          RIG00940
      READ (5,110) PNH(I),TNH(I),DELPN(I),ROTA(I),TBURN(I),TUPT(I),         RIG00950
     *PUPT(I),PPLN(I),TAMB(I)                                               RIG00960
110   FORMAT (10 F8.3)                                                      RIG00970
C                                                                           RIG00980
C                                                                           RIG00990
```

```
C                                                                       RIG01000
CCC   ************************                                        RIG01010
CCC     DATA REDUCTION                                                  RIG01020
C                                                                       RIG01030
        TUPTR=TUPT(I)+C3                                                RIG01040
        TAMBR=TAMB(I)+C3                                                RIG01050
        TNHR=TNH(I)+C3                                                  RIG01060
        WPA(I)=1.746190501260D0*DSQRT((PNH(I)+B)*DELPN(I)/TNHR) +       RIG01070
       *0.039475965810D0                                                RIG01080
        WF(I)=ROTA(I)                                                   RIG01090
        IF (ROTA(I) .NE. 0.0D0) WF(I)=(0.40475919622D0*ROTA(I)-         RIG01100
       *3.07159427360D0)*1.0D-3                                         RIG01110
        WP(I)=WPA(I)+WF(I)                                              RIG01120
        RHOUP=C1*(B+(PUPT(I)/C2))/TUPTR                                 RIG01130
        RHOS=C1*(B-(PPLN(I)/C2))/TAMBR                                  RIG01140
        RHOP=RHOS*TAMBR/TUPTR                                           RIG01150
        RHOA=C1*B/TAMBR                                                 RIG01160
        WS(I)=.123808D0*SECAIR(I)*DSQRT(RHOA*PPLN(I))                   RIG01170
        WSTR(I)=WS(I)/WP(I)                                             RIG01180
        UP(I)=WP(I)/RHOP/AP                                             RIG01190
        PSTR(I)=(PPLN(I)*C4/RHOS)/(UP(I)*UP(I)/64.348D0)                RIG01200
        UU(I)=WP(I)/RHOUP/AUP                                           RIG01210
        RHOM=(WP(I)+WS(I))/((WS(I)/RHOS)+(WP(I)/RHOP))                  RIG01220
        UM(I)=(WP(I)+WS(I))/RHOM/AM                                     RIG01230
        TSTR(I)=TAMBR/TUPTR                                             RIG01240
        WSTR(I)=WS(I)/WP(I)                                             RIG01250
        PRTR(I)=PSTR(I)/TSTR(I)                                         RIG01260
        WSTR44(I)=WSTR(I)*TSTR(I)**.44D0                                RIG01270
        UMACH(I)=UU(I)/41.42658D0/DSQRT(GAMMA*TUPTR)                    RIG01280
90      CONTINUE                                                        RIG01290
CCC                                                                     RIG01300
CCC                                                                     RIG01310
CCC                                                                     RIG01320
CCC                                                                     RIG01330
CCC                                                                     RIG01340
CCC   ************************                                        RIG01350
CCC     TABULAR OUTPUT                                                  RIG01360
C                                                                       RIG01370
        WRITE (04,500) MTUPT,MR                                         RIG01380
500     FORMAT('1',/T49,'***   HOT RIG PERFORMANCE   ***',              RIG01390
       *20X,'TUPT:  ',I3/T57,I1,' RING DIFFUSER'//)                     RIG01400
        WRITE (04,510) DATE                                             RIG01410
510     FORMAT (/T4,'DATE:  ',2A8,T65,'DATA TAKEN BY I J EICK')         RIG01420
        WRITE (04,520)NNOZ,LMS                                          RIG01430
520     FORMAT(/T4,'NUMBER OF PRIMARY NOZZLES:  ',I2,T65,'MIXING STACK',RIG01440
       *' LENGTH:  ',F5.2,'  INCHES')                                   RIG01450
        WRITE (04,530) DP,DM                                            RIG01460
530     FORMAT (T4,'PRIMARY NOZZLE DIAMETER:  ',F5.2,'  INCHES',T65,    RIG01470
```

```
     *'MIXING STACK DIAMETER:  ',F6.3,'  INCHES')                          RIG01480
      WRITE (04,540) DU,LD                                                 RIG01490
540   FORMAT(T4,'UPTAKE DIAMETER:  ',F5.3,'  INCHES',T65,                  RIG01500
     *'MIXING STACK L/D:  ',F4.2)                                          RIG01510
      WRITE (04,550) AMAP,SD                                               RIG01520
550   FORMAT (T4,'AREA RATIO, AM/AP:  ', F4.2,T65,                         RIG01530
     *'STANDOFF RATIO:  ',F4.2)                                            RIG01540
      WRITE (04,560) GAMMA,B                                               RIG01550
560   FORMAT(T4,'GAMMA:  ',F6.4,T65,'AMBIENT PRESSURE:  ',F5.2,            RIG01560
     *'  INCHES HG')                                                       RIG01570
      WRITE (04,570)                                                       RIG01580
570   FORMAT (///1X,'NR',T7,'PNH',T16,'DELPN',T25,'TNH',T34,'ROTA',        RIG01590
     *T41,'TBURN',T50,'TUPT',T59,'TAMB',T68,'PUPT',T77,'PPLN',             RIG01600
     *T86,'SEC AREA')                                                      RIG01610
      WRITE (04,580)                                                       RIG01620
580   FORMAT(1X,T6,'IN HG',T16,'IN H2O',T25,'DEG F',T41,'DEG F'            RIG01630
     *,T50,'DEG F',T59,'DEG F',T68,'IN H2O',T77,'IN H2O',T88,'SQ IN')      RIG01640
      WRITE (04,590) (I,PNH(I),DELPN(I),TNH(I),ROTA(I),TBURN(I),           RIG01650
     *TUPT(I),TAMB(I),PUPT(I),PPLN(I),SECAIR(I),I=1,12)                    RIG01660
590   FORMAT(/1X,I2,T7,F5.2,T16,F5.2,T25,F5.1,T33,F5.1,T41,F6.1,T50,       RIG01670
     *F5.1,T59,F4.1,T68,F5.2,T78,F4.2,T87,F6.3)                            RIG01680
      WRITE (04,600)                                                       RIG01690
600   FORMAT (///1X,'NR',T7,'WPA',T16,'WF',T25,'WP',T34,'WS',T43,'W*',     RIG01700
     *T52,'P*',T61,'T*',T69,'P*/T*',T77,'W*T**.44',T88,'UP',T97,           RIG01710
     *'UM',T106,'UU',T113,'UMACH')                                         RIG01720
      WRITE (04,610)                                                       RIG01730
610   FORMAT(1X,T6,4('LBM/S',4X),T87,3('FT/S',5X))                         RIG01740
      WRITE (04,620) (I,WPA(I),WF(I),WP(I),WS(I),WSTR(I),PSTR(I),          RIG01750
     *TSTR(I),PRTR(I),WSTR44(I),UP(I),UM(I),UU(I),UMACH(I),I=1,12)         RIG01760
620   FORMAT(/1X,I2,T6,F5.3,T15,F5.3,T24,F5.3,T33,F5.3,T42,F5.3,T51,       RIG01770
     *F5.3,T60,F5.3,T69,F5.3,T78,F5.3,T87,F5.1,T96,F5.1,T105,F5.1,         RIG01780
     *T113,F6.4)                                                           RIG01790
C                                                                          RIG01800
C                                                                          RIG01810
C     **************************                                           RIG01820
C                                                                          RIG01830
C                                                                          RIG01840
555   CONTINUE                                                             RIG01850
      STOP                                                                 RIG01860
      END                                                                  RIG01870
```

LIST OF REFERENCES

1. Moss, C. M., Effects of Several Geometric Parameters on the Performance of a Multiple Nozzle Eductor System, Master's Thesis, Naval Postgraduate School, September 1977.

2. Ellin, C. R., Model Test of Multiple Nozzle Exhaust Gas Eductor Systems for Gas Turbine Powered Ships, Engineer's Thesis, Naval Postgraduate School, June 1977.

3. Pucci, P. F., Simple Eductor Design Parameters, Ph.D. Thesis, Stanford University, September 1954.

4. Harrell, J. P., Jr., Experimentally Determined Effects of Eductor Geometry on the Performance of Exhaust Gas Eductors for Gas Turbine Powered Ships, Engineer's Thesis, Naval Postgraduate School, September 1981.

5. Ross, P. D., Combustion Gas Generator for Gas Turbine Exhaust Systems Modelling, Master's Thesis, Naval Postgraduate School, December 1977.

6. Welch, D. R., Hot Flow Testing of Multiple Nozzle Exhaust Eductor Systems, Engineer's Thesis, Naval Postgraduate School, September 1978.

7. Lemke, R. J. and Staehli, C. P., Performance of Multiple Nozzle Eductor Systems with Several Geometric Configurations, Master's Thesis, Naval Postgraduate School, September 1977.

8. Hill, J. A., Hot Flow Testing of Multiple Nozzle Exhaust Eductor Systems, Master's Thesis, Naval Postgraduate School, September 1979.

9. Shaw, R. S., Performance of a Multiple Nozzle Exhaust Gas Eductor System for Gas Turbine Powered Ships, Master's Thesis, Naval Postgraduate School, December 1980.

10. Ryan, D. L., Flow Characteristics of a Multiple Nozzle Exhaust Gas Eductor System, Master's Thesis, Naval Postgraduate School, March 1981.

11. Davis, C. C., Performance of Multiple, Angled Nozzles with Short Mixing Stack Eductor Systems, Master's Thesis, Naval Postgraduate School, September 1981.

12. Drucker, J. C., Characteristics of a Four-Nozzle, Slotted Short Mixing Stack with Shroud, Gas Eductor System, Master's Thesis, Naval Postgraduate School, March 1982.

13. AGA Thermovision 750, Operating Manual, AGA Infrared Systems AB, 1973.

14. Kline, S. J. and McClintock, F. A., "Describing Uncertainties in Single-Sample Experiments," Mechanical Engineering, p. 3-8, January 1953.

INITIAL DISTRIBUTION LIST

		No. Copies
1.	Defense Technical Information Center Cameron Station Alexandria, Virginia 22314	2
2.	Library, Code 0142 Naval Postgraduate School Monterey, California 93940	2
3.	Department Chairman, Code 69 Department of Mechanical Engineering Naval Postgraduate School Monterey, California 93940	2
4.	Professor Paul F. Pucci, Code 69Pc Department of Mechanical Engineering Naval Postgraduate School Monterey, California 93940	4
5.	Dean of Reasearch, Code 012 Naval Postgraduate School Monterey, California 93940	1
6.	Commander Attn: NAVSEA Code 0331 Naval Ship Systems Command Washington, DC 20362	1
7.	Mr. Olin M. Pearcy NSRDC Code 2833 Naval Ship Research and Development Center Annapolis, Maryland 21402	1
8.	Mr. Mark Goldberg NSRDC Code 2833 Naval Ship Research and Development Center Annapolis, Maryland 21402	1
9.	Mr. Eugene P. Wienert Head, Combined Power and Gas Turbine Branch Naval Ship Engineering Center Philadelphia, Pennsylvania 19112	1

10. Mr. Donald N. McCallum 1
NAVSEC Code 6136
Naval Ship Engineering Center
Washington, DC 21362

11. LCDR Ira J. Eick, USN 1
P.O. Box 248
Lebanon, New Jersey 08833

12. LT Carl J. Drucker, USN 1
1032 Marlborough Street
Philadelphia, Pennsylvania 19125

13. LCDR C. M. Moss, USN 1
625 Midway Road
Powder Springs, Georgia 30073

14. LCDR J. P. Harrell, Jr., USNR 1
1600 Stanley
Ardmore, Oklahoma 73401

15. LCDR J. A. Hill, USN 1
RFD 2, Box 116B
Elizabeth Lane
York, Maine 03909

16. LCDR R. J. Lemke, USN 1
2902 No. Cheyenne
Tacoma, Washington 98407

17. LCDR C. P. Staehli, USN 1
2808 39th St., N.W.
Gig Harbor, Washington 98335

18. Lt R. S. Shaw, USN 1
147 Wampee Curve
Summerville, South Carolina 29483

19. LCDR D. L. Ryan, USN 1
6393 Caminito Luisito
San Diego, California 92111

20. LCDR C. C. Davis, USN 1
1608 Linden Drive
Florence, South Carolina 29501

21. LCDR D. Welch, USN 1
1036 Brestwick Commons
Virginia Beach, Virginia 23464

22. CDR P. D. Ross, Jr., USN 1
6050 Henderson Drive No. 8
La Mesa, California 92041

23. Mr. John King 1
Civil Engineering Laboratory, Code L63
Naval Construction Battalion Center
Port Hueneme, California 93043